

FACIAL FEATURE EXTRACTION USING DEFORMABLE TEMPLATES

A THESIS SUBMITTED TO
THE GRADUATE SCHOOL OF INFORMATICS
OF
THE MIDDLE EAST TECHNICAL UNIVERSITY

BY

HAKAN SERÇE

IN PARTIAL FULFILLMENT OF THE REQUIREMENTS FOR THE DEGREE OF
MASTER OF SCIENCE
IN
THE DEPARTMENT OF INFORMATION SYSTEMS

DECEMBER 2003

Approval of the Graduate School of Informatics.

Prof. Dr. Neşe Yalabık
Director

I certify that this thesis satisfies all the requirements as a thesis for the degree of Master of Science.

Assoc. Prof. Dr. Onur
Demirörs
Head of Department

This is to certify that we have read this thesis and that in our opinion it is fully adequate, in scope and quality, as a thesis for the degree of Master of Science.

Prof. Dr. Uğur Halıcı
Supervisor

Examining Committee Members

Prof. Dr. Kemal Leblebicioğlu

Prof. Dr. Neşe Yalabık

Prof. Dr. Uğur Halıcı

Assoc. Prof. Dr. Volkan Atalay

Assist. Prof. Dr. Erkan Mumcuoğlu

ABSTRACT

FACIAL FEATURE EXTRACTION USING DEFORMABLE TEMPLATES

Serçe, Hakan

M.Sc., Department of Information Systems

Supervisor: Prof. Dr. Uğur Halıcı

December 2003, 181 pages

The purpose of this study is to develop an automatic facial feature extraction system, which is able to identify the detailed shape of eyes, eyebrows and mouth from facial images. The developed system not only extracts the location information of the features, but also estimates the parameters pertaining the contours and parts of the features using parametric deformable templates approach.

In order to extract facial features, deformable models for each of eye, eyebrow, and mouth are developed. The development steps of the geometry, imaging model and matching algorithms, and energy functions for each of these templates are presented in detail, along with the important implementation issues. In addition, an eigenfaces based multi-scale face detection algorithm which incorporates standard facial proportions is implemented, so that when a face is detected the rough search regions for the facial features are readily available.

The developed system is tested on JAFFE (Japanese Females Facial Expression Database), Yale Faces, and ORL (Olivetti Research Laboratory) face image databases. The performance of each deformable templates, and the face

detection algorithm are discussed separately.

Keywords: Computer Vision, Facial Feature Finding, Deformable Templates, Eye Template, Eyebrow Template, Mouth Template, Active Contours (Snakes), Eigenfaces, Image Pyramid

ÖZ

ŞEKİL DEĞİŞTİREBİLEN ŞABLONLAR KULLANARAK YÜZ ÖZNİTELİKLERİNİ BULMA

Serçe, Hakan

Yüksek Lisans, Bilişim Sistemleri Bölümü

Tez Yöneticisi: Prof. Dr. Uğur Halıcı

Aralık 2003, 181 sayfa

Bu çalışma yüz görüntüleri üzerinde gözler, kaşlar ve ağzın detaylı şekillerini belirleyebilen bir otomatik *yüz öznitelikleri bulma* sistemi geliştirmek amacı ile yapılmıştır. Geliştirilen sistem, sadece özniteliklerin yerlerini belirlemekle kalmayıp, özniteliklerin dış hatları ve parçaları ile ilgili parametreleri de keşsetmektedir.

Yüz özniteliklerini çıkarabilmek için, göz, kaş ve ağız *şekil değiştirebilen şablonları* ayrı ayrı geliştirilmiştir. Bu şablonların herbirinin geometrisi, görüntüleme modeli, eşleme algoritması ve enerji fonksiyonlarının geliştirilmesi adımları, gerçekleştirmeye yönelik önemli noktaları ile birlikte detaylı bir şekilde sunulmuştur. Ayrıca, eigen-yüz tabanlı çok-ölçekli ve standart yüz oranlarını içeren bir yüz tespit etme algoritması geliştirilmiştir, öyle ki görüntüde bir yüz tespit edildiğinde yüz özniteliklerinin kabaca yerleri de bulunmuş olmaktadır.

Geliştirilen sistem, JAFFE (Japanese Females Facial Expression Database), Yale Faces, ve ORL (Olivetti Research Laboratory) yüz görüntüleri veri taban-

ları kullanılarak test edilmiştir. Geliştirilen herbir şablon ile yüz tespit etme algoritmasının performansları ayrı ayrı tartışılmıştır.

Anahtar Kelimeler: Bilgisayarlı Görme, Yüz Öz Niteliklerinin Yerlerinin Saptanması, Şekil Değiştirebilen Şablonlar, Göz Şablonu, Kaş Şablonu, Ağız Şablonu, Aktif Eğriler, Eigen Yüz, Görüntü piramidi

To Fatma Cemile, my beloved wife . . .

ACKNOWLEDGMENTS

I would like to thank my supervisor, Prof. Dr. Uğur Halıcı, who encouraged and guided me in writing of this thesis. I also express my sincere appreciation to the other committee members, Prof. Dr. Neşe Yalabık, Prof. Dr. Kemal Leblebicioğlu, Assoc. Prof. Dr. Volkan Atalay, Assist. Prof. Dr. Erkan Mumcuoğlu for their comments and suggestions.

I would like to express my deepest gratitude to my wife, Fatma Cemile, who encouraged and supported me in this demanding study in the first months of our marriage with her never ending patience. She helped me generate most of the drawings used in this thesis, and performed long-lasting tests of the developed system. I should admit that, I would never finish this study without her endless support.

I would also like to thank to my employer, MilSOFT, for providing me time for studying whenever I needed, and for tolerating me when I was so tired and sleepy after a sleepless night of studying.

Thanks are also to all of my friends for their direct or indirect help.

Finally, my deepest thanks are to my parents who supported and motivated me with their never ending patience, tolerance and understanding throughout the study.

TABLE OF CONTENTS

ABSTRACT	iii
ÖZ	v
DEDICATON	vii
ACKNOWLEDGMENTS	viii
TABLE OF CONTENTS	ix
LIST OF TABLES	xiii
LIST OF FIGURES	xv
LIST OF ALGORITHMS	xviii
CHAPTER	
1 Introduction	1
1.1 Background and Rationale of the Study	1
1.2 Approach	3
1.3 Road Map	3
2 Image Processing Background	5
2.1 Low Level Image Processing	5
2.1.1 Histogram Equalization	6
2.1.2 Smoothing	8
2.1.3 Edge Detection	10
2.1.4 Corner Detection	12
2.1.5 Peak Valley Detection	14
2.2 Object Description and Recognition	16
2.2.1 Classical Template Matching	16

	2.2.2	Deformable Template Matching	17
	2.2.3	Active Contours (Snakes)	19
	2.2.3.1	Internal Energy	20
	2.2.3.2	External Energy	21
	2.2.3.3	Image Energy Functionals	21
	2.2.3.4	Snake Minimization	21
3		Previous Work on Facial Feature Extraction	23
	3.1	Face Detection	23
	3.1.1	Eigenfaces	24
	3.1.2	Neural Networks	25
	3.2	Facial Feature Extraction	27
	3.2.1	Eigenfeatures	27
	3.2.2	Gabor Jets	28
	3.2.3	Classical Template Matching	31
	3.2.4	Deformable Templates	32
	3.2.4.1	An Eye Deformable Template	32
	3.2.4.2	A More Robust Eye Deformable Template	36
	3.2.4.3	Deformable Templates using a spring model	36
	3.2.4.4	Multi-state templates for mouth extraction	38
	3.2.4.5	Other Deformable Template Research	41
	3.2.5	Active Contours (Snakes)	42
	3.2.6	Integral Projection	44
4		Implementation	48
	4.1	Face Detection	49
	4.1.1	Calculation of the Eigenfaces	51
	4.1.2	Face Detection Algorithm	55
	4.2	Extraction of Eyebrow: Eyebrow Deformable Template	58
	4.2.1	Template Geometry	58
	4.2.2	Imaging Model	61
	4.2.3	Matching Algorithm	62

4.2.4	Implementation Issues	64
4.2.4.1	Template Geometry Issues	64
4.2.4.2	Image Boundary Considerations	66
4.2.4.3	Energy Calculation Issues	67
4.2.4.4	Use of Downhill Simplex	69
4.2.4.5	Coefficients of the Energy Function	70
4.3	Extraction of Eye: Eye Deformable Template	70
4.3.1	Template Geometry	70
4.3.2	Imaging Model	72
4.3.3	Matching Algorithm	73
4.3.4	Implementation Issues	74
4.3.4.1	Template Geometry Issues	74
4.3.4.2	Image Boundary Considerations	74
4.3.4.3	Energy Calculation Issues	75
4.3.4.4	Use of Downhill Simplex	77
4.3.4.5	Coefficients of the Energy Function	77
4.4	Extraction of Mouth: Mouth Deformable Template	78
4.4.1	Template Geometry	78
4.4.2	Imaging Model	79
4.4.3	Matching Algorithm	81
4.4.4	Implementation Issues	81
4.4.4.1	Template Geometry Issues	82
4.4.4.2	Image Boundary Considerations	83
4.4.4.3	Energy Calculation Issues	84
4.4.4.4	Use of Downhill Simplex	85
4.4.4.5	Coefficients of the Energy Function	85

	4.4.4.6	Selection of Open vs. Closed Mouth Template	85
5		Results	86
	5.1	Test Settings	86
	5.2	Performance of the Face Detection Algorithm	87
	5.3	Test Settings for Deformable Templates	88
	5.4	Performance of the Eyebrow Template	89
	5.5	Performance of the Eye Template	91
	5.6	Performance of the Mouth Template	94
	5.7	General Findings on Deformable Templates	102
6		Conclusion	107
	6.1	Limitations and Future Work	108
		6.1.1 Face Detection	108
		6.1.2 Feature Extraction	110
	6.2	Application Areas	110
		REFERENCES	111
		APPENDICES	117
	A	Test Sets	117
	B	Polygonal Eyebrow Template Detailed Test Results	121
	C	Spline-based Eyebrow Template Detailed Test Results	128
	D	Spline-based Eye Template Detailed Test Results	135
	E	Polygonal Eye Template Detailed Test Results	142
	F	Polygonal Mouth-Closed Template Detailed Test Results	149
	G	Spline-based Mouth-Closed Template Detailed Test Results	156
	H	Polygonal Mouth-Open Template Detailed Test Results	163
	I	Spline-based Mouth-Open Template Detailed Test Results	170
	J	Face Detection Training Set	177

LIST OF TABLES

4.1	The geometrical constraints of the eyebrow template	59
4.2	The imaging model of the eyebrow template	61
4.3	The geometrical constraints of the eye template	72
4.4	The imaging model of the eye template	73
4.5	The geometrical constraints of the Mouth template	80
4.6	The imaging model of the Mouth template	80
5.1	The results of the face detection algorithm tests	87
5.2	Polygonal eyebrow templates analysis results of JAFFE, YALE & ORL (%)	89
5.3	Spline-based templates analysis results of JAFFE, YALE & ORL (%)	89
5.4	Polygonal eyebrow template analysis results of JAFFE, YALE & ORL in average pixels difference	90
5.5	Spline-based eyebrow template analysis results of JAFFE, YALE & ORL in average pixels difference	90
5.6	Comparison of polygonal and spline-based eyebrow templates . .	91
5.7	Polygonal eye templates analysis results of JAFFE, YALE & ORL (%)	91
5.8	Spline-based eye template analysis results of JAFFE, YALE & ORL (%)	92
5.9	Polygonal eye templates analysis results of JAFFE, YALE & ORL in average pixels difference	92
5.10	Spline-based eye templates analysis results of JAFFE, YALE & ORL in average pixels difference	93
5.11	Comparison of polygonal and spline-based eye templates	93
5.12	Polygonal mouth-closed template analysis results of JAFFE, YALE & ORL (%)	94
5.13	Spline-based mouth-closed template analysis results of JAFFE, YALE & ORL (%)	94
5.14	Polygonal mouth-open template analysis results of JAFFE, YALE & ORL (%)	95
5.15	Spline-based mouth-open template analysis results of JAFFE, YALE & ORL (%)	95
5.16	Polygonal mouth-closed template analysis results of JAFFE, YALE & ORL in average pixels difference	96

5.17	Spline-based mouth-closed template analysis results of JAFFE, YALE & ORL in average pixels difference	97
5.18	Polygonal mouth-open template analysis results of JAFFE, YALE & ORL in average pixels difference	98
5.19	Spline-based mouth-open template analysis results of JAFFE, YALE & ORL in average pixels difference	99
5.20	Comparison of polygonal and spline-based mouth-closed templates	100
5.21	Comparison of polygonal and spline-based mouth-open templates	101

LIST OF FIGURES

2.1	Histograms of a synthetic image and a real-life image.	7
2.2	The effect of histogram equalization on the image and its histogram	7
2.3	Smoothing with median filtering	8
2.4	Smoothing with different averaging kernels	9
2.5	A plot of the gaussian function	9
2.6	Smoothing using gaussian kernels	10
2.7	Edge magnitude orientation	11
2.8	Edge detection using Sobel kernels	12
2.9	Results of different corner detection algorithms	14
2.10	Peak and valley potentials	14
2.11	Valley template geometry and image model	15
3.1	Standard eigenfaces	25
3.2	Neural network for face detection	26
3.3	Bunch graph	30
3.4	Templates for matching different facial regions	32
3.5	Eye template (Yuille)	33
3.6	Mouth template	37
3.7	Eye template (Malciu and Preteux)	38
3.8	The parameterized deformable templates	39
3.9	Lip outline parameters	40
3.10	Deformable templates	43
3.11	Lower lip template	44
3.12	Integral projection	45
3.13	Y-Relief and X-Reliefs for an example image	46
4.1	Overview of the system	50
4.2	The face model used in face detection	52
4.3	Normalization of training Images	53
4.4	An image pyramid	55
4.5	A sample screen depicting the face detection process	57
4.6	The geometry of the deformable eyebrow template	59
4.7	Eyebrow rough localization epoch	63
4.8	Eyebrow rough deforming epoch	63
4.9	Eyebrow fine tuning epoch	63
4.10	An invalid eyebrow template geometry	66

4.11	The geometry of the deformable eye template	71
4.12	The geometry of the deformable mouth template	79
5.1	Sample results of the polygonal eyebrow template	102
5.2	Sample results of the spline-based eyebrow template	102
5.3	Sample results of the polygonal eye template	103
5.4	Sample results of the spline-based eye template	104
5.5	Sample results of the polygonal mouth template	104
5.6	Sample results of the spline-based mouth template	105
5.7	A case where spline based template outperformed polygonal tem- plate	105
5.8	Sample results of the system	106
A.1	Randomly selected JAFFE images	118
A.2	Randomly selected YALE images	119
A.3	Randomly selected ORL images	120
B.1	JAFFE polygonal left eyebrow template test results	122
B.2	JAFFE polygonal right eyebrow template test results	123
B.3	YALE polygonal left eyebrow template test results	124
B.4	YALE polygonal right eyebrow template test results	125
B.5	ORL polygonal left eyebrow template test results	126
B.6	ORL polygonal right eyebrow template test results	127
C.1	JAFFE spline-based left eyebrow template test results	129
C.2	JAFFE spline-based right eyebrow template test results	130
C.3	YALE spline-based left eyebrow template test results	131
C.4	YALE spline-based right eyebrow template test results	132
C.5	ORL spline-based left eyebrow template test results	133
C.6	ORL spline-based right eyebrow template test results	134
D.1	JAFFE spline-based left eye template test results	136
D.2	JAFFE spline-based right eye template test results	137
D.3	YALE spline-based left eye template test results	138
D.4	YALE spline-based right eye template test results	139
D.5	ORL spline-based left eye template test results	140
D.6	ORL spline-based right eye template test results	141
E.1	JAFFE polygonal left eye template test results	143
E.2	JAFFE polygonal right eye template test results	144
E.3	YALE polygonal left eye template test results	145
E.4	YALE polygonal right eye template test results	146
E.5	ORL polygonal left eye template test results	147
E.6	ORL polygonal right eye template test results	148
F.1	JAFFE polygonal mouth-closed template test results	150
F.2	JAFFE polygonal mouth-closed template test results (%)	151

F.3	YALE polygonal mouth-closed template test results	152
F.4	YALE polygonal mouth-closed template test results (%)	153
F.5	ORL polygonal mouth-closed template test results	154
F.6	ORL polygonal mouth-closed template test results (%)	155
G.1	JAFFE spline-based mouth-closed template test results	157
G.2	JAFFE spline-based mouth-closed template test results(%)	158
G.3	YALE spline-based mouth-closed template test results	159
G.4	YALE spline-based mouth-closed template test results(%)	160
G.5	ORL spline-based mouth-closed template test results	161
G.6	ORL spline-based mouth-closed template test results (%)	162
H.1	JAFFE polygonal mouth-open template test results	164
H.2	JAFFE polygonal mouth-open template test results (%)	165
H.3	YALE polygonal mouth-open template test results	166
H.4	YALE polygonal mouth-open template test tesults (%)	167
H.5	ORL polygonal mouth-open template test results	168
H.6	ORL polygonal mouth-open template test results (%)	169
I.1	JAFFE spline-based mouth-open template test results	171
I.2	JAFFE spline-based mouth-open template test results (%)	172
I.3	YALE spline-based mouth-open template test results	173
I.4	YALE spline-based mouth-open template test results (%)	174
I.5	ORL spline-based mouth-open template test results	175
I.6	ORL spline-based mouth-open template test results (%)	176
J.1	Face detection training set (part 1)	178
J.2	Face detection training set (part 2)	179
J.3	Face detection training set (part 3)	180
J.4	Face detection training set (part 4)	181

LIST OF ALGORITHMS

2.1	Forming the histogram of an image	6
2.2	Histogram equalization	8
2.3	Edge detection algorithm	11
3.1	Eye feature localizing using the more robust template	37
4.1	Face image normalization	54
4.2	Computing the initial geometry of the eyebrow template	65
4.3	Penalty mechanism for the eyebrow template	66
4.4	Finding where a given point lies in the eyebrow template geometry	68
4.5	Collecting statistics of eyebrow template	69
4.6	Computing the initial geometry of the eye template	75
4.7	Penalty mechanism for the eye template	76
4.8	Finding where a given point lies in the eye template geometry .	77
4.9	Collecting statistics of eye template	78
4.10	Computing the initial geometry of the mouth template	82
4.11	Penalty mechanism for the mouth template	83
4.12	Finding where a given point lies in the mouth template geometry	84
4.13	Collecting Statistics of Mouth Template	84

CHAPTER 1

Introduction

1.1 Background and Rationale of the Study

Facial feature extraction is the process of segmentation of facial features such as eyes, eyebrows, and lips, from static images or video sequences that contain faces. In general, the term *facial feature extraction* is widely used when static images are the concern, and *tracking* is used for referring the process of continuously extracting and tracking the features from video sequences. Facial feature extraction has long been a popular area of research mainly because of its wide range of application areas including: face recognition [1, 2], facial expression analysis [3], security systems (iris), photography (red eye correction), multi modal speech recognition and lipreading [4, 5], gaze tracking, human computer interfaces [6, 7], driver monitoring systems, and automatic facial animation[8],[9, p.6].

The starting problem in most of the cases of facial feature extraction is face detection, which deals with locating faces in images. Face detection is a problem on its own, on which significant research has been conducted. Principle component analysis (PCA) based [10], and connectionist approaches [11] have been successfully used in previous researches for face detection in arbitrary images.

Different approaches have been applied to facial feature extraction success-

fully. One of these approaches is the eigenfeatures method, which is a PCA based technique. Eigenlips for tracking lips for multi-modal speech and speaker recognition is used in [12]. Their approach concentrated on estimating the outer lip contour from the lip intensity image using PCA. Eigeneyes as an alternative to eigenfaces for face recognition is used in [1]. The idea behind the study is that the regions around the eyes are enough to recognize peoples, which is proved with the reported results of their study.

Elastic bunch graph technique used in [13] exploits Gabor jets for registering facial feature points. Their method aim face recognition by using similarity measures on the elastic bunch graph and the Gabor wavelet responses of facial feature points at different scales and orientations.

Classical template matching is most of the time too simplistic and rigid for facial feature detection, but it yields considerable performance when used in controlled conditions. Eye, eyebrow and mouth templates for detecting facial feature extraction is used in [14], in initializing step of their facial expression synthesis system. This method is also used in [15] for locating mouth and eye corners. The study does not use templates for detection of the features as a whole, but only for detecting corners of these features.

Integral projection method uses the maxima and minima of horizontal and vertical integral projections of the human face for locating the facial features. An in-depth analysis of this technique is provided in [16].

Deformable templates approach [17] proposes a solution to the limitations of classical template matching, by allowing deformation of the template geometry and providing relative invariance to illumination conditions. Deformable templates are successfully employed for facial feature extraction in the literature [18, 19, 20, 17, 21, 22, 23, 24, 25, 26, 27].

Active contours, which can be considered as generic deformable templates based on parametric curves, are used for extracting the contours of facial features [5].

1.2 Approach

In this thesis, deformable templates approach is exploited for developing an automatic facial feature extraction system. The system extracts location and detailed shape information of eye, eyebrow, and mouth features from static images. Deformable template geometries, imaging models, and matching algorithms are designed and developed for each of these features. The study provides the steps for developing a parametric deformable template in detail, along with important implementation issues.

The developed system is tested on randomly selected images from JAFFE, ORL and Yale Faces databases. The performance of the deformable models are assessed by comparing the parameters of automatically fitted models against the hand-fitted models. The deviations of the two are used to measure the performance of the models.

In addition, an eigenfaces based multi-scale face detection algorithm is implemented. A face model which incorporates standard facial proportions is designed and used in the face detection algorithm. This provides that the rough search regions for the facial features are readily available when a face is detected. This algorithm is tested on all the images available in the three image databases, and the results are discussed.

1.3 Road Map

Chapter 2 provides image processing background information on low-level image processing operations, and object description and recognition techniques. Histogram equalization, smoothing, edge detection, corner detection and peak-valley detection are explained as relevant low level image processing operations. Then, classical template matching, deformable template matching, and active contours(snakes) are discussed as important approaches related to object shape description and recognition.

Chapter 3 presents some of the important studies on facial feature extraction. The chapter first gives a brief literature survey on face detection. Then, it

present the studies on facial feature extraction.

Chapter 4 provides detailed information pertaining the design and development of the facial feature extraction system, which extracts the detailed shape and position information of eyes, eyebrows and lips. The chapter presents the geometries, imaging models and matching algorithms of the deformable templates, and the development of the energy functions is explained in details. In addition, the algorithm developed for providing automatic initialization is also presented.

Chapter 5 presents our testing approach and discusses the results of the tests.

Chapter 6 concludes the study by summarizing the overall study and results, and providing the limitations and further improvement opportunities.

Lastly the complete results of the tests, the images in the test sets, and the training sets are provided in the Appendices.

CHAPTER 2

Image Processing Background

This chapter presents foundations of image processing related to the following areas in the study: low-level image processing operations such as histogram equalization, smoothing, edge detection, corner detection and peak-valley detection, and object description recognition operations such as classical template matching, deformable template matching, and active contours(snakes).

2.1 Low Level Image Processing

Low level image processing is needed for extracting useful information in order to build higher level operations upon, and eliminate irrelevant data. Low level processing does not produce any information that is not available in the unprocessed or raw image. Instead, it filters out the irrelevant bulk of information. Numerous low level processing operations have been developed, each providing useful outputs for different purposes. In the following sections, The following low level image processing operations are explained:

- histogram equalization,
- smoothing,
- edge detection,

- corner detection, and
- valley/peak detection.

2.1.1 Histogram Equalization

The histogram of an image shows the distribution of pixels according to the grey levels [28, 29]. Figure 2.1 depicts the histograms of a synthetic image, and a real-life image.

The Algorithm 2.1 from [29] defines how the histogram of an image is formed.

```

Let  $I(x, y)$  be the input image
Let  $b$  be the bits used per pixel in the image
1. Create an array histogram with  $2^b$  elements
2. for all grey levels,  $i$ , do
2.1 histogram[ $i$ ]=0
3. for all pixel coordinates  $x$  and  $y$  , do
3.1 Increment histogram[ $I(x, y)$ ] by 1

```

Algorithm 2.1: Forming the histogram of an image

Histogram is not a unique property of an image, i.e. two completely different images can have the same histograms. One of the most important benefits provided by histograms is the means to perform optimal contrast improvement [29]. Histogram equalization, performs a non-linear mapping of grey levels, so that the histogram is flattened as much as possible. The non-linear mapping of histogram equalization provides that more gray levels are allocated for the gray levels with higher number of pixels in the original histogram. Figure 2.2 shows the effect of histogram equalization. The Algorithm 2.2 adapted from [29] defines how histogram equalization is performed. Instead of performing the histogram equalization globally for the whole image, one can do it for smaller patches of an image locally. This approach is used in adaptive histogram equalization technique. Although adaptive histogram equalization yields better results in many cases, it suffers from high computational needs.

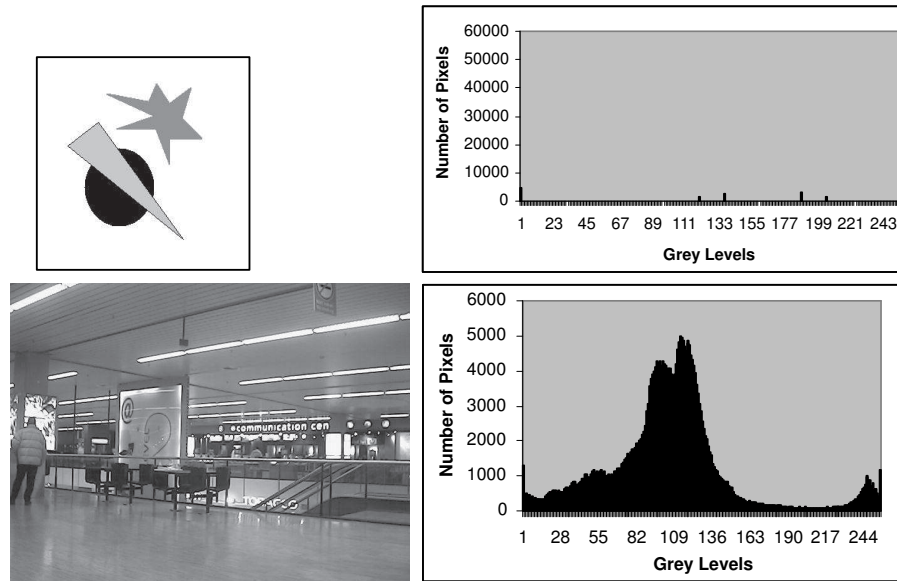


Figure 2.1: Histograms of a synthetic image and a real-life image. The synthetic image contains only a few levels of grey, while the real-life image contains all available levels of grey.

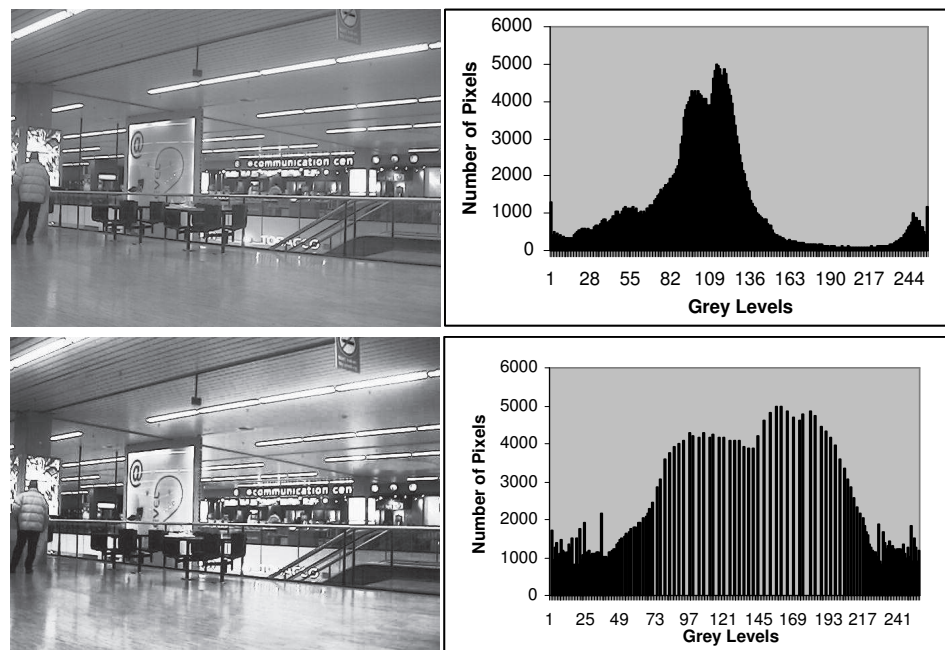


Figure 2.2: The effect of histogram equalization on the image and its histogram. The histogram of the histogram equalized image is more spread on the x axis.

Let $I(x, y)$ be the input image
 Let $g(x, y)$ be the resulting image

1. Compute the scaling factor, $\alpha = 255/\text{number of pixels}$
2. Calculate histogram using Algorithm 2.1
3. $c[0] = \alpha \times \text{histogram}[0]$
4. **for all** grey levels, i , **do**
- 4.1 $c[i] = c[i-1] + \alpha \times \text{histogram}[i]$
5. **for all** pixel coordinates x and y , **do**
- 5.1 $g(x, y) = c[I(x, y)]$

Algorithm 2.2: Histogram equalization

2.1.2 Smoothing

Smoothing is a neighborhood operation that performs low pass filtering. Smoothing is mostly used for elimination of sudden changes caused by noise in the image and it is usually implemented in two different ways: median filtering, and averaging. Median filtering relies on selection of the median¹ grey level in a neighborhood. Median filtering is a powerful scheme for smoothing, but it is computationally expensive, because it requires sorting for the neighborhood of each pixel. Figure 2.3 illustrates the power of median filtering.

Averaging is mostly preferred to median filtering because of computational considerations. This type of smoothing is equivalent to convolving the image with a kernel containing the averaging weights. The result of smoothing

¹ Median is the value in the middle in an ordered set of values.

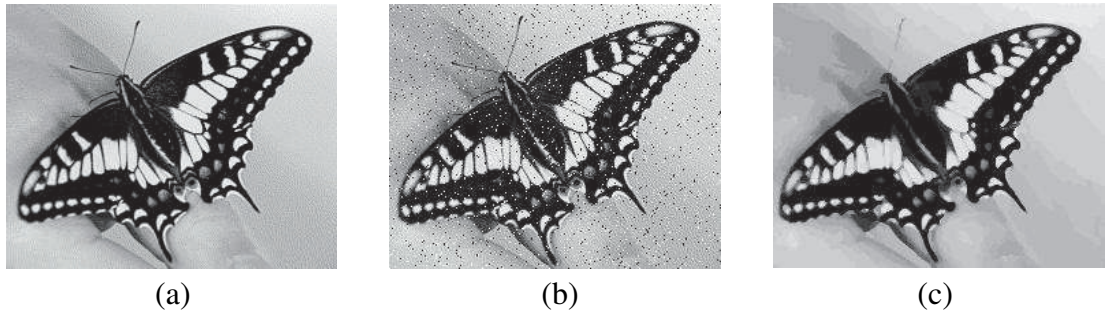


Figure 2.3: Smoothing with median filtering. a)Original image b)Noisy (Salt and pepper noise) image c)Smoothing of (b) with median filtering

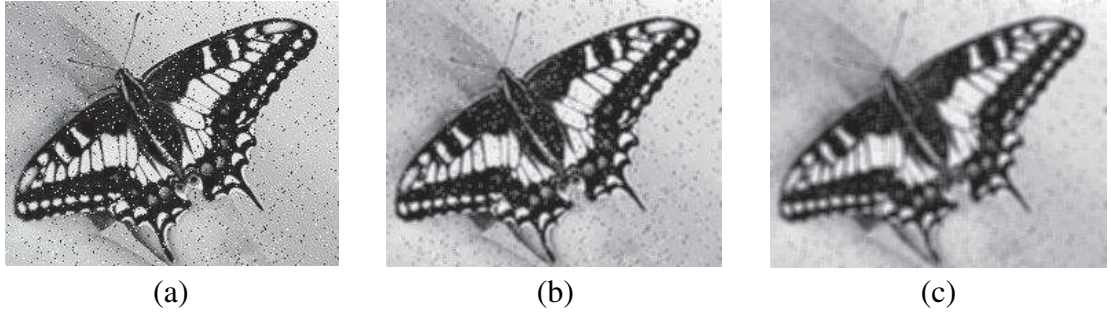


Figure 2.4: Smoothing with different averaging kernels. a)Original noisy image b)Smoothing with a 3x3 averaging filter c)Smoothing with a 5x5 averaging filter

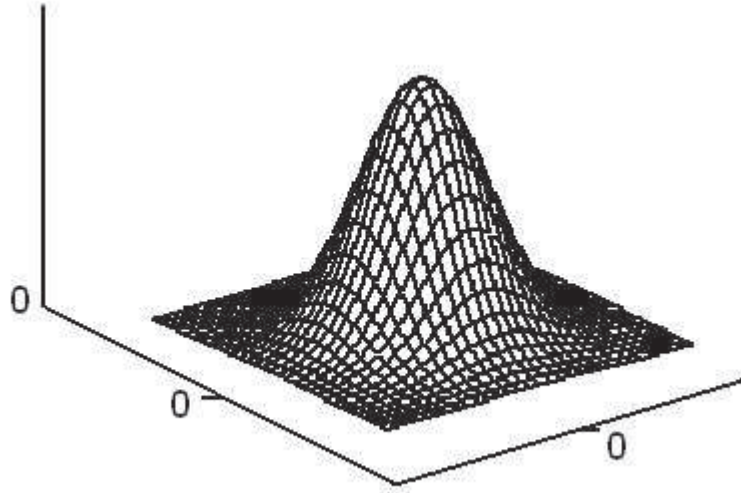


Figure 2.5: A plot of the gaussian function $g(x, y) = e^{\frac{-(x^2+y^2)}{2\sigma^2}}$

with sample smoothing kernels is given in Figure 2.4. Smoothing can be performed using weighted averaging as well. Giving a higher weight to the pixel in question is quite reasonable, for instance. Probably the most popular example for such a weighted averaging is smoothing with a Gaussian kernel. A Gaussian kernel is generated by discretization of the continuous Gaussian function $g(x, y) = e^{\frac{-(x^2+y^2)}{2\sigma^2}}$. A plot of this function is given in Figure 2.5. The following are two discretizations of Gaussian function:

$$h_1 = \frac{1}{16} \begin{bmatrix} 1 & 2 & 1 \\ 2 & 4 & 2 \\ 1 & 2 & 1 \end{bmatrix} \quad h_2 = \frac{1}{10} \begin{bmatrix} 1 & 1 & 1 \\ 1 & 2 & 1 \\ 1 & 1 & 1 \end{bmatrix} \quad (2.1)$$

Figure 2.6 shows an example of smoothing an image by using these two discretizations of Gaussian function, h_1 and h_2 .



Figure 2.6: Smoothing using gaussian kernels

2.1.3 Edge Detection

Edge detection is a very important low level operation, which is used for isolating the edges on an image. Edges are important because edges provide invaluable information that can be used for recognizing objects.

Edge detection is usually performed by detecting pixels of sudden brightness change. In calculus, change is measured by means of derivatives. In the case of edge detection, horizontal and vertical derivatives at each pixel are used for estimating the magnitude and orientation of the edge on a pixel. Different kernels have been developed for estimating the horizontal and vertical derivatives on images. Prewitt kernels and Sobel kernels used for this purpose are given below:

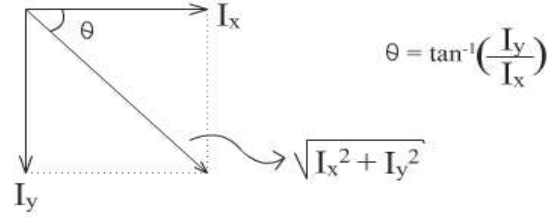


Figure 2.7: Edge magnitude orientation

$$h_x(Prewitt) = \begin{bmatrix} -1 & 0 & 1 \\ -1 & 0 & 1 \\ -1 & 0 & 1 \end{bmatrix} \quad h_y(Prewitt) = \begin{bmatrix} -1 & -1 & -1 \\ 0 & 0 & 0 \\ 1 & 1 & 1 \end{bmatrix} \quad (2.2)$$

$$h_x(Sobel) = \begin{bmatrix} -1 & 0 & 1 \\ -2 & 0 & 2 \\ -1 & 0 & 1 \end{bmatrix} \quad h_y(Sobel) = \begin{bmatrix} -1 & -2 & -1 \\ 0 & 0 & 0 \\ 1 & 2 & 1 \end{bmatrix} \quad (2.3)$$

Calculation of the magnitude and orientation from the horizontal and vertical derivatives are performed as follows:

Let $I(x,y)$ be the image function. And let $I_x(x_0, y_0)$ be the horizontal derivative and $I_y(x_0, y_0)$ is the vertical derivative of the coordinate (x_0, y_0) . Then the magnitude of the edge of (x_0, y_0) is defined as $\sqrt{I_x^2 + I_y^2}$ and the orientation is $\Theta = \tan^{-1}(\frac{I_y}{I_x})$. This can be seen more clearly in Figure 2.7.

Different approaches exist for detecting edges using horizontal and vertical derivatives. A simple algorithm is provided for detecting edges in Algorithm 2.3:

1. Calculate I_x and I_y
2. Calculate edge magnitude image as $\sqrt{I_x^2 + I_y^2}$
3. Threshold the edge magnitude image

Algorithm 2.3: Edge detection algorithm

This simple algorithm can give satisfying results for many applications. Figure 2.8 illustrates the effect of this algorithm with different thresholds, using Sobel kernel.

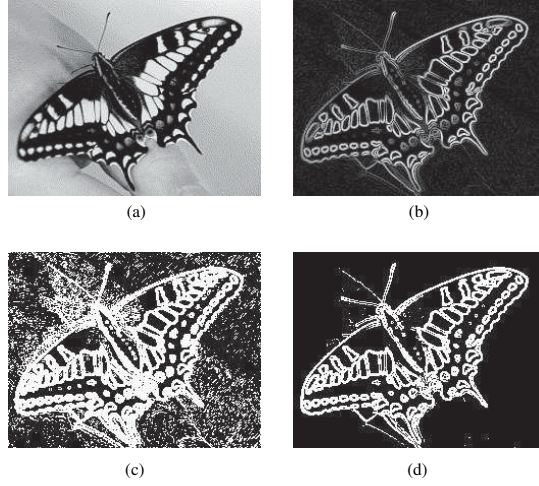


Figure 2.8: Edge detection using Sobel kernels. a)Original image, b)Edge magnitudes, c)Edge magnitudes thresholded with $T=50$, d)Edge magnitudes thresholded with $T=150$)

A more sophisticated method based on derivatives is Canny edge detection. Canny's edge detector makes use of different scales, hysteresis thresholding and non-maximal suppression. The details of Canny's edge detector can be found in [28, 29].

2.1.4 Corner Detection

Corners are the region, where two or more edges join with a high curvature. Similar to edges, corners provide valuable information for object matching. The simplest corner detector is the Moravec detector [28]. Moravec operator generates high responses for corners and sharp edges. The Moravec operator given in [28] is:

$$MO(i, j) = \frac{1}{8} \times \sum_{k=i-1}^{i+1} \sum_{l=j-1}^{j+1} |I(k, l) - I(i, j)| \quad (2.4)$$

Another corner detector based on scale-space analysis is given in [30] as:

$$I_{xx}I_y^2 - 2I_xI_yI_{xy} + I_{yy}I_x^2 \quad (2.5)$$

where the subscripts denote partial derivatives. This operator gives high response at corners.

Another well-known corner detector is Plessey Feature Point Detector [31]. Plessey feature point detector uses the following matrix:

$$M = \begin{bmatrix} \sum I_x^2 & \sum I_{xy} \\ \sum I_{xy} & \sum I_y^2 \end{bmatrix} \quad (2.6)$$

where the summations are calculated in the neighbourhood of a given pixel. If the two eigen values of the matrix M are large in the neighborhood of a certain point, then a small motion in any direction will cause an important change in grey level. This property indicates that a given pixel is a corner. Considering this, the following cornerness measure is proposed by Harris [31]:

$$R = \det M - k(\text{trace } M)^2 \quad (2.7)$$

where k is a parameter suggested to be set to 0.04 by Harris. Figure 2.9 gives the responses of Moravec, Plessey and scale-space corner detectors.

Other more sophisticated methods for corner detection are SUSAN [32] corner detector, and Kitchen-Rosenfeld [33] corner detectors.

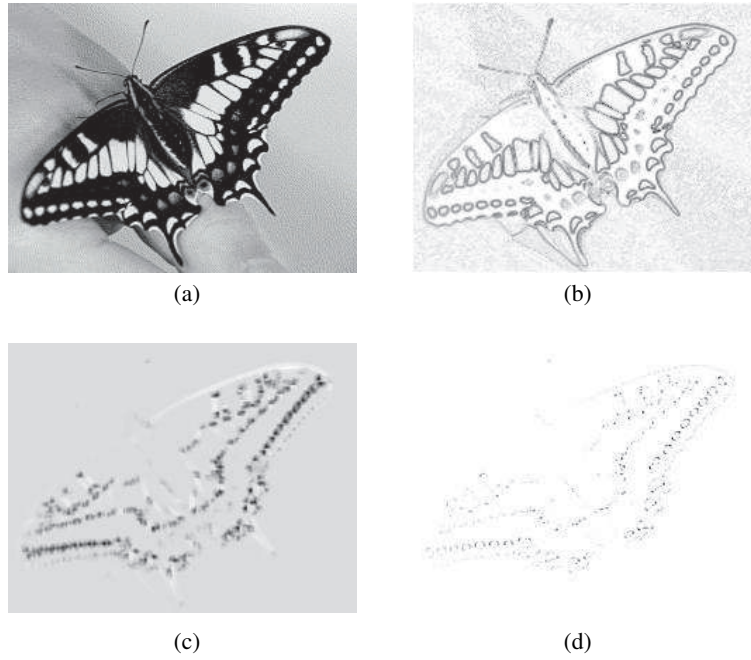


Figure 2.9: Results of different corner detection algorithms. a)The original image, b)Corners detected by Moravec operator, c)Corners detected by Plessey corner detector, d)Corners detected by Scale-space theory based corner detector. Note that (b), (c) and (d) are inverted for improving visibility.)

2.1.5 Peak Valley Detection

Peak and Valley potentials depict useful proportion of images. A peak is a pixel or a region that has a high intensity value compared to its surroundings. And conversely a valley is a pixel or a region that has a low intensity value compared to its surroundings. Figure 2.10 illustrated peak and valley potentials of an image considering a small neighborhood.

Peak and valley potentials are used for locating eyes in [34, 21]. Peak and

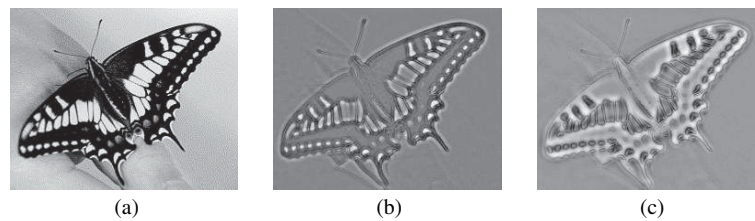


Figure 2.10: Peak and valley potentials. a)Original image, b)Peak potential, c)Valley potential

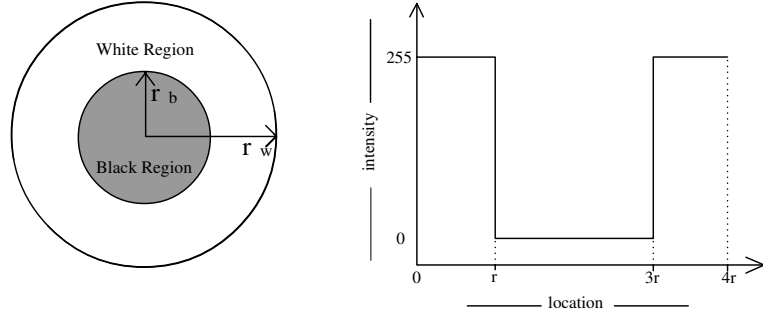


Figure 2.11: Valley template geometry and image model [18]

valley potentials are calculated using a morphological technique in [35, 36]. A more interesting approach to peak and valley computation is described in [18]. Their approach is based on deformable templates, which will be described in section 2.2.2. The valley template, the geometry and its relation to the intensity values is depicted in Figure 2.11.

The geometric model for valley is a circle of radius r_b and a surrounding of radius r_w (See Figure 2.11). The imaging model specifies that the intensities inside the valley and its surroundings conform to normal distribution with means μ_b and μ_w , and with standard deviation σ_b and σ_w . Based on this assumptions, a measure of fitness related to Fisher's linear discriminant [37] is proposed in [34] as:

$$M = \frac{\hat{\mu}_b - \hat{\mu}_w}{h + \gamma \sqrt{\tilde{n}_b \hat{\sigma}_b^2 + \tilde{n}_w \hat{\sigma}_w^2}} \quad (2.8)$$

which depicts the ratio of between classes scatter to within class scatter. In this formula:

$$\tilde{n}_b = \frac{n_b}{(n_b + n_w)} \quad \text{and} \quad \tilde{n}_w = \frac{n_w}{(n_b + n_w)} \quad (2.9)$$

where n_b and n_w are the number of pixels in the valley and its surroundings. $h = \max(I(x, y)) - \min(I(x, y))$ which is an adjustment value for preventing M to take very large values for very small σ_b and σ_w values and γ is a dimensionless constant.

μ_b and μ_w , σ_b and σ_w are the means and standard deviations of the a-trimmed

valley and surrounding pixel intensities. a-trimming provides robustness to noise by excluding the extremes from the samples. In order to calculate a-trimmed estimates, the data is first ordered and the lowest a1 percent and highest a2 percent of the data is thrown away, ie. trimmed. The template is used successfully in [34] in their eye template.

2.2 Object Description and Recognition

The notion of shape representation is first introduced in [38]. Shape representation is an essential step for object recognition. The low level image processing operations explained in section 2.1 extracts useful information from the image, but a means to combine this data for recognition is missing without the notion of shape representation. Shape representation or object description is a difficult process which may involve one or more of the followings [28, p.229] :

- boundary description (2D / 3D),
- region based descriptions,
- statistical properties, and
- feature points.

Different object descriptions and shape representation methods are used in different studies. In the following sections some of the object recognition techniques are described along with the shape representation used in the technique.

2.2.1 Classical Template Matching

Classical template matching uses correlation for finding likeness to a fixed size template. Correlation is usually implemented using convolution. The template (the convolution kernel) gives higher responses in the regions where the feature being searched appears.

Classical Template Matching is an easy and fast approach, and it performs very well in certain problems, but it has the following major limitations [18]:

Templates have a fixed size. Objects appear in different sizes in reality. In addition, the same object might appear in different sizes because of the proximity to the imaging device (objects far away appear smaller, and objects closer to the imaging device appear larger).

Templates have a rigid shape. In reality objects does not have ideal, fixed shapes. Usually impurities and variations exist for the same kind of objects. Even the same object can appear in different shapes because of 2D projection to the imaging surface (rotated circular objects may appear as elliptical objects).

Lightning conditions are not considered. Classical templates does not take into account the differences in lightning conditions enough. However, different lightning conditions can dramatically affect the result of correlation calculation used for template matching.

2.2.2 Deformable Template Matching

Deformable templates propose solution to the limitations of classical template matching, by allowing deformation of the template geometry and providing relative invariance to lightening condition.

A deformable template consists of three basic elements [34]:

- 1. Geometrical Model.** A parametric geometrical model defines the geometry for the template and introduces constraints on the deformation of the geometry. This model includes the prior probabilities for the parameters. These prior probabilities correspond to a geometric measure of fitness. Considering an eye template, for instance, the prior probabilities should yield higher values for a normal eye, and lower probabilities for an abnormal eye, and even less values for objects that are not eyes.
- 2. Imaging Model.** The imaging model specifies how a deformable template of specific geometry is related to specific intensity values (or colors) in a

given image. This corresponds to an imaging measure of fitness. Considering an eye template again, for instance, the imaging model should state that iris would be much darker than the whites of the eye, and it should also state that the boundaries of iris and eye correspond to high edge values in the image.

3. Matching Algorithm. An algorithm using the geometrical and imaging measures of fitness to match the template to the image. The algorithm might define how the template will be initialized, which optimization algorithm will be used for energy minimization (gradient descent, downhill simplex, genetic algorithms, etc), which states will be involved during the minimization, and so on.

A probabilistic formalization of the definition of deformable templates is also provided in [34]. Suppose $T(\mathbf{g})$ specifies the geometrical model of the template with prior probability $P(T(\mathbf{g}))$ on the template parameters denoted as \mathbf{g} (*note that \mathbf{g} is a vector*). The imaging model $P(I|T(\mathbf{g}))$ gives the probability of producing an image I from a template $T(\mathbf{g})$. Thus $P(I|T(\mathbf{g}))P(T(\mathbf{g}))$ gives the probability of producing a feature (which is to be detected with the template) from a template $T(\mathbf{g})$.

Based on these probabilities, a measure of fitness, which can be expressed as probability of detection of a template, can be defined by using Bayes' theorem. The probability of detection of a template is $P(T(\mathbf{g})|I)$. We can calculate this probability as follows :

$$P(T(\mathbf{g})|I) = \frac{P(I|T(\mathbf{g}))P(T(\mathbf{g}))}{P(I)} \quad (2.10)$$

Equation 2.10 gives the probability of detection of a template, $P(T(\mathbf{g})|I)$, in terms of the imaging model and the prior probabilities. By maximizing this probability with respect to the template parameters (\mathbf{g}) candidate matches for the template can be found. This probability can also be used as a confidence measure for the matches.

In practice, usually energy minimization approach is employed instead of probabilistic approaches [34, 21]. Energy minimization approach involves developing energy functions which will favor a normal object geometry conforming to the imaging model when minimized. Thus, the total energy of the template is defined as

$$E(\mathbf{g}) = E_{prior}(\mathbf{g}) + E_{data}(\mathbf{g}), \quad (2.11)$$

where E_{prior} dictates the geometrical model or the geometrical constraints and E_{data} dictates the imaging model. In [18] the connection between the energy minimization approach and the probabilistic approach is presented by means of Gibbs distribution [39]. Gibbs distribution is defined as $P(\mathbf{g}) = e^{-\beta E(\mathbf{g})}/Z$, where β and Z are constants. In this representation, maximizing $P(\mathbf{g})$ is equivalent to minimizing $E(\mathbf{g})$.

Deformable templates have been successfully applied to facial feature extraction as explained in Chapter 3.

2.2.3 Active Contours (Snakes)

Active contours or snakes are proposed in [40]. An active contour is defined as an energy minimizing spline. The energy function of a snake involves terms to attract the snake to the desired features on an image. Snakes are usually employed for detecting object boundaries especially in occluded or noisy images. Snakes deform continuously for minimizing their energy function, so they can be considered as a special case of a general technique for matching a deformable mode to an image [28].

Snake energy function is composed of the following terms: [41, 42, 43]

1. **Internal Forces.** Internal forces provide the smoothness of the snake by introducing tension and stiffness terms.
2. **External Forces.** External forces come from high level sources such as human operators or automatic initialization procedures.

3. Image Forces. Image intensity and other potentials derived from image intensity are used to drive the model towards salient features such as light and dark regions, edges, and terminations.

Snake is represented as a parametrically defined function as $\mathbf{v}(s) = [x(s), y(s)]$, where $x(s)$, $y(s)$ are x, y coordinates and $s \in [0, 1]$. The energy of the snake can be written as

$$\begin{aligned} E_{snake} &= \int_0^1 E_{snake}(\mathbf{v}(s)) ds \\ &= \int_0^1 \{[E_{intern}(\mathbf{v}(s))] + [E_{extern}(\mathbf{v}(s))] + [E_{image}(\mathbf{v}(s))]\} ds \end{aligned} \quad (2.12)$$

where E_{intern} represents the internal energy of the spline due to bending, E_{extern} external constraint forces, and E_{image} denotes image forces. Usually, snakes are implemented using spline curves, for ensuring the smoothness of the curve effortlessly [9, 28].

2.2.3.1 Internal Energy

The internal energy of a snake element is defined as follows:

$$E_{intern} = \underbrace{\alpha(s)|\mathbf{v}_s(s)|^2}_{\text{Tension}} + \underbrace{\beta(s)|\mathbf{v}_{ss}(s)|^2}_{\text{Stiffness}} \quad (2.13)$$

Equation 2.13 contains a first derivative term controlled by $\alpha(s)$, and a second derivative term controlled by $\beta(s)$. The first derivative term introduces tension, resulting in the contraction of the snake like an elastic band. The second derivative introduces a force which makes the snake resist bending (stiffness). Another description of Equation 2.13 is as follows: the snake, by construction, tries to zero out (or at least keep constant) its velocity and acceleration with respect to its parameter.

In the absence of any other constraints, a snake collapses to a point in order to minimize E_{intern} . Adjusting $\alpha(s)$ and $\beta(s)$ allows controlling the relative importance of tension and stiffness terms. For example, a corner can be allowed by setting $\beta(s) = 0$ in one part of the snake. However, in most applications $\alpha(s)$ and $\beta(s)$ are selected as uniform weights (simply α and β).

2.2.3.2 External Energy

External energy terms reflect attraction and repulsion constraints coming from human operators or automatic initialization procedures. Attraction and repulsion forces drive snakes to or from specified features. In order to introduce an attractive force between a snake element and a spatial point \mathbf{x} in an image, for instance, the following energy term can be used.

$$E_{extern}(\mathbf{v}(s)) = k|\mathbf{x} - \mathbf{v}(s)|^2 \quad (2.14)$$

This energy is minimum when a $\mathbf{v} = \mathbf{x}$, thus it is an attractive force. Energy terms for repulsive forces can be introduced similarly.

2.2.3.3 Image Energy Functionals

The potential energy P is generated by processing an image $I(x, y)$, and it produces a force that can be employed to drive snakes towards features of interest. The potential energy can be constructed by considering application specific requirements. However, in general, lines, edges and terminations are used in order to construct the image potential energy.

$$P = E_{image} = w_{line}E_{line} + w_{edge}E_{edge} + w_{term}E_{term} \quad (2.15)$$

The minimization of the potential energy P given in Equation 2.15 can be performed by gradient descent.

2.2.3.4 Snake Minimization

Previous paragraphs described the energy function of a snake, which needs to be minimized to find the optimum configuration of the snake which reveals the salient features in the image. Different approaches were proposed for this minimization problem. Originally [40] proposed a semi-implicit method, which considers explicit use of forces in addition to the variational calculus based minimization method. A more efficient method is proposed in [44], which makes use of a greedy algorithm. Another method used for snake minimization is

dynamic programming, which performs the minimization as a straightforward search instead of by means of derivatives as used in the variational approach.

The methods employed for minimizing the snake energy usually suffer from oscillations. A number of methods have been proposed for eliminating the oscillation, during the minimization. [45] proposed a method which starts minimizing in highly blurred images and then gradually reduces the image blurring making the snake fit more accurately to the salient features. Gradient vector flow based snakes provide a wider range of attraction to the features, which eliminates the issues related the initialization of the snakes comparably [42, 43].

CHAPTER 3

Previous Work on Facial Feature Extraction

Facial feature extraction has long been a popular area of research, because it is a prerequisite for face recognition and facial expression analysis, which are research areas of longing interest on their own [46, 3, 47, 48].

This chapter will first present a brief literature survey on Face Detection. Then, some of the important studies on facial feature extraction will be described.

3.1 Face Detection

The first problem to be solved by a system that performs automatic facial feature extraction is detection of a face or faces in an image or image sequence. In most of the works in automatic facial expression analysis, controlled conditions are assumed for the image or image sequence that will be used to obtain face images.

Human perceptual system effortlessly detects faces in uncontrolled conditions. Moreover, human observers can detect not only a single face in a scene but multiple faces having different alignments, scales, lighting conditions at first sight of a scene, even if they are partially occluded by other objects. We are not only able to detect faces that are partially occluded, but our perceptual system can also guess the occluded part as well. This is a very difficult problem for a computer vision system. Even the most sophisticated computer vision systems developed for face detection purposes are far from reaching the

performance of human vision system.

In automated face detection systems, usually, the presence of one face in the image is known beforehand, and the facial image is assumed to occur in frontal view. In addition, the head alignment is assumed to be nearly vertical, i.e. only minimal rotation of the head is tolerated. In spite of these controlled conditions, detection of the exact location of a face is not an easy problem, because faces can occur in different scales, part of a face can be occluded (by a hand), etc.

In this section some of the well-established face detection methods will be explained. An exhaustive survey on face detection techniques is given in [11].

3.1.1 Eigenfaces

Eigenfaces approach [10] is a PCA (Principle Component Analysis) based approach for detecting faces. In this approach, faces are represented as points in a space called eigenspace. Face detection is performed by computing the distance of image windows to the space of faces. Assuming raw images as points in a high dimensional space (for an $N \times M$ image, the dimension of such a space is $N \times M$) is impractical for two reasons. Firstly, working in very high dimensional spaces is computationally too expensive, and secondly, raw images contain statistically irrelevant data which degrades the performance of the system. Principal component analysis reduces the dimensionality of a feature space by restricting the attention to those directions along which the scatter is greatest [37]. Thus, principal component analysis is used for projecting the raw face images onto the eigenspace of a representative set of normalized face images, for eliminating redundant and irrelevant information. Figure 3.1 depicts the standard eigenfaces presented in the eigenfaces demo web page of the MIT Media Lab [49]. Eigenfaces approach is used for both detection and recognition of faces. For the recognition part, the Euclidian distances of a given image to each of the images in the training set is computed in the eigenspace and recognition is performed by choosing the shortest distance image in the training set. For the detection of faces, the distance to the space of faces (eigenspace) is used. Distance to

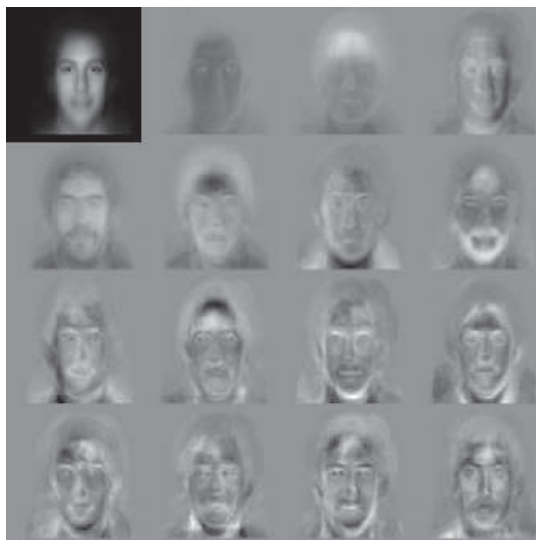


Figure 3.1: Standard eigenfaces [49]

the space of faces is the reconstruction error, which occurs when an image is projected onto the face space and then projected back to the original space. If the distance of a given image from the eigenspace is less than a predetermined threshold value then the image is accepted as a face image. This topic will be elaborated later in Chapter 4.

3.1.2 Neural Networks

Neural networks, especially multi layer perceptron, have been used by many researchers for face detection and face recognition, and promising results were reported [50]. The first advanced neural approach which performed reasonably on a large and difficult dataset was Rowley et al. [11].

The system described in [51] incorporates prior knowledge of face in a retinally connected neural network shown in Figure 3.2. The system works in two stages: filtering, and arbitrating. Filtering is performed using neural networks at each location in the image at different scales for the occurrence of a face. Then, arbitrating is performed for merging and eliminating the overlapping detections.

The first component of the system is a neural-network based filter that receives a 20x20 pixel region of the image, and signals the existence or non-existence of a face in the region by outputting a number between -1 and 1. The

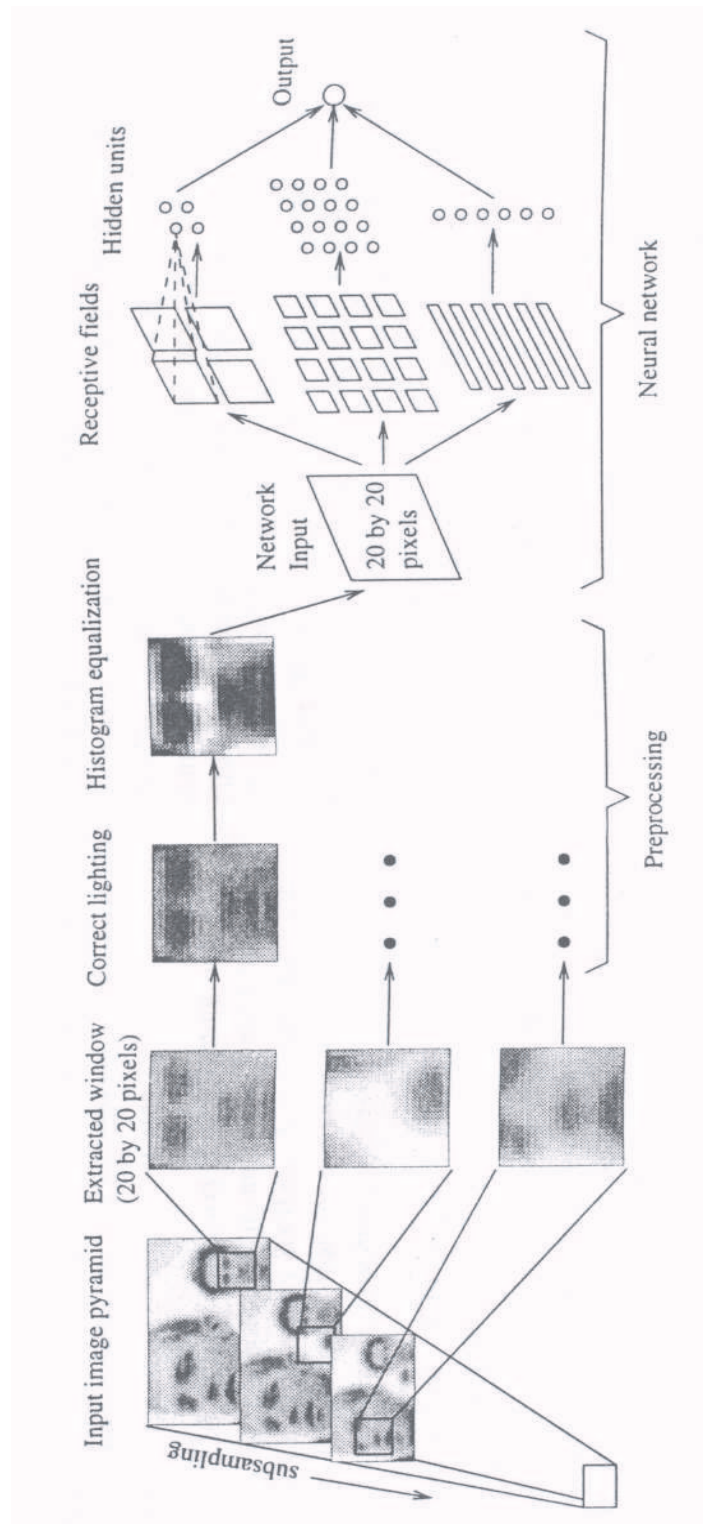


Figure 3.2: Neural network for face detection [51]

system aims multi scale face detection by repeatedly sub-sampling the input image by a factor of 1.2, and re-applying the filter at each scale.

The filtering algorithm performs lightning correction and histogram equalization before testing the existence of a face using a neural network. The neural network has retinal connections to its input layer, and the hidden layer contains three different types of hidden units which are chosen to allow the hidden units to represent features that might be important for face detection.

As a last step the system merges overlapping detections, and eliminates some of the false detections by employing a simple heuristic.

Their system was trained using a very large set of face images at different scales and rotations. They performed tests on a variety of images from newspapers, web, and TV images, and they reported up to % 92.7 face detection rates.

3.2 Facial Feature Extraction

In this section previous research on facial feature extraction is presented in the following categories:

- Eigenfeatures,
- Gabor Jets,
- Template Matching,
- Deformable Templates,
- Snakes, and
- Integral Projection.

3.2.1 Eigenfeatures

Eigenfeatures approach is similar in nature to the eigenfaces approach described in Section 3.1.1. The main difference is that, PCA is performed for each of the

features to be detected, instead of for the whole face. After applying PCA to a representative training set of images; eigeneyes, eigenmouth, eigennose etc. are calculated. Individual eigenfeature responses and combined responses of eigenfeatures are used in [2] for face recognition. The study reports that eigenfeatures approach yields superior results.

Eigenlips is employed in [12] for tracking lips mainly for multi-modal speech and speaker recognition purposes. Instead of using lip intensity images directly, their approach concentrated on estimating the outer lip contour from the lip intensity image. They first developed an eigenlip classifier using PCA on 105 images (3 different poses of 35 different speakers) for locating the mouth region. Then, they manually labeled the outer lip contours on these images and applied PCA again, this time trying to reduce the dimensionality of the lip contour (eigencontour). They then developed a linear regression based method for estimating the outer lip contour when lip intensities are given, using eigenlips and eigencontours. The resulting lip contour estimator is reported to be estimate the rough outer corner of the lips reasonably well.

Eigeneyes is used in [1] as an alternative to eigenfaces for face recognition. The study is motivated with the idea that the regions around the eyes are enough to recognize peoples. The system developed with this study is superior to the classical eigenfaces approach with respect to computational needs, because the eigeneyes approach uses much smaller vectors than the eigenfaces approach. The reported results demonstrated that eigeneyes are comparable to eigenfaces face recognition systems, and most of the time eigeneyes performed better than eigenfaces.

3.2.2 Gabor Jets

In [13], elastic bunch graphs (face bunch graphs) are employed for face recognition. In their study, the nodes of the graph corresponds to fiducial points, and at each node Gabor wavelet responses at different scales and orientations are stored. Gabor wavelets are biologically motivated convolution kernels which

has the shape of plane waves restricted by a Gaussian envelop function. Gabor wavelets of different orientations and scales respond differently to the features having different orientations and scales. The research employs this property of Gabor wavelets for collecting scale and orientation invariant metrics for matching. A jet is a set of Gabor wavelet coefficients at different orientations and scales. In their study, a jet contains 40 coefficients corresponding to 5 scales and 8 orientations. Figure 3.3 illustrates the elastic bunch graph approach.

In their study, a small number of representative training images are used for constructing a model face bunch graph. Then, fiducial points are located at input images using jet comparison and matching algorithms for face recognition purposes.

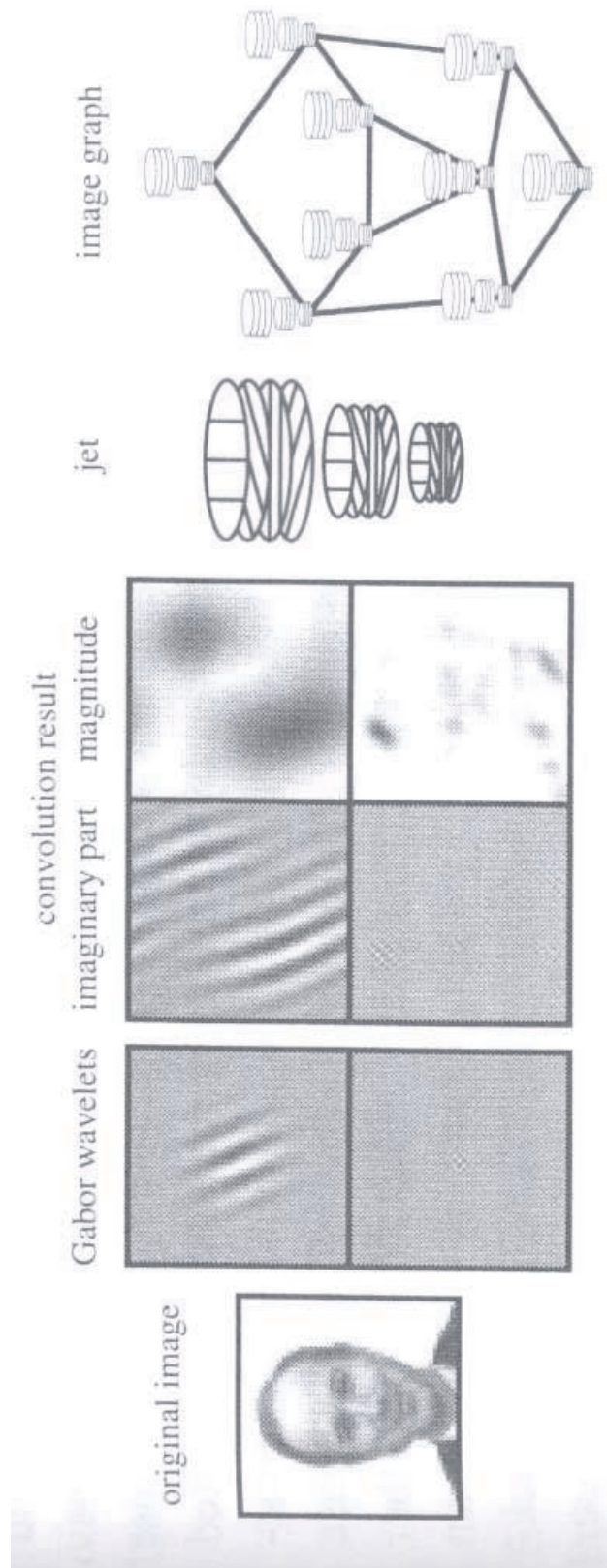


Figure 3.3: The graph representation of a face is based on the Gabor wavelets transform, a convolution with a set of wavelet kernels[13].

3.2.3 Classical Template Matching

Template matching is one of the basic approaches used in feature detection. Simple template matching involves convolution of an image with a mask that corresponds to the feature to be detected. High values of the convolved image indicate good matches between the template and the image. Good matches are interpreted as detected features.

Classical template matching performs reasonably only in controlled lightening conditions, and when the size of the features does not vary. Although these assumptions are unrealistic, in specific applications they can be satisfied. One such case is reported in [14]. They developed a system for facial expression synthesis from single neutral (showing no expression) face images. Their system employs eye, eyebrow and mouth templates for extracting facial features. In their study binary templates shown in Figure 3.4 are used and the facial feature extraction algorithm is initialized manually by setting the position of the tip of the nose. After manual initialization, the algorithm tries to determine the region of eyes by using the *Eyes Template*, then it uses the single eye template for finding the locations of individual eyes, and lastly eyebrow template is used for finding eyebrows. Mouth template is applied to the region below the nose tip to find mouth.

In [15] an application of template matching for locating mouth and eye corners is presented. Their study does not use templates for the whole eye or mouth, instead it uses smaller templates for detecting corners of these features. After detecting corner locations, geometrical verification conditions are considered for eliminating irrelevant matches. The geometrical conditions used for verification are :

1. The eye orientations, and mouth orientation (the lines connecting the left and right corners for each feature) is approximately parallel to the line connecting the center of the eyes,
2. The length of the left and right eyes are equal,

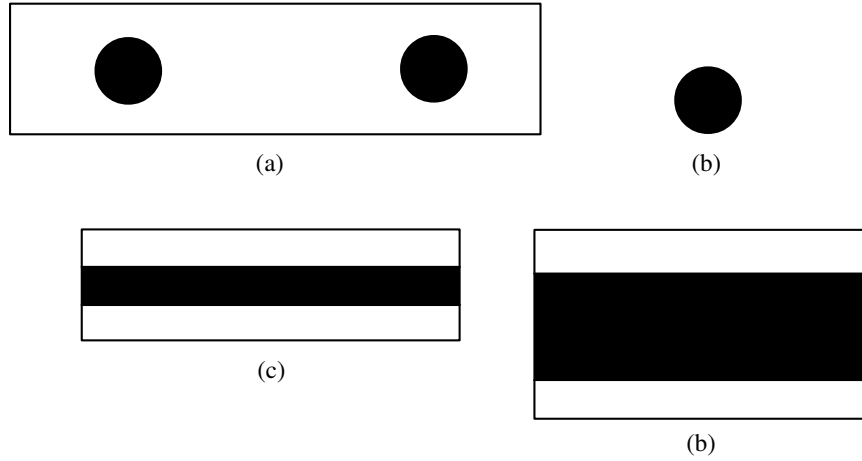


Figure 3.4: Templates for matching different facial regions. a)The eyes template for locating eyes, b)The single eye template for locating left(right) eye, c)The eyebrow template for locating left(right) eyebrow, d)The mouth template for locating mouth. [14]

3. The calculated center of the mouth is equally distant to mouth corners.

The system is tested on *Miss America* and *Claire* video sequences and performed up to %91 correct tracking rate for mouth corners and up to %74 for eye corners.

3.2.4 Deformable Templates

In this section, some of the important studies on facial feature extraction by using deformable templates are explained.

The pioneering study on facial feature detection using deformable templates was presented in [17] and [18]. Most of the studies afterwards use variations of the templates developed in these studies [24, 25, 26, 27]. In this section we will first provide an in-depth review of the eye templates presented in [18]. Then some of the other important contributions will also be reviewed.

3.2.4.1 An Eye Deformable Template

Peak and valley potentials (see section 2.1.5) are used in [17] in the design of their eye template. The geometry of the eye template is shown in Figure 3.5, in which the parabolas specified by the template correspond to the following

parametric curves:

$x(\alpha) = x_t + e_1 + a - (\frac{a}{b^2})^2 e_2$ for the upper parabola and

$x(\alpha) = x_t + e_1 - c - (\frac{c}{b^2})^2 e_2$ for the lower parabola, where e_1 and e_2 are directions defined by Θ , namely $e_1 = (\cos\Theta, \sin\Theta)$ and $e_2 = (-\sin\Theta, \cos\Theta)$.

The positions of the centers of the peaks are $x_t + p_1 e_1$ and $x_t + p_2 e_1$, where p_2 is a negative number.

In order to specify the prior probabilities an energy term, E_{prior} , is defined. This energy term imposes relations on the template parameters, such as the center of the eye is close to the center of the iris. The energy term used for specifying prior probabilities is given as follows:

$$E_{prior} = \frac{k_1}{2} \|x_t - x_c\|^2 + \frac{k_2}{2} (p_1 - p_2 - (r + b))^2 + \frac{k_3}{2} (b - 2r)^2 + k_4 (2c - a)^2 + (b - 2a)^2 \quad (3.1)$$

where k_1, k_2, k_3 , and k_4 are the coefficients used to combine the energy terms.

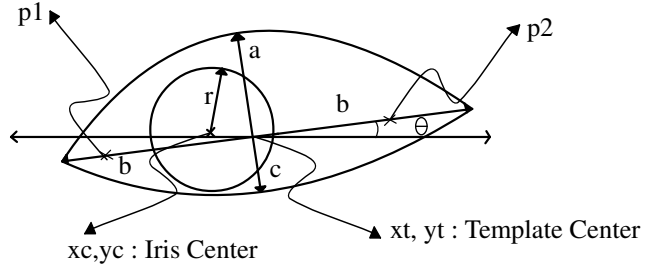


Figure 3.5: Eye template. The geometry of the eye template is specified by eleven parameters $g = (x_t, x_c, r, a, b, c, \Theta, p_1, p_2)$. x_t : The center of the whole template (x_t, y_t) ; x_c : The center of the iris, modelled as a circle (x_c, y_c) ; r : The radius of the iris; a, b, c : The parameters of the parabolas which bound the eye template; Θ : The orientation of the template; p_1 and p_2 : The parameters used to locate the position of the centers of the peaks in the left and right side of the iris [17].

The imaging model of the template uses the following assumptions:

- The iris corresponds to a valley in the image intensity,
- The whites of the eye correspond to peaks in the image intensity,
- The boundaries of the eye and the iris correspond to edges in the image,

- The iris is a dark (low intensity values) region in the image, and
- The whites of the eye are bright (high intensity values) regions in the image

Thus in order to utilize this imaging model, peak, valley and edges of an image are extracted. In [17], peak, valley and edges are computed by using morphological filters and then smoothed by convolving with a Gaussian filter, given the edge, valley and peak fields $\Psi_e(x, y)$, $\Psi_v(x, y)$ and $\Psi_p(x, y)$

The algorithm used for matching the template to the image defines an energy function, E , which makes use of the geometrical model and the imaging model. The energy function is minimized by changing the parameters of the template using gradient descent algorithm.

E has contributions from the valley (the iris), peaks (the whites of the eyes) and edges (boundaries of the iris and the eyes).

$$E = E_v + E_p + E_e + E_I + E_{prior} + E_{inertia} , \quad (3.2)$$

where

E_v : The part of the energy function which considers valleys,

E_p : The part of the energy function which considers peaks,

E_e : The part of the energy function which considers edges,

E_I : The part of the energy function which considers intensities,

E_{prior} : The part of the energy function which considers the prior probabilities as defined before, and

$E_{inertia}$: The part of the energy function which is used for fixing the iris parameters after the first epochs.

The detailed formula of these energy functions are given below [17]:

$$E_v = -\frac{C_1}{|R_b|} \int_{R_b} \Psi_v(x) dA, \quad (3.3)$$

$$E_p = -C_6 |\Psi_p(x_t + p_1 e_1) + \Psi_p(x_t + p_2 e_1)|, \quad (3.4)$$

$$E_e = -\frac{c_2}{|\partial R_b|} \int_{\partial R_b} \Psi_e(x) ds - \frac{c_3}{|\partial R_w|} \int_{\partial R_w} \Psi_e(x) ds \quad (3.5)$$

$$E_I = -\frac{c_4}{|R_b|} \int_{R_b} I(x) dA - \frac{c_5}{|R_w|} \int_{R_w} I(x) ds \quad (3.6)$$

$$E_{inertia} = -\frac{k_5}{2} (r - r_{old})^2 + \frac{k_6}{2} \|x_t^{old} - x_t\|^2 \quad (3.7)$$

and E_{prior} is defined in Equation 3.1 before while explaining the prior probabilities .

Some of the terms used in the formula above are explained below:

R_b : The region corresponding to the iris,

R_w : The region corresponding to the whites of the eyes,

∂R_b : The region corresponding to the iris boundary,

∂R_w : The region corresponding to the eye boundary,

$|R_b|$: The area of the iris,

$|R_w|$: The area of the whites of the eye,

$|\partial R_b|$: The length of the iris boundary,

$|\partial R_w|$: The length of the eye boundary, and

c_i and k_i are coefficients.

The algorithm tries to minimize the energy function, E , by using a search strategy based on steepest descent. It first locates the iris by using the valley potentials, the peaks are used to orient the template and then the intensity values are used for fine tuning, etc. The updating of the parameters $g = (x_t, x_c, r, a, b, c, , p_1, p_2)$ is done by steepest descent in each epoch, that is:

$$\frac{d_g}{dt} = -\nabla E = -\left(\frac{\partial E}{\partial x_t}, \frac{\partial E}{\partial x_c}, \frac{\partial E}{\partial r}, \frac{\partial E}{\partial a}, \frac{\partial E}{\partial b}, \frac{\partial E}{\partial c}, \frac{\partial E}{\partial \Theta}, \frac{\partial E}{\partial p_1}, \frac{\partial E}{\partial p_2}\right) \quad (3.8)$$

In the first epoch c_1 is the only non-zero coefficient. This means only the valley fields are considered. The center of the eye template, x_t , is set equal to the center of the iris, x_c . So in the first epoch the iris drags the template towards

the eye. In the next epoch the coefficients c_2 and c_4 are switched on to better localize the iris. After this stage the position and size of the iris is considered fixed and k_5 and k_6 are switched on, in order to fix these. This assures that the parameter values of iris can affect the remainder of the template, but the other parameters cannot affect the iris.

3.2.4.2 A More Robust Eye Deformable Template

A more robust deformable template is proposed in [18] for extracting eyes, which considers a number of aspects where it is possible to make improvements on the template presented in [17]. These aspects are as follows:

1. Instead of detecting the valley and peak fields by using morphological filters, it would be better to use deformable templates for this purpose,
2. Instead of using a fixed scale for detecting peaks and valleys, an automated approach should be employed.
3. The deformable templates should be made more invariant to occlusion and degradations caused by noise. This can be achieved by using a more sophisticated measure of fitness.
4. The initialization of the templates should be automated, which was done manually in the template explained previously.

In order to satisfy these aspects, Algorithm 3.1 is provided in [18]:

3.2.4.3 Deformable Templates using a spring model

Deformable templates for extracting eye and mouth features are proposed in [21]. One of the distinctive properties of these templates is that, the geometrical model of these templates are defined on a spring model which tries to avoid deformations on an initially set template. The simplified geometry of mouth and eye templates used in [21] are given Figure 3.6 and Figure 3.7.

1. Valley template runs over the whole image with different scales. The iris candidates who are very close to each other are eliminated and the iris candidates above the threshold are selected as potential iris candidates.
2. The same process is repeated for peak template
3. The possible eye candidates are determined by selecting linear white/black/white regions
4. The eye template runs over all possible eye candidates
5. The eye is selected from the candidates which gives higher results.

Algorithm 3.1: Eye Feature Localizing using the more robust template. The valley and peaks templates referred in the algorithm are explained in section 2.1.5.

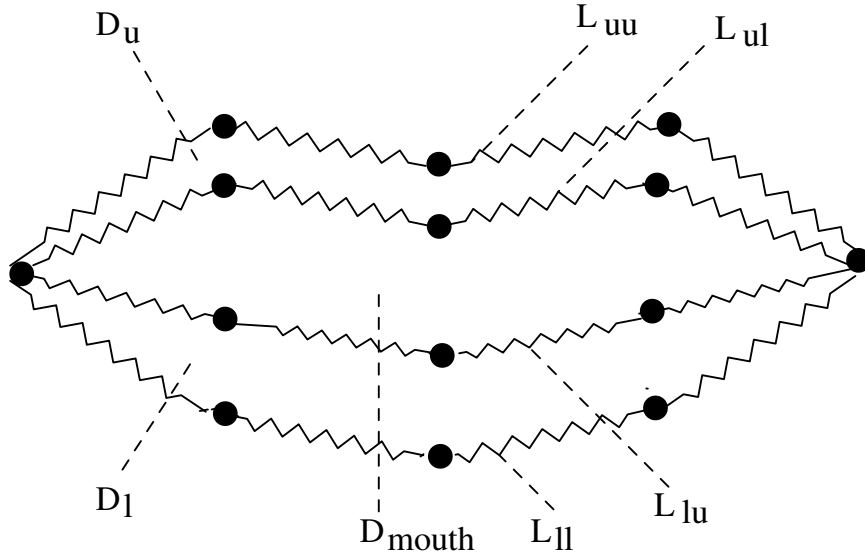


Figure 3.6: Mouth Template. L_{uu} : upper boundary of upper lip, L_{ul} : lower boundary of upper lip, L_{lu} : upper boundary of lower lip, L_{ll} : lower boundary of lower lip, D_u : upper lip region, D_l : lower lip region, D_{mouth} : the regions between the two lips

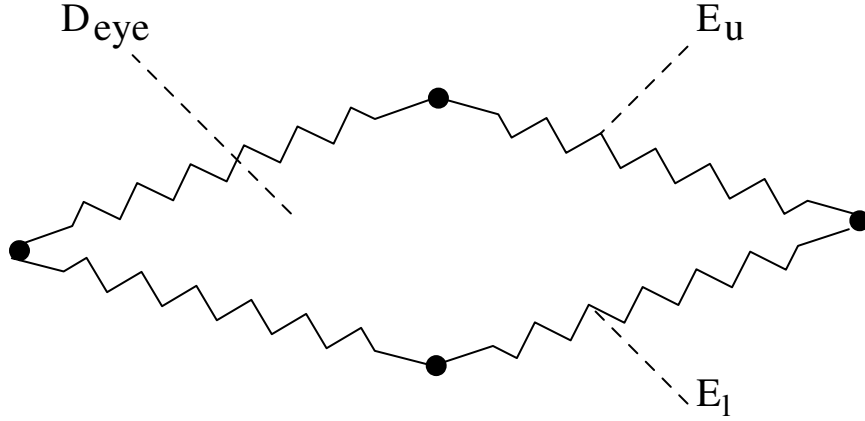


Figure 3.7: Eye template. E_u : upper boundary of the eye model, E_l :lower boundary of the eye model, D_{eye} :inner region of the eye

As seen in Figure 3.6 and Figure 3.7, a deformable template framework is developed in [21] for representing the geometric constraints by using a spring model in order to allow minimum deformation from the initial geometry. The elastic energy of the deformable template $\tau(T)$ is defined as:

$$E_{elastic}(T, \tau) = \sum_{i \in \tau(T)} k_i (l_i - l'_i)^2 \quad (3.9)$$

where l_i and l'_i are the lengths of natural and current length and k_i is the stiffness.

3.2.4.4 Multi-state templates for mouth extraction

There are some problems with the approach of using deformable templates in estimating mouth features [19]. One of the problems is about the complexity of the cost functions to be minimized for finding a good match. The other problem is that the selection of the open or close mouth template is done manually.

In order to solve these problems, [19] introduced, a deformable template-based algorithm for estimating mouth feature automatically in a head-and-shoulder videophone sequence. The features of the mouth are then described by a mouth-closed and a mouth-open deformable template as seen in Figure 3.8. The mouth features are represented by the corners points of the mouth and lip outline parameters.

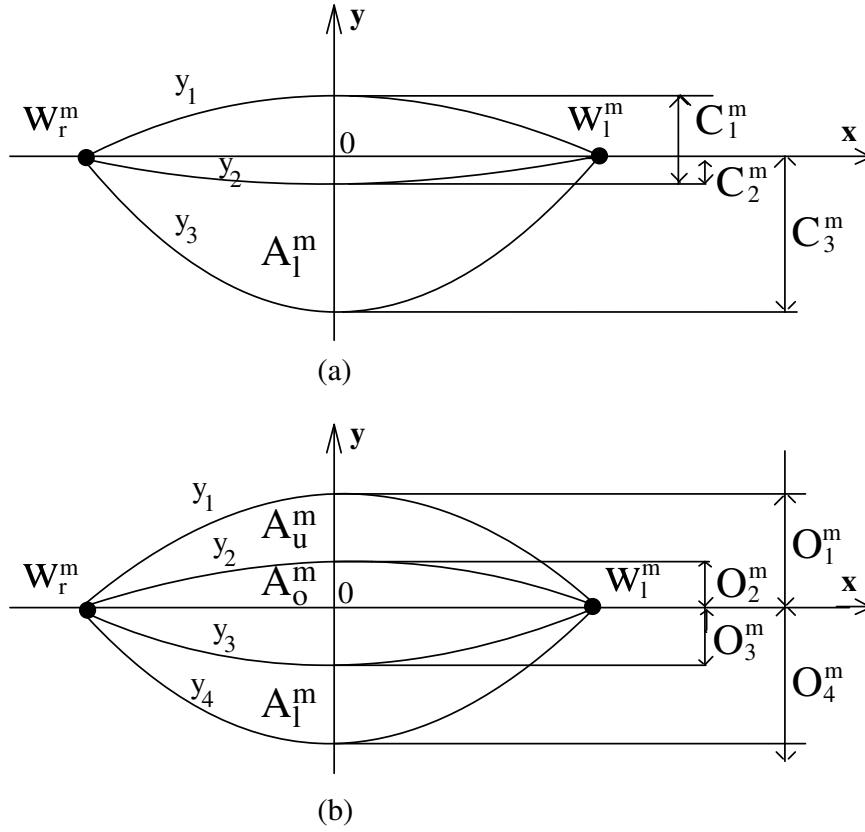


Figure 3.8: The parameterized Deformable Templates for a)Mouth-closed deformable template, b)Mouth-open deformable template. W_l^m and W_r^m are the mouth corner points. $C_i^m (i = 1, 2, 3)$ and $O_i^m (i = 1, 2, 3, 4)$ are the lip outline parameters. [19]

Lip outline parameters include the information about the opening of the mouth and the thickness of the lips. Estimation of the lip outline parameters includes four steps:

1. The estimation of the candidates for the lip outline parameters
2. The determination of whether the mouth is open or close
3. The deformable template matching
4. The verification of the estimates for lip outline parameters

Figure 3.9 depicts the candidates for the lip outline parameters and determination of whether the mouth is closed or open.

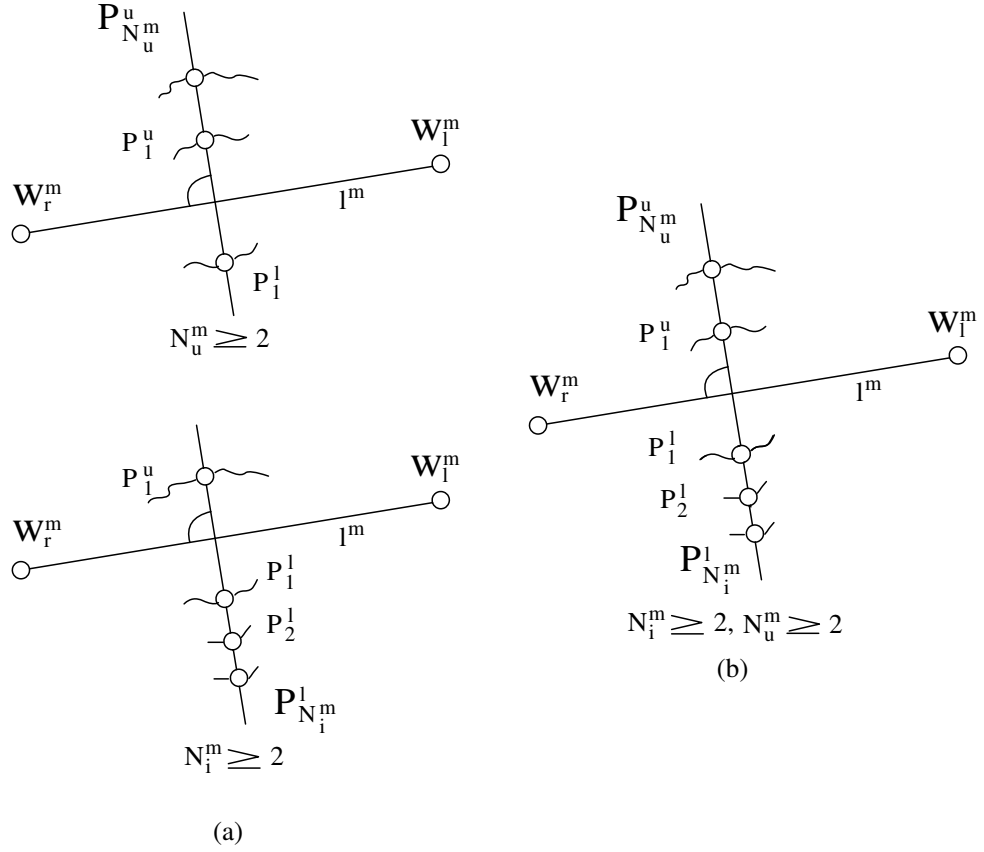


Figure 3.9: Lip outline parameters [19]

After the determination of the state of the mouth, deformable template matching was used to select the upper and lower lip outline parameters. The study introduced a simplified cost functions for both mouth-open and mouth-closed templates.

The Mouth-open function is given as follows:

$$\int_0^m k_1 f_1 + k_2 f_2 + k_3 f_3 \rightarrow MIN \quad (3.10)$$

with f_1 being

$$f_1 = - \sum_{i=1}^4 \frac{1}{L_{yi}} \oint E_y(X) ds \quad (3.11)$$

where E_y is the edge strength extracted from the y component of the image using a morphological edge detector, $L_{yi} (i = 1, 2, 3, 4)$ are the lengths of the parabolas seen in Figure 3.8(b), so that f_1 is the average of the edge strength

over $L_{y_i} (i = 1, 2, 3, 4)$, f_2 being

$$f_2 = -|m_{A_u^m} - m_{A_o^m}| - |m_{A_l^m} - m_{A_o^m}| + \sigma_{A_u^m} + \sigma_{A_o^m} + \sigma_{A_l^m} \quad (3.12)$$

and f_3 being

$$f_3 = |\sigma_{A_u^m} - \sigma_{A_o^m}| + |\sigma_{A_o^m} - \sigma_{A_l^m}| + |\sigma_{A_l^m} - \sigma_{A_u^m}| \quad (3.13)$$

, where $m_{A_u^m}$, $m_{A_l^m}$, $m_{A_o^m}$ and $\sigma_{A_u^m}^2$, $\sigma_{A_l^m}^2$, $\sigma_{A_o^m}^2$ are the means and the variances of the C_r component of the image in the regions of the upper lip A_u^m , the lower lip A_l^m and in the region between the lips A_o^m .

The mouth-closed cost function[19]:

$$\int_m^c k_1 f_1 + k_2 f_2 + k_3 f_3 \rightarrow MIN \quad (3.14)$$

with f_1 being

$$f_1 = -\sum_{i=1}^3 \frac{1}{L_{y_i}} \oint E_y(X) ds \quad (3.15)$$

where $L_{y_i} (i = 1, 2, 3)$ are the lengths of the parabolas (Figure 3.8.a), f_2 being

$$f_2 = -|m_{A_u^m} - m_{A_l^m}| + \sigma_{A_u^m} + \sigma_{A_l^m} \quad (3.16)$$

f_3 being

$$f_3 = |\sigma_{A_u^m} - \sigma_{A_l^m}| \quad (3.17)$$

Coefficients $k_i (i = 1, 2, 3)$ are the weighting factors which were set to 1 in the experiments.

In order to validate the study, experimental results obtained with typical videophone sequence were used. The results of this evaluation indicated that this deformable template-based algorithm was 37 % successful in automatically estimating the mouth features of the images.

3.2.4.5 Other Deformable Template Research

A robust method of tracking lip contours is proposed in [52]. The authors used a multi-state mouth model which involves three lip states such as open, relatively

closed, and tightly closed. They also combined lip color, shape and motion in information in their model. The system is tested on 5000 images by using a facial expression database which consists of image sequences of children and adults of European, African and Asian ancestry. It is reported that the method accurately tracked lip motion and was robust to variation in facial appearance among subjects, specularities, mouth state, and head motion.

A system to track head position and facial features in real time is presented in [22]. This system processes head and facial feature tracking separately. In the system, first, the head position is reconstructed by means of a model based head tracker, which matches a 3D generic textured head model and 2D image features extracted from the input sequence. After the pose reconstruction, the input image is warped into the texture map of the model. The result of this process is the stabilized view of the face. By using this stabilized view of the face, the system uses multi-state deformable templates for detecting the face features such as eyebrows, eyes and lips (Figure 3.10).

Head tracking and facial feature tracking algorithms are tested in [22]. According to the results, it was found out that the performance of the head tracking algorithm was about 30 frame/s on a Pentium III 600, while face expression reconstruction process running at about 45 frame/s.

Deformable templates are used for the automatic estimation of the chin and cheek contours of a person is used in [23].

Lip extraction and tracking through Bayesian models which involves designing parametric template modes for describing the shape of the lips are conducted in [20]. The lower lip template proposed in [20] is shown in Figure 3.11.

3.2.5 Active Contours (Snakes)

Snakes are in a way generic deformable templates which use an imaging model that considers the image potentials on the contour of the snake only. The main source of problem when using snakes is that they need a good starting configuration. The initialization of the snakes are usually performed manually or by

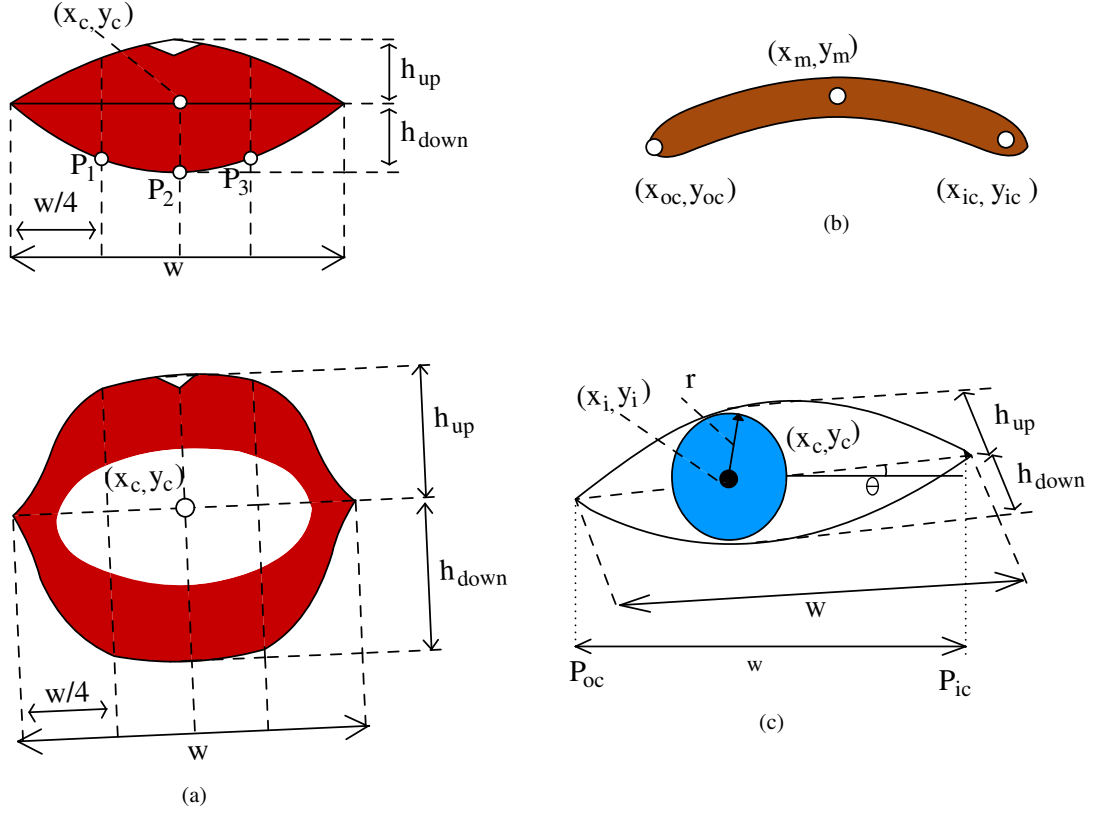


Figure 3.10: a)Mouth Template, b)Eye Template and c)Eye Template [22]

employing other techniques beforehand to estimate the rough location of the features of interest. In the following paragraphs some of the studies that use snakes for facial feature extraction are explained.

An active contour lip model is used in [4] to track the lips of a speaker in a bimodal speech recognition system. The active contour model used in their study is based on cubic B-splines. In order to overcome the initialization problem, the study employs a color segmentation algorithm. The authors performed color segmentation on hue-saturation space of the sub-sampled image. Then they choose the largest connected component with position and aspect ratio lying within some reasonable constraints. The cubic B-spline based active contour model is defined as follows:

$$X_k(u) = \Phi_0(u)P_{k-1} + \Phi_1(u)P_k + \Phi_2(u)P_{k+1} + \Phi_0(3)P_{k+2}, \quad (3.18)$$

where $X_k(u)$ is the points in the k^{th} segment, $\Phi_i(u)$'s are the cubic B-spline basis

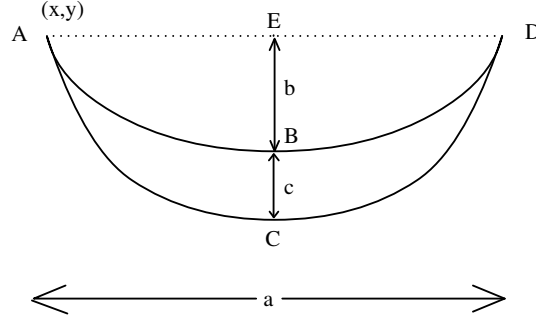


Figure 3.11: Lower lip template [20]

functions, and P_k 's are control points of the spline defined as affine transformations of the control points of the initial contour as follows:

$$P_k = c + A.\overline{P_k} \quad (3.19)$$

The study used a coarse-to-fine search strategy for estimating lip contours by moving in the normal direction of the snake control points and looking for lip boundaries. They then deformed the active contour model towards the boundaries. The study reports real-time performance.

Catmull-Rom splines are used for implementing the active contour used for extracting lip boundaries in [5]. Catmull-Rom splines have desirable properties such as *local control* and interpolation of control points. Their system is initialized by another face tracker system. They used the coordinate of the tip of the nose as an input, and they first estimated the corners of the mouth by extracting the line connecting the corners. They used a snake growing algorithm to detect the upper and lower lip contours separately. The system is reported to yield real-time performance.

3.2.6 Integral Projection

The integral projection of a potential $\Psi(x, y)$ is calculated by summing the values in a specific direction. Usually the horizontal and vertical integral projections have been exploited for determining the vertical and horizontal positions of facial features. Horizontal and vertical integral projections denoted by $\Psi_H(x)$

and $\Psi_V(y)$ are calculated according to the following formula (generalized from [53]) :

$$\Psi_H(x) = \sum_y \Psi(x, y) , and \quad (3.20)$$

$$\Psi_V(y) = \sum_x \Psi(x, y) . \quad (3.21)$$

The horizontal and vertical projections - $\Psi_H(y)$, $\Psi_V(x)$ - of an image is depicted in Figure 3.12.

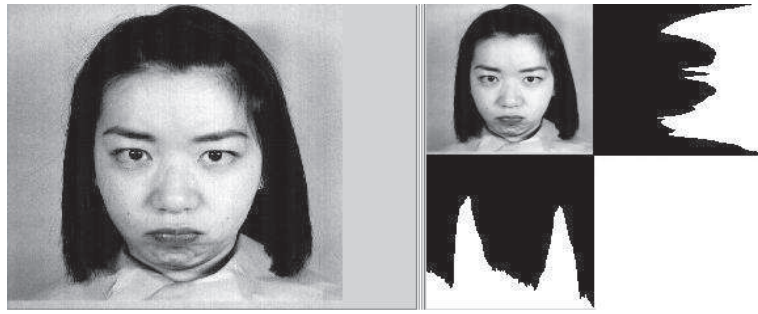


Figure 3.12: Integral projection

The local minima and maxima of $\Psi_H(y)$ and $\Psi_V(x)$ provide cues on the positions of facial features.

An in-depth analysis of integral projections is provided in [16]. Instead of horizontal and vertical integral projections, the terms X-Relief and Y-Relief are used. The boundaries of facial features is extracted in [16] by evaluating the topographical grey level y-projection (Y-Relief) and x-projection (X-Relief) (Figure 3.13). Matching of minima in Y-Relief is used as a base for feature extraction. Moreover, the X-Relief characteristics of each feature is determined through extensive experimentation with many face images [16].

Both X-Relief and Y-Relief proposed in [16] can be used to determine left and right, and upper and lower boundaries of a facial feature. According to that study, the following steps are used to find the boundaries:

1. Calculate the mean gray-level for every row of the face region, which is $YR()$

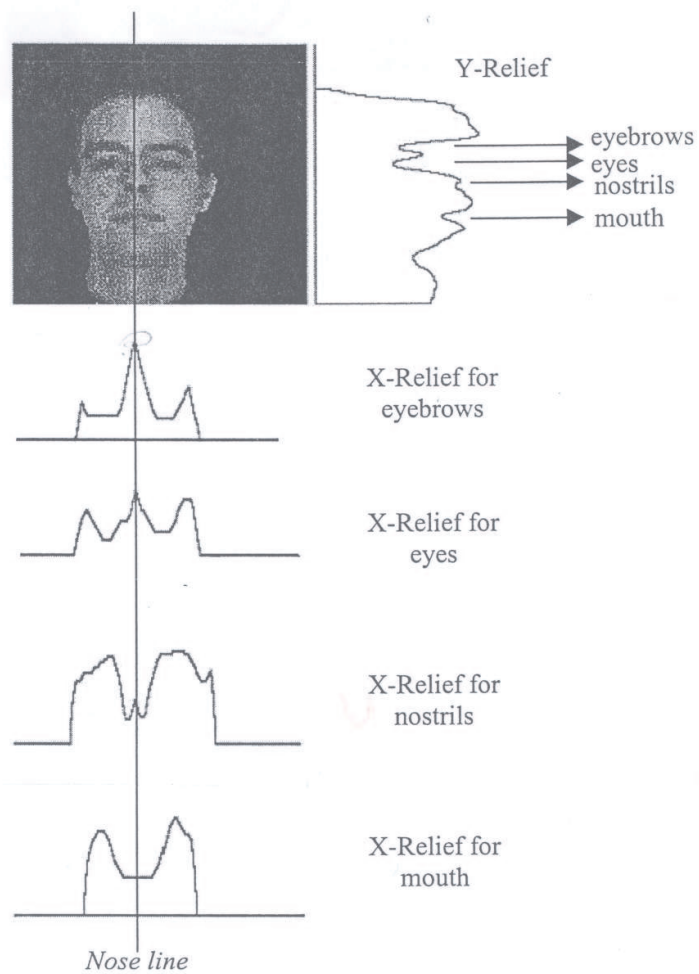


Figure 3.13: Y-Relief and X-Reliefs for an example image [16]

2. Determine the minima in $YR()$
3. Find preceding maxima and succeeding maxima for each minima
4. Find the point where maximum change in $YR()$ occurs in between the current minimum and preceding maximum. This will be a candidate for upper boundary
5. Find the point where maximum change in $YR()$ occurs in between the current minimum and succeeding maximum. This will be a candidate for lower boundary
6. For each significant minimum in Y-Relief, calculate X-Relief. Each X-

Relief element is calculated by taking the average of 3 pixels on the same column but on neighboring rows. After that, X-Relief is smoothed in horizontal direction by a filter of width 3 points (columns) to get rid of small variations

7. Determine the minima in $XR()$
8. Find preceding maxima and succeeding maxima for each minima
9. Find the point where maximum change in $XR()$ occurs in between the current minimum and preceding maximum. This point will be a candidate for left boundary
10. Find the point where maximum change in $YR()$ occurs in between the current minimum and succeeding maximum. This point will be a candidate for right boundary

X-Relief and Y-Relief are used together to obtain more precise information about facial features. The position of the minimum in Y-Relief and the shape of corresponding X-Relief are processed together to match a minimum with a facial feature. Fuzzy Set Theory was used in order to calculate the similarity between the relief of a feature candidate and the characteristic relief.

CHAPTER 4

Implementation

In this chapter the implementation of the facial feature extraction system is explained. The system extracts the detailed shape and position information of eyes, eyebrows and lips, which are the features that are considered important in facial expression analysis, face recognition, lipreading and multi-modal speech analysis systems.

The first step in fully automatic facial feature extraction systems is the detection of key feature points or localizing the face. In this study an eigenfaces based multi-scale face detection algorithm is developed for this purpose. The algorithm performs a sequential search on the Gaussian pyramid of the input image starting from the lowest sized level of the pyramid. A face model based on adult facial proportions is developed and used in the face detection algorithm. This provides that the rough search regions for the facial features are readily available when a face is detected. After the algorithm finds the initial search regions for the facial features, each of the deformable model is matched separately.

The deformable models used in this study are parametric deformable templates, which define the geometry and imaging model for the desired features. The geometry of the templates are inspired from previous studies, however the energy functions are developed in this work. The geometrical models of each de-

formable model are developed using both polygonal and spline-based geometries. Spline based geometries seem to approximate the real geometries of the facial features better. By implementing both polygonal and spline-based geometries, we tried to achieve quantitative results on their performance in representing facial features. In order to perform a coarse-to-fine grain matching, multiple epochs are used in the matching algorithms of the templates. Energy minimization is performed by using the *Downhill Simplex* algorithm described in [54]. Our decision on the minimization algorithm is shaped by the simplicity of Downhill simplex. Minimization algorithms based on derivatives (Gradient Descent, Conjugate Gradients, etc.) are not considered, because they require that the derivatives of the energy functions are available, and in our case the derivatives are not easily available. An overview of our system is given in Figure 4.1.

In the following sections we first explain in detail the face detection algorithm developed for detecting faces and rough search regions for desired facial features. Then, we present the deformable models developed for extracting eye, eyebrow and mouth features.

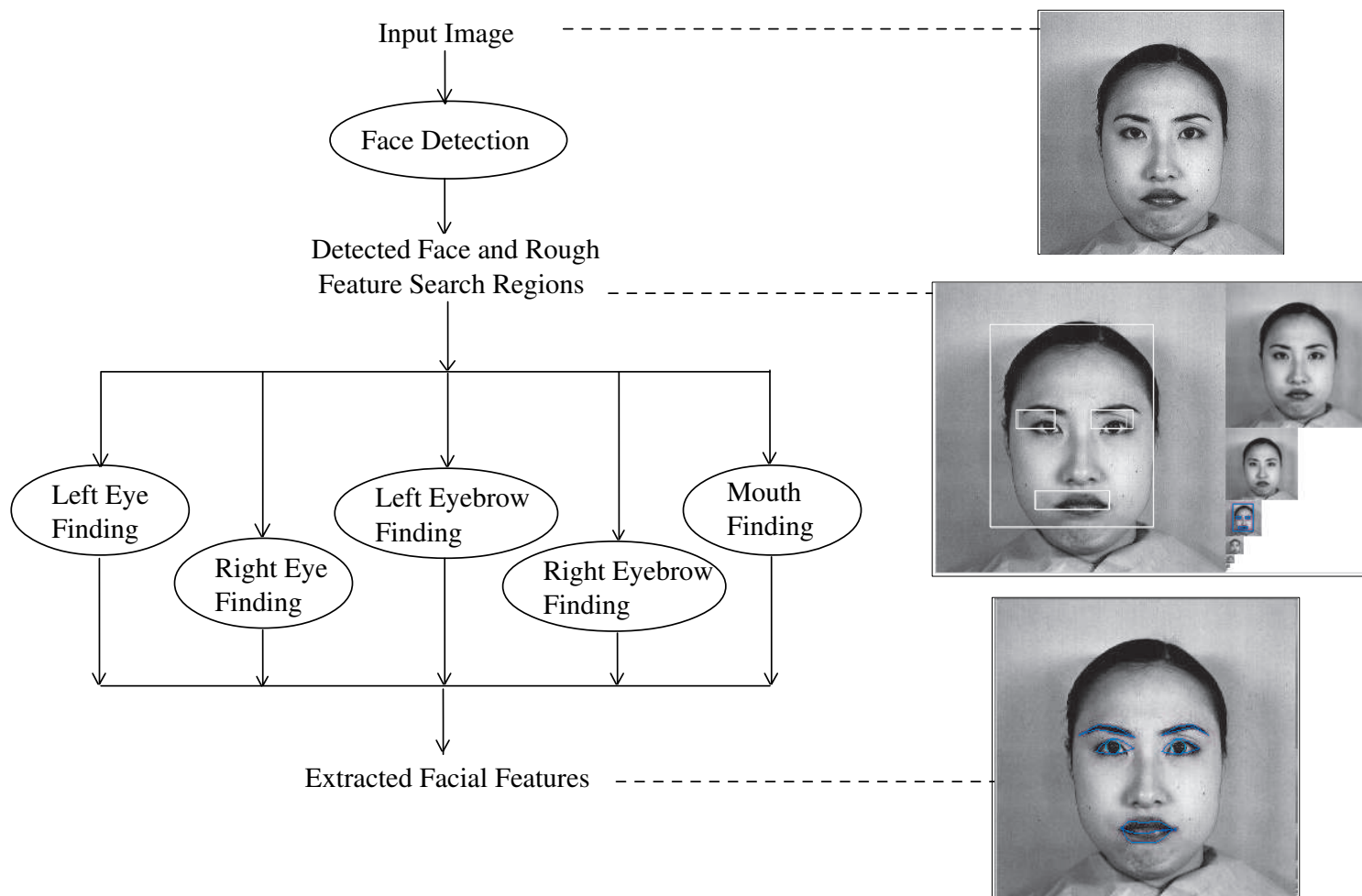
4.1 Face Detection

The face detection algorithm implemented in this study is based on the eigenfaces approach. Eigenfaces approach uses principle component analysis (PCA) technique on a representative set of facial images in order to construct a lower dimensional face space. In order to classify a given image as a face or non-face image, the distance-to-eigenspace measure is used.

In the eigenface calculations, we use face images having 18x24 pixels resolution, which is reported to be the smallest resolution at which human beings can perform recognition [55]. This small sizes provides high speed.

In addition, we developed an 18x24 face model corresponding to the search window of our algorithm, and embedded adult facial proportions into this model, so that the locations of facial features are readily available when a face is detected.

Figure 4.1: Overview of the system



Our algorithm performs a sequential face search based on the distance-to-space measure on the Gaussian pyramid of the input image. Searching on the Gaussian pyramid provides multi-scale face detection capability to our algorithm.

In the following sections the details pertaining the calculation of the eigenfaces, the developed face model, and the pyramid search algorithm is explained.

4.1.1 Calculation of the Eigenfaces

In the calculation of eigenfaces, images of the same size have to be used. In addition, using images which has the same features on the same spatial locations is important. In order to satisfy these requirements, we normalized the images in size, and orientation before starting PCA calculations. Before discussing the details of the normalization procedure, the developed face model will be presented, because the face model shapes the normalization procedure.

Face Model

The study presented in [55] reports that human beings are able to recognize faces having as small as 18x24 pixels resolution. Probably even a smaller resolution is sufficient for detection (compared to recognition) , however we decided to use 18x24 pixels in our algorithm, because we were unable to find a similar study for face detection.

Our face model incorporates standard adult facial proportions used in drawing and similar arts [56, 57]. These proportions can be summarized as follows:

- eyes divide the face vertically into two halves,
- nose tip divides the eyes-to-chin region vertically into two halves,
- mouth divides the nose-tip-to-chin region vertically into two halves,
- eyes divide the face horizontally into five equal parts,
- and mouth corners are vertically aligned with the centers of the eyes.

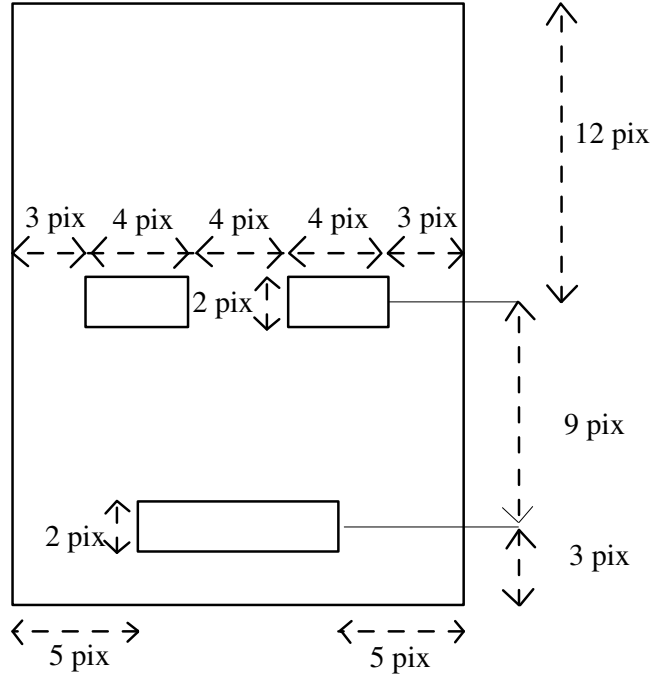


Figure 4.2: The face model used in face detection. The size of the face model is 18x24 and adult facial proportions are incorporated to define the rough locations of the facial features.

In addition to these ratios, we have assumed that the eye and mouth heights are equal to one half of the width of one eye. The face model conforming to developed based on these assumptions are given in Figure 4.2.

Normalization of Face Images

Considering this face model we have designed a normalization procedure which rotates and scales the image such that at the end we have an 18x24 image, which contains inner eye corners in the screen coordinates $\mathbf{x}_{\text{lefteye}} = (7, 12)$ and $\mathbf{x}_{\text{righteye}} = (11, 12)$ (Note that when we say *left eye* we mean the eye that appears to the left on the screen, not the left eye of the face). In order to normalize the images we manually marked the inner corners of the eyes in each image. The normalization procedure is given in Algorithm 4.1. A sample screen depicting the normalization operation is provided in Figure 4.3.

PCA Calculations

The normalized M number of face images I_i are first converted to 432x1

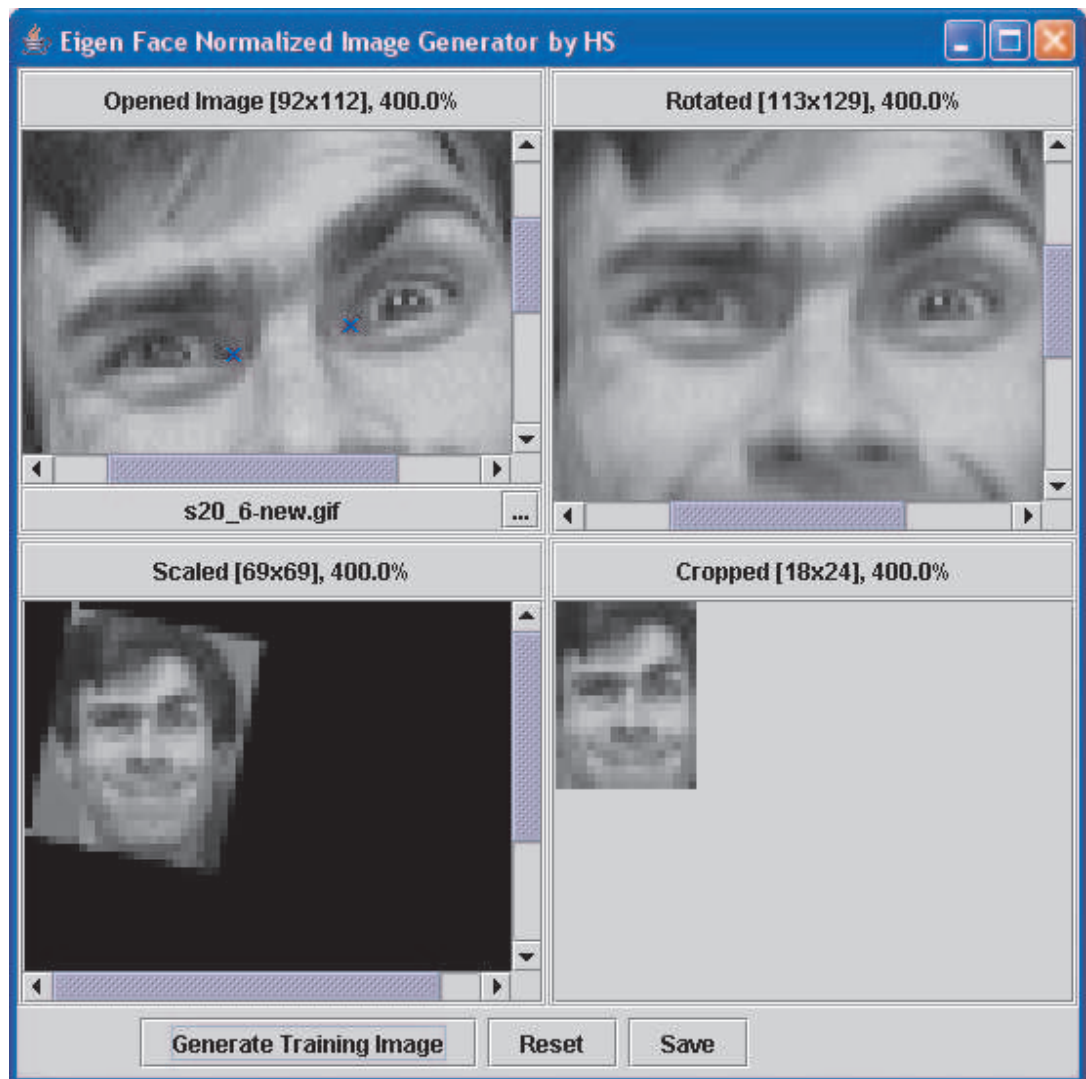


Figure 4.3: Normalization of training Images

Let x_l and x_r be the manually selected inner eye corner locations
Let I be the image
Assume screen coordinates (y gets larger while going down)
1. if $x_l.y \neq x_r.y$ then
1.1. Correction angle $\theta = -\tan^{-1}((x_r.y - x_l.y)/(x_r.x - x_l.x))$
1.2. Rotate I by θ around x_l , rotate x_l and x_r
2. Calculate the scaling factor $\rho = 4/(x_r.x - x_l.x)$,
because 4 is the normalized difference between the corners.
3. Scale I by ρ , scale x_l and x_r
4. Crop I so that the resulting image contains only the rectangle
 $Rect(x_l.x - 7, x_l.y, 18, 24)$
5. Return the cropped image

Algorithm 4.1: Face image normalization for eigenface calculations

(432=18x24) vectors Γ_i . Then we compute the average face vector as follows:

$$\Psi = \frac{1}{M} \sum_{i=1}^M \Gamma_i \quad (4.1)$$

Then we subtract the mean face from the vectors as follows:

$$\Phi_i = \Gamma_i - \Psi \quad (4.2)$$

We compute the covariance matrix:

$$C = \frac{1}{M} \sum_{n=1}^M \Phi_n \Phi_n^T = AA^T \quad (432 \times 432 \text{ matrix}), \quad (4.3)$$

where $A = [\Phi_1 \Phi_2 \dots \Phi_M]$ (432xM matrix). Then we compute the eigenvalues and eigenvectors of the covariance matrix and select the eigenvectors u_i corresponding to K largest value eigenvalues as the eigenfaces. The selected K eigenfaces define a K dimensional space (eigenspace). In this space, a face image Φ_i is represented by a vector :

$$\Omega_i = \begin{bmatrix} w_1^i \\ w_2^i \\ \dots \\ w_K^i \end{bmatrix}, \quad i = 1, 2, \dots, M \quad (4.4)$$

where $w_j^i = u_j^T \Phi_i$, and u_j is the j th eigenface.



Figure 4.4: An image pyramid

4.1.2 Face Detection Algorithm

Using the face model explained in 4.1.1 and eigenfaces approach, we implemented a face detection algorithm which performs a sequential search on the Gaussian pyramid of the input image.

Image pyramids are distinguished as M-Pyramids (Matrix Pyramids) and T-Pyramids (Tree Pyramids) [28]. T-Pyramids are used when simultaneous access to multiple resolution data is required, on the other hand M-Pyramids are used when it is necessary to work with an image at different resolutions. Our algorithm employs M-Pyramid data structure, which is a sequence $\{M_L, M_{L-1}, \dots, M_0\}$ of images, where M_L has the same dimensions and elements as the original data, and M_{i-1} is derived from M_i by reducing the dimensions by one half (sub-sampling). A Gaussian pyramid is a special case of an image pyramid in which the image is blurred with a Gaussian kernel before sub-sampling. Figure 4.4 illustrates an image pyramid.

Our algorithm performs a sequential search starting from the smallest sized pyramid level which is larger than our 18x24 search window. Searching in the smaller sized levels of the pyramid allows our algorithm to detect faces much

larger than 18x24 at a very high speed. Searching in different levels of the pyramid provides that faces with different scales can be detected. In the sequential search, our algorithm scans each 18x24 window in the levels of the pyramids and constructs 432x1 vectors. Then the distance to face space is calculated. Distance to face space is defined as follows :

$$e_d = ||\Phi - \hat{\Phi}|| \quad (4.5)$$

where $\Phi = \Gamma - \Psi$ and $\hat{\Phi} = \sum_{i=1}^K w_i u_i (w_i = u_i^T \Phi)$. In order to decide that the currently considered search window is a face we check e_d against a threshold T_d . If $e_d < T_d$, then Γ is a face. In other words, distance to face space measure is the reconstruction error. We first project the currently considered search window onto the face space and then we project it back to the original space. If the window is a face then the reconstruction process results in a very low error, otherwise a considerable error is observed, because the face space is specialized to represent face images. The images used in this study contain single faces, and in order to provide high speed we employed this fact, i.e. the algorithm stops searching when a face is found. Figure 4.5 illustrates the face detection algorithm in action.

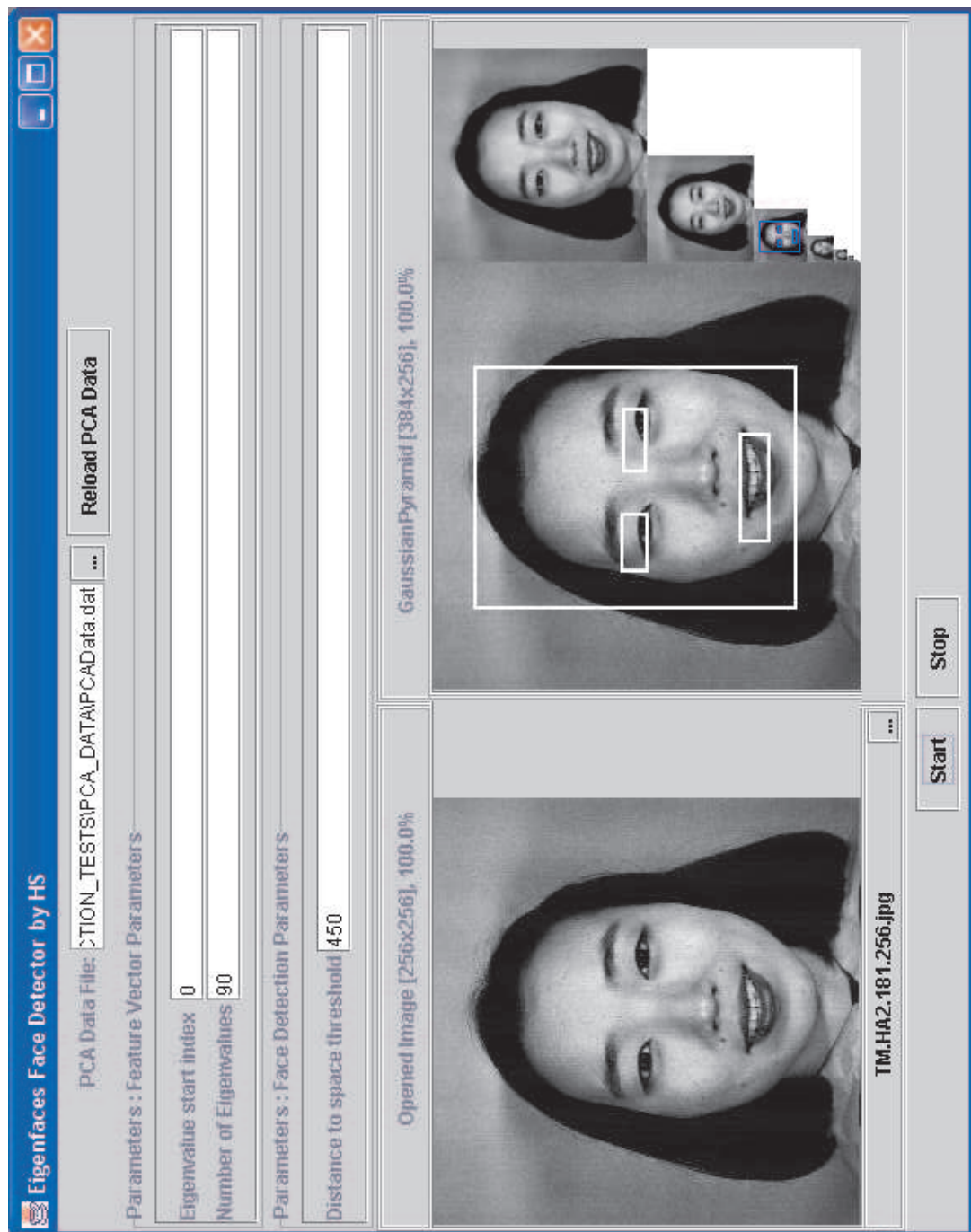


Figure 4.5: A sample screen depicting the face detection process

4.2 Extraction of Eyebrow: Eyebrow Deformable Template

For the extraction of the left and right eyebrows a parametric deformable template is developed. The template exploits the intensity, edge and corner potentials of the eyebrow. The details of the template is given in the following sections.

4.2.1 Template Geometry

The geometry of the Eyebrow template is illustrated in Figure 4.6. The geometry of the template is constructed by considering the possible occurrences of an eyebrow, analyzing the occurrences in the available databases, and determining the most likely deformation segments informally. An eyebrow template geometry composed of three points is used in [22]. Three points are enough to describe the rough shape of the eyebrow, but we considered this template unsatisfactory for describing the shape of the eyebrow in detail. As a result, a template with more parameters is designed in this study.

After developing the geometry of the template, we constructed a list of constraints pertaining the geometry. Those constraints are listed in Table 4.1. The constraints are used to develop an energy function (E_{prior}) which will aid us during matching. Before starting to construct the energy function E_{prior} , reviewing some facts will be helpful in understanding the process.

Fact 4.1 *Let f and g be arbitrary variables that are required to be equal. Then minimizing the function $(f - g)^2$ is enough.*

Justification: $(f - g)^2$ can take only non-negative values, thus minimizing $(f - g)^2$ yields $(f - g)^2 = 0$. And this means $f = g$.

Fact 4.1 provides enough information for forming the energy functions for each of the constraints listed in Table 4.1, but we need to combine these energy functions without violating each other.

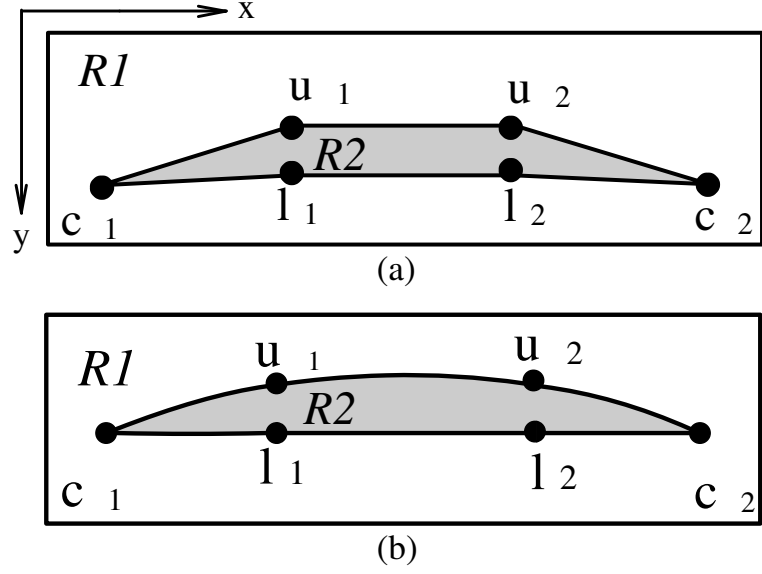


Figure 4.6: The geometry of the deformable eyebrow template. R_2 is the planar domain that represents the eyebrow, and R_1 is the planar domain that represents the surroundings of the eyebrow. c_1 and c_2 correspond to the corners of the eyebrow, and l_1, l_2, u_1, u_2 are points that define the upper and lower contour of the eyebrow a) The polygonal geometry b) Spline based geometry

Table 4.1: The geometrical constraints of the eyebrow template. The constraints are developed by trial and error.

	Constraint	Formal Representation
1.	u_1 and l_1 align vertically	$u_{1x} = l_{1x}$
2.	u_2 and l_2 align vertically	$u_{2x} = l_{2x}$
3.	u_1 and u_2 are horizontally evenly spaced	$3 u_{1x} - c_{1x} = c_{1x} - c_{2x} $, and $3 u_{2x} - c_{2x} = c_{1x} - c_{2x} $
4.	l_1 and l_2 are horizontally evenly spaced	$3 l_{1x} - c_{1x} = c_{1x} - c_{2x} $, and $3 l_{2x} - c_{2x} = c_{1x} - c_{2x} $
5.	Height is uniform between the curls of the eyebrow	$ u_{1y} - l_{1y} = u_{2y} - l_{2y} $
6.	The width of the template is ten times the height	$10 u_{1y} - l_{1y} = c_{1x} - c_{2x} $

Fact 4.2 *Let E_1 and E_2 be energy functions that are required to be minimized. If both E_1 and E_2 can take only non-negative values, and if E_1 and E_2 are independent, then minimizing $E = E_1 + E_2$ minimizes both E_1 and E_2 .*

Justification: *Minimizing E yield $E = E_1 + E_2 = 0$, and this means $E_1 = 0$ and $E_2 = 0$, because E_1 and E_2 can take only non-negative values. Thus, both E_1 and E_2 are minimized.*

Fact 4.2 requires that the energy functions that need to be combined have to be independent. However, we cannot use fact 4.2 in this form, because most of our constraints (and thus the energy functions representing them) are dependent to the same variables. Fact 4.3 offers a solution to our problem.

Fact 4.3 *Let E_1 and E_2 be energy functions that are required to be minimized. If both E_1 and E_2 can take only non-negative values, and if E_1 and E_2 are dependent, then minimizing $E = k_1E_1 + k_2E_2$ does not guarantee that both E_1 and E_2 are minimized, but the positive coefficients k_1 and k_2 shapes the preference between E_1 and E_2 during minimization.*

Justification: *This time minimizing E is not guaranteed to yield $E = k_1E_1 + k_2E_2 = 0$, because it is not guaranteed that both E_1 and E_2 can be zero at the same time. Minimization will favor the energy function with the larger coefficient, because otherwise a larger coefficient will be multiplied with a positive number and this will result in a larger energy.*

With the help of the Fact 4.3, constructing E_{prior} is straightforward. In the following paragraphs, we will first develop the energy functions corresponding to the first and second constraints in Table 4.1, then we will combine them. And finally we will present the full E_{prior} .

The energy function E_1 corresponding to the first constraint is $E_1 = (u_{1x} - l_{1x})^2$ by Fact 4.1. Similarly, the energy function E_2 corresponding to the second constraint is $E_2 = (u_{2x} - l_{2x})^2$. E_1 and E_2 are independent functions, however to be general we use Fact 4.3 to get the combined energy function $E = k_1(u_{1x} -$

Table 4.2: The imaging model of the eyebrow template. $I(x, y)$ denotes the intensities, $\Psi_c(x, y)$ denotes the corner potential, and $\Psi_e(x, y)$ denotes the edge potential. ∂T denotes the border of the template, and it is defined as the union of the line segments as follows : $\partial T = |c_1 u_1| \cup |u_1 u_2| \cup |u_2 c_2| \cup |c_2 l_2| \cup |l_2 l_1| \cup |l_1 c_1|$. The measure of darkness M_D is adapted from the measure of fit proposed for valley detection [34] described in Section 2.1.5.

	Property	Formal Representation
1.	Eyeblink corners c_1 and c_2 correspond to regions having high corner values in the image	Choose c_1 and c_2 to maximize $\Psi_c(c_1) + \Psi_c(c_2)$
2.	Eyeblink boundary correspond to regions having high edge values in the image	Choose all parameters to maximize $\int_{s \in \partial T} \Psi_e(x, y) ds$
3.	The pixels inside the template boundary have very low intensity values compared to the pixels outside the template, i.e. eyebrow is darker than its surroundings	Choose all parameters to maximize the darkness measure $M_D = \frac{\hat{\mu}_1 - \hat{\mu}_2}{h + \gamma \sqrt{\hat{n}_1 \hat{\sigma}_1^2 + \hat{n}_2 \hat{\sigma}_2^2}}$ <p>where the subscript 1 denotes the region R_1, and subscript 2 denotes the region R_2 (See Figure 4.6)</p>

$l_{1x})^2 + k_2(u_{2x} - l_{2x})^2$. Final E_{prior} is given as follows:

$$\begin{aligned}
E_{prior} = & k_1(u_{1x} - l_{1x})^2 + k_2(u_{2x} - l_{2x})^2 \\
& + k_3 [(3|u_{1x} - c_{1x}| - |c_{1x} - c_{2x}|)^2 + (3|u_{2x} - c_{2x}| - |c_{1x} - c_{2x}|)^2] \\
& + k_4 [(3|l_{1x} - c_{1x}| - |c_{1x} - c_{2x}|)^2 + (3|l_{2x} - c_{2x}| - |c_{1x} - c_{2x}|)^2] \\
& + k_5 (|u_{1y} - l_{1y}| - |u_{2y} - l_{2y}|)^2 + k_6 (10|u_{1y} - l_{1y}| - |c_{1x} - c_{2x}|) \quad (4.6)
\end{aligned}$$

4.2.2 Imaging Model

The imaging model of the eyebrow template is designed to exploit the intensity, edge and corner potentials of the underlying image. The imaging model is given in Table 4.2.

The developed geometry and imaging model is used for locating the detailed shape and position information of the left and right eyebrows. At first, we planned to develop separate templates for each of the right and left eyebrows,

but experimenting with the template showed that it is reasonable to use a single template for both of the eyebrows.

The energy function E_{data} that combines the properties listed in Table 4.2 is developed as follows :

$$E_{data} = -k_7(\Psi_c(c_1) + \Psi_c(c_2)) - k_8 \int_{s \in \partial T} \Psi_e(x, y) ds - k_9 \left(\frac{\hat{\mu}_1 - \hat{\mu}_2}{h + \gamma \sqrt{\tilde{n}_1(\hat{\sigma}_1^2) + \tilde{n}_2(\hat{\sigma}_2^2)}} \right) \quad (4.7)$$

4.2.3 Matching Algorithm

The designed matching algorithm is an energy minimization algorithm. The energy of the template $E_{brow} = E_{prior} + E_{data}$ is given below:

$$\begin{aligned} E_{brow} = & k_1(u_{1x} - l_{1x})^2 + k_2(u_{2x} - l_{2x})^2 \\ & + k_3 [(3|u_{1x} - c_{1x}| - |c_{1x} - c_{2x}|)^2 + (3|u_{2x} - c_{2x}| - |c_{1x} - c_{2x}|)^2] \\ & + k_4 [(3|l_{1x} - c_{1x}| - |c_{1x} - c_{2x}|)^2 + (3|l_{2x} - c_{2x}| - |c_{1x} - c_{2x}|)^2] \\ & + k_5(|u_{1y} - l_{1y}| - |u_{2y} - l_{2y}|)^2 + k_6(10|u_{1y} - l_{1y}| - |c_{1x} - c_{2x}|) \\ & - k_7(\Psi_c(c_1) + \Psi_c(c_2)) - k_8 \int_{s \in \partial T} \Psi_e(x, y) ds \\ & - k_9 \frac{\hat{\mu}_1 - \hat{\mu}_2}{h + \gamma \sqrt{\tilde{n}_1 \hat{\sigma}_1^2 + \tilde{n}_2 \hat{\sigma}_2^2}} \quad (4.8) \end{aligned}$$

The minimization of this energy function is performed by employing a variety of the Downhill Simplex algorithm. In order to find the optimum parameters c_1 , c_2 , u_1 , u_2 , l_1 , and l_2 that minimizes the energy function we developed a multi-epoch algorithm. The epochs explained below provide a coarse to fine grain optimization.

Rough Localization. In the first epoch only the location of the whole template is modified, and this way a fast rough localization is performed. This epoch is especially helpful when the initialization procedure performs poorly (See Figure 4.7).

Rough Deforming. After the template is roughly located on the eyebrow, this epoch starts. This epoch is a rough deforming state, in which we move

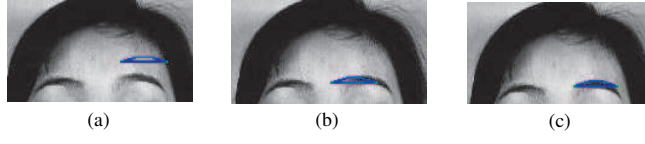


Figure 4.7: Eyebrow rough localization epoch

u_1 and l_1 together, and likewise u_2 and l_2 are also moved together(See Figure 4.8).

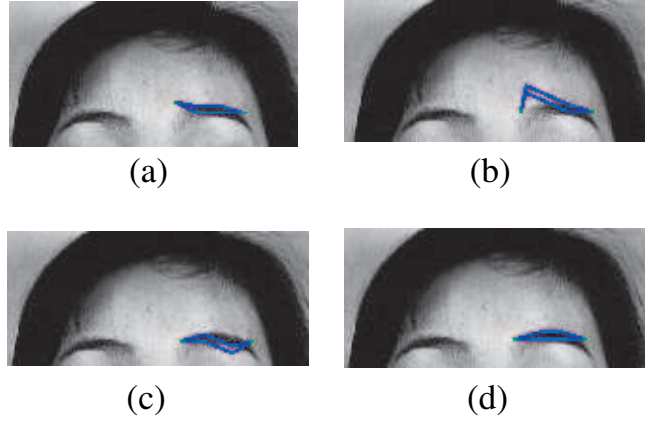


Figure 4.8: Eyebrow rough deforming epoch

Fine Tuning. Finally, all parameters are freely optimized in order to fine tune the template (Figure 4.9).

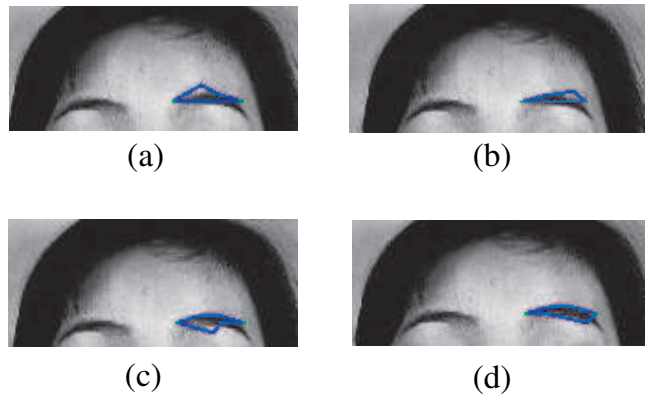


Figure 4.9: Eyebrow fine tuning epoch

4.2.4 Implementation Issues

In this section, we will provide the important issues regarding the implementation of the eyebrow template.

4.2.4.1 Template Geometry Issues

In the following the implementation issues regarding the geometry of the template is discussed.

4.2.4.1.1 Computing The Initial Geometry The developed deformable eyebrow template needs to be initialized by an external procedure. In order to provide a uniform interface for any external procedure to set the initial configuration of the template, we developed an initialization procedure based on a rectangular bounding box. A specialized external procedure can directly provide the initial geometry of the template, but we did not limit the template to such specialized procedure. In addition, general purpose facial feature locating algorithms like the one presented in [16] exist which compute a rectangular bounding box for facial features. Considering these and the geometric constraints of the eyebrow template given in Table 4.1, we compute the initial geometry using Algorithm 4.2

4.2.4.1.2 Surroundings of The Eyebrow The imaging model of the eyebrow template requires that a finite surroundings region be given (see property 3 given in Table 4.2). The surroundings of the eyebrow is not calculated directly, but it is calculated from the eyebrow geometry as top, down, right and left margins. By considering the anatomical properties of the human face, the margins specifying the surrounding is calculated as follows:

- top margin = half of the eyebrow height
- bottom margin = $\frac{1}{4}$ of the eyebrow height
- left margin = 3 pixels

Let *box* be the rectangular bounding box

1. Calculate auxiliary variables
 - 1.1. Set $width = box.width$
 - 1.2. Set $height = width/10$ (Using constraint 6)
 - 1.3. Set $upY = box.y$
 - 1.4. Set $downY = box.y + height$
 - 1.5. Set $c1x = box.x$
 - 1.6. Set $u1x = c1x + width/3$ (Using constraint 3)
 - 1.7. Set $u2x = c1x + 2*width/3$ (Using constraint 3)
 - 1.8. Set $c2x = c1x + width$
2. Calculate the final geometry parameters
 - 2.1 Set $c_1 = \text{new Point}(c1x, downY)$
 - 2.1 Set $c_2 = \text{new Point}(c2x, downY)$
 - 2.2 Set $u_1 = \text{new Point}(u1x, upY)$
 - 2.3 Set $l_1 = \text{new Point}(u1x, downY)$
 - 2.2 Set $u_2 = \text{new Point}(u2x, upY)$
 - 2.3 Set $l_2 = \text{new Point}(u2x, downY)$

Algorithm 4.2: Computing the initial geometry of the eyebrow template. The algorithm calculates initial geometry parameters (c_1 , u_1 , u_2 , l_1 , l_2 and c_2) given a rectangular bounding box. The calculated geometry conforms to the constraints given in Table 4.1

- right margin = 3 pixels

These values are obtained by experimenting with the template. Bottom margin is selected to be very small, because it is possible that eyes or eyelids, which are usually as dark as the eyebrow, can appear just below the eyebrow. Left and right margins are chosen just to provide some flexibility. Choosing larger margins for left, right, and top margins seems meaningful, as there is large regions of facial skin (which appear brighter than the eyebrow, providing a good M_D given in Table 4.2) in these directions. However, hair can cover some of the skin in these regions. Thus the values are chosen as listed above.

4.2.4.1.3 Preventing The Geometry From Building An Invalid Shape

The geometry constraint provided in Table 4.1, and thus E_{prior} tries to impose a well defined shape on the template. However, in some cases the minimization

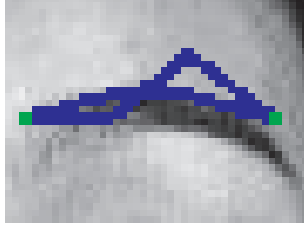


Figure 4.10: An invalid eyebrow template geometry. The minimization algorithm sometimes gets caught to an invalid shape and it cannot recover, if the penalty mechanism is not considered.

1. if u_1 appears below l_1 , then add $PENALTY \times |u_{1y} - l_{1y}|$ to E_{brow}
2. if u_2 appears below l_2 , then add $PENALTY \times |u_{2y} - l_{2y}|$ to E_{brow}

Algorithm 4.3: Penalty mechanism for the eyebrow template, used for preventing the geometry from building an invalid shape. $PENALTY$ is a large enough number, such that minimizing E will guarantee that $E_{u-lpenalty}$ is minimized.

algorithm happens to try invalid geometrical configurations and some times the geometry becomes so tangled to be able to recover. Figure 4.10 shows one such case. In order to prevent these cases we developed a mechanism which adds penalty terms to E_{brow} when an invalid geometry occurs. The penalty mechanism is given in Algorithm 4.3

4.2.4.2 Image Boundary Considerations

Image boundaries need to be considered carefully, because E_{brow} causes unexpected behavior when some part of the template is out of the image boundaries. If some part of the template is out of the image boundary, then nothing is calculated for that part. Consider for example that the template as a whole is out of the image boundary, then this means that we will not process any points. This results in $E_{brow} = 0$, which is a good enough minimum to drive the minimization algorithm. The situation explained here results in nonsense minima, and needs to be avoided. In order to avoid this, we add another penalty term

$$E_{boundarypenalty} = PENALTY \times Area\ of\ (\partial T \setminus \partial I) \quad (4.9)$$

to E_{brow} , where ∂T denotes the planar domain representing the eyebrow template, ∂I denotes the planar domain representing the image region, and $\partial T \setminus \partial I$ denotes the planar domain that represents the region that lies outside the image boundary.

4.2.4.3 Energy Calculation Issues

In order to calculate the energy of a given template geometry and the image on which the template matching will be performed, we implemented an algorithm that traverses the image regions corresponding to the template geometry for collecting statistics on the template which will be used for calculating E_{data} . Calculation of E_{prior} is independent of the image and straightforward, with a given geometry as given in Equation 4.6. In the following paragraphs we will discuss the issues pertaining the calculation of E_{data} .

4.2.4.3.1 Finding where a given point lies in the template geometry

Collecting statistics from the image for calculating E_{data} will be discussed later, but in order to collect those statistics we need to be able to understand whether a given point lies on the boundary, inside the brow region (R_2), inside the surroundings region (R_1) or near a corner. This classification is performed as given in Algorithm 4.4. The algorithm classifies a given point as one of the followings:

- corner,
- on boundary,
- inside, or
- outside.

4.2.4.3.2 Collecting Statistics In order to collect the statistics needed for calculating E_{data} , each point falling into the rectangular bounding box of the

Let p be a given point for which we need to be classified

1. If $\|p - c_1\| \leq 1$ or $\|p - c_2\| \leq 1$
 - 1.1 return CORNER
2. else if distance of p to at least one of the line segments $|c_1u_1|$, $|u_1u_2|$, $|u_2c_2|$, $|c_2l_2|$, $|l_2l_1|$, and $|l_1c_1|$ is smaller than or equal to 1.
 - 2.1 return ON BOUNDARY
3. else if the polygon $c_1u_1u_2c_2l_2l_1$ contains p
 - 3.1 return INSIDE
4. else return OUTSIDE

Algorithm 4.4: Finding where a given point lies in the eyebrow template geometry

template geometry is traversed and different statistics are updated depending on where this point lies in the geometry. The algorithm used for Collecting Statistics is given in Algorithm 4.5.

4.2.4.3.3 Collected Template Statistics The algorithm collect four different statistics on the image:

Corner Statistics The corner potential of the image is calculated using the Plessey corner detection technique explained in Section 2.1.4. Corner potential is then normalized so that the values lie in the range $[0, 1]$. The corner potential is then smoothed in order provide a smooth energy surface for the minimization algorithm. The collected corner statistics are the values of this normalized-smoothed corner potential near the corner points of the template geometry (c_1 and c_2).

Boundary Edge Statistics The edge potential of the image is calculated using the Sobel kernels explained in Section 2.1.3. Edge potential is then normalized so that the values lie in the range $[0, 1]$. Then edge potential is smoothed similar to the corner potential. The collected boundary edge statistics are the values of this normalized-smoothed edge potential near the boundary of the template geometry.

Let R_I be the bounding box of the image
Let R_T be the bounding box of the template

1. Set $box = R_I \cap R_T$
2. for each point p in box
 - 2.1 if p is a CORNER point
 - 2.1.1 collect corner statistics for p
 - 2.1.2 collect boundary edge statistics for p
 - 2.2. if p is INSIDE the eyebrow region
 - 2.2.1 collect inside intensity statistics for p
 - 2.3. if p is OUTSIDE the eyebrow region
 - 2.3.1 collect outside intensity statistics for p
 - 2.4. if p is ON BOUNDARY of the eyebrow region
 - 2.4.1 collect boundary edge statistics for p
 - 2.4.1 collect inside intensity statistics for p

Algorithm 4.5: Collecting statistics of eyebrow template. The algorithm collects four different statistical samples: 1)corners 2)boundary edges 3)inside intensities 4)outside intensities.

Inside Intensity Statistics The intensity potential of the image is normalized so that the values lie in the range $[0, 1]$. Then smoothing is performed for aiding the minimization. The collected inside intensity statistics are the values of this normalized-smoothed intensity potential in region R_2 shown in Figure 4.6.

Outside Intensity Statistics Similar to the previous item, normalized-smoothed intensity potential in region R_1 shown in Figure 4.6 are collected.

4.2.4.4 Use of Downhill Simplex

Downhill simplex is an easy to implement algorithm, which provides optimization without using any derivative information. This algorithm tries to find a minimum by searching the energy surface by trial. Experimentation showed that the algorithm gets unreasonably slower when the dimensionality of the searched space increases. In our case, a search space of dimension 4 was enough to put the algorithm into a very long lasting search. In order to overcome this

limitation, we tried to perform optimization by modifying one-or two variables at a time. Experimenting with the eyebrow template proved that this technique performs reasonably fast for research purposes. We performed the minimization in multiple epochs, each epoch having its own parameters which are modified one after another in the downhill simplex algorithm.

First epoch has only one parameter : the location of the whole template. Thus downhill simplex performs a fast optimization in the two dimensional space. Second epoch has four parameters: one for c_1 , one for c_2 , one for u_1 and l_1 and one for u_2 and l_2 . These parameters are minimized one after another, just like a two dimensional minimization. And lastly, six parameters are introduced, one for each of the template geometry parameters.

4.2.4.5 Coefficients of the Energy Function

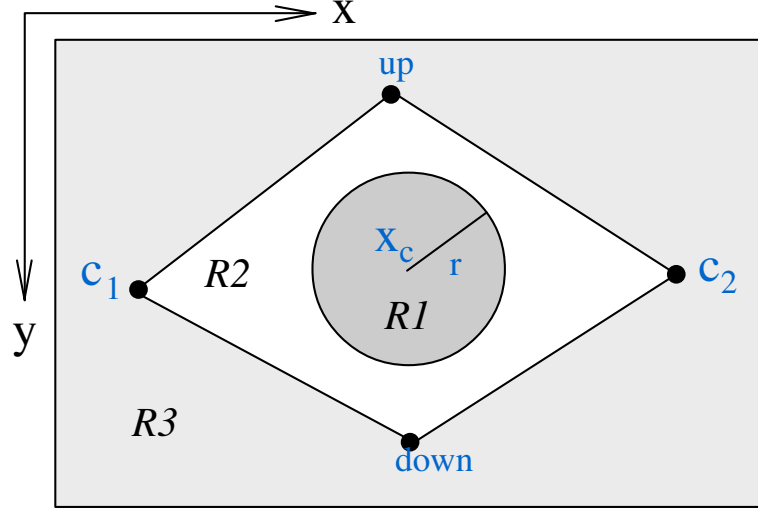
We decided that each epoch should have its own set of coefficients, because different constraints may need to be emphasized in different epochs. Thus we implemented our model to support different coefficients in different epochs. The selection of the coefficient values proved to be an important step which will be discussed later.

4.3 Extraction of Eye: Eye Deformable Template

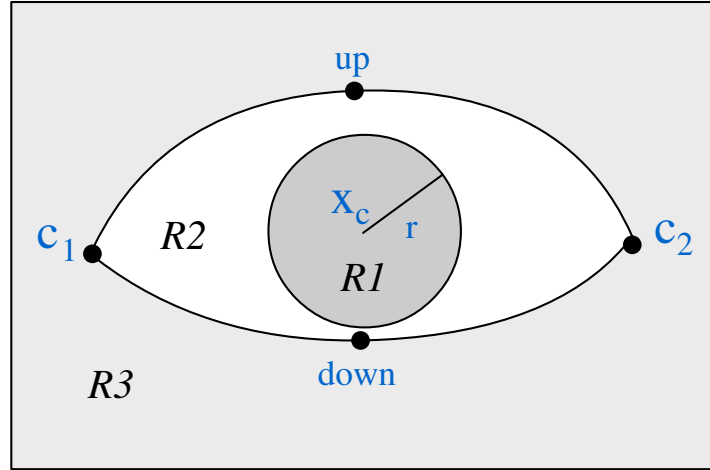
For the extraction of the left and right eyes a parametric deformable template is developed. The template exploits the intensity, and edge potentials of the eye. The details of the template is given in the following sections.

4.3.1 Template Geometry

The geometry of the Eye template is illustrated in Figure 4.11. The geometry of the template is taken from [21]. The template proposed in [18] (given in Section 3.2.4) is also evaluated, and a draft implementation is completed, but as a less rigid template we have chosen the template geometry proposed in [21].



(a)



(b)

Figure 4.11: The geometry of the deformable eye template. R_1 is the planar domain that represents the iris, R_2 is the planar domain that represents the whites of the eye, and R_3 is the planar domain that represents the surroundings of the eye. x_c is the iris center, r is the iris radius, c_1 and c_2 correspond to the corners of the eye, and up , $down$ are points that define the upper and lower contour of the eye

Table 4.3: The geometrical constraints of the eye template. The constraints are adapted from the energy function developed in [18]. XT denotes the template center, $XT = (c_1 + c_2 + up + down)/4$, and TW denotes the template width, which is $TW = ||c_1 - c_2||$.

	Constraint	Formal Representation
1.	Iris center coincides with the template center	$xc = XT$
2.	Iris radius is a fourth of the template width	$4r = TW$
3.	up is twice as far from the template center as $down$	$ XT - up = 2 XT - down $
4.	Distance from up to template center is a fourth of template width	$4 XT - up = TW$
5.	up and $down$ are horizontally in the middle	$up_x = XT_x$ $down_x = XT_x$
6.	template is truly horizontal	$c_{1y} = c_{2y}$

After developing the geometry of the template, we constructed a list of constraints pertaining the geometry. This constraints are listed in Table 4.3

The constraints presented in Table 4.3 are used to develop an energy function (E_{prior}) which will aid us during matching. E_{prior} is developed using the facts presented in Section 4.2.1 as follows:

$$\begin{aligned}
E_{prior} = & k_1(xc - XT)^2 + k_2(4r - TW)^2 \\
& + k_3(||XT - up|| - 2||XT - down||)^2 + k_4(4||XT - up|| - TW)^2 \\
& + k_5 [(up_x - XT_x)^2 + (down_x - XT_x)^2] + k_6(c_{1y} - c_{2y})^2 \quad (4.10)
\end{aligned}$$

4.3.2 Imaging Model

The imaging model of the eye template is designed to exploit the intensity, and edge potentials of the underlying image. The imaging model is given in Table 4.4. The developed geometry and imaging model is used for locating the detailed shape and position information of the left and right eyes.

The energy function E_{data} that combines the properties listed in Table 4.4 is

Table 4.4: The imaging model of the eye template. $I(x, y)$ denotes the intensities, and $\Psi_e(x, y)$ denotes the edge potential. ∂T denotes the border of the template, and it is defined as the union of the line segments as follows : $\partial T = |c_1 up| \cup |upc_2| \cup |c_2 down| \cup |downc_1|$. The measure of darkness M_D is adapted from the measure of fit proposed for valley detection [34] described in Section 2.1.5.

	Property	Formal Representation
1.	Eye boundary correspond to regions having high edge values in the image	Choose all parameters to maximize $\int_{s \in \partial T} \Psi_e(x, y) ds$
2.	Iris is darker than eye whites	Choose all parameters to maximize the darkness measure $M_D = \frac{\hat{\mu}_2 - \hat{\mu}_1}{h + \gamma \sqrt{\tilde{n}_2 \hat{\sigma}_2^2 + \tilde{n}_1 \hat{\sigma}_1^2}}$ <p>where the subscript 1 denotes the region R_1, and subscript 2 denotes the region R_2 (See Figure 4.11)</p>

developed as follows :

$$E_{data} = -k_7 \int_{s \in \partial T} \Psi_e(x, y) ds - k_8 \left(\frac{\hat{\mu}_2 - \hat{\mu}_1}{h + \gamma \sqrt{\tilde{n}_2 \hat{\sigma}_2^2 + \tilde{n}_1 \hat{\sigma}_1^2}} \right) \quad (4.11)$$

The matching algorithm of the deformable template and implementation issues will be described in the following sections.

4.3.3 Matching Algorithm

The designed matching algorithm is an energy minimization algorithm. The energy of the template $E_{eye} = E_{prior} + E_{data}$ is given below:

$$\begin{aligned}
E_{eye} = & k_1(xc - XT)^2 + k_2(4r - TW)^2 \\
& + k_3(||XT - up|| - 2||XT - down||)^2 + k_4(4||XT - up|| - TW)^2 \\
& + k_5 [(up_x - XT_x)^2 + (down_x - XT_x)^2] + k_6(c_{1y} - c_{2y})^2 \\
& - k_7 \int_{s \in \partial T} \Psi_e(x, y) ds - k_8 \left(\frac{\hat{\mu}_2 - \hat{\mu}_1}{h + \gamma \sqrt{\tilde{n}_2 \hat{\sigma}_2^2 + \tilde{n}_1 \hat{\sigma}_1^2}} \right) \quad (4.12)
\end{aligned}$$

The minimization of this energy function is performed by employing the Downhill Simplex algorithm. In order to find the optimum parameters c_1 , c_2 ,

up , $down$, r , and xc that minimizes the energy function we developed a multi-epoch algorithm. The epochs provide a coarse to fine grain optimization.

4.3.4 Implementation Issues

In this section, we will provide the important issues regarding the implementation of the eye template.

4.3.4.1 Template Geometry Issues

In the following paragraphs the implementation issues regarding the geometry of the template is discussed.

4.3.4.1.1 Computing The Initial Geometry Similar to Eyebrow template, considering the geometric constraints of the eye template given in Table 4.3, we compute the initial geometry using Algorithm 4.6

4.3.4.1.2 Surroundings of The Eye Eye template does not rely on any computations based on its surroundings, thus the margins are not as important as those of the Eyebrow template. For that reason we just set a 2 pixel margin for all sides.

4.3.4.1.3 Preventing The Geometry From Building An Invalid Shape Similar to Eyebrow template, we developed a penalty mechanism for preventing the template to get stuck to invalid shapes. Experimentation proved that eye template is more likely to get stuck in invalid shapes, so we developed a more thorough penalty mechanism. The penalty mechanism is given in Algorithm 4.7

4.3.4.2 Image Boundary Considerations

Image boundary considerations for the Eye template is the same as those of Eyebrow template presented in section 4.2.4.2.


```

Assume screen coordinates (y increases downwards)
Let box be the rectangular bounding box
Let  $\lambda$  a number showing the preference of valleyiness to circle measure
Let  $N$  be the number of top scoring circles to consider using Hough
transform
1. Find the iris parameters
1.1. Find top  $N$  circles using Hough transform in box, as iris candidates
1.2. For each candidate circle calculate an iris measure
 $M = \lambda * ValleyMeasure_{candidate} + HoughCircleMeasure_{candidate}$ 
1.3. Select the circle with maximum  $M$  as the circle identifying iris (iris)
2. Calculate auxiliary variables
2.1. Set  $width = 6 \times iris.radius$ 
3. Calculate the final geometry parameters
3.1 Set  $c_1 = \text{new Point}( iris.x - width/2, iris.y )$ 
3.1 Set  $c_2 = \text{new Point}( iris.x + width/2, iris.y )$ 
3.2 Set  $up = \text{new Point}( iris.x, iris.y - iris.radius )$ 
3.3 Set  $down = \text{new Point}( iris.x, iris.y + iris.radius )$ 
3.2 Set  $xc = \text{new Point}( iris.x, iris.y )$ 
3.3 Set  $r = iris.radius$ 

```

Algorithm 4.6: Computing the initial geometry of the eye template. The algorithm calculates initial geometry parameters (c_1 , c_2 , up , $down$, xc and r) given a rectangular bounding box.

4.3.4.3 Energy Calculation Issues

In the following paragraphs we will discuss the issues pertaining the calculation of E_{data}

4.3.4.3.1 Finding Where A Given Point Lies In The Template Ge-

ometry Similar to eyebrow template, a mechanism is needed to find where the a point lies in the template geometry. This classification is performed as given in Algorithm 4.8. The algorithm classifies a given point as one of the followings:

- outside,
- eye boundary,
- eye white,

1. if *up* appears below *down*, then add $PENALTY \times |up_y - down_y|$ to E_{eye}
2. if *up* appears below c_1 , then add $PENALTY \times |up_y - c_{1y}|$ to E_{eye}
3. if *up* appears below c_2 , then add $PENALTY \times |up_y - c_{2y}|$ to E_{eye}
4. if *down* appears above c_1 , then add $PENALTY \times |down_y - c_{1y}|$ to E_{eye}
5. if *down* appears above c_2 , then add $PENALTY \times |down_y - c_{2y}|$ to E_{eye}
6. if c_2 appears in the left side of c_1 , then add $PENALTY \times |c_{2x} - c_{1x}|$ to E_{eye}
7. if *up* appears in the left side of c_1 , then add $PENALTY \times |up_x - c_{1x}|$ to E_{eye}
8. if *down* appears in the left side of c_1 , then add $PENALTY \times |down_x - c_{1x}|$ to E_{eye}
9. if *up* appears in the right side of c_2 , then add $PENALTY \times |up_x - c_{2x}|$ to E_{eye}
10. if *down* appears in the right side of c_2 , then add $PENALTY \times |down_x - c_{2x}|$ to E_{eye}

Algorithm 4.7: Penalty mechanism for the eye template, used for preventing the geometry from building an invalid shape.

Let p be a given point for which we need to be classified

1. If p is outside the boundary of the polygon defined by points c_1 , c_2 , up and $down$
 - 1.1 return OUTSIDE
2. else if distance of p to at least one of the line segments $|c_1up|$, $|upc_2|$, $|c_2down|$, $|downc_1|$ is smaller than or equal to 1.
 - 2.1 return EYE BOUNDARY
3. else if $||xc - p|| < R$ contains p
 - 3.1 return IRIS
4. else if $||xc - p|| \leq R + 1$
 - 4.1. return IRIS BOUNDARY
5. else return EYE WHITE

Algorithm 4.8: Finding where a given point lies in the eye template geometry

- iris boundary, or
- iris.

4.3.4.3.2 Collecting Statistics In order to collect the statistics needed for calculating E_{data} , each point falling into the rectangular bounding box of the template geometry is traversed and different statistics are updated depending on where in the geometry this point lies. The algorithm used for collecting statistics is given in Algorithm 4.9.

4.3.4.3.3 Collected Template Statistics The algorithm collects 8 different statistics (normalized-smoothed intensity and edge statistics for four different regions: eye boundary, eye white, iris, boundar, iris) on the image.

4.3.4.4 Use of Downhill Simplex

Downhill simplex is used in the manner explained in section 4.2.4.4.

4.3.4.5 Coefficients of the Energy Function

The coefficients of the energy function is explained in section 4.2.4.2.

<p>Let R_I be the bounding box of the image</p> <p>Let R_T be the bounding box of the template</p> <ol style="list-style-type: none"> 1. Set $box = R_I \cap R_T$ 2. for each point p in box <ol style="list-style-type: none"> 2.1 if p is a EYE BOUNDARY point <ol style="list-style-type: none"> 2.1.1 collect eye boundary edge statistics for p 2.1.2 collect eye boundary intensity statistics for p 2.2. if p is an EYE WHITE point <ol style="list-style-type: none"> 2.2.1 collect white edge statistics for p 2.2.2 collect white intensity statistics for p 2.3 if p is an IRIS BOUNDARY point <ol style="list-style-type: none"> 2.3.1 collect iris boundary edge statistics for p 2.3.2 collect iris boundary intensity statistics for p 2.4 if p is an IRIS point <ol style="list-style-type: none"> 2.4.1 collect iris edge statistics for p 2.4.2 collect iris intensity statistics for p

Algorithm 4.9: Collecting statistics of eye template.

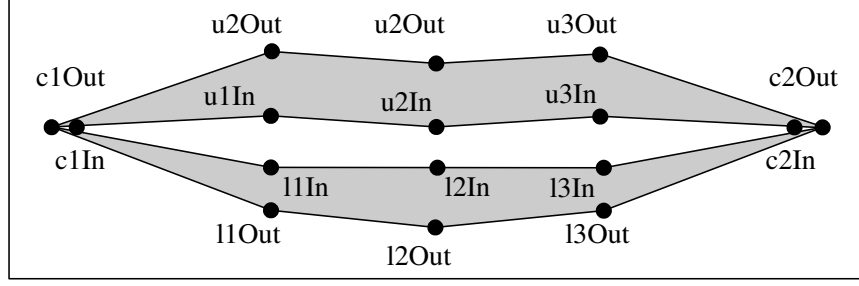
4.4 Extraction of Mouth: Mouth Deformable Template

For the extraction of the mouth, a parametric deformable template is developed. The template exploits the intensity and edge potentials of the mouth. The details of the template is given in the following sections.

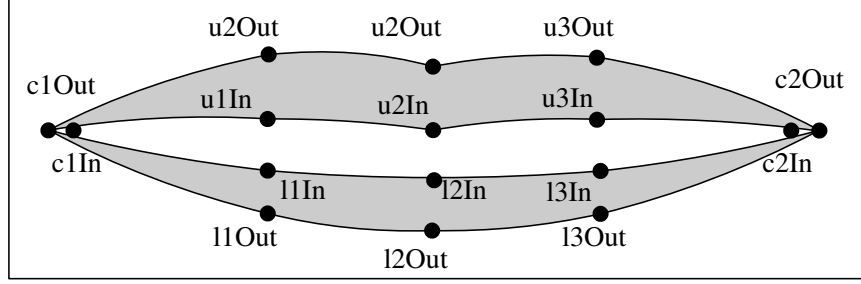
4.4.1 Template Geometry

The geometry of the Mouth template is illustrated in Figure 4.12. The geometry of the template is taken from [21]. After developing the geometry of the template. We constructed a list of constraints pertaining the geometry. This constraints are listed in Table 4.5. A closed mouth template is also constructed by combining u_1In with l_1In , u_2In with l_2In , and u_3In with l_3In .

The constraints presented in Table 4.5 are used to develop an energy function (E_{prior}) which will aid us during matching. E_{prior} is developed using the facts presented in Section 4.2.1 as follows:



(a)



(b)

Figure 4.12: The geometry of the deformable mouth template. The geometry is composed of points defining two polygons, one for the outer boundary of the mouth, and another for the inner boundary.

$$\begin{aligned}
E_{prior} = & k_1[(4||u1Out - u2Out|| - TW)^2 + (4||u2Out - u3Out|| - TW)^2 \\
& + (4||u3Out - c2Out|| - TW)^2 + (4||c2Out - l3Out|| - TW)^2 \\
& + (4||l3Out - l2Out|| - TW)^2 + (4||l2Out - l1Out|| - TW)^2 \\
& + (4||l1Out - c1Out|| - TW)^2 + (4||c1In - u1In|| - TW)^2 \\
& + (4||u1In - u2In|| - TW)^2 + (4||u2In - u3In|| - TW)^2 \\
& + (4||u3In - c2In|| - TW)^2 + (4||c2In - l3In|| - TW)^2 \\
& + (4||l3In - l2In|| - TW)^2 + (4||l2In - l1In|| - TW)^2 \\
& + (4||l1In - c1In|| - TW)^2] + k_2(||c2Out - c2In||)^2 \quad (4.13)
\end{aligned}$$

4.4.2 Imaging Model

The imaging model of the mouth template is designed to exploit the edge potentials of the underlying image. The imaging model is given in Table 4.6.

Table 4.5: The geometrical constraints of the Mouth template. TW denotes the width of the template.

	Constraint	Formal Representation
1.	points are horizontally evenly spaced in each polygons	$4 c1Out - u1Out = TW$ $4 u1Out - u2Out = TW$ $4 u2Out - u3Out = TW$ $4 u3Out - c2Out = TW$ $4 c2Out - l3Out = TW$ $4 l3Out - l2Out = TW$ $4 l2Out - l1Out = TW$ $4 l1Out - c1Out = TW$ $4 c1In - u1In = TW$ $4 u1In - u2In = TW$ $4 u2In - u3In = TW$ $4 u3In - c2In = TW$ $4 c2In - l3In = TW$ $4 l3In - l2In = TW$ $4 l2In - l1In = TW$ $4 l1In - c1In = TW$
2.	Inner and outer corners are close	$ c1Out - c1In = 0$ $ c2Out - c2In = 0$

Table 4.6: The imaging model of the Mouth template. $\Psi_e(x, y)$ denotes the edge potential. ∂T denotes the border of the template.

	Property	Formal Representation
1.	Mouth boundary correspond to regions having high edge values in the image	Choose all parameters to maximize $\int_{s \in \partial T} \Psi_e(x, y)$

The developed geometry and imaging model is used for locating the detailed shape and position information of the mouth.

The energy function E_{data} that represents the property listed in Table 4.6 is developed as follows :

$$E_{data} = -k_3 \int_{s \in \partial T} \Psi_e(x, y) ds \quad (4.14)$$

The matching algorithm of the deformable template and implementation issues will be described in the following sections.

4.4.3 Matching Algorithm

The designed matching algorithm is an energy minimization algorithm. The energy of the template $E_{mouth} = E_{prior} + E_{data}$ is given below:

$$\begin{aligned} E_{mouth} = & k_1[(4||u1Out - u2Out|| - TW)^2 + (4||u2Out - u3Out|| - TW)^2 \\ & + (4||u3Out - c2Out|| - TW)^2 + (4||c2Out - l3Out|| - TW)^2 \\ & + (4||l3Out - l2Out|| - TW)^2 + (4||l2Out - l1Out|| - TW)^2 \\ & + (4||l1Out - c1Out|| - TW)^2 + (4||c1In - u1In|| - TW)^2 \\ & + (4||u1In - u2In|| - TW)^2 + (4||u2In - u3In|| - TW)^2 \\ & + (4||u3In - c2In|| - TW)^2 + (4||c2In - l3In|| - TW)^2 \\ & + (4||l3In - l2In|| - TW)^2 + (4||l2In - l1In|| - TW)^2 \\ & + (4||l1In - c1In|| - TW)^2] + k_2(||c2Out - c2In||)^2 \\ & - k_3 \int_{s \in \partial T} \Psi_e(x, y) ds \quad (4.15) \end{aligned}$$

The minimization of this energy function is performed by employing the Downhill Simplex algorithm. The epochs provide a coarse to fine grain optimization.

4.4.4 Implementation Issues

In this section, we will provide the important issues regarding the implementation of the mouth template.

```

Let box be the rectangular bounding box
1. Calculate auxiliary variables
1.1. Set width = box.width
1.2. Set height = box.height
1.3. Set x = box.x
1.4. Set y = box.y
2. Calculate the final geometry parameters
2.1 Set c1Out = new Point( box.x, box.y + height/2 )
2.2 Set u1Out = new Point( box.x + width/4, box.y )
2.3 Set u2Out = new Point( box.x + width/2, box.y )
2.4 Set u3Out = new Point( box.x + 3*width/4, box.y )
2.5 Set c2Out = new Point( box.x + width, box.y + height/2 )
2.6 Set l3Out = new Point( box.x + 3*width/4, box.y + height )
2.7 Set l2Out = new Point( box.x + width/2, box.y + height )
2.8 Set l1Out = new Point( box.x + width/4, box.y + height )
2.9 Set c1In = new Point( box.x, box.y + height/2 )
2.10 Set u1In = new Point( box.x + width/4, box.y + height/3 )
2.11 Set u2In = new Point( box.x + width/2, box.y + height/3 )
2.12 Set u3In = new Point( box.x + 3*width/4, box.y + height/3 )
2.13 Set c2In = new Point( box.x + width, box.y + height/2 )
2.14 Set l3In = new Point( box.x + 3*width/4, box.y + 2*height/3 )
2.15 Set l2In = new Point( box.x + width/2, box.y + 2*height/3 )
2.16 Set l1In = new Point( box.x + width/4, box.y + 2*height/3 )

```

Algorithm 4.10: Computing the initial geometry of the mouth template. The algorithm calculates initial geometry parameters given a rectangular bounding box. The calculated geometry conforms to all of the constraints given in Table 4.5

4.4.4.1 Template Geometry Issues

In the following paragraphs the implementation issues regarding the geometry of the template is discussed.

4.4.4.1.1 Computing The Initial Geometry Similar to Eyebrow template, considering the geometric constraints of the eye template given in Table 4.5, we compute the initial geometry using Algorithm 4.10

- | |
|---|
| <ol style="list-style-type: none"> 1. for each point x of the inner polygon <ol style="list-style-type: none"> 1.1. if x is not in the outer domain <ol style="list-style-type: none"> 1.1.1. find the minimum distance of x to the outer polygon ($dist_x$) 1.1.2. Add $PENALTY \times (ADJUSTMENT + dist_x)$ to E_{mouth} 2. if $u1Out$ appears below $d1Out$, then add $PENALTY \times u1Out_y - d1Out_y$ to E_{mouth} 3. if $u2Out$ appears below $d2Out$, then add $PENALTY \times u2Out_y - d2Out_y$ to E_{mouth} 4. if $u3Out$ appears below $d3Out$, then add $PENALTY \times u3Out_y - d3Out_y$ to E_{mouth} 5. if $u1In$ appears below $d1In$, then add $PENALTY \times u1In_y - d1In_y$ to E_{mouth} 6. if $u2In$ appears below $d2In$, then add $PENALTY \times u2In_y - d2In_y$ to E_{mouth} 7. if $u3In$ appears below $d3In$, then add $PENALTY \times u3In_y - d3In_y$ to E_{mouth} |
|---|

Algorithm 4.11: Penalty mechanism for the mouth template, used for preventing the geometry from building an invalid shape.

4.4.4.1.2 Surroundings of The Mouth Mouth template does not rely on any computations based on its surroundings, thus the margins are not as important as those of the Eyebrow template. For that reason we just set a 2 pixel margin for all sides.

4.4.4.1.3 Preventing The Geometry From Building An Invalid Shape

Similar to Eyebrow template, we developed a penalty mechanism for preventing the template to get stuck to invalid shapes. The penalty mechanism is given in Algorithm 4.11

4.4.4.2 Image Boundary Considerations

Image boundary considerations for the Mouth template is the same as those of Eyebrow template presented in section 4.2.4.2.

Let p be a given point for which we need to be classified

1. Calculate the minimum distance of the p to the polygons
2. If any of the distances is less than or equal to 1 return BOUNDARY
3. else return NON BOUNDARY

Algorithm 4.12: Finding where a given point lies in the mouth template geometry

Let R_I be the bounding box of the image
Let R_T be the bounding box of the template

1. Set $box = R_I \cap R_T$
2. for each point p in box
 - 2.1 if p is a BOUNDARY point
 - 2.1.1 collect boundary edge statistics for p
 - 2.1.2 collect boundary intensity statistics for p

Algorithm 4.13: Collecting Statistics of Mouth Template.

4.4.4.3 Energy Calculation Issues

In the following paragraphs we will discuss the issues pertaining the calculation of E_{data}

4.4.4.3.1 Finding Where A Given Point Lies In The Template Geometry Similar to eyebrow template, a mechanism is needed to find where the a point lies in the template geometry. This classification is performed as given in Algorithm4.12. The algorithm classifies a given either a boundary or non-boundary.

4.4.4.3.2 Collecting statistics In order to collect the statistics needed for calculating E_{data} , each point falling into the rectangular bounding box of the template geometry is traversed and boundary statistics are collected. The algorithm used for Collecting Statistics is given in Algorithm 4.13.

4.4.4.3.3 Collected Template Statistics The algorithm collects 2 different statistics (normalized-smoothed intensity and edge statistics for boundaries) on the image.

4.4.4.4 Use of Downhill Simplex

Downhill simplex is used in the manner explained in section 4.2.4.4.

4.4.4.5 Coefficients of the Energy Function

The coefficients of the energy function is explained in section 4.2.4.2.

4.4.4.6 Selection of Open vs. Closed Mouth Template

The selection of open or closed mouth template for a given face image is currently performed manually.

CHAPTER 5

Results

In this chapter performance of the system is presented. Firstly, the image databases used in this study are explained. Then, the test results for the developed face detection algorithm is provided, and a discussion on the performance of the algorithm is provided. Then, the results observed for each of the deformable models are discussed separately, because each model has its own dynamics. And lastly the performance of the system as a whole is discussed.

5.1 Test Settings

Images from JAFFE (Japanese Female Facial Expression Database) [58], ORL (Olivetti Research Laboratory) [59] and Yale Faces [60] databases are used for assessing the performance of the developed face detection algorithm, deformable models and the system as a whole. JAFFE database contains 213 images of 7 facial expressions (six basic expressions plus neutral expression) belonging to 10 Japanese female models. ORL database contains 10 different images of each of 40 distinct subjects. For some of the subjects, the database contains the images taken at different times, varying lighting, facial expressions, and facial details (glasses/no glasses). And lastly, Yale Faces database contains 165 images of 15 subjects. There are 11 images per subject, one for each of the following facial

expressions or configurations: center-light, w/glasses, happy, left-light, w/no glasses, normal, right-light, sad, sleepy, surprised, and wink.

5.2 Performance of the Face Detection Algorithm

In order to assess the performance of the developed face detection algorithm, we divided all of images from JAFFE, ORL and Yale databases into two sets, one for training and the other for testing. The training set contains 100 images of faces with different illumination and facial expression, at different scales. The images are first normalized as explained in section 4.1.1, and PCA computations are performed on the normalized images. The randomly selected training images are shown in Appendix J. Then the images in the test set are used for testing the algorithm in the databases. In the tests first 90 eigenfaces are selected, and a distance to face space threshold value of 450 is used. The results of the tests are presented in Table 5.1.

Table 5.1: The results of the face detection algorithm tests

	False Detection		Correct Detection		Failure to Detect	
Name	#	%	#	%	#	%
JAFFE:	35	18	160	82	0	0
ORL:	0	0	209	100	0	0
YALE:	110	78	30	22	0	0
TOTAL:	145	26	379	74	0	0

The performance of the face detection algorithm is very poor in Yale face database, because the illumination conditions in this database are quite different from the other two databases. In fact, the illumination conditions are even different within the Yale face database. Since our algorithm does not perform any brightness equalization, varying illumination conditions dramatically affected the test results.

The 100 % success in ORL database is mainly because of the nature of the images in that database. The database consists of images that contain only a face.

5.3 Test Settings for Deformable Templates

This section describes the test settings applicable for the tests of the each of the deformable templates. The template specific settings will be provided later in the appropriate sections if applicable.

Three sets of test images are constructed by randomly selecting from each of these databases. The first set contains 20 images from the JAFFE database, the second set contains 20 images from the Yale Faces database and the last set contains 25 images from ORL database. The images contained in this sets are shown in Appendix A.

After the image sets are constructed, templates are handfitted to the images in the test sets, for right eyebrow, left eyebrow, right eye, left eye, and mouth, and the results are stored. Then, the automatic deformable template matching is performed and the results are compared with the handfitted results. The comparison is performed by taking the absolute difference of parameters between the handfitted and automatically fitted models. In order to normalize the pixel differences, we divided them to the widths of the handfitted templates in order to obtain differences between parameter values as *percent of template width* instead of *pixels*. Also an analysis is performed for classifying the templates as one of the followings:

No-hit: Template does not localize the feature at all.

Hit: Template barely finds the position of the feature, but half of its parameters are more than 20 % different from the handfitted values. (20 % is a subjective measure decided on by analysing the results)

Good: Almost all of the template parameters are within the 10 % range, with at most two points lying within the 10-20 % range.

Very Good: All of the template parameters are within the 10 % range.

The results of each template is classified using above measure, in the following sections.

5.4 Performance of the Eyebrow Template

The detailed results of the eyebrow template is given in Appendix B and Appendix C. Both polygonal and spline-based eyebrow templates are tested. The results of each test are given in detail.

The number of events and the percentage values of polygonal eyebrow template test results are given in Table 5.2.

Table 5.2: Polygonal eyebrow templates analysis results of JAFFE, YALE & ORL (%)

	$JAFFE_{avg}$				$YALE_{avg}$				ORL_{avg}			
	Left		Right		Left		Right		Left		Right	
Name	#	%	#	%	#	%	#	%	#	%	#	%
No Hit:	0	0	0	0	0	0	1	5	1	4	0	0
Hit:	0	0	0	0	2	1	0	0	2	8	0	0
Good:	8	40	5	25	7	35	4	0.2	14	58	13	54
Very Good:	12	60	15	75	11	55	15	75	7	29	11	46

The number of events and the percentage values of spline-based eyebrow template test results are given in Table 5.3.

Table 5.3: Spline-based templates analysis results of JAFFE, YALE & ORL (%)

	$JAFFE_{avg}$				$YALE_{avg}$				ORL_{avg}			
	Left		Right		Left		Right		Left		Right	
Name	#	%	#	%	#	%	#	%	#	%	#	%
No Hit:	0	0	0	0	0	0	0	0	1	04	0	0
Hit:	1	5	0	0	9	1	1	5	0	0	0	0
Good:	6	30	5	25	14	70	3	15	14	58	4	17
Very Good:	13	65	15	75	6	30	16	8	9	38	20	83

Table 5.4 depicts the performance of polygonal deformable model with regard to each template parameters. Table 5.5 depicts the performance of spline-based deformable model with regard to each template parameters. In order the understand the difference between polygonal and spline-based eyebrow templates, the comparison of the results of both templates are shown in Table 5.6.

Table 5.4: Polygonal eyebrow template analysis results of JAFFE, YALE & ORL in average pixels difference

	$JAFFE_{avg}$		$YALE_{avg}$		ORL_{avg}		$TOTAL_{avg}$	
Paramater	Left	Right	Left	Right	Left	Right	Left	Right
$c1_x$	2.16	4.97	2.73	6.38	2.88	4.65	2.59	5.33
$c1_y$	3.23	2.25	4.85	3.89	4.10	2.20	4.06	2.78
$u1_x$	3.87	3.83	4.17	3.05	4.54	2.50	4.19	3.12
$u1_y$	1.12	0.86	1.84	1.23	1.17	1.02	1.38	1.04
$u2_x$	3.86	3.50	3.90	2.70	4.49	3.33	4.08	3.18
$u2_y$	1.02	1.03	2.09	1.30	1.28	1.20	1.46	1.18
$c2_x$	5.28	2.29	6.78	4.22	5.24	2.78	5.77	3.09
$c2_y$	4.41	3.11	2.60	2.60	2.09	2.17	3.03	2.63
$l2_x$	4.42	3.02	3.76	2.30	4.99	3.22	4.39	2.85
$l2_y$	1.46	1.36	2.07	1.59	1.29	1.25	1.61	1.40
$l1_x$	3.88	3.43	3.31	3.26	4.05	0.72	3.75	3.14
$l2_y$	1.38	1.60	0.00	2.50	1.34	1.10	1.54	1.73

Table 5.5: Spline-based eyebrow template analysis results of JAFFE, YALE & ORL in average pixels difference

	$JAFFE_{avg}$		$YALE_{avg}$		ORL_{avg}		$TOTAL_{avg}$	
Parameter	Left	Right	Left	Right	Left	Right	Left	Right
$c1_x$	2.91	7.75	2.50	5.76	1.70	4.14	2.37	5.88
$c1_y$	3.01	5.02	7.26	3.82	3.04	1.57	4.44	3.47
$u1_x$	3.17	2.81	4.09	2.47	3.28	1.71	3.51	2.33
$u1_y$	1.09	0.90	1.10	1.18	0.92	0.86	1.01	0.98
$u2_x$	4.14	2.95	4.01	2.52	3.81	2.38	3.99	2.62
$u2_y$	1.08	0.89	1.57	1.25	0.70	0.89	1.12	1.01
$c2_x$	6.76	2.37	7.16	3.95	5.19	1.43	6.37	2.58
$c2_y$	4.75	2.30	1.74	1.82	1.61	2.95	2.70	2.36
$l2_x$	4.51	2.47	3.90	2.05	4.30	2.33	4.24	2.28
$l2_y$	1.26	0.85	1.53	1.26	0.74	0.81	1.18	0.97
$l1_x$	3.23	3.81	3.20	2.39	2.81	2.18	3.08	2.79
$l2_y$	1.34	1.24	2.21	1.44	0.99	1.02	1.51	1.23

Table 5.6: Comparison of polygonal and spline-based eyebrow templates

	$JAFFE_{avg}$		$YALE_{avg}$		ORL_{avg}	
Parameter	Eyebrow	Eyebrow2	Eyebrow	Eyebrow2	Eyebrow	Eyebrow2
$c1_x$	3.56	5.33	4.55	4.13	3.77	2.92
$c1_y$	2.74	4.02	4.37	5.54	3.15	2.31
$u1_x$	3.85	2.99	3.61	3.28	3.52	2.50
$u1_y$	0.99	0.99	1.54	1.14	1.10	0.89
$u2_x$	3.68	3.55	3.30	3.26	3.91	3.09
$u2_y$	1.02	0.98	1.69	1.141	1.24	0.80
$c2_x$	3.78	4.56	5.50	5.56	4.01	3.31
$c2_y$	3.76	3.2	2.60	1.78	2.13	2.28
$l2_x$	3.72	3.49	3.03	2.97	4.10	3.31
$l2_y$	1.41	1.06	1.83	1.39	1.27	0.77
$l1_x$	3.66	3.52	3.28	2.79	3.39	2.49
$l2_y$	1.49	1.29	2.21	1.82	1.22	1.00

5.5 Performance of the Eye Template

The detailed results of the eye template is given in Appendix D and Appendix E. Both polygonal and spline-based eye templates are tested. The results of each test are given in detail.

The number of events and the percentage values of polygonal eye template test results are given in Table 5.9.

Table 5.7: Polygonal eye templates analysis results of JAFFE, YALE & ORL (%)

	$JAFFE_{avg}$				$YALE_{avg}$				ORL_{avg}			
	Left		Right		Left		Right		Left		Right	
Name	#	%	#	%	#	%	#	%	#	%	#	%
No Hit:	0	0	0	0	1	5	2	10	0	0	0	0
Hit:	0	0	0	0	1	5	2	10	1	4	0	0
Good:	0	0	0	0	1	5	2	10	5	21	5	21
Very Good:	20	100	15	100	17	85	14	70	18	75	19	79

The number of events and the percentage values of spline-based eye template test results are given in Table 5.10.

Table 5.9 depicts the performance of polygonal deformable model with regard to each template parameters.

Table 5.8: Spline-based eye template analysis results of JAFFE, YALE & ORL (%)

	$JAFFE_{avg}$				$YALE_{avg}$				ORL_{avg}			
	Left		Right		Left		Right		Left		Right	
Name	#	%	#	%	#	%	#	%	#	%	#	%
No Hit:	0	0	0	0	0	0	3	15	0	0	0	0
Hit:	0	0	0	0	1	5	0	0	0	0	0	0
Good:	0	0	0	0	2	1	1	5	9	38	7	29
Very Good:	20	100	20	100	17	85	16	80	15	63	17	71

Table 5.9: Polygonal eye templates analysis results of JAFFE, YALE & ORL in average pixels difference

Parameter	$JAFFE_{avg}$		$YALE_{avg}$		ORL_{avg}		$TOTAL_{avg}$	
	Left	Right	Left	Right	Left	Right	Left	Right
xc	0.61	0.73	7.75	11.15	1.28	0.76	3.21	4.22
yc	0.73	0.95	7.47	7.78	0.58	0.53	2.93	3.09
r	0.80	0.77	0.82	0.78	0.54	0.47	0.72	0.67
$c1_x$	2.10	2.06	7.31	11.33	3.22	3.20	4.21	5.53
$c1_y$	3.66	1.38	8.86	8.50	0.78	0.76	4.43	3.55
$c2_x$	2.54	2.42	8.87	13.20	2.89	1.90	4.77	5.4
$c2_y$	3.02	1.35	7.89	7.80	1.39	1.86	4.10	3.67
up_x	1.86	1.85	8.46	12.48	1.99	2.02	4.10	5.45
up_y	1.61	1.59	7.81	8.01	1.05	1.28	3.49	3.63
$down_x$	1.28	1.33	7.47	11.56	1.24	0.97	3.33	4.62
$down_y$	0.95	0.87	8.30	7.87	2.88	2.26	4.04	3.67

Table 5.10 depicts the performance of spline-based deformable model with regard to each template parameters.

In order the understand the difference between polygonal and spline-based eye templates, the comparison of the results of both templates are shown in Table 5.11.

Table 5.10: Spline-based eye templates analysis results of JAFFE, YALE & ORL in average pixels difference

	$JAFFE_{avg}$		$YALE_{avg}$		ORL_{avg}		$TOTAL_{avg}$	
Parameter	Left	Right	Left	Right	Left	Right	Left	Right
xc	0.72	1.32	7.30	1.16	1.10	0.89	3.04	1.12
yc	1.15	0.90	7.62	1.04	0.53	0.51	3.10	0.82
r	0.63	0.53	0.87	0.80	0.64	0.43	0.71	0.59
$c1_x$	1.89	2.74	7.18	1.92	3.70	3.28	4.26	2.65
$c1_y$	4.52	1.91	8.83	1.67	0.63	0.94	4.66	1.50
$c2_x$	2.25	1.91	8.39	2.75	2.36	1.24	4.33	1.97
$c2_y$	2.55	1.50	7.96	1.21	1.42	1.88	3.98	1.53
up_x	2.57	2.56	8.71	2.77	2.43	2.66	4.57	2.66
up_y	1.73	1.61	7.76	1.64	1.38	1.59	3.62	1.61
$down_x$	1.77	1.85	7.07	1.55	1.11	1.07	3.31	1.49
$down_y$	1.37	1.35	8.08	1.22	1.90	1.97	3.78	1.51

Table 5.11: Comparison of polygonal and spline-based eye templates

	$JAFFE_{avg}$		$YALE_{avg}$		ORL_{avg}	
Parameter	Eye	Eye2	Eye	Eye2	Eye	Eye2
xc	0.67	1.02	9.45	4.23	1.02	0.99
yc	0.84	1.03	7.62	4.33	0.56	0.52
r	0.78	0.58	0.80	0.84	0.51	0.53
$c1_x$	2.08	2.31	9.32	4.55	3.21	3.49
$c1_y$	2.52	3.21	8.68	5.25	0.77	0.79
$c2_x$	2.48	2.08	11.03	5.57	2.40	1.80
$c2_y$	2.18	2.02	7.84	4.59	1.63	1.65
up_x	1.85	2.57	10.47	5.74	2.01	2.54
up_y	1.60	1.67	7.91	4.70	1.17	1.49
$down_x$	1.31	1.81	9.51	4.31	1.10	1.09
$down_y$	0.91	1.36	8.09	4.65	2.57	1.94

5.6 Performance of the Mouth Template

Test results are in Appendix F, Appendix G, Appendix H, and Appendix I. Both polygonal and spline-based mouth templates are tested. The results of each test are given in detail.

The number of occurrences and the percentage values of polygonal mouth closed template test results are given in Table 5.16.

Table 5.12: Polygonal mouth-closed template analysis results of JAFFE, YALE & ORL (%)

Name	$JAFFE_{avg}$		$YALE_{avg}$		ORL_{avg}	
Name	#	%	#	%	#	%
No Hit:	0	0	0	0	1	7
Hit:	0	0	0	0	0	0
Good:	0	0	9	50	2	14
Very Good:	14	100	9	50	11	79

The number of occurrences and the percentage values of spline-based mouth closed template test results are given in Table 5.16.

Table 5.13: Spline-based mouth-closed template analysis results of JAFFE, YALE & ORL (%)

Name	$JAFFE_{avg}$		$YALE_{avg}$		ORL_{avg}	
Name	#	%	#	%	#	%
No Hit:	0	0	0	0	2	13
Hit:	0	0	0	0	1	7
Good:	0	0	8	44	2	13
Very Good:	14	100	10	56	12	80

The number of events and the percentage values of polygonal mouth open template test results are given in Table 5.18.

The number of occurrences and the percentage values of spline-based mouth open template test results are given in Table 5.19.

Table 5.16 depicts the performance of polygonal mouth-closed deformable model with regard to each template parameters.

Table 5.17 depicts the performance of spline-based mouth-closed deformable model with regard to each template parameters.

Table 5.14: Polygonal mouth-open template analysis results of JAFFE, YALE & ORL (%)

Name	$JAFFE_{avg}$		$YALE_{avg}$		ORL_{avg}	
Name	#	%	#	%	#	%
No Hit:	0	0	0	0	0	0
Hit:	0	0	0	0	0	0
Good:	0	0	1	50	0	0
Very Good:	6	100	1	50	9	100

Table 5.15: Spline-based mouth-open template analysis results of JAFFE, YALE & ORL (%)

Name	$JAFFE_{avg}$		$YALE_{avg}$		ORL_{avg}	
Name	#	%	#	%	#	%
No Hit:	0	0	0	0	0	0
Hit:	0	0	0	0	0	0
Good:	0	0	1	50	1	11
Very Good:	6	100	1	50	8	89

Table 5.18 depicts the performance of polygonal mouth open deformable model with regard to each template parameters.

Table 5.19 depicts the performance of spline-based mouth open deformable model with regard to each template parameters.

In order to understand the difference between polygonal and spline-based mouth-closed templates, the comparison of the results of both templates are shown in Table 5.20.

In order to understand the difference between polygonal and spline-based mouth open templates, the comparison of the results of both templates are shown in Table 5.21.

Table 5.16: Polygonal mouth-closed template analysis results of JAFFE, YALE & ORL in average pixels difference

Parameter	$JAFFE_{avg}$	$YALE_{avg}$	ORL_{avg}	$TOTAL_{avg}$
$c1_{out_x}$	2.81	9.96	2.62	5.13
$c1_{out_y}$	2.12	4.51	3.52	3.39
$u1_{out_x}$	2.05	6.52	2.34	3.63
$u1_{out_y}$	1.47	1.91	2.22	1.87
$u2_{out_x}$	2.84	6.34	2.23	3.81
$u2_{out_y}$	1.33	3.97	2.18	2.49
$u3_{out_x}$	1.26	7.35	2.00	3.54
$u3_{out_y}$	2.36	1.72	2.41	2.16
$c2_{out_x}$	4.63	9.10	2.85	5.53
$c2_{out_y}$	2.43	4.34	3.27	3.35
$d3_{out_x}$	1.60	7.42	2.31	3.77
$d3_{out_y}$	4.10	2.70	2.65	3.15
$d2_{out_x}$	2.74	6.28	2.51	3.85
$d2_{out_y}$	3.19	4.88	3.13	3.74
$d1_{out_x}$	2.35	6.61	2.72	3.89
$d1_{out_y}$	4.27	2.75	3.26	3.43
$c1_{in_x}$	2.81	9.96	2.62	5.13
$c1_{in_y}$	2.12	4.51	3.52	3.39
$u1_{in_x}$	2.98	6.16	2.45	3.87
$u1_{in_y}$	3.76	2.70	2.97	3.14
$u2_{in_x}$	2.68	6.45	2.25	3.79
$u2_{in_y}$	3.87	4.32	2.72	3.64
$u3_{in_x}$	2.99	8.00	2.29	4.43
$u3_{in_y}$	3.35	3.11	2.58	3.01
$c2_{in_x}$	4.63	9.10	2.85	5.53
$c2_{in_y}$	2.43	4.34	3.27	3.35
$d3_{in_x}$	2.99	8.00	2.29	4.43
$d3_{in_y}$	3.35	3.11	2.58	3.01
$d2_{in_x}$	2.68	6.45	2.25	3.79
$d2_{in_y}$	3.87	4.32	2.72	3.64
$d1_{in_x}$	2.98	6.16	2.45	3.87
$d1_{in_y}$	3.76	2.70	2.97	3.14

Table 5.17: Spline-based mouth-closed template analysis results of JAFFE, YALE & ORL in average pixels difference

Parameter	$JAFFE_{avg}$	$YALE_{avg}$	ORL_{avg}	$TOTAL_{avg}$
$c1_{out_x}$	1.63	5.67	1.47	2.92
$c1_{out_y}$	1.59	4.09	3.05	2.91
$u1_{out_x}$	2.29	5.38	1.61	3.09
$u1_{out_y}$	1.01	2.15	2.32	1.83
$u2_{out_x}$	2.73	5.25	2.33	3.44
$u2_{out_y}$	1.61	3.59	2.92	2.71
$u3_{out_x}$	2.28	6.05	2.37	3.56
$u3_{out_y}$	1.54	2.07	2.22	1.94
$c2_{out_x}$	1.90	6.37	2.40	3.56
$c2_{out_y}$	1.18	3.87	3.49	2.85
$d3_{out_x}$	1.92	5.74	2.08	3.25
$d3_{out_y}$	2.70	3.40	3.05	3.05
$d2_{out_x}$	2.47	4.89	2.20	3.19
$d2_{out_y}$	1.68	4.45	4.28	3.47
$d1_{out_x}$	2.86	5.39	1.77	3.34
$d1_{out_y}$	2.75	3.56	3.12	3.14
$c1_{in_x}$	1.63	5.67	1.47	2.92
$c1_{in_y}$	1.59	4.09	3.05	2.91
$u1_{in_x}$	2.99	5.24	2.07	3.43
$u1_{in_y}$	3.24	3.04	2.79	3.02
$u2_{in_x}$	2.95	4.81	2.08	3.28
$u2_{in_y}$	2.88	4.18	3.25	3.44
$u3_{in_x}$	2.20	5.53	1.81	3.18
$u3_{in_y}$	3.05	3.46	2.37	2.96
$c2_{in_x}$	1.90	6.37	2.40	3.56
$c2_{in_y}$	1.18	3.87	3.49	2.85
$d3_{in_x}$	2.20	5.53	1.81	3.18
$d3_{in_y}$	3.05	3.46	2.37	2.96
$d2_{in_x}$	2.95	4.81	2.08	3.28
$d2_{in_y}$	2.88	4.18	3.25	3.44
$d1_{in_x}$	2.99	5.24	2.07	3.43
$d1_{in_y}$	3.24	3.04	2.79	3.02

Table 5.18: Polygonal mouth-open template analysis results of JAFFE, YALE & ORL in average pixels difference

Parameter	$JAFFE_{avg}$	$YALE_{avg}$	ORL_{avg}	$TOTAL_{avg}$
$c1_{out_x}$	1.88	7.03	1.79	4.19
$c1_{out_y}$	5.81	6.14	2.80	6.85
$u1_{out_x}$	1.46	7.16	1.73	3.94
$u1_{out_y}$	2.08	0.73	1.25	2.05
$u2_{out_x}$	1.77	7.25	2.16	4.32
$u2_{out_y}$	4.33	5.49	1.34	5.16
$u3_{out_x}$	2.10	7.74	1.73	4.55
$u3_{out_y}$	1.33	0.23	1.12	1.34
$c2_{out_x}$	3.21	10.04	2.36	6.27
$c2_{out_y}$	4.53	7.40	2.50	6.32
$d3_{out_x}$	2.07	7.47	2.08	4.57
$d3_{out_y}$	2.52	3.00	1.80	3.28
$d2_{out_x}$	1.93	5.70	2.29	3.95
$d2_{out_y}$	7.13	7.84	3.15	8.42
$d1_{out_x}$	2.15	4.77	1.77	3.61
$d1_{out_y}$	2.99	3.46	2.06	3.84
$c1_{in_x}$	2.39	6.70	1.86	4.45
$c1_{in_y}$	4.45	5.98	2.27	5.71
$u1_{in_x}$	2.09	6.16	1.99	4.11
$u1_{in_y}$	2.92	4.86	2.35	4.35
$u2_{in_x}$	2.14	8.25	2.45	5.00
$u2_{in_y}$	4.67	8.28	2.34	6.66
$u3_{in_x}$	4.24	9.41	2.68	6.85
$u3_{in_y}$	3.48	4.52	2.40	4.63
$c2_{in_x}$	5.81	11.86	3.82	9.10
$c2_{in_y}$	4.03	7.09	2.28	5.81
$d3_{in_x}$	4.41	10.54	3.67	7.68
$d3_{in_y}$	1.61	4.95	2.12	3.43
$d2_{in_x}$	1.63	6.38	1.96	3.86
$d2_{in_y}$	3.77	0.48	2.23	3.41
$d1_{in_x}$	2.76	3.81	1.61	3.64
$d1_{in_y}$	2.55	3.32	2.22	3.54

Table 5.19: Spline-based mouth-open template analysis results of JAFFE, YALE & ORL in average pixels difference

Parameter	$JAFFE_{avg}$	$YALE_{avg}$	ORL_{avg}	$TOTAL_{avg}$
$c1_{out_x}$	3.19	5.16	1.59	2.66
$c1_{out_y}$	6.98	10.73	2.50	5.49
$u1_{out_x}$	2.32	3.79	1.39	2.01
$u1_{out_y}$	1.60	2.67	1.32	1.50
$u2_{out_x}$	2.86	2.38	2.70	2.81
$u2_{out_y}$	2.43	7.42	2.09	2.31
$u3_{out_x}$	3.36	1.94	2.41	3.04
$u3_{out_y}$	0.79	2.17	1.70	1.09
$c2_{out_x}$	2.93	1.90	2.42	2.76
$c2_{out_y}$	5.70	11.39	2.40	4.60
$d3_{out_x}$	3.12	3.20	1.96	2.73
$d3_{out_y}$	3.49	8.12	2.34	3.11
$d2_{out_x}$	2.60	1.62	2.36	2.52
$d2_{out_y}$	2.33	9.30	2.41	2.36
$d1_{out_x}$	1.86	1.43	2.09	1.94
$d1_{out_y}$	4.21	7.94	2.73	3.72
$c1_{in_x}$	2.80	4.83	1.36	2.32
$c1_{in_y}$	5.53	10.56	1.84	4.30
$u1_{in_x}$	3.12	2.79	1.31	2.52
$u1_{in_y}$	2.02	5.79	1.87	1.97
$u2_{in_x}$	3.41	3.38	2.59	3.14
$u2_{in_y}$	1.80	9.22	2.22	1.94
$u3_{in_x}$	4.27	3.04	2.26	3.60
$u3_{in_y}$	2.41	5.46	2.00	2.27
$c2_{in_x}$	5.07	3.49	2.43	4.19
$c2_{in_y}$	5.20	10.56	2.12	4.17
$d3_{in_x}$	3.43	3.90	2.44	3.10
$d3_{in_y}$	1.11	3.69	1.72	1.31
$d2_{in_x}$	2.43	1.51	2.45	2.43
$d2_{in_y}$	2.82	6.63	2.72	2.79
$d1_{in_x}$	2.89	1.20	2.13	2.63
$d1_{in_y}$	1.96	2.28	1.83	1.92

Table 5.20: Comparison of polygonal and spline-based mouth-closed templates

	$JAF F E_{avg}$		$Y A L E_{avg}$		$O R L_{avg}$	
Parameter	Polygonal	Spline	Polygonal	Spline	Polygonal	Spline
$c1_{out_x}$	2.81	1.63	9.96	5.67	2.62	1.47
$c1_{out_y}$	2.12	1.59	4.51	4.09	3.52	3.05
$u1_{out_x}$	2.05	2.29	6.52	5.38	2.34	1.61
$u1_{out_y}$	1.47	1.01	1.91	2.15	2.22	2.32
$u2_{out_x}$	2.84	2.73	6.34	5.25	2.23	2.33
$u2_{out_y}$	1.33	1.61	3.97	3.59	2.18	2.92
$u3_{out_x}$	1.26	2.28	7.35	6.05	2.00	2.37
$u3_{out_y}$	2.36	1.54	1.72	2.07	2.41	2.22
$c2_{out_x}$	4.63	1.90	9.10	6.37	2.85	2.40
$c2_{out_y}$	2.43	1.18	4.34	3.87	3.27	3.49
$d3_{out_x}$	1.60	1.92	7.42	5.74	2.31	2.08
$d3_{out_y}$	4.10	2.70	2.70	3.40	2.65	3.05
$d2_{out_x}$	2.74	2.47	6.28	4.89	2.51	2.20
$d2_{out_y}$	3.19	1.68	4.88	4.45	3.13	4.28
$d1_{out_x}$	2.35	2.86	6.61	5.39	2.72	1.77
$d1_{out_y}$	4.27	2.75	2.75	3.56	3.26	3.12
$c1_{in_x}$	2.81	1.63	9.96	5.67	2.62	1.47
$c1_{in_y}$	2.12	1.59	4.51	4.09	3.52	3.05
$u1_{in_x}$	2.98	2.99	6.16	5.24	2.45	2.07
$u1_{in_y}$	3.76	3.24	2.70	3.04	2.97	2.79
$u2_{in_x}$	2.68	2.95	6.45	4.81	2.25	2.08
$u2_{in_y}$	3.87	2.88	4.32	4.18	2.72	3.25
$u3_{in_x}$	2.99	2.20	8.00	5.53	2.29	1.81
$u3_{in_y}$	3.35	3.05	3.11	3.46	2.58	2.37
$c2_{in_x}$	4.63	1.90	9.10	6.37	2.85	2.40
$c2_{in_y}$	2.43	1.18	4.34	3.87	3.27	3.49
$d3_{in_x}$	2.99	2.20	8.00	5.53	2.29	1.81
$d3_{in_y}$	3.35	3.05	3.11	3.46	2.58	2.37
$d2_{in_x}$	2.68	2.95	6.45	4.81	2.25	2.08
$d2_{in_y}$	3.87	2.88	4.32	4.18	2.72	3.25
$d1_{in_x}$	2.98	2.99	6.16	5.24	2.45	2.07
$d1_{in_y}$	3.76	3.24	2.70	3.04	2.97	2.79

Table 5.21: Comparison of polygonal and spline-based mouth-open templates

Parameter	$JAFPE_{avg}$		$YALE_{avg}$		ORL_{avg}	
	Polygonal	Spline	Polygonal	Spline	Polygonal	Spline
$c1_{out_x}$	1.88	3.19	7.03	5.16	1.79	1.59
$c1_{out_y}$	5.81	6.98	6.14	10.73	2.80	2.50
$u1_{out_x}$	1.46	2.32	7.16	3.79	1.73	1.39
$u1_{out_y}$	2.08	1.60	0.73	2.67	1.25	1.32
$u2_{out_x}$	1.77	2.86	7.25	2.38	2.16	2.70
$u2_{out_y}$	4.33	2.43	5.49	7.42	1.34	2.09
$u3_{out_x}$	2.10	3.36	7.74	1.94	1.73	2.41
$u3_{out_y}$	1.33	0.79	0.23	2.17	1.12	1.70
$c2_{out_x}$	3.21	2.93	10.04	1.90	2.36	2.42
$c2_{out_y}$	4.53	5.70	7.40	11.39	2.50	2.40
$d3_{out_x}$	2.07	3.12	7.47	3.20	2.08	1.96
$d3_{out_y}$	2.52	3.49	3.00	8.12	1.80	2.34
$d2_{out_x}$	1.93	2.60	5.70	1.62	2.29	2.36
$d2_{out_y}$	7.13	2.33	7.84	9.30	3.15	2.41
$d1_{out_x}$	2.15	1.86	4.77	1.43	1.77	2.09
$d1_{out_y}$	2.99	4.21	3.46	7.94	2.06	2.73
$c1_{in_x}$	2.39	2.80	6.70	4.83	1.86	1.36
$c1_{in_y}$	4.45	5.53	5.98	10.56	2.27	1.84
$u1_{in_x}$	2.09	3.12	6.16	2.79	1.99	1.31
$u1_{in_y}$	2.92	2.02	4.86	5.79	2.35	1.87
$u2_{in_x}$	2.14	3.41	8.25	3.38	2.45	2.59
$u2_{in_y}$	4.67	1.80	8.28	9.22	2.34	2.22
$u3_{in_x}$	4.24	4.27	9.41	3.04	2.68	2.26
$u3_{in_y}$	3.48	2.41	4.52	5.46	2.40	2.00
$c2_{in_x}$	5.81	5.07	11.86	3.49	3.82	2.43
$c2_{in_y}$	4.03	5.20	7.09	10.56	2.28	2.12
$d3_{in_x}$	4.41	3.43	10.54	3.90	3.67	2.44
$d3_{in_y}$	1.61	1.11	4.95	3.69	2.12	1.72
$d2_{in_x}$	1.63	2.43	6.38	1.51	1.96	2.45
$d2_{in_y}$	3.77	2.82	0.48	6.63	2.23	2.72
$d1_{in_x}$	2.76	2.89	3.81	1.20	1.61	2.13
$d1_{in_y}$	2.55	1.96	3.32	2.28	2.22	1.83

5.7 General Findings on Deformable Templates

According to the test results the following findings are obtained:

1. The developed deformable templates for eye, eyebrow, and mouth produced reasonable results. In some cases the deformable templates performed badly. Sample results are provided in Figure 5.1, 5.2, 5.4, 5.4. Sample results of the system as a whole is provided in Figure 5.8.

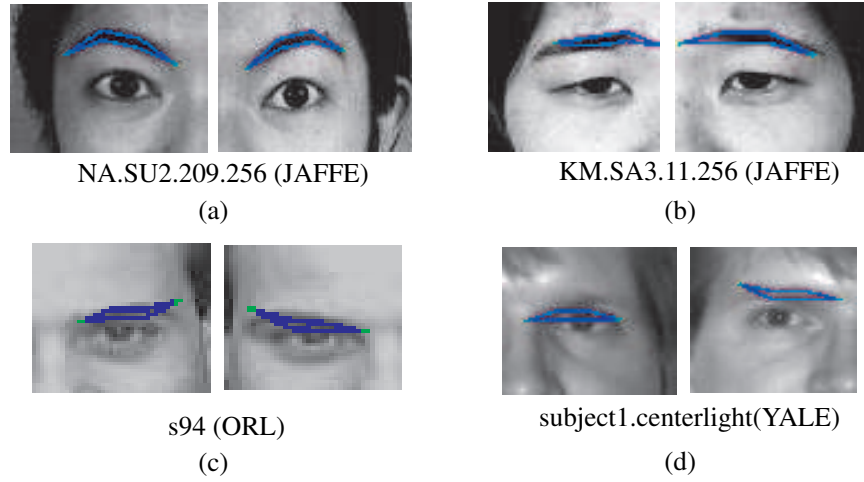


Figure 5.1: Sample results of the polygonal eyebrow template

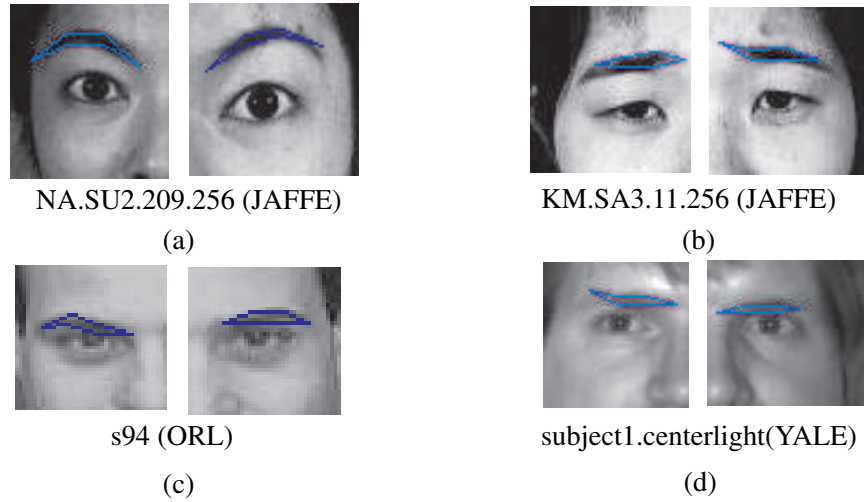


Figure 5.2: Sample results of the spline-based eyebrow template

2. Using a single eye and eyebrow template for both left and right features yields acceptable results.

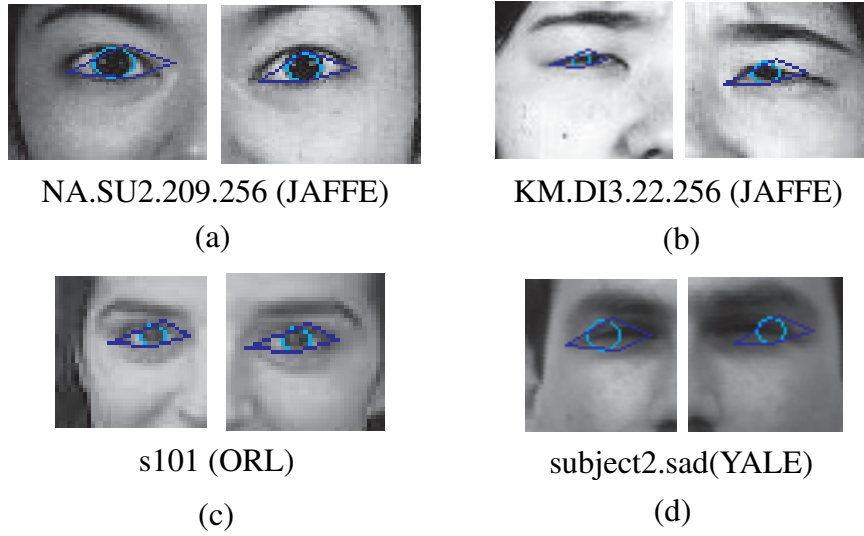


Figure 5.3: Sample results of the polygonal eye template

3. Using splines or polygons for representing the template geometries did not produce considerably different results. Although splines represent the facial features more realistically, the results did not point out a difference. The main reason for this is that, minimization with splines is more difficult as they show more complex behavior when the template parameters are modified. However, during the tests in some cases it is observed that spline-based template performed superior compared to polygonal template. One such case is depicted in Figure 5.7

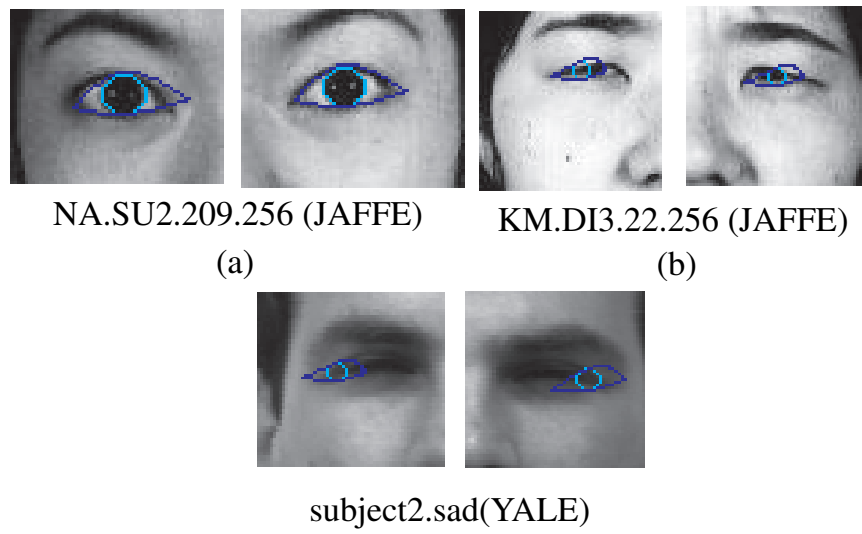


Figure 5.4: Sample results of the spline-based eye template

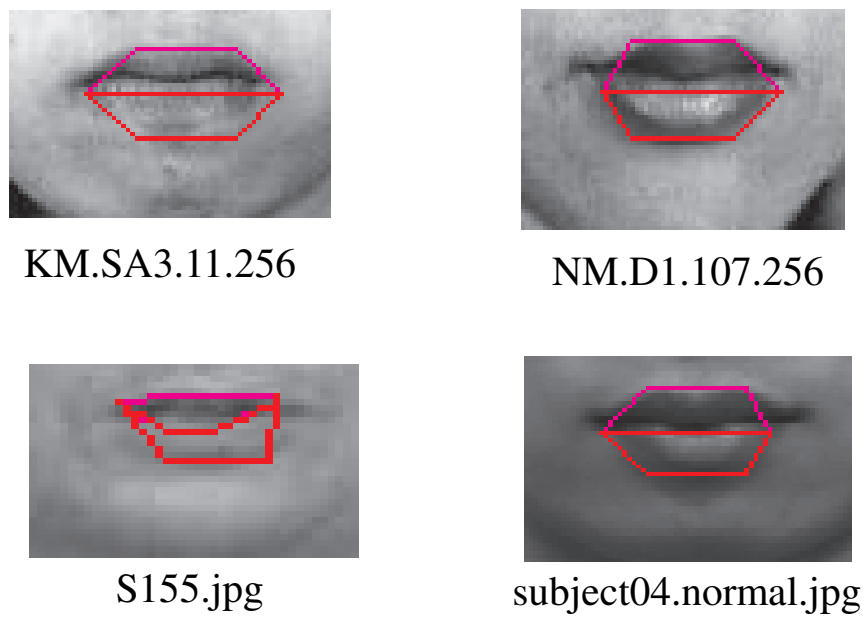
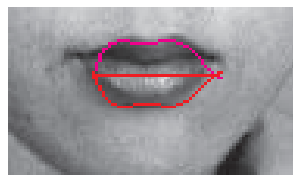


Figure 5.5: Sample results of the polygonal mouth template



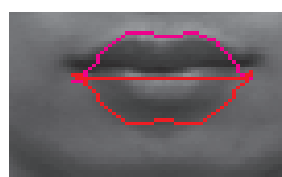
KM.SA3.11.256



NM.D1.107.256

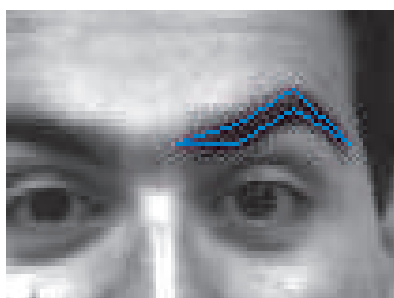


S155.jpg



subject04.normal.jpg

Figure 5.6: Sample results of the spline-based mouth template



(a)



(b)

Figure 5.7: A case where spline based template outperformed polygonal template

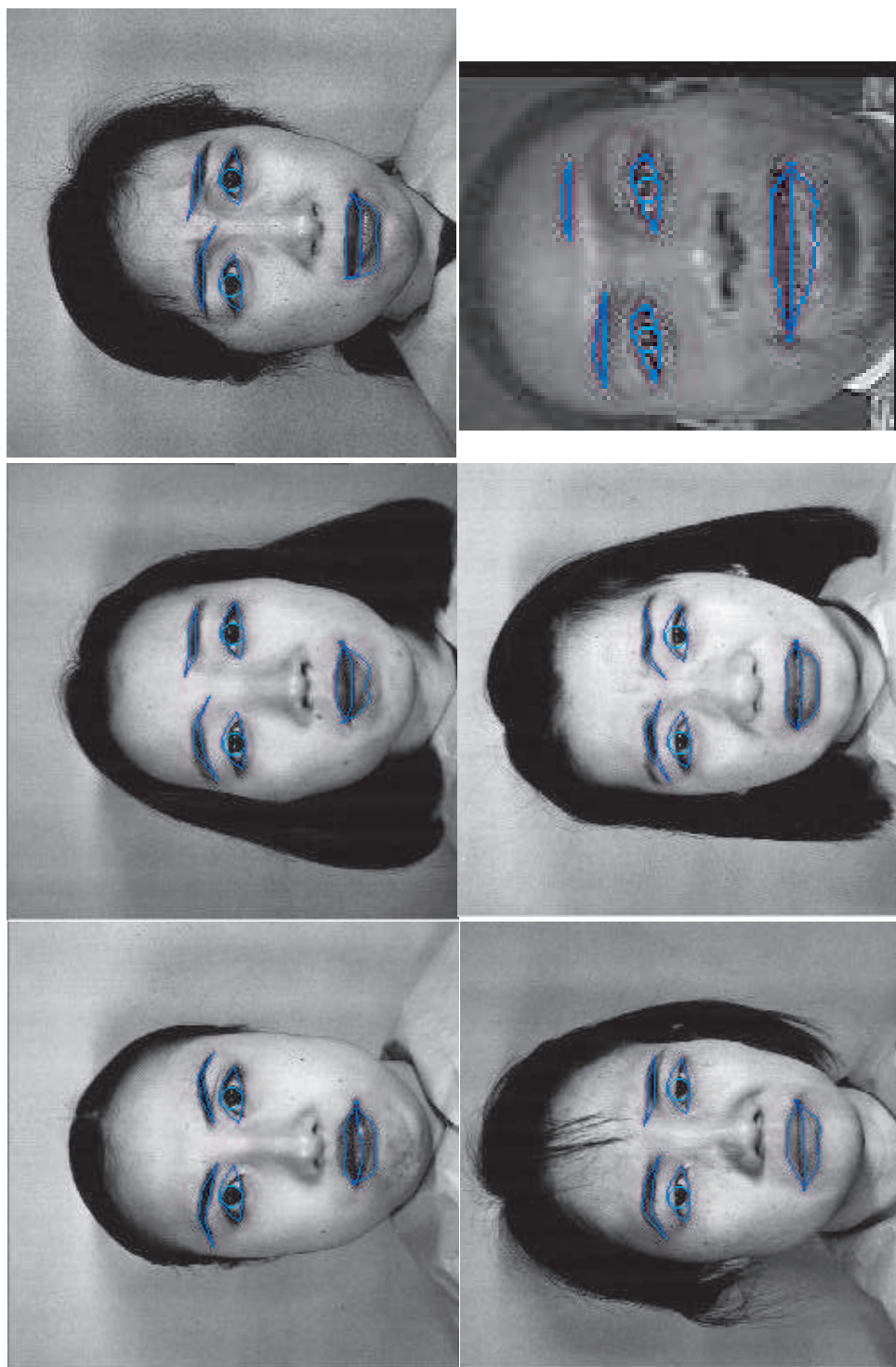


Figure 5.8: Sample results of the system

CHAPTER 6

Conclusion

In this study, an automatic facial feature extraction system is developed. The system first detects a face on a given static gray-scale image, and determines rough search regions for facial features. Then, deformable templates developed for each of eye, eyebrow and mouth are run on these search regions separately for extracting facial feature parameters.

In order to detect faces with different sizes, an eigenfaces-based detection algorithm is developed. Given a static gray-scale image, the algorithm builds the Gaussian pyramid of the image, and then performs the search starting from the smallest sized level of the pyramid to the higher sized levels. This search allows the algorithm to detect faces in multiple scales. Our algorithm performs the search using an 18x24 pixels face window, which is reported to be the smallest resolution at which human beings can perform recognition. The average adult facial proportions are used to embed the locations of facial features into our face model, so that the rough locations of the facial features are readily available when a face is detected.

The extraction of detailed location and shape information of facial features is performed by using deformable models. Polygonal and spline based models for each of the eyes, eyebrows and mouths are developed. The same eye model is used for extracting left and right eye parameters. Similarly, the same eyebrow

model is used for extracting left and right eyebrow parameters. For each of the deformable models, geometrical and imaging models, energy functions and matching algorithms are developed.

The system is tested on JAFFE, ORL and Yale facial image databases. The developed face detection algorithm yielded on average 74% rates. In order to assess the performance of the deformable models, the deviations of the feature parameters from the hand-fitted values are used. These deviations are interpreted by using a subjective measure of goodness in addition to the pixel deviations. According to the test results the acceptable (including *good* and *very good* subjective measures) correct extraction of the feature parameters for the eyebrow template is 77%, eye template is 90%, and mouth template is 70%.

6.1 Limitations and Future Work

The limitations of the face detection and feature extraction sub-systems of the developed system is discussed separately in the following paragraphs. Future work anticipated for overcoming the limitations are also presented.

6.1.1 Face Detection

The limitations of the developed face detection algorithm is summarized as follows.

Multiple face detection The algorithm is inherently suitable for multiple face detection. In this study we stopped the search when a face is found for achieving high speed, because we know in advance that the images contain a single face. In order to apply the system on real-life cases, we need to continue our search after finding a face, and some kind of non-maxima suppression method should be employed to eliminate multiple detections of the same face.

Invariance to illumination conditions Our algorithm does not perform any brightness normalization. In order to provide illumination invariance, a

preprocessing step using an overall brightness equalization, and histogram equalization should be added.

Invariance to rotation The face detection algorithm developed in this thesis can tolerate only a minimal rotation in the image plane. In order to provide rotation invariance, multi-orientation eigenfaces can be used.

Improved Search Mechanism Our algorithm uses a sequential search window. A faster search mechanism can be developed based on saccadic search.

Embedding Color Information Our algorithm is developed considering gray-scale images, and thus we were unable to use color information. Using color information in color images can drastically reduce the detection time, because a fast skin-color filtering can narrow our search region in the beginning.

Improving the accuracy of the detected face location Our algorithm performs a search on a Gaussian pyramid. When a face is found on smaller size levels of the pyramid, the location of the face is calculated by finding the location in the bottommost level of the pyramid. A pixel in one level of the pyramid corresponds to four pixels in the next level, 16 pixels in the next, and this goes on exponentially. So when we detect a face on the third level from the bottom, then our point corresponds to $4^3 = 64$ pixels (a 8x8 region) in the original image, so on average we are 4 pixels away from the real location of the face. In order to overcome this limitation, multiple eigenfaces for different scales can be developed. Then, when a face is found at level k , a finer level search can be performed in the 2x2 region in level $k + 1$. This can improve the accuracy with negligible computational burden.

6.1.2 Feature Extraction

The limitations and future work related to the feature extraction sub-system of the developed system are summarized as follows:

- The geometrical model should be developed based on statistical observations rather than empirical observations. A statistical approach can be developed for constructing the geometrical model from a representative sample data.
- Inter-feature validity checks should be employed in the system in order to be more robust.
- Better initialization algorithms (such as the one used in eye template) should be developed for each of the deformable models, because initial configuration of the template affects the performance.
- More sophisticated optimization algorithms (Direction Set methods, Conjugate Gradient methods, etc.) should be used in order to provide more speed and accuracy.
- In order to be a more general and complete facial feature extraction system, deformable models for more facial features (nose, ears, etc.) can be developed.
- Parallel implementation should be considered for faster processing, because the extraction of each facial feature can be performed independently after a face is detected and rough search regions are identified.

6.2 Application Areas

The system developed in this study can be used as a starting point in many areas including the following:

- face recognition,

- facial expression analysis,
- security systems (iris recognition),
- photography (red eye correction, etc.),
- multi modal speech recognition and lipreading,
- human computer interfaces,
- driver monitoring systems, and
- automatic facial animation.

REFERENCES

- [1] T. E. de Campos, R. S. Feris, and R. M. C. Junior, "Eigenfaces versus eigeneyes: First steps toward performance assesment of representations for face recognition," in *Lecture Notes in Artificial Intelligence, MICAI-2000*, vol. 1793, (Acapulco), pp. 197–206, April 2000.
- [2] A. Pentland, B. Moghaddam, and T. Starner, "View-based and modular eigenspaces for face recognition," MIT Media Laboratory Perceptual Computing Section Technical Report 245, Vision and Modeling Group, The Media Laboratory, Massachusetts Institute of Technology, 20 Ames St, Cambridge MA 02139, 1994. Appeared in IEEE Conference on Computer Vision and Pattern Recognition, 1994.
- [3] I. A. Essa, *Analysis, Interpretation and Synthesis of Facial Expressions*. PhD thesis, Massachusetts Institute of Technology, February 1995.
- [4] M. T. Chan, Y. Zhang, and T. S. Huanz, "Real time lip tracking and bimodal continous speec recognition," in *Electronic Proceedings of 1998 Workshop on Multimedia Signal Processing*, (Los Angeles, California, USA), IEEE Signal Processing Society, December 1998.
- [5] M. Nilsson and N. Kilander, "Machine vision based lip tracking in real-time video streams using active contour models," Master's thesis, Department of Computing Science, Umea University, June 2002.
- [6] D. O. Gorodnichy, S. Malik, and G. Roth, "Nouse 'use your nose as a mouse'-a new technology for hands-free games and interfaces," in *Proceedings of International Conference on Vision Interface (VI'2002)*, (Calgary), pp. 354–361, May 27-29 2002.
- [7] J. G. Ko, K. N. Kim, and R. S. Ramakrishna, "Facial feature tracking for eye-head controlled human computer interface," in *IEEE TENCON*, 1999.
- [8] D. Terzopoulos and K. Waters, "Analysis and sysnthesis of facial image sequences using physical and anatomical models," *IEEE Transactions on Pattern Analysis and Machine Intelligence*, vol. 15, June 1993.
- [9] A. Blake and M. Isard, *Active Contours*. Springer-Verlag London Limited, 1998.

- [10] M. Turk and A. Pentland, "Face recognition using eigenfaces," in *IEEE Conference on Computer Vision and Pattern Recognition*, pp. 586–591, 1991.
- [11] E. Hjelmås and B. K. Low, "Face detection: A survey," *Computer Vision and Image Understanding*, vol. 83, pp. 236–274, 2001.
- [12] S. Lucey, S. Sridharan, and V. Chandran, "Initialized eigenlip estimator for fast lip tracking using linear regression," in *International Conference on Pattern Recognition (ICPR'00)*, vol. 3, (Barcelona, Spain), pp. 31–82, September 2000.
- [13] L. Wiskott, J.-M. Fellous, N. Kruger, and C. von der Malsburg, *Intelligent Biometric Techniques in Fingerprint and face recognition*, ch. 7: Introduction to Face Recognition, Face Recognition by Elastic Bunch Graph Matching, pp. 357–396. CRC Press, 1999.
- [14] I. King and X. Q. Li, *Intelligent Biometric Techniques in Fingerprint and face recognition*, ch. 7: Introduction to Face Recognition, Facial Expression Synthesis Using Radial basis Function Networks, pp. 399–421. CRC Press, 1999.
- [15] L. Zhang, "Estimation of the eye and mouth corner point positions in a knowledge-based coding system," *Digital Compression Technologies and Systems for Video Communications*, vol. 2952, pp. 21–28, 1996.
- [16] S. Baskan, "Segmentation of human face," Master's thesis, Middle East Technical University, 2000.
- [17] A. Yuille, C. D.S., and H. P.W., "Feature extraction from faces using deformable templates," in *In Proc. CVPR*, pp. 104–109, 1989.
- [18] A. Blake and A. Yuille, *Active Vision*. Massachusetts Institute of Technology, 1992.
- [19] L. Zhang, "Estimation of the mouth features using deformable templates," in *International Conference on Image Processing (ICIP '97)*, vol. 3, (Washington DC), p. 328, October 26-29 1997.
- [20] D. Shah and S. Marshall, *Nonlinear Model-Based Image/Video Processing and Analysis*, ch. 8: Image Models for Facial Feature Tracking, pp. 299–319. 2001.
- [21] M. Malciu and F. Preteux, "Tracking facial features in video sequences using a deformable model based approach," in *Proceedings SPIE Conference on Mathematical Modeling, Estimation and Imaging*, vol. 4121, (San Diego, CA), pp. 51–62, 2000.

- [22] A. Bottion, "Real time head and facial features tracking from uncalibrated monocular views," in *The 5th Asian Conference on Computer Vision*, (Melbourne, Australia), pp. 23–25, January 2002.
- [23] M. Kampmann, "Estimation of the chin and cheek contours for precise face model adaptation," in *International Conference on Image Processing (ICIP-97)*, (Santa Barbara, CA), pp. 300–303, October 1997.
- [24] F. J. Huang, "Project-audio-visual speech processing," tech. rep., Advanced Multimedia Processing Lab, Electrical & Computer Engineering, Carnegie Mellon. <http://amp.ece.cmu.edu/projects/AudioVisulSpeechProcessing>.
- [25] M. Kampmann and L. Zhang, "Estimation of eye, eyebrow and noise features in videophone sequences," in *International Workshop on Very Low Bitrate Video Coding (VLBV 98)*, (Urbana, USA), pp. 101–104, October 1998.
- [26] J. Nikkanen, "Eye detection from a facial image." Digital Image Processing III-Presentation (<http://www.cs.tut.fi/jtn/80573/eyedetection.html>).
- [27] Y. Zhang, "Automatic feature extraction." <http://dino.cis.udel.edu:8080/fets/paper/node4.html>, 1999.
- [28] M. Sonka, V. Hlavac, and R. Boyle, *Image Processing, Analysis, and Machine Vision*. Brooks/Cole Publishing Company, second ed., 1999.
- [29] N. Efford, *Digital Image Processing: a practical introduction using JavaTM*. Pearson Education Limited, 2000.
- [30] M. B. ter Haar Romeny, "Scale-space theory for multiscale geometric image analysis," in *CVPR'99 IEEE International Conference on Computer Vision and Pattern Recognition*, June 1999.
- [31] C. Harris and M. Stephens, "A combined corner and edge detector," in *Fourth Alvey Vision Conference*, pp. 147–151, 1988.
- [32] S. Smith and J. Brady, "Susan - a new approach to low-level image processing," *International Journal of Computer Vision*, vol. 23, no. 1, pp. 45–78, 1997.
- [33] L. A. Kitchen and Rosenfeld, "Gray level corner detection," *Pattern Recognition Letters*, vol. 1, pp. 95–102, 1982.
- [34] A. L. Yuille, P. Hallinan, and D. Cohen, "Detecting facial features using deformable templates," *International Journal of Computer Vision*., 1992.
- [35] P. Maragos, "Tutorial on advances in morphological image processing and analysis," *Optical Engineering*, vol. 26, pp. 623–632, 1987.

- [36] S. J., *Image Analysis and Mathematical Morphology*. London,: Academic Press, 1982.
- [37] R. O. Duda, P. E. Hart, and D. G. Stork, *Pattern Classification*. John Wiley and Sons, Inc., second ed., 2001.
- [38] R. N. Shepard and J. Metzler, “Mental rotation of three-dimensional objects,” *Science* 171, pp. 701–703, 1971. In David Marr, Vision, p.11, W. H. Freeman and Company,1980.
- [39] G. Parisi, *Statistical Field Theory*. MA: Addison-Wesley, 1988. In Blake and Yuille, Active Vision, p.24, The MIT Press,1992.
- [40] K. M., W. A., and T. D., “Snakes: Active contour models,” in *1st Conference on Computer Vision*, pp. 259–268, 1996.
- [41] J. Ivins and J. Porrill, “Everything you always wanted to know about snakes (but were afraid to ask),” AIVRU Technical Memo 86, Artificial Intelligence Vision Research Unit, University of Sheffield, England, March 2000.
- [42] C. Xu and J. L. Prince, “Gradient vector flow: A new external force for snakes,” *IEEE Proceedings on Computer Vision and Pattern Recognition*, 1997.
- [43] C. Xu and J. L. Prince, “Snakes, shapes and gradient vector flow,” *IEEE Transactions on Image Processing*, vol. 7, no. 3, 1998.
- [44] D. J. Williams and M. Shah, “A fast algorithm for active contours and curvature estimation,” *CVGIP: Image Understanding*, vol. 55, pp. 14–26, January 1992.
- [45] W. A., T. D., and K. M., “Signal matching through scale space,” *American Association for Artificial Intelligence*, pp. 714–719. In Ivins J. and Porrill J., Everything You Always Wanted To Know About Snakes (But Were Afraid To Ask), AIVRU Technical Memo, 2000.
- [46] R. Brunelli and T. Poggio, “Face recognition: Features versus templates,” *IEEE Transactions on Pattern Analysis and Machine Intelligence*, vol. 15, no. 10, pp. 1042–1052, 1993.
- [47] G. Donato, M. S. Bartlett, J. C. Hager, P. Ekman, and T. J. Sejnowski, “Classifying facial actions,” *IEEE Transactions on Pattern Analysis and Machine Intelligence*, vol. 21, no. 10, pp. 974–989, 1999.
- [48] M. J. Black and Y. Yacoob, “Recognizing facial expressions in image sequences using local parametrized models of image motion,” *International Journal of Computer Vision*, vol. 25, no. 1, pp. 23–48, 1997.

- [49] B. Moghaddam, "Photobook eigenfaces demo." MIT Media Lab. Photobook Eigenfaces Demo Web Page ([www-white.media.mit.edu /vis-mod/demos/facerec/basic.html](http://www-white.media.mit.edu/~vis-mod/demos/facerec/basic.html)).
- [50] A. S. Pandya and R. R. Szabo, *Intelligent Biometric Techniques in Fingerprint and face recognition*, ch. 7: Introduction to Face Recognition, Neural Networks For Face Recognition, pp. 287–314. CRC Press, 1999.
- [51] H. A. Rowley, S. Baluja, and T. Kanade, "Neural network-based detection," *IEEE*, pp. 1063–6919, 1996.
- [52] Y. li Tian, T. Kanade, and J. F. Cohn, "Robust lip tracking by combining shape, color and motion," in *ACCV'2000*, pp. 1040–1045, 2000.
- [53] M.-M. Chuang, R.-F. Chang, and Y.-L. Huang, "Automatic facial feature extraction in model-based coding," *Journal of Information Science and Engineering*, no. 16, pp. 447–458, 2000.
- [54] W. H. Press, S. A. Teukolsky, W. T. Vetterling, and B. P. Flannery, *Numerical Recipes in C : The Art of Scientific Computing*. Cambridge University Press, Cambridge, second ed., 1992. Fully available at www.library.cornell.edu/nr/bookcpdf.html.
- [55] T. Bachmann, "Identification of spatially quantized tachiscopic images of faces: how many pixels does it take to carry identity?," *European Journal of Cognitive Psychology*, no. 3, pp. 87–103, 1991. In A. Jonathan Howel, Introduction to Face Recognition, Intelligent Biometric Techniques in Fingerprinting and Face Recognition, 1999.
- [56] B. Hoddinott, "Adult facial proportions (t-20)," March 2001. www.finearteducation.com/prebeginner/t-20.htm.
- [57] L. M. Larmann, "Standard human facial proportions," February 2000. www2.evansville.edu/drawinglab/face.html.
- [58] M. J. Lyons, J. Budynek, and S. Akamatsu, "Automatic classification of single facial images," *IEEE Transactions on Pattern analysis and Machine Intelligence*, vol. 21, no. 12, pp. 1357–1362, 1999. As a reference for the JAFFE database (www.mis.atri.co.jp/~mlyons/jaffe.html).
- [59] F. Samaria and A. Harter, "Parameterization of a stochastic model for human face identification," in *Proceedings of 2nd IEEE Workshop on Applications of Computer Vision*, (Sarasota FL), December 1994. As a reference for the ORL database (www.uk.research.att.com/facedatabase.html).
- [60] D. Kriegman and P. Belhumeur, "Yale face database," <http://cvc.yale.edu/projects/yalefaces/yalefaces.html> (Last updated: February 19, 1999).

APPENDIX A

Test Sets



Figure A.1: Randomly selected JAFFE images

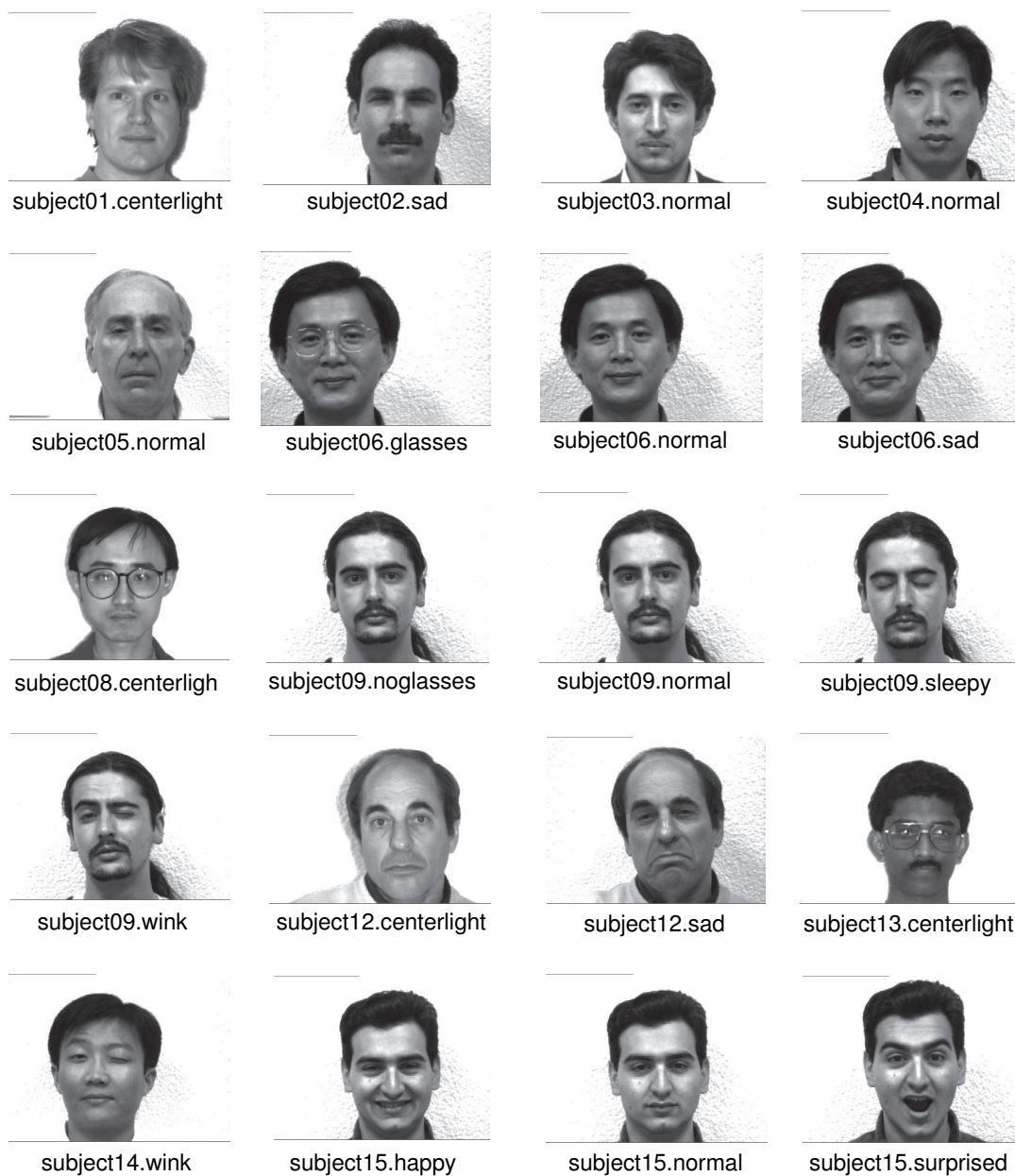


Figure A.2: Randomly selected YALE images

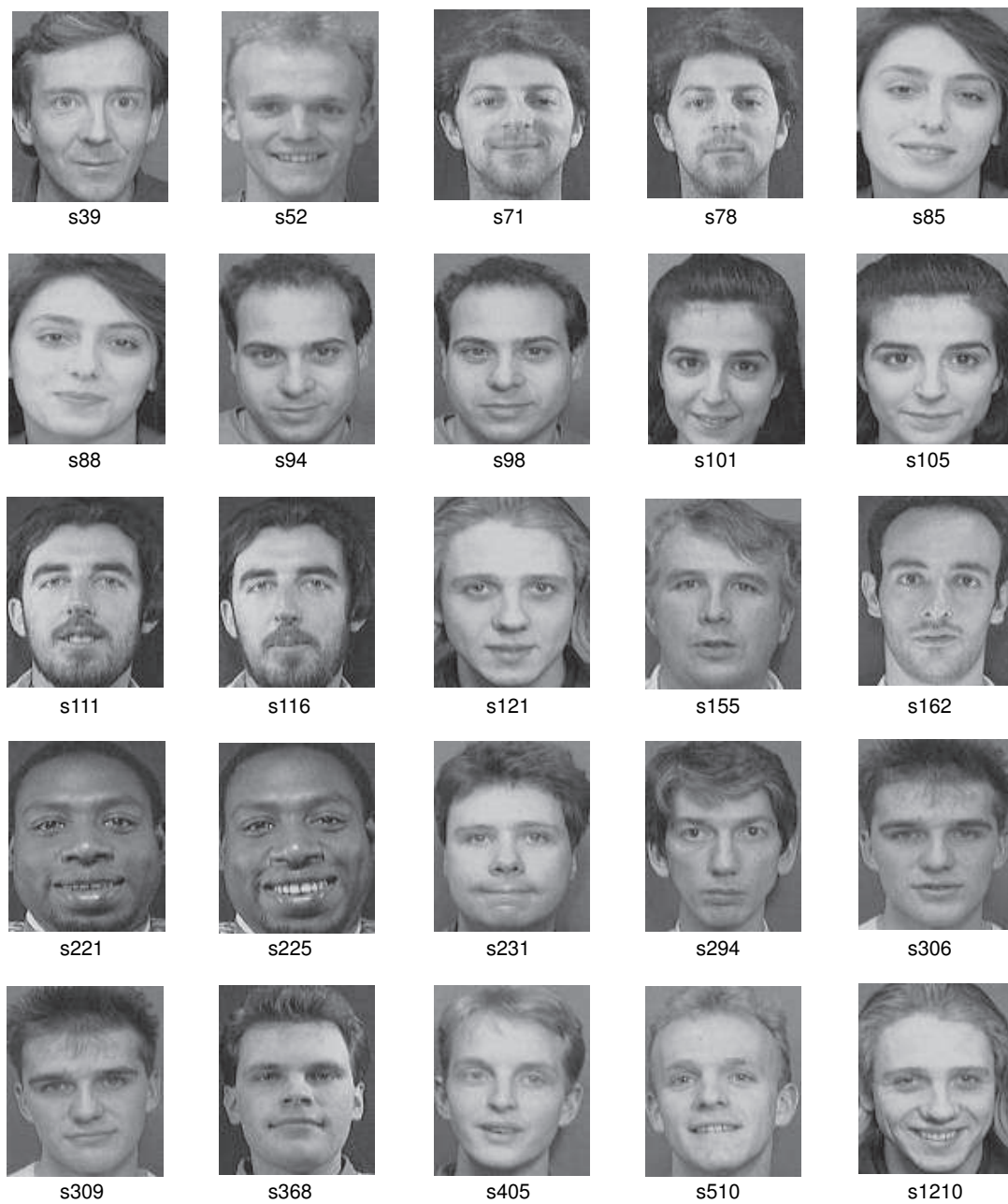


Figure A.3: Randomly selected ORL images

APPENDIX B

Polygonal Eyebrow Template Detailed Test Results

Absolute Difference Pixel Values																																				
% Param Name	K.A.DI	K.A.HA	K.A.SA	K.A.SU	KL	AN	KL	FE	KM	DI	KM	SA	KR	AN	MK	SA	NA	HA	NA	SU	NM	DI	TM	FE	TM	SA	UY	AN	UY	DI	YM	DI	YM	HA	Average	
c1_x	2.83	0.494	4.29	0.29	2.07	1.5	1.56	4.929	2.83	3.59	3.74	1.85	0.4	1.62	2.313	1.2	2.8	1.4	2.24	1.18	2.16															
c1_y	3.01	7.081	1.38	0.52	2.53	2.5	1	3.727	0.57	1	1.37	3.01	4.35	1.18	7.531	2.66	4.18	6.24	3.98	6.82	3.23															
u1_x	5.83	5.803	5.96	4.33	1.93	1.16	3.92	3.858	1.5	4.4	2.79	2.48	0.27	2.96	8.695	4.86	2.2	5.06	5.09	4.26	3.87															
u1_y	1.87	0.637	0.75	2	0.19	0.6	0.62	0.09	0.35	0.92	0.67	1.13	1.75	0.39	3.009	2.33	0.44	0.29	3.51	0.94	1.12															
u2_x	5.5	6.803	6.92	3.84	0.76	0.5	3	5.112	0.16	5.26	0.31	2.15	1.4	0.43	11.31	7.86	1.13	4.57	4.91	5.26	3.86															
u2_y	0.87	0.303	1.41	1.35	0.98	0.73	0	0.874	1.52	1.59	0.98	0.54	1.92	1.26	2.264	1.66	0.22	1.65	0.18	0.06	1.02															
c2_x	7.83	11.14	10.3	3	0.36	2.83	0.43	6.887	2.03	7.65	1.45	5.48	3.27	3.71	9.98	7.2	3.87	5.73	7.58	4.93	5.28															
c2_y	0.33	10.63	0.72	9.5	1.76	5.84	2.14	0.419	2.06	1.31	1.62	4.99	2.32	4.18	2.136	2.01	0.49	8.42	9.02	6.47	4.41															
l2_x	4.83	7.136	7.96	7.1	0.66	0.83	1.33	6.087	1.29	6.95	3.31	4.81	0.93	0.77	8.98	6.53	0.8	5.98	6.91	5.26	4.42															
l2_y	1.34	0.703	1.05	1.61	1.72	1.16	0.3	2.515	0.68	0.37	0.42	1.01	3.02	0.82	3.864	3.33	1.16	0.37	2.62	1.19	1.46															
l1_x	4.83	5.136	6.63	5.67	1.6	1.83	2.58	7.191	0.16	5.07	1.34	3.48	0.27	4.29	9.029	5.2	0.53	6.4	3.75	2.6	3.88															
l1_y	2.01	1.037	1.05	3.17	0.19	0.5	0.65	2.157	0.12	1.21	2.43	0.34	0.02	0.82	3.943	4.99	1.16	0.91	0.38	0.53	1.38															
Average	3.55	5.08	4.30	3.56	1.32	1.77	1.54	3.79	1.20	4.54	1.64	2.81	1.81	1.96	6.28	4.08	1.62	4.19	4.53	3.54																

Percentage (of width) Diff																																				
% Param Name	K.A.DI	K.A.HA	K.A.SA	K.A.SU	KL	AN	KL	FE	KM	DI	KM	SA	KR	AN	MK	SA	NA	HA	NA	SU	NM	DI	TM	FE	TM	SA	UY	AN	UY	DI	YM	DI	YM	HA	Average	
c1_x	7.66	1.47	13.84	0.92	5.49	4.34	4.29	14.22	7.78	9.70	9.84	5.35	1.13	3.56	6.37	3.52	7.50	3.20	6.12	3.09	5.97															
c1_y	8.13	21.03	4.46	1.64	6.71	7.20	2.76	10.75	1.56	2.89	3.61	8.68	12.31	2.58	20.73	7.83	11.19	14.29	10.85	17.78	8.84															
u1_x	15.77	17.24	19.22	13.68	5.13	3.36	10.78	11.13	4.12	11.89	7.34	7.15	0.75	6.48	23.93	14.31	5.89	11.59	13.87	11.12	10.74															
u1_y	5.07	1.89	2.42	6.32	0.52	1.74	1.70	0.26	0.98	2.49	1.76	3.25	4.95	0.85	8.28	6.85	1.19	0.67	9.57	2.45	3.16															
u2_x	14.86	20.21	22.32	12.13	2.01	1.43	8.26	14.75	0.44	14.21	0.82	6.19	3.96	0.95	31.14	23.13	3.03	10.47	13.39	13.73	10.87															
u2_y	2.36	0.90	4.54	4.27	2.61	2.11	0.00	2.52	4.19	4.29	2.59	1.56	5.42	2.75	6.23	4.89	0.60	3.77	0.49	0.16	2.81															
c2_x	21.17	33.08	33.20	9.47	0.96	8.16	1.19	19.87	5.60	20.68	3.81	15.81	9.24	8.12	27.47	21.17	10.36	13.12	20.66	12.86	14.80															
c2_y	0.88	31.57	2.31	30.00	4.66	16.84	5.89	1.21	5.66	35.46	4.26	14.40	6.56	9.15	5.88	5.90	1.31	19.29	24.61	16.89	12.14															
l2_x	13.06	21.20	25.67	22.41	1.75	2.39	3.67	17.56	3.56	18.79	8.72	13.88	2.64	1.68	24.72	19.21	2.14	13.69	18.83	13.73	12.46															
l2_y	3.63	2.09	3.39	5.08	4.56	3.36	0.83	7.26	1.88	1.00	1.10	2.91	8.54	1.81	10.64	9.79	3.10	0.86	7.15	3.11	4.10															
l1_x	13.06	15.26	21.37	17.89	4.24	5.28	7.11	20.74	0.45	13.70	3.53	10.04	0.75	9.40	24.85	15.29	1.43	14.65	10.23	6.77	10.80															
l1_y	5.43	3.08	3.39	10.00	0.52	1.43	1.79	6.22	0.33	3.27	6.40	0.99	0.05	1.80	10.85	14.69	3.10	2.08	1.02	1.38	3.89															
Average	9.26	14.08	13.01	11.15	3.26	4.80	4.02	10.54	3.05	11.51	4.48	7.52	4.69	4.09	16.76	12.21	4.24	8.97	11.40	8.59																

Figure B.1: JAFFE polygonal left eyebrow template test results

Absolute Difference Pixel Values																					
%ParamName	K.A.Dif	K.A.Hd	K.A.Sd	K.A.Su	KL.AN	KL.FE	KM.DI	KM.Sd	KR.AN	MK.Sd	NA.AN	NA.Hd	NA.Su	NM.DI	TM.FE	TM.Sd	UY.AN	UY.DI	YM.DI	YMHd	Average
e1_x	11.14	6.27	6.22	9.45	1.00	0.66	6.46	7.59	0.41	6.43	3.74	3.04	2.65	6.99	5.03	7.25	5.55	1.46	3.32	4.72	4.97
e1_y	6.81	0.08	5.09	3.07	0.73	1.08	2.55	2.50	1.53	0.03	1.37	0.19	1.98	0.17	3.87	3.82	1.14	3.72	0.68	4.51	2.25
u1_x	8.47	1.27	5.48	8.12	0.33	3.95	0.13	5.21	3.93	3.43	2.79	7.23	4.69	3.32	3.36	5.59	2.12	2.88	3.08	1.21	3.83
u1_y	0.15	0.48	0.61	0.30	1.26	0.91	0.55	0.46	2.37	0.23	0.67	3.29	3.46	0.10	0.27	0.48	0.51	0.08	1.06	0.02	0.86
u2_x	7.47	2.32	5.83	4.72	1.33	3.01	3.55	2.69	4.93	2.77	0.31	10.67	7.69	0.66	2.70	4.92	1.38	0.05	0.99	2.02	3.50
u2_y	3.15	0.92	0.98	2.55	1.40	1.52	1.31	0.51	0.97	0.23	0.98	0.90	0.88	0.23	1.07	0.15	0.87	0.32	0.35	1.32	1.03
e2_x	4.47	0.61	1.31	2.47	2.00	2.68	0.13	3.21	5.93	0.77	1.45	7.73	4.04	1.34	0.30	1.98	0.88	0.07	0.01	4.38	2.29
e2_y	5.48	5.08	2.42	0.53	2.06	1.75	2.78	2.31	0.20	1.97	1.62	2.12	2.07	1.83	7.87	4.54	5.14	2.66	2.35	7.49	3.11
l2_x	5.14	4.41	6.50	5.72	2.33	3.01	1.55	2.55	1.59	0.43	3.31	7.15	5.93	0.34	0.36	4.59	2.21	0.28	1.65	1.36	3.02
l2_y	3.48	2.39	1.45	3.45	0.60	0.59	1.64	0.31	1.13	0.30	0.42	1.21	1.06	0.17	1.47	1.85	1.47	2.29	1.35	0.56	1.36
l1_x	7.80	4.61	5.82	9.12	1.33	1.02	2.13	3.55	0.26	1.77	1.34	4.23	4.69	3.32	4.03	8.59	2.55	0.54	0.41	1.54	3.43
l1_y	0.48	0.42	1.74	0.60	1.40	1.64	0.78	1.31	1.87	1.30	2.43	2.39	4.69	0.17	1.13	1.52	1.47	3.38	0.03	3.25	1.60
Average	5.34	2.41	3.62	4.17	1.32	1.82	1.96	2.68	2.09	1.64	1.70	4.18	3.65	1.55	2.62	3.77	2.11	1.48	1.27	2.70	

Percentage (of width) Diff																					
%ParamName	K.A.Dif	K.A.Hd	K.A.Sd	K.A.Su	KL.AN	KL.FE	KM.DI	KM.Sd	KR.AN	MK.Sd	NA.AN	NA.Hd	NA.Su	NM.DI	TM.FE	TM.Sd	UY.AN	UY.DI	YM.DI	YMHd	Average
e1_x	33.41	17.76	16.53	27.52	2.57	1.61	19.20	22.32	1.05	15.95	9.84	8.30	7.78	19.60	16.41	20.92	17.16	4.17	8.37	11.60	14.10
e1_y	20.44	0.24	13.51	8.93	1.87	2.65	7.58	7.36	3.96	0.09	3.61	0.51	5.81	0.48	12.61	11.01	3.52	10.62	1.72	11.09	6.38
u1_x	25.41	3.61	14.56	23.64	0.86	9.72	0.39	15.34	10.16	8.51	7.34	19.71	13.79	9.32	10.97	16.11	6.56	8.21	7.75	2.98	10.75
u1_y	0.44	1.36	1.62	0.88	3.24	2.24	1.64	1.34	6.12	0.57	1.76	8.96	10.17	0.29	0.87	1.40	1.56	0.24	2.68	0.05	2.37
u2_x	22.41	6.57	15.48	13.76	3.42	7.40	10.53	7.90	12.74	6.86	0.82	29.09	22.61	1.84	8.80	14.19	4.26	0.15	2.48	4.98	9.82
u2_y	9.44	2.61	2.60	7.42	3.60	3.74	3.89	1.51	2.50	0.57	2.59	2.45	2.57	0.64	3.48	0.44	2.69	0.91	0.89	3.26	2.89
e2_x	13.41	1.72	3.47	7.19	5.12	6.58	0.39	9.46	15.33	1.90	3.81	21.08	11.89	3.77	0.99	5.71	2.72	0.21	0.04	10.78	6.28
e2_y	16.44	14.39	6.42	1.53	5.29	4.29	8.26	6.80	0.51	4.87	4.26	5.77	6.08	5.13	25.65	13.10	15.89	7.60	5.92	18.42	8.83
l2_x	15.41	12.49	17.25	16.67	5.99	7.40	4.59	7.49	4.12	1.08	8.72	19.49	17.43	0.96	1.19	13.23	6.85	0.80	4.17	3.34	8.43
l2_y	10.44	6.75	3.84	10.04	1.55	1.44	4.88	0.91	2.93	0.74	1.10	3.29	3.11	0.48	4.79	5.33	4.55	6.53	3.40	1.37	3.87
l1_x	23.41	13.04	15.44	26.55	3.42	2.50	6.33	10.44	0.68	4.38	3.53	11.53	13.79	9.32	13.15	24.77	7.88	1.55	1.03	3.80	9.83
l1_y	1.44	1.18	4.63	1.75	3.58	4.02	2.32	3.86	4.82	3.22	6.40	6.51	13.80	0.48	3.70	4.37	4.55	9.67	0.07	8.00	4.42
Average	16.01	6.81	9.61	12.16	3.38	4.47	5.83	7.89	5.41	4.06	4.48	11.39	10.74	4.36	8.55	10.88	6.52	4.22	3.21	6.64	

Figure B.2: JAFFE polygonal right eyebrow template test results

Absolute Difference Pixel Values																			
% Param	r	l	right	2.sad	brmal	brmal	s	s	brmal	6.sad	r	l	right	s	brmal	leepy	wink	2.sad	subje
c1_x	4.13	4.46	0.06	6.83	1.83	5.00	2.89	0.58	2.00	0.55	1.85	0.13	1.81	7.25	4.00	4.54	1.90	0.03	2.14
c1_y	0.97	0.49	4.04	5.00	3.92	13.17	5.26	4.67	1.00	6.39	3.95	4.39	3.39	5.13	4.20	4.40	10.71	4.45	5.40
u1_x	10.46	2.20	6.06	0.50	5.84	5.00	1.11	2.75	1.67	4.78	3.49	3.87	6.48	0.75	2.33	7.26	4.64	5.97	6.48
u1_y	2.38	2.45	1.37	2.33	1.68	0.33	0.34	1.17	1.00	1.35	2.32	1.65	3.01	0.50	3.67	9.02	0.20	0.58	0.37
u2_x	12.79	2.54	4.73	2.17	3.17	6.33	0.11	4.75	1.00	1.78	3.15	1.88	3.15	4.08	3.00	7.26	5.97	4.64	4.14
u2_y	1.04	2.11	0.71	0.00	3.68	0.67	0.01	0.17	0.67	0.31	4.32	2.65	3.34	2.50	7.67	7.68	0.13	0.91	1.37
c2_x	17.79	4.87	9.40	6.13	6.84	10.67	3.11	7.08	1.00	7.45	4.82	5.21	5.48	8.42	2.33	12.60	7.97	8.30	4.48
c2_y	0.97	0.18	1.71	3.98	3.08	0.83	0.92	2.00	2.33	2.05	2.05	1.28	0.28	1.13	4.80	8.78	1.24	3.11	4.40
l2_x	14.46	2.54	3.40	2.17	2.51	3.33	0.22	4.08	0.33	2.11	2.15	3.21	2.81	4.42	0.67	8.26	6.64	4.97	5.48
l2_y	0.64	0.18	1.71	2.00	1.75	0.50	1.92	2.33	2.33	1.05	2.05	0.95	0.94	0.47	4.80	8.78	1.90	1.45	2.07
l1_x	12.79	0.87	5.06	1.17	4.51	0.67	0.78	3.08	1.00	2.78	2.15	2.87	4.48	0.25	0.33	8.26	4.31	3.97	5.14
l1_y	1.97	0.51	1.71	2.33	0.08	0.17	2.92	3.67	2.33	2.39	0.72	0.72	0.28	1.87	0.80	8.45	2.24	1.45	2.07
Average	6.70	1.95	3.33	2.88	3.24	3.89	1.63	3.03	1.39	2.75	2.75	2.40	2.95	3.06	3.22	7.94	3.99	3.32	3.63
Percentage (of width) Diff																			
% Param	r	l	right	2.sad	brmal	brmal	s	s	brmal	6.sad	r	l	right	s	brmal	leepy	wink	2.sad	subje
c1_x	12.76	12.88	0.20	24.70	5.17	17.05	10.32	2.13	5.41	1.58	4.95	0.33	5.61	26.52	12.63	13.62	7.02	0.08	5.27
c1_y	3.02	1.40	13.18	18.07	11.09	44.89	18.77	17.07	2.70	18.25	10.58	11.85	10.48	18.78	13.26	13.20	39.68	11.21	13.29
u1_x	32.35	6.36	19.77	1.81	16.52	17.05	3.96	10.06	4.50	13.66	9.34	10.29	20.04	2.74	7.37	21.79	17.19	15.05	15.35
u1_y	7.35	7.06	4.48	8.43	4.76	1.14	1.23	4.27	2.70	3.87	6.21	4.37	9.31	1.83	11.58	27.05	0.75	1.46	0.91
u2_x	39.56	7.32	15.42	7.83	8.98	21.59	0.39	17.38	2.70	5.09	8.45	4.98	9.73	14.94	9.47	21.79	22.13	11.69	10.19
u2_y	3.22	6.10	2.31	0.00	10.42	2.27	0.04	0.61	1.80	0.89	11.57	7.02	10.34	9.15	24.21	23.05	0.48	2.30	3.37
c2_x	55.03	14.05	30.64	22.14	19.35	36.36	11.10	25.91	2.70	21.28	12.91	13.83	16.95	30.79	7.37	37.79	29.53	20.93	11.01
c2_y	3.02	0.52	5.57	14.38	8.72	2.84	3.30	7.32	6.31	5.87	5.49	3.40	0.86	4.15	15.16	26.35	4.58	7.85	10.83
l2_x	44.72	7.32	11.07	7.83	7.09	11.36	0.80	14.94	0.90	6.04	5.77	8.52	8.70	16.16	2.11	24.79	24.59	12.53	13.47
l2_y	1.98	0.52	5.57	7.23	4.95	1.70	6.87	8.54	6.31	3.01	5.49	2.51	2.92	1.71	15.16	26.35	7.05	3.65	5.09
l1_x	39.56	2.51	16.51	4.22	12.75	2.27	2.77	11.28	2.70	7.95	5.77	7.63	13.85	0.91	1.05	24.79	15.95	10.01	12.65
l1_y	6.11	1.48	5.57	8.43	0.23	0.57	10.44	13.41	6.31	6.82	1.92	1.91	0.86	6.83	2.53	25.35	8.28	3.65	5.09
Average	20.72	5.63	10.86	10.42	9.17	13.26	5.83	11.08	3.75	7.86	7.37	6.37	9.14	11.21	10.16	23.82	14.77	8.37	8.92
Average	20.72	5.63	10.86	10.42	9.17	13.26	5.83	11.08	3.75	7.86	7.37	6.37	9.14	11.21	10.16	23.82	14.77	8.37	8.92
Average	20.72	5.63	10.86	10.42	9.17	13.26	5.83	11.08	3.75	7.86	7.37	6.37	9.14	11.21	10.16	23.82	14.77	8.37	8.92

Figure B.3: YALE polygonal left eyebrow template test results

Absolute Difference Pixel Values																			
% Param	r	flight	2.sad	brmal	brmal	sses	brmal	6.sad	rflight	sses	brmal	6.sad	rflight	sses	brmal	leepy	wink	rflight	2.sad
c1_x	19.36	9.30	5.00	6.84	4.90	2.81	7.50	10.08	7.30	2.29	0.69	1.42	4.93	8.96	9.25	5.26	11.92	2.74	6.02
c1_y	6.25	0.45	3.07	3.80	5.13	0.96	4.52	3.73	0.40	3.12	3.49	4.32	0.99	4.68	2.56	0.53	7.53	5.72	5.74
u1_x	15.50	2.30	0.33	1.84	2.33	5.19	1.86	0.25	1.30	0.29	4.31	2.26	1.07	2.96	1.91	0.26	2.92	6.00	0.64
u1_y	6.18	0.35	1.00	0.97	0.67	1.13	0.27	1.17	0.86	0.75	0.59	0.23	0.64	0.42	0.13	1.57	0.17	1.83	1.54
u2_x	11.08	0.30	1.67	0.16	1.00	9.19	5.86	2.92	0.30	1.29	0.98	3.07	1.27	1.96	1.58	0.08	4.58	2.33	0.69
u2_y	5.17	2.65	1.33	1.70	1.33	0.54	1.07	1.17	0.53	1.42	0.74	0.56	0.64	0.75	0.13	0.91	0.50	0.83	1.13
c2_x	4.42	1.70	2.67	2.49	4.00	9.19	12.53	9.92	5.70	2.04	6.65	1.59	1.40	4.04	6.09	2.08	1.75	2.33	0.02
c2_y	4.27	0.45	3.73	2.13	1.63	1.38	1.53	1.40	2.40	1.45	2.49	2.66	2.01	6.02	4.56	3.47	0.47	2.37	3.07
l2_x	9.75	2.64	1.00	1.17	0.67	3.52	5.53	4.58	0.63	1.63	1.98	1.07	0.27	1.96	0.75	1.26	3.25	0.67	3.36
l2_y	6.27	2.45	3.07	0.54	0.30	0.71	0.87	1.73	1.73	1.12	0.18	1.66	1.01	2.68	1.90	1.81	0.13	1.70	1.07
l1_x	15.17	5.30	2.00	3.51	3.00	1.19	0.80	2.42	1.30	1.29	1.98	1.07	1.07	5.29	3.58	1.26	5.25	3.33	2.36
l1_y	6.62	0.55	2.73	2.54	3.63	0.71	0.80	2.07	1.40	1.12	1.82	1.66	1.67	3.02	1.56	1.47	1.80	3.70	7.12
Average	9.17	2.37	2.30	2.31	2.38	3.04	3.60	3.45	1.99	1.48	2.16	1.80	1.41	3.56	2.83	1.66	3.36	2.80	4.20

Percentage (of width) Diff																			
% Param	r	flight	2.sad	brmal	brmal	sses	brmal	6.sad	rflight	sses	brmal	6.sad	rflight	sses	brmal	leepy	wink	rflight	2.sad
c1_x	74.45	25.14	17.65	21.60	12.79	8.52	26.79	32.53	20.86	5.25	1.57	3.09	10.57	24.88	27.47	15.61	35.75	6.36	14.34
c1_y	24.05	1.20	10.82	11.99	13.37	2.90	16.15	12.04	1.13	7.14	7.99	9.40	2.13	13.01	7.61	1.57	22.60	13.30	13.66
u1_x	59.61	6.22	1.18	5.81	6.09	15.72	6.65	0.81	3.72	0.67	9.88	4.91	2.29	8.22	5.69	0.76	8.75	13.95	1.53
u1_y	23.78	0.96	3.53	3.06	1.74	3.41	0.95	3.76	2.46	1.72	1.35	0.50	1.37	1.16	0.39	4.67	0.50	4.26	3.66
u2_x	42.63	0.82	5.88	0.51	2.61	27.84	20.94	9.41	0.86	2.96	2.25	6.68	2.71	5.44	4.70	0.23	13.75	5.43	1.65
u2_y	19.87	7.15	4.71	5.36	3.48	1.64	3.81	3.76	1.51	3.24	1.70	1.22	1.37	2.08	0.39	2.69	1.50	1.94	7.16
c2_x	16.99	4.59	9.41	7.88	10.43	27.84	44.75	31.99	16.28	4.68	15.22	3.46	3.00	11.23	18.08	6.17	5.25	5.43	0.06
c2_y	16.41	1.20	13.18	6.73	4.26	4.17	5.48	4.52	6.85	3.32	5.70	5.79	4.30	16.71	13.56	10.32	1.40	5.50	7.31
l2_x	37.50	7.12	3.53	3.70	1.74	10.67	19.75	14.78	1.81	3.72	4.54	2.33	0.57	5.44	2.24	3.73	9.75	1.55	8.00
l2_y	24.10	6.61	10.82	1.69	0.78	2.15	3.10	5.59	4.94	2.56	0.41	3.61	2.16	7.45	5.63	5.37	0.40	3.95	2.55
l1_x	58.33	14.33	7.06	11.07	7.83	3.60	2.87	7.80	3.72	2.96	4.54	2.33	2.29	14.70	10.64	3.73	15.75	7.75	5.61
l1_y	25.45	1.50	9.65	8.01	9.48	2.15	2.85	6.67	3.99	2.56	4.17	3.61	3.59	8.38	4.64	4.38	5.40	8.60	18.09
Average	35.26	6.40	8.12	7.28	6.22	9.22	12.84	11.14	5.68	3.40	4.94	3.91	3.03	9.89	8.42	4.93	10.07	6.50	5.90

Figure B.4: YALE polygonal right eyebrow template test results

Absolute Difference Pixel Values																									
% Param	s101	s105	s111	s116	s121	s1210	s155	s162	s221	s225	s231	s294	s306	s309	s39	s405	s510	s52	s71	s78	s85	s88	s94	s98	Average
c1_x	0.52	0.32	2.05	1.47	7.12	5.85	0.03	1.09	4.59	5.54	4.89	3.61	1.77	1.77	2.93	15.67	0.69	1.83	0.32	2.53	2.17	0.49	0.91	1.22	2.88
c1_y	1.42	0.60	5.47	4.25	1.91	2.14	3.24	1.85	4.21	3.77	0.83	1.50	1.06	1.13	1.27	13.23	1.76	6.47	2.54	8.45	6.43	1.11	11.27	12.56	4.10
u1_x	2.86	4.66	4.38	4.14	8.45	6.65	3.70	2.27	6.59	7.88	7.22	6.27	2.56	4.11	4.26	15.67	0.69	1.83	2.99	4.12	2.75	0.17	1.43	3.22	4.54
u1_y	0.15	1.27	0.67	0.42	0.02	0.12	0.59	0.58	1.24	0.17	0.03	0.23	0.53	0.53	0.44	11.33	1.91	1.17	0.06	0.96	1.38	0.79	2.21	1.37	1.17
u2_x	2.86	6.66	4.29	3.47	6.45	6.65	6.03	1.20	4.92	5.88	7.22	6.94	3.89	4.44	3.93	13.00	1.64	0.17	3.65	4.45	3.09	1.51	2.09	3.22	4.49
u2_y	0.15	1.27	0.85	1.75	1.35	1.46	0.59	0.33	0.24	0.49	0.97	0.43	0.19	0.80	0.77	13.67	0.76	0.83	0.61	0.63	0.04	0.55	1.21	0.71	1.28
c2_x	3.19	8.99	3.21	3.14	6.45	5.31	5.70	2.75	5.59	4.21	8.22	10.27	6.89	5.77	5.59	14.67	1.36	2.83	4.65	2.45	6.75	3.34	0.09	4.22	5.24
c2_y	0.08	2.27	4.46	3.58	1.42	2.52	3.09	0.03	0.46	0.23	0.84	0.17	0.94	1.53	0.06	17.57	4.76	0.13	0.54	0.43	0.22	1.58	2.06	1.11	2.09
l2_x	2.52	7.32	5.29	3.47	9.78	6.31	6.37	0.87	5.92	5.88	6.89	10.61	4.56	5.77	4.93	14.00	0.31	0.17	5.32	4.12	3.42	1.84	0.76	3.22	4.99
l2_y	0.25	1.94	0.39	0.09	1.42	1.86	0.76	0.16	0.13	0.11	0.84	0.50	0.27	0.47	1.60	14.23	1.42	0.13	0.12	1.43	0.11	0.11	0.94	1.77	1.29
l1_x	3.19	3.32	4.38	3.80	8.12	4.31	3.70	0.61	5.59	5.88	7.22	5.94	1.89	5.11	4.59	17.00	0.36	0.17	3.32	4.12	0.75	0.16	0.57	3.22	4.05
l1_y	0.92	1.94	2.47	1.91	0.42	0.86	0.57	0.08	0.13	0.11	0.84	0.50	0.27	0.47	0.60	12.57	0.42	0.47	0.79	1.10	0.44	0.89	1.61	1.77	1.34
Average	1.51	3.38	3.16	2.62	4.41	3.65	2.87	0.98	3.30	3.34	3.84	3.91	2.07	2.66	2.58	14.38	1.34	1.35	2.08	2.90	2.30	1.05	2.09	3.13	

Percentage (of width) Diff																									
% Param	s101	s105	s111	s116	s121	s1210	s155	s162	s221	s225	s231	s294	s306	s309	s39	s405	s510	s52	s71	s78	s85	s88	s94	s98	Average
c1_x	2.86	1.51	9.92	8.01	28.85	23.20	0.17	5.09	17.65	21.88	26.20	18.65	9.17	8.87	13.11	71.21	3.57	8.33	1.63	14.04	8.67	1.80	3.95	5.79	13.09
c1_y	7.73	2.83	26.48	23.16	7.76	8.80	16.75	8.67	16.18	14.89	4.43	7.77	5.49	5.67	5.68	60.15	9.08	29.39	12.93	46.93	25.74	4.07	49.01	59.82	19.14
u1_x	15.59	21.83	21.21	22.56	34.25	27.31	19.14	10.66	25.34	31.09	38.70	32.45	13.24	20.54	19.08	71.21	3.57	8.33	15.18	22.86	11.02	0.64	6.20	15.31	21.14
u1_y	0.81	5.96	3.25	2.29	0.08	0.51	3.07	2.70	4.77	0.68	0.15	1.20	2.73	2.67	1.95	51.52	9.88	5.30	0.29	5.36	5.51	2.88	9.59	6.53	5.40
u2_x	15.59	31.20	20.78	18.92	26.15	27.31	31.21	5.62	18.93	23.19	38.70	35.89	20.14	22.20	17.59	59.09	8.50	0.76	18.57	24.72	12.35	5.52	9.10	15.31	21.14
u2_y	0.81	5.96	4.14	9.57	5.49	5.99	3.07	1.54	0.92	1.95	5.21	2.25	1.00	4.00	3.44	62.12	3.91	3.79	3.10	3.50	0.17	2.00	5.24	3.36	5.94
c2_x	17.40	42.14	15.53	17.11	26.15	21.83	29.48	12.88	21.49	16.61	44.06	53.14	35.66	28.87	25.05	66.67	7.02	12.88	23.66	13.60	27.02	12.22	0.40	20.07	24.62
c2_y	0.46	10.64	21.58	19.52	5.76	10.38	15.00	0.14	1.77	0.90	4.50	0.87	4.86	7.67	0.29	79.85	24.60	0.61	2.76	2.39	0.89	5.79	8.96	5.26	9.85
l2_x	13.77	34.33	25.61	18.92	39.66	25.94	37.93	4.06	22.78	23.19	36.92	54.86	23.59	28.87	22.07	63.64	1.60	0.76	27.05	22.86	13.68	6.74	3.30	15.31	23.43
l2_y	1.36	9.08	1.88	0.48	5.76	7.64	3.93	0.76	0.49	0.42	4.50	2.58	1.41	2.33	7.17	64.70	7.36	0.61	0.63	7.95	0.44	0.42	4.08	8.44	6.02
l1_x	17.40	15.58	21.21	20.74	32.90	17.72	19.14	2.84	21.49	23.19	38.70	30.72	9.80	25.54	20.57	77.27	1.84	0.76	16.88	22.86	3.02	0.58	2.50	15.31	19.11
l1_y	5.00	9.08	11.96	10.43	1.70	3.53	2.96	0.36	0.49	0.42	4.50	2.58	1.41	2.33	2.70	57.12	2.19	2.12	4.02	6.10	1.77	3.24	6.98	8.44	6.31
Average	8.23	15.84	15.29	14.31	17.87	15.01	14.82	4.61	12.69	13.20	20.55	20.25	10.71	13.30	11.56	65.38	6.93	6.14	10.56	16.10	9.19	3.82	9.11	14.91	

Figure B.5: ORL polygonal left eyebrow template test results

Absolute Difference Pixel Values																										
% Param	s101	s105	s111	s116	s121	s1210	s155	s162	s221	s225	s231	s294	s306	s309	s39	s405	s510	s52	s71	s78	s85	s88	s94	s98	Average	
c1_x	4.87	7.00	1.73	3.07	5.87	4.53	5.94	4.70	1.53	1.27	6.43	5.54	1.59	6.10	1.67	7.00	4.25	8.15	3.89	4.35	5.86	6.72	1.39	8.15	4.65	
c1_y	5.10	0.29	7.50	4.10	3.25	0.91	1.69	4.84	2.82	5.07	0.10	2.61	0.81	3.53	2.13	0.01	1.02	4.64	0.38	0.80	0.31	0.23	0.41	0.13	2.20	
u1_x	2.20	2.66	1.09	1.93	1.54	0.81	1.88	0.64	3.86	4.06	4.09	1.87	2.41	4.76	5.00	4.00	0.25	2.33	0.44	1.35	3.52	4.05	3.72	1.48	2.50	
u1_y	0.47	0.19	0.27	1.50	2.45	0.74	0.55	0.82	0.38	2.21	1.23	1.02	0.13	2.27	1.73	2.51	0.91	1.41	0.35	1.07	0.05	0.60	0.48	1.07	1.02	
u2_x	5.87	5.00	2.24	3.40	5.20	0.86	1.88	0.70	3.20	1.40	10.09	1.87	0.92	4.43	3.67	3.67	0.58	1.67	0.89	2.35	6.19	9.05	2.05	2.81	3.33	
u2_y	0.47	0.53	0.27	0.16	3.11	0.74	0.88	0.51	2.28	2.46	1.10	0.64	0.21	3.93	1.07	2.18	0.91	1.74	0.02	0.74	0.05	0.94	2.52	1.41	1.20	
c2_x	3.20	0.00	0.91	1.40	3.20	0.19	1.21	2.97	2.20	1.60	7.76	2.54	0.92	2.76	5.00	4.33	1.58	3.67	2.11	2.35	5.52	7.05	2.72	1.48	2.78	
c2_y	2.56	0.71	2.76	3.43	3.25	1.57	4.85	2.51	0.82	1.07	2.57	0.61	1.14	2.87	2.47	0.01	0.02	2.71	0.38	1.53	6.02	5.77	1.25	1.13	2.17	
l2_x	5.54	5.66	1.91	3.07	4.87	0.19	1.21	1.03	1.53	0.73	7.09	1.87	0.92	3.76	4.00	4.33	2.58	3.67	0.77	2.69	6.52	8.05	2.39	2.81	3.22	
l2_y	0.77	2.29	1.09	1.76	3.91	1.24	0.18	0.84	1.85	1.26	0.10	0.28	0.47	2.53	1.13	2.01	0.36	2.37	0.38	0.80	0.31	0.23	2.59	1.21	1.25	
l1_x	3.20	5.00	0.76	0.93	1.54	0.86	3.21	0.30	1.20	0.06	7.43	5.21	0.59	5.76	3.67	5.00	0.58	2.00	0.89	3.02	3.52	4.05	3.72	2.81	2.72	
l1_y	0.56	0.63	0.09	2.43	3.58	0.91	0.15	0.51	1.48	2.41	0.43	2.06	0.14	2.20	1.13	1.01	0.36	2.37	0.62	0.53	0.31	0.23	1.08	1.13	1.10	
Average	2.90	2.50	1.72	2.27	3.48	1.13	1.97	1.70	1.93	1.97	4.04	2.18	0.85	3.74	2.72	3.01	1.12	3.06	0.93	1.80	3.18	3.91	2.03	2.13	2.13	

Percentage (of width) Diff																										
% Param	s101	s105	s111	s116	s121	s1210	s155	s162	s221	s225	s231	s294	s306	s309	s39	s405	s510	s52	s71	s78	s85	s88	s94	s98	Average	
c1_x	22.83	29.16	7.77	13.75	23.17	21.90	26.60	21.02	21.02	4.49	27.54	27.70	6.81	26.90	7.35	31.35	19.93	37.03	18.54	19.78	22.81	22.81	6.11	38.19	21.02	
c1_y	23.91	1.22	33.60	18.34	12.82	4.39	7.55	21.68	17.91	0.41	13.05	3.45	15.59	9.41	0.05	4.80	21.10	1.83	3.66	1.22	1.22	1.82	0.59	10.06	10.06	
u1_x	10.33	11.10	4.87	8.64	6.06	3.91	8.42	2.86	2.86	14.34	17.54	9.37	10.33	21.02	22.06	17.91	1.18	10.61	2.09	6.14	13.72	13.72	16.41	6.94	10.10	
u1_y	2.20	0.80	1.22	6.70	9.66	3.58	2.46	3.69	3.69	7.79	5.27	5.12	0.55	10.00	7.65	11.24	4.26	6.40	1.67	4.87	0.19	0.19	2.11	5.04	4.43	
u2_x	27.51	20.82	10.05	15.24	20.54	4.16	8.42	3.11	3.11	4.93	43.26	9.37	3.96	19.55	16.18	16.42	2.74	7.58	4.25	10.69	24.11	24.11	9.05	13.19	13.43	
u2_y	2.20	2.19	1.22	0.73	12.29	3.58	3.95	2.28	2.28	8.68	4.73	3.21	0.88	17.36	4.71	9.75	4.26	7.91	0.09	3.36	0.19	0.19	11.12	6.60	4.74	
c2_x	15.01	0.01	4.08	6.28	12.64	0.93	5.43	13.30	13.30	5.66	33.26	12.70	3.96	12.19	22.06	19.41	7.43	16.67	10.03	10.69	21.52	21.52	11.99	6.94	11.96	
c2_y	12.02	2.95	12.36	15.36	12.82	7.61	21.71	11.23	11.23	3.79	11.02	3.05	4.88	12.85	10.88	0.05	0.11	12.31	1.83	6.95	23.45	23.45	5.53	5.28	9.69	
l2_x	25.95	23.60	8.56	13.75	19.22	0.93	5.43	4.61	4.61	2.57	30.40	9.37	3.96	16.60	17.65	19.41	12.12	16.67	3.68	12.21	25.41	25.41	10.52	13.19	13.58	
l2_y	3.60	9.55	4.90	7.89	15.45	6.00	0.82	3.77	3.77	4.44	0.41	1.38	2.02	11.18	5.00	9.00	1.68	10.79	1.83	3.66	1.22	1.22	11.42	5.66	5.28	
l1_x	15.01	20.82	3.38	4.16	6.06	4.16	14.39	1.36	1.36	0.22	31.83	26.04	2.53	25.43	16.18	22.39	2.74	9.09	4.25	13.72	13.72	16.41	13.19	11.76	11.76	
l1_y	2.65	2.61	0.42	10.88	14.14	4.39	0.67	2.28	2.28	8.50	1.84	10.29	0.60	9.71	5.00	4.53	1.68	10.79	2.93	2.40	1.22	1.22	4.76	5.28	4.63	
Average	13.60	10.40	7.70	10.14	13.74	5.46	8.82	7.60	7.60	6.94	17.29	10.89	3.66	16.52	12.01	13.46	5.24	13.91	4.42	8.18	12.40	12.40	8.94	10.00	10.00	

Figure B.6: ORL polygonal right eyebrow template test results

APPENDIX C

Spline-based Eyebrow Template Detailed Test Results

Absolute Difference Pixel Values																						
% Param Name	K.A.DI	K.A.HA	K.A.SA	K.A.SU	K.L.AN	K.L.FE	K.M.DI	K.M.SA	K.R.AN	M.K.SA	N.A.AN	N.A.HA	N.A.SU	N.M.DI	T.M.FE	T.M.SA	U.Y.AN	U.Y.DI	Y.M.H	Average		
c1_x	3.32	1.56	0.4	7.54	4.73	2.90	0.54	2.16	6.28	0.33	3.86	0.76	3.37	3.74	3.37	2.78	3.93	3.96	1.76	0.97	2.91	
c1_y	1.72	1.86	1.61	5.81	4.61	0.33	0	3.07	0.70	8.61	1.17	4.53	3.55	3.79	1.03	4.78	3.23	2.48	4.82	2.57	3.01	
u1_x	1.78	5.82	5.14	0.20	0.49	1.47	0.15	2.69	3.33	0.34	4.23	3.08	1.37	3.05	7.63	7.20	2.13	0.68	6.03	6.52	3.17	
u1_y	1.27	0.68	0.66	1.16	1.64	0.49	1.14	0.86	0.41	0.26	0.74	1.50	2.15	0.67	1.46	1.65	0.58	1.65	2.48	0.32	1.09	
u2_x	4.60	5.90	10.2	2.17	1.25	2.83	2.45	6.63	0.28	2.01	2.12	2.03	1.71	0.46	8.37	10.93	0.69	0.68	7.25	10.25	4.14	
u2_y	0.04	0.83	0.52	0.95	1.71	0.39	1.48	1.15	1.30	0.74	1.18	0.73	1.51	0.08	1.14	2.65	0.89	0.78	0.33	3.20	1.08	
c2_x	9.20	7.55	16.9	3.80	2.32	6.66	6.33	9.77	3.39	4.67	2.29	4.95	4.29	6.13	5.20	10.62	5.13	2.76	11.60	11.66	6.76	
c2_y	10.12	10.97	10.3	1.14	2.19	7.65	4.07	0.42	2.63	1.94	1.71	2.53	3.12	1.18	5.39	14.18	0.15	1.56	6.19	7.48	4.75	
l2_x	3.93	6.23	10.9	4.46	1.51	3.16	4.11	7.96	1.72	0.34	0.88	4.69	0.63	0.13	6.04	9.85	0.35	2.68	8.25	12.43	4.51	
l2_y	0.37	0.03	1.42	0.52	0.50	0.23	1.88	1.41	0.70	1.06	1.85	0.17	2.21	0.85	3.34	5.10	0.16	0.12	1.20	2.16	1.26	
l1_x	0.78	5.11	5.06	1.13	0.07	2.13	0.41	5.28	2.00	1.01	3.90	4.08	1.37	4.39	7.96	8.62	0.46	2.02	4.70	4.11	3.23	
l1_y	0	0.61	1.58	0	1.52	1.23	0.99	0.69	2.36	0.68	2.39	2.74	0.07	0.79	0.27	3.00	4.09	0.82	2.65	0.05	0.38	1.34
Average																						
	3.38	4.23	5.74	2.63	1.91	2.57	2.05	3.76	2.07	1.94	2.18	2.64	2.30	2.22	4.63	7.12	1.61	1.76	4.96	5.61		

Percentage (of width) Diff

% Param Name	K.A.DI	K.A.HA	K.A.SA	K.A.SU	K.L.AN	K.L.FE	K.M.DI	K.M.SA	K.R.AN	M.K.SA	N.A.AN	N.A.HA	N.A.SU	N.M.DI	T.M.FE	T.M.SA	U.Y.AN	U.Y.DI	Y.M.H	Average	
c1_x	8.98	4.64	1.29	23.80	12.56	8.35	1.49	6.22	17.28	0.89	10.17	2.19	9.55	8.19	9.29	8.16	10.53	9.08	4.79	2.52	8.00
c1_y	4.66	5.53	5.20	18.35	12.25	0.96	0.01	8.85	1.93	23.26	3.07	13.07	10.04	8.31	2.84	14.06	8.65	5.68	13.15	6.70	8.33
u1_x	4.80	17.29	16.56	0.64	1.29	4.23	0.41	7.76	9.18	0.91	11.14	8.89	3.89	6.69	21.00	21.16	5.69	1.56	16.45	17.00	8.83
u1_y	3.44	2.02	2.14	3.65	4.36	1.42	3.14	2.47	1.13	0.70	1.94	4.33	6.10	1.46	4.03	4.85	1.56	3.79	6.78	0.83	3.01
u2_x	12.43	17.52	33.00	6.85	3.32	8.17	6.74	19.1	0.76	5.42	5.58	5.84	4.83	1.00	23.05	32.15	1.84	1.56	19.77	26.73	11.79
u2_y	0.11	2.48	1.66	2.99	4.55	1.14	4.09	3.31	3.58	2.00	3.10	2.11	4.28	0.18	3.15	7.80	2.38	1.80	0.91	8.34	3.00
c2_x	24.86	22.43	54.57	11.99	6.17	19.20	17.4	28.2	9.33	12.63	6.04	14.27	12.15	13.41	14.30	31.23	13.73	6.32	31.65	30.43	19.02
c2_y	27.35	32.58	33.36	3.61	5.83	22.07	11.2	1.21	7.25	5.24	4.51	7.30	8.83	2.59	14.84	41.71	0.40	3.58	16.87	19.50	13.49
l2_x	10.63	18.51	35.15	14.10	4.01	9.13	11.3	23	4.74	0.91	2.32	13.54	1.77	0.27	16.62	28.98	0.95	6.14	22.50	32.43	12.85
l2_y	1.01	0.10	4.57	1.65	1.33	0.66	5.19	4.07	1.93	2.87	4.86	0.48	6.26	1.86	9.20	14.99	0.42	0.27	3.27	5.64	3.53
l1_x	2.10	15.17	16.32	3.57	0.20	6.16	1.13	15.2	5.51	2.72	10.27	11.78	3.89	9.61	21.91	25.37	1.23	4.62	12.81	10.72	9.01
l1_y	1.64	4.69	0.01	4.81	3.26	2.86	1.91	6.8	1.87	6.47	7.20	0.19	2.23	0.58	8.25	12.02	2.19	6.08	0.13	1.00	3.71
Average																					
	8.50	11.91	16.99	8.00	4.93	7.03	5.34	10.52	5.37	5.34	5.85	7.00	6.15	4.51	12.37	20.21	4.13	4.21	12.42	13.49	

Figure C.1: JAFFE spline-based left eyebrow template test results

Absolute Difference Pixel Values																																				
Param Name	K_A	D_H	K_A	H_A	K_A	S_A	K_L	A_N	K_L	F_E	K_M	D_C	K_M	S_A	K_R	A_N	K_M	S_A	A_N	H_A	N_A	S_L	N_M	D_F	T_M	F_E	T_M	S_A	A_N	U_Y	D_C	U_Y	D_F	Y_M	H_A	Average
c1_x	13.06	3.5	6.53	8.11	3.62	6	10.8	9.9	3.22	4.24	8.95	8.62	8.14	10.4	7.6	6.92	11	6.52	8.45	9.22	7.74															
c1_y	2.97	3.38	4.11	12.8	4.73	5.03	2.18	2.21	2.33	0.97	0.21	2.06	2.55	10.1	13.5	0.96	9.14	5.17	6.29	5.21	4.80															
u1_x	9.71	1.09	7.6	7.11	1.88	0.67	2.9	5.28	1.98	0.95	3.21	5.3	0.86	5.77	4.27	4.36	0.95	0.35	0.53	0.94	3.29															
u1_y	0.12	1.56	0.53	0.16	0.66	0.00	1.36	0	0.79	0.15	1.82	3.45	1.97	0.22	0.58	0.8	0.19	1.72	0.56	0.87	0.88															
u2_x	7.89	0.87	7.78	4.11	1.12	0.5	4.48	2.82	3.84	0.05	7.19	6.04	5.53	2.1	2.01	2.5	1.33	1.22	2.47	2.55	3.32															
u2_y	2.23	0.55	1.48	1.5	0.8	1.52	0.99	0.4	1.04	0.15	1.67	1.12	0.95	0.56	0.23	1.33	0.41	0.31	0.11	1.92	0.96															
c2_x	3.94	1.6	4.49	2.44	2.38	0.33	0.52	1.15	5.55	2.39	5.39	7	3.86	0.9	2.73	1.85	0.66	0.85	0.2	1.88	2.51															
c2_y	4.72	1.97	4.46	2.17	1.6	0.63	1.85	2.33	3.5	1.78	0.87	4.87	1.55	1.86	2.52	3.8	0.14	0.53	2.09	6.79	2.50															
i2_x	5.55	2.13	8.89	5.11	2.55	0.5	2.48	2.15	0.51	2.39	5.86	5.12	2.97	1.1	0.32	2.17	3.01	0.4	3.14	1.88	2.91															
i2_y	2.27	2.35	2.85	2.5	0.3	0.88	0.82	0.33	0.47	0.11	0.1	1.13	0.99	0.14	0.13	2.83	1.19	0.69	1.09	0.46	1.08															
i11_x	9.04	2.99	7.63	11.3	2.88	2	3.91	2.63	2.15	0.72	0.21	1.97	0.86	8.01	5.98	8.11	5.62	2.68	3.18	2.26	4.20															
i11_y	0.09	0.53	0.99	0.91	0.83	2.3	0.31	1.49	0.15	1.11	0.72	2.45	2.71	0.03	1.38	0.94	0.46	0.98	0.99	3.36	1.14															
Average																																				
5.59	2.00	5.12	5.21	2.05	1.64	2.94	2.65	2.31	1.26	3.22	4.24	2.75	3.75	3.63	3.24	3.06	1.86	2.56	3.09																	
Percentage (of width) Diff																																				
Param Name	K_A	D_H	K_A	H_A	K_A	S_A	K_L	A_N	K_L	F_E	K_M	D_C	K_M	S_A	K_R	A_N	K_M	S_A	A_N	H_A	N_A	S_L	N_M	D_F	T_M	F_E	T_M	S_A	A_N	U_Y	D_C	U_Y	D_F	Y_M	H_A	Average
c1_x	39.18	9.91	17.34	23.62	9.29	14.75	32.13	29.11	8.32	10.52	24.40	24.64	23.94	29.26	24.79	19.95	34.04	18.64	21.30	22.67	21.89															
c1_y	8.90	9.56	10.91	37.37	12.14	12.38	6.48	6.50	6.02	2.41	0.57	5.87	7.51	28.44	44.09	2.76	28.27	14.78	15.86	12.81	13.68															
u1_x	29.12	3.08	20.19	20.71	4.81	1.84	8.60	15.53	5.13	2.35	8.76	15.14	2.54	16.17	13.92	12.59	2.94	0.99	1.34	2.31	9.39															
u1_y	0.36	4.41	1.41	0.48	1.69	0.00	4.04	0.01	2.05	0.36	4.97	9.87	5.81	0.63	1.89	2.30	0.60	4.92	1.41	2.14	2.47															
u2_x	23.66	2.47	20.67	11.97	2.87	1.23	13.32	8.28	9.94	0.13	19.61	17.27	16.26	5.89	6.57	7.21	4.10	3.48	6.23	6.27	9.37															
u2_y	6.70	1.56	3.92	4.38	2.04	3.73	2.93	1.18	2.69	0.36	4.55	3.20	2.80	1.56	0.76	3.85	1.26	0.89	0.27	4.73	2.67															
c2_x	11.82	4.53	11.93	7.12	6.10	0.82	1.53	3.38	14.36	5.91	14.69	20.01	11.36	2.52	8.90	5.35	2.04	2.43	0.50	4.63	7.00															
c2_y	14.15	5.58	11.85	6.32	4.10	1.56	5.49	6.87	9.06	4.41	2.38	13.91	4.57	5.21	8.22	10.97	0.43	1.50	5.28	16.70	6.93															
i2_x	16.66	6.02	23.59	14.89	6.53	1.23	7.38	6.32	1.32	5.91	15.97	14.63	8.72	3.09	1.04	6.25	9.30	1.13	7.91	4.63	8.13															
i2_y	6.80	6.65	7.57	7.29	0.76	2.18	2.43	0.98	1.23	0.28	0.27	3.24	2.91	0.40	0.44	8.17	3.69	1.98	2.75	1.13	3.06															
i11_x	27.12	8.46	20.25	32.84	7.38	4.92	11.61	7.73	5.56	1.78	0.58	5.62	2.54	22.47	19.51	23.38	17.37	7.66	8.02	5.56	12.02															
i11_y	0.26	1.49	2.64	2.66	2.12	5.66	0.93	4.37	0.38	2.76	1.97	7.01	7.96	0.07	4.51	2.70	1.43	2.80	2.51	8.26	3.12															
Average																																				
15.39	5.31	12.69	14.14	4.99	4.17	8.07	7.52	5.51	3.10	8.23	11.70	8.08	9.64	11.22	8.79	8.79	5.10	6.11	7.65																	

Absolute Difference Pixel Values																					
% Param	right	2.sad	brmal	brmal	sses	brmal	6.sad	right	sses	brmal	leppy	wink	right	2.sad	subje	subje	subje	subje	subje	Average	
c1_x	0.84	3.59	4.49	5.75	3.06	4.78	1.11	3.42	3.07	0.77	1.73	1.71	0.51	5.19	0.72	1.48	2.82	0.56	1.37	3.07	2.50
c1_y	5.78	18.29	4.42	9.53	16.25	17.84	3.67	5.19	2.04	7.30	5.57	5.86	5.91	9.99	7.55	0.82	7.93	6.48	4.56	0.18	7.26
u1_x	4.84	2.81	6.94	1.13	5.63	4.37	4.22	1.25	1.68	5.47	4.27	4.69	5.18	2.81	5.95	0.12	2.16	6.58	7.17	4.44	4.09
u1_y	2.44	1.93	0.91	3.63	0.58	0.06	1.53	2.09	0.16	1.40	0.44	1.17	0.18	0.37	0.21	0.11	0.19	1.55	1.33	1.75	1.10
u2_x	6.78	3.94	1.94	0.13	4.29	4.55	4.55	4.58	2.54	2.81	4.02	1.79	1.85	6.15	6.95	0.57	5.50	6.03	6.24	4.93	4.01
u2_y	1.58	2.35	0.24	1.30	1.42	1.29	1.19	0.76	0.45	0.32	2.32	0.65	0.51	2.37	4.21	1.77	1.57	2.51	1.08	3.45	1.57
c2_x	11.51	6.18	3.26	1.54	9.29	7.89	8.89	8.25	3.54	9.48	5.76	3.93	4.18	10.48	6.61	3.76	9.86	10.06	7.79	10.93	7.16
c2_y	0.94	0.28	3.43	3.13	1.22	1.16	0.66	2.52	2.63	1.75	0.62	0.15	3.80	1.01	1.45	0.80	0.21	3.79	4.08	1.15	1.74
l2_x	8.44	3.89	0.61	0.46	3.63	1.55	4.22	3.91	1.00	3.14	3.02	3.12	1.51	6.48	4.61	0.43	6.33	6.37	7.58	7.60	3.90
l2_y	1.08	1.29	2.34	4.70	0.12	0.83	0.34	2.86	2.61	0.75	0.26	1.15	1.89	0.34	1.45	0.87	0.73	2.74	1.38	2.85	1.53
l1_x	7.18	0.80	5.94	1.79	4.29	0.33	3.89	1.58	0.98	3.47	2.93	4.20	3.18	1.81	3.28	1.12	1.82	5.02	5.84	4.44	3.20
l1_y	1.94	0.12	2.34	4.13	1.78	0.28	1.34	4.19	2.78	2.14	1.84	3.76	2.55	1.99	2.55	0.66	1.52	2.28	2.63	3.35	2.21
Average																					
Average	4.45	3.79	3.07	3.10	4.30	3.74	2.97	3.38	1.96	3.23	2.73	2.68	2.60	4.08	3.80	1.04	3.39	4.50	4.26	4.01	

Percentage (of width) Diff																					
% Param	right	2.sad	brmal	brmal	sses	brmal	6.sad	right	sses	brmal	leppy	wink	right	2.sad	subje	subje	subje	subje	subje	Average	
c1_x	2.61	10.35	14.65	20.78	8.67	16.30	3.97	12.51	8.29	2.20	4.64	4.53	1.59	18.98	2.27	4.45	10.46	1.41	3.38	7.66	7.99
c1_y	17.88	52.75	14.41	34.44	46.00	60.82	13.11	18.98	5.50	20.87	14.93	15.56	18.27	36.55	23.85	2.47	29.36	16.32	11.21	0.46	22.69
u1_x	14.98	8.10	22.64	4.08	15.92	14.91	15.08	4.56	4.55	15.64	11.43	12.46	16.02	10.29	18.78	0.36	7.99	16.60	17.63	11.11	12.16
u1_y	7.54	5.56	2.96	13.12	1.65	0.20	5.46	7.64	0.43	4.01	1.19	3.11	0.56	1.37	0.67	0.33	0.69	3.90	3.28	4.38	3.40
u2_x	20.95	11.38	6.33	0.46	12.15	15.52	16.27	16.76	6.86	8.02	10.78	4.75	5.71	22.48	21.94	1.72	20.38	15.21	15.36	12.34	12.27
u2_y	4.88	6.77	0.78	4.69	4.01	4.40	4.27	2.76	1.22	0.92	6.22	1.72	1.59	8.69	13.31	5.32	5.82	6.33	2.65	8.62	4.75
c2_x	35.60	17.83	10.61	5.56	26.30	26.88	31.74	30.17	9.57	27.07	15.43	10.44	12.93	38.34	20.89	11.3	36.54	25.35	19.17	27.34	21.95
c2_y	2.90	0.79	11.20	11.31	3.44	3.95	2.36	9.23	7.10	4.99	1.67	0.41	11.76	3.69	4.57	2.41	0.77	9.57	10.04	2.88	5.25
l2_x	26.11	11.21	1.99	1.66	10.26	5.29	15.08	14.32	2.70	8.98	8.10	8.29	4.68	23.70	14.57	1.28	23.45	16.05	18.63	19.00	11.77
l2_y	3.33	3.71	7.63	16.97	0.33	2.81	1.21	10.45	7.05	2.13	0.69	3.06	5.83	1.25	4.57	2.62	2.69	6.92	3.39	7.12	4.69
l1_x	22.20	2.31	19.38	6.49	12.15	1.12	13.89	5.78	2.66	9.92	7.86	11.15	9.83	6.63	10.36	3.36	6.75	12.66	14.36	11.11	9.50
l1_y	5.99	0.34	7.63	14.93	5.05	0.94	4.78	15.32	7.50	6.11	4.94	9.98	7.90	7.29	8.06	1.97	5.63	5.75	6.48	8.38	6.75
Average																					
Average	13.75	10.93	10.02	11.21	12.16	12.76	10.60	12.37	5.29	9.24	7.32	7.12	8.05	14.94	11.99	3.13	12.54	11.34	10.46	10.03	

Figure C.3: YALE spline-based left eyebrow template test results

Absolute Difference Pixel Values																			
% Param	right	2.sad	brmal	brmal	sses	brmal	6.sad	right	sses	brmal	leepy	wink	right	2.sad	subje	subje	subje	subje	Average
c1_x	12.26	5.54	8.06	4.86	3.10	3.67	5.64	2.69	5.34	5.87	2.66	1.40	4.36	8.74	10.04	4.12	9.23	3.90	5.76
c1_y	4.27	1.94	0.70	3.76	4.68	2.76	7.13	6.82	0.67	5.04	3.57	6.84	0.61	6.22	1.89	0.77	7.06	5.88	3.82
u1_x	11.26	0.36	1.58	0.04	3.02	3.74	2.50	4.45	0.35	2.00	1.22	1.98	1.53	3.07	2.70	0.57	0.43	4.80	2.47
u1_y	5.09	1.06	1.47	1.67	1.82	1.08	0.23	1.15	0.60	0.11	0.16	0.00	0.57	1.42	1.28	0.18	0.08	0.52	1.18
u2_x	9.92	0.54	1.18	1.53	0.38	6.89	5.15	4.26	1.05	1.52	2.50	3.62	0.63	2.43	2.61	0.52	2.56	1.29	2.52
u2_y	4.42	0.30	1.07	1.01	3.58	1.87	1.25	1.78	1.26	1.34	0.17	2.55	0.09	0.88	0.14	0.56	0.87	0.75	1.25
c2_x	6.23	1.26	5.07	3.63	2.38	6.49	10.52	8.42	6.68	3.97	1.92	0.95	1.74	3.26	5.00	2.33	3.44	1.49	3.95
c2_y	1.25	1.13	1.76	0.33	0.32	0.58	0.56	3.38	2.23	1.68	1.80	3.22	1.87	4.88	2.77	3.01	0.94	0.57	1.82
l2_x	8.59	1.95	1.42	0.26	0.04	2.14	4.66	6.00	0.68	1.58	0.41	1.39	0.37	2.43	0.33	1.40	1.23	1.54	2.05
l2_y	4.62	1.07	0.14	0.10	1.65	0.22	0.26	3.82	1.56	2.12	0.20	2.22	0.36	2.65	0.10	1.40	0.61	0.29	1.26
l1_x	10.92	2.64	3.25	1.71	2.31	0.26	0.17	1.78	0.35	3.00	0.80	1.36	1.53	5.41	4.37	0.43	2.76	2.14	2.39
l1_y	4.62	1.66	0.23	0.01	2.78	0.55	1.16	2.95	1.23	1.38	1.69	1.53	1.50	2.12	0.15	0.18	1.82	2.39	1.44
Average																			
	6.95	1.62	2.16	1.57	2.17	2.52	3.27	3.96	1.83	2.47	1.43	2.25	1.26	3.62	2.61	1.29	2.59	2.13	2.23

Percentage (of width) Diff																			
% Param	right	2.sad	brmal	brmal	sses	brmal	6.sad	right	sses	brmal	leepy	wink	right	2.sad	subje	subje	subje	subje	Average
c1_x	47.1	14.97	28.46	15.35	8.08	11.11	20.13	8.69	15.25	13.44	6.09	3.04	9.35	24.28	29.83	12.24	27.69	9.07	16.90
c1_y	16.4	5.23	2.48	11.87	12.21	8.38	25.45	22.02	1.91	11.54	8.19	14.87	1.31	17.27	5.60	2.30	21.18	13.67	10.81
u1_x	43.3	0.99	5.59	0.12	7.88	11.33	8.93	14.34	0.99	4.58	2.79	4.30	3.27	8.54	8.02	1.68	1.28	11.17	7.45
u1_y	19.6	2.87	5.17	5.28	4.76	3.28	0.82	3.71	1.70	0.25	0.37	0.00	1.21	3.94	3.80	0.53	0.25	1.22	3.56
u2_x	38.2	1.47	4.17	4.83	0.98	20.87	18.39	13.74	3.01	3.48	5.74	7.87	1.34	6.74	7.75	1.55	7.69	3.01	7.76
u2_y	17	0.80	3.79	3.18	9.35	5.68	4.46	5.73	3.60	3.08	0.39	5.54	0.19	2.45	0.42	1.67	2.62	1.73	3.72
c2_x	24	3.40	17.90	11.46	6.20	19.67	37.57	27.18	19.09	9.09	4.40	2.06	3.72	9.06	14.85	6.92	10.31	3.46	12.04
c2_y	4.8	3.07	6.21	1.04	0.83	1.77	1.99	10.90	6.37	3.84	4.13	7.01	4.01	13.56	8.22	8.94	2.82	1.33	5.05
l2_x	33	5.26	5.02	0.81	0.11	6.50	16.64	19.37	1.95	3.62	0.94	3.02	0.80	6.74	0.99	4.15	3.69	3.59	6.37
l2_y	17.8	2.88	0.49	0.32	4.30	0.65	0.93	12.32	4.46	4.87	0.46	4.83	0.77	7.37	0.30	4.17	1.82	0.68	3.70
l1_x	42	7.12	11.47	5.39	6.03	0.79	0.59	5.74	0.99	6.87	1.84	2.95	3.27	15.02	12.97	1.29	8.28	4.97	7.19
l1_y	17.8	4.49	0.82	0.02	7.24	1.67	4.15	9.52	3.51	3.15	3.87	3.34	3.21	5.88	0.46	0.53	5.45	1.33	4.13
Average																			
	26.74	4.38	7.63	4.97	5.66	7.64	11.67	12.77	5.24	5.65	3.27	4.90	2.71	10.07	7.77	3.83	7.76	4.96	5.66

Figure C.4: YALE spline-based right eyebrow template test results

Absolute Difference Pixel Values																									
% Param Name	s101	s105	s111	s116	s121	s1210	s155	s162	s221	s225	s231	s294	s306	s309	s39	s405	s510	s52	s71	s78	s85	s88	s94	s98	Average
c1_x	11.08	1.55	0.78	0.48	0.32	1.16	1.15	1.91	0.17	2.18	0.62	4.41	0.86	1.32	1.50	0.80	4.31	1.43	0.74	1.33	0.67	0.17	0.91	0.86	1.70
c1_y	0.60	8.43	5.73	5.05	2.83	3.17	3.48	2.16	3.80	4.71	1.60	2.50	1.50	1.12	0.07	10.07	0.18	2.09	2.55	3.34	1.84	1.33	0.84	3.99	3.04
u1_x	6.08	2.93	4.16	3.85	4.32	3.83	3.29	1.82	3.89	5.85	2.70	7.72	4.07	2.38	3.17	0.99	2.20	2.76	2.93	3.33	2.67	0.51	1.14	2.15	3.28
u1_y	0.17	0.59	1.52	0.88	1.69	0.66	0.26	1.19	3.14	1.51	1.28	0.04	1.33	0.75	1.00	2.02	0.31	1.15	0.25	0.24	0.26	0.67	0.70	0.59	0.92
u2_x	3.42	5.20	5.23	4.94	4.99	5.49	6.88	1.64	3.83	5.18	3.50	9.07	5.87	4.04	2.72	0.33	2.64	2.09	4.22	4.00	1.33	1.51	1.63	1.66	3.81
u2_y	0.17	1.22	1.00	0.17	0.36	0.64	0.02	0.76	0.33	0.84	0.75	3.36	0.42	0.58	0.15	0.67	0.10	0.27	1.14	0.57	1.07	0.66	0.79	0.81	0.70
c2_x	0.42	7.54	5.32	6.31	7.66	5.83	7.52	3.83	6.18	4.85	5.50	13.03	9.21	7.02	5.17	2.97	2.36	6.43	5.97	2.33	3.33	2.84	0.95	1.92	5.19
c2_y	0.73	0.63	1.17	1.19	0.51	2.20	3.29	2.63	0.23	0.71	0.58	6.90	0.82	0.62	1.40	3.34	3.30	0.03	0.39	0.67	1.84	2.66	2.04	0.75	1.61
l2_x	3.75	5.93	6.23	4.94	8.32	5.16	7.22	1.31	4.83	5.18	3.17	12.02	6.54	5.38	3.72	0.67	1.31	2.43	5.89	3.66	1.67	1.84	0.36	1.58	4.30
l2_y	1.07	0.18	1.16	1.00	0.51	1.54	0.49	0.73	0.53	1.04	0.58	3.13	0.15	0.28	0.78	0.83	0.03	0.03	0.10	0.33	1.51	0.33	1.31	0.08	0.74
l1_x	5.75	1.59	4.16	3.52	3.99	1.49	3.29	0.15	2.89	3.85	2.70	7.39	3.40	3.38	3.50	2.32	2.53	1.09	3.26	3.33	0.67	0.17	0.86	2.15	2.81
l1_y	1.73	0.18	3.02	2.71	0.49	0.58	0.60	1.49	1.27	1.04	0.11	0.50	0.43	0.28	0.73	1.18	2.05	0.85	0.79	0.00	1.17	0.67	1.40	0.39	0.99
Average	2.91	3.00	3.29	2.92	3.00	2.65	3.12	1.63	2.59	3.08	1.92	5.84	2.88	2.26	1.99	2.18	1.78	1.72	2.35	1.93	1.50	1.11	1.08	1.41	

Percentage (of width) Diff																									
% Param Name	s101	s105	s111	s116	s121	s1210	s155	s162	s221	s225	s231	s294	s306	s309	s39	s405	s510	s52	s71	s78	s85	s88	s94	s98	Average
c1_x	60.45	7.24	3.75	2.63	1.31	4.77	5.95	8.95	0.64	8.61	3.31	22.80	4.44	6.60	6.72	3.65	22.29	6.49	3.76	7.39	2.67	0.64	3.98	4.07	8.46
c1_y	3.27	39.52	27.75	27.53	11.46	13.01	17.98	10.12	14.62	18.59	8.55	12.94	7.76	5.60	0.30	45.76	0.94	9.48	12.95	18.54	7.36	4.85	3.67	19.00	14.23
u1_x	33.18	13.72	20.13	21.01	17.53	15.73	17.03	8.52	14.97	23.09	14.44	39.94	21.06	11.88	14.18	4.49	11.37	12.55	14.88	18.50	10.66	1.86	4.95	10.25	15.66
u1_y	0.91	2.76	7.36	4.80	6.86	2.70	1.37	5.58	12.08	5.96	6.86	0.19	6.86	3.75	4.48	9.17	1.62	5.23	1.25	1.32	1.04	2.46	3.05	2.79	4.19
u2_x	18.64	24.38	25.29	26.97	20.23	22.58	35.61	7.69	14.74	20.46	18.75	46.94	30.39	20.21	12.17	1.52	13.67	9.52	21.47	22.21	5.33	5.51	7.10	7.91	18.30
u2_y	0.91	5.71	4.82	0.91	1.46	2.62	0.10	3.57	1.28	3.33	4.02	17.40	2.16	2.92	0.67	3.03	0.52	1.23	5.78	3.17	4.29	2.42	3.43	3.86	3.32
c2_x	2.27	35.33	25.72	34.43	31.04	23.95	38.90	17.94	23.77	19.14	29.46	67.37	47.63	35.10	23.13	13.49	12.20	29.21	30.35	12.95	13.33	10.39	4.15	9.13	24.60
c2_y	4.00	2.95	5.67	6.50	2.06	9.06	17.02	12.34	0.89	2.80	3.13	35.67	4.22	3.11	6.27	15.19	17.07	0.13	1.99	3.72	7.36	9.73	8.87	3.56	7.64
l2_x	20.45	27.78	30.13	26.97	33.74	21.21	37.33	6.13	18.59	20.46	16.96	62.16	33.84	26.88	16.65	3.03	6.77	11.03	29.94	20.36	6.66	6.73	1.58	7.54	20.54
l2_y	5.82	0.83	5.62	5.45	2.06	6.32	2.51	3.41	2.05	4.12	3.13	16.19	0.78	1.42	3.51	3.79	0.17	0.13	0.53	1.83	6.02	1.20	5.70	0.39	3.46
l1_x	31.36	7.47	20.13	19.19	16.17	6.14	17.03	0.71	11.12	15.19	14.44	38.21	17.61	16.88	15.67	10.55	13.10	4.97	16.58	18.50	2.66	0.64	3.75	10.25	13.68
l1_y	9.45	0.83	14.62	14.80	2.00	2.37	3.11	6.98	4.90	4.12	0.61	2.61	2.20	1.42	3.28	5.38	10.58	3.87	4.00	0.02	4.69	2.46	6.09	1.84	4.68
Average	15.89	14.04	15.92	15.93	12.16	10.87	16.16	7.66	9.97	12.16	10.31	30.20	14.91	11.31	8.92	9.92	9.19	7.82	11.96	10.71	6.01	4.07	4.69	6.72	

Figure C.5: ORL spline-based left eyebrow template test results

Absolute Difference Pixel Values																											
% Param	s101	s105	s111	s116	s121	s1210	s155	s162	s221	s225	s231	s294	s306	s309	s39	s405	s510	s52	s71	s78	s85	s88	s94	s98	Average		
c1_x	5.49	3.25	2.40	3.63	6.36	4.22	6.61	1.81	5.05	1.47	6.04	4.74	2.91	4.97	3.46	6.79	5.89	3.90	0.20	4.48	5.30	5.09	0.94	4.34	4.14		
c1_y	0.66	1.50	2.42	3.63	0.31	0.49	2.66	0.89	2.84	6.47	0.81	0.46	0.40	1.49	1.06	0.75	0.91	0.06	1.18	0.06	4.09	3.24	0.63	0.72	1.57		
u1_x	1.82	0.80	0.54	2.03	0.80	0.64	1.55	1.52	1.38	3.96	1.99	0.87	1.81	2.90	0.79	2.68	0.55	0.56	2.47	1.48	3.79	1.31	2.33	2.52	1.71		
u1_y	0.59	1.10	0.31	1.54	1.65	0.53	0.15	0.37	0.81	2.73	0.60	1.27	0.50	0.56	1.08	1.19	0.62	1.46	0.95	0.33	0.82	0.10	0.86	0.58	0.86		
u2_x	4.49	4.79	2.40	2.63	3.04	1.36	0.36	1.81	0.71	1.86	6.17	1.21	0.24	1.88	2.79	1.34	0.45	1.56	0.60	2.48	6.96	5.91	0.70	1.33	2.38		
u2_y	0.59	1.33	0.18	0.21	0.53	0.20	0.46	0.96	1.86	1.07	1.60	1.56	0.73	2.02	0.42	0.86	0.62	1.13	1.97	0.01	0.98	0.62	1.11	0.33	0.89		
c2_x	0.82	1.69	1.12	0.03	0.07	1.17	1.43	0.15	0.38	1.23	2.13	1.66	0.26	0.58	2.13	0.85	0.78	0.10	0.81	2.32	6.96	2.99	1.70	2.98	1.43		
c2_y	5.82	3.39	2.95	5.78	1.05	0.20	4.95	3.56	2.72	4.32	3.07	4.13	1.71	0.95	2.02	2.49	0.09	0.06	1.48	3.76	7.24	5.77	0.05	3.29	2.95		
l2_x	4.15	5.45	2.07	2.30	2.71	0.69	0.31	2.15	2.38	2.80	3.32	1.21	0.24	1.21	2.46	2.01	1.55	0.44	1.06	2.81	7.30	4.91	1.04	1.33	2.33		
l2_y	0.01	0.16	1.08	1.61	0.67	0.10	1.46	1.89	1.82	0.12	0.03	1.30	0.70	0.82	0.88	0.99	0.25	0.39	2.10	0.06	0.91	0.84	1.28	0.13	0.81		
l1_x	2.82	3.13	0.21	1.03	0.80	1.03	2.89	1.19	4.05	0.35	5.32	4.20	1.19	3.90	2.13	3.68	0.89	0.90	1.14	3.14	3.79	1.05	2.33	1.18	2.18		
l1_y	1.32	1.26	0.04	2.28	0.11	0.50	1.15	1.56	1.51	2.92	0.30	0.34	0.47	0.70	0.68	0.01	0.25	0.39	2.41	1.27	0.89	1.15	1.36	1.62	1.02		
Average	2.38	2.32	1.31	2.23	1.51	0.93	2.00	1.49	2.13	2.44	2.62	1.91	0.93	1.83	1.64	1.97	1.07	0.91	1.36	1.85	4.08	2.75	1.20	1.70			
Percentage (of width) Diff																											
% Param	s101	s105	s111	s116	s121	s1210	s155	s162	s221	s225	s231	s294	s306	s309	s39	s405	s510	s52	s71	s78	s85	s88	s94	s98	Average		
c1_x	25.71	13.53	10.73	16.26	25.11	20.44	29.62	8.12	17.81	5.17	25.88	23.69	12.46	21.94	15.26	30.42	27.60	17.71	0.96	20.35	20.63	20.11	4.16	20.34	18.08		
c1_y	3.08	6.24	10.81	16.26	1.20	2.37	11.92	3.99	10.03	22.84	3.45	2.31	1.73	6.56	4.67	3.37	4.28	0.27	5.60	0.28	15.93	12.77	2.76	3.35	6.50		
u1_x	8.52	3.32	2.43	9.11	3.16	3.08	6.95	6.81	4.87	13.97	8.53	4.33	7.76	12.80	3.49	11.98	2.60	2.56	11.76	6.71	14.75	5.17	10.29	11.79	7.36		
u1_y	2.76	4.57	1.38	6.91	6.50	2.58	0.65	1.68	2.86	9.64	2.59	6.35	2.14	2.48	4.78	5.34	2.91	6.63	4.51	1.49	3.19	0.39	3.81	2.71	3.70		
u2_x	21.02	19.95	10.74	11.79	11.99	6.58	1.60	8.12	2.51	6.57	26.45	6.03	1.03	8.30	12.32	6.01	2.09	7.10	2.88	11.26	27.13	23.33	3.10	6.25	10.17		
u2_y	2.76	5.53	0.82	0.94	2.10	0.96	2.05	4.29	6.55	3.77	6.88	7.82	3.12	8.89	1.84	3.85	2.91	5.11	9.36	0.02	3.81	2.46	4.92	1.56	3.85		
c2_x	3.84	7.04	5.03	0.15	0.28	5.66	6.39	0.65	1.34	4.32	9.12	8.28	1.09	2.54	9.37	3.82	3.65	0.47	3.87	10.55	27.13	11.81	7.51	13.96	6.16		
c2_y	27.30	14.13	13.19	25.87	4.13	0.97	22.15	15.93	9.59	15.24	13.14	20.66	7.35	4.18	8.90	11.16	0.41	0.27	7.06	17.07	28.23	22.79	0.23	15.44	12.72		
l2_x	19.46	22.72	9.25	10.29	10.68	3.35	1.39	9.61	8.40	9.90	14.24	6.03	1.03	5.35	10.85	9.00	7.29	1.99	5.06	12.77	28.43	19.38	4.57	6.25	9.89		
l2_y	0.05	0.67	4.85	7.21	2.64	0.50	6.52	8.47	6.44	0.42	0.12	6.49	2.98	3.60	3.01	4.44	1.16	1.78	10.00	0.28	3.55	3.33	5.65	0.62	3.53		
l1_x	13.21	13.04	0.93	4.63	3.16	4.98	12.92	5.32	14.28	1.22	22.81	20.99	5.10	17.21	9.37	16.46	4.16	4.07	5.41	14.29	14.75	4.13	10.29	5.54	9.51		
l1_y	6.20	5.26	0.19	10.20	0.44	2.42	5.13	6.98	5.33	10.30	1.30	1.68	1.99	3.07	3.01	0.03	1.16	1.78	11.49	5.78	3.45	4.54	6.02	7.60	4.39		
Average	11.16	9.67	5.86	9.97	5.95	4.49	8.94	6.66	7.50	8.61	11.21	9.55	3.98	8.08	7.24	8.82	5.02	4.14	6.50	8.40	15.91	10.85	5.28	7.95			

Figure C.6: ORL spline-based right eyebrow template test results

APPENDIX D

Spline-based Eye Template Detailed Test Results

Absolute Difference Pixel Values																																											
% Param Name	KA	DI1	KA	HA	KA	SA	KA	SU	KL	AN	KL	FE	KM	DI	KM	SA	KR	AN	MK	SA	NA	AN	NA	HA	NA	SU	NM	DI	TM	FE	TM	SA	UY	AN	UY	DI	YM	DI	YM	HA	Average		
xc	1.00	0.00	0.33	0.67	0.00	0.67	2.33	1.67	0.67	1.00	0.33	0.33	0.00	0.33	0.33	0.00	0.33	0.33	0.00	0.33	0.33	0.33	0.33	0.33	0.33	0.33	0.33	0.33	0.33	0.33	0.33	0.33	0.33	0.33	0.33	0.33	0.67	0.67	0.67	0.67	0.60		
yc	0.00	0.33	0.00	1.67	2.67	0.33	0.33	0.67	0.00	0.67	0.00	0.67	0.00	0.67	0.00	0.00	0.67	0.00	0.67	0.00	0.67	0.00	0.67	0.00	0.67	0.00	0.67	0.00	0.67	0.00	0.67	0.00	0.67	0.00	0.67	0.00	0.67	0.00	0.67	0.00	0.73		
r	0.67	0.67	0.33	1.00	2.00	1.00	2.00	1.00	0.33	2.00	0.33	0.33	0.67	1.00	0.33	0.67	1.00	0.33	0.33	2.00	0.33	0.33	0.33	0.33	0.33	0.67	1.00	0.33	0.33	0.00	0.33	0.00	0.00	1.00	0.00	0.33	1.00	0.33	1.00	0.33	1.00	0.80	
c1x	1.71	2.48	2.29	0.85	3.89	3.22	3.87	0.89	1.96	2.22	0.29	0.96	1.52	4.29	0.63	2.63	1.63	1.63	1.63	2.22	0.29	0.96	1.52	4.29	0.63	2.63	1.63	1.63	1.63	1.63	1.63	1.63	1.63	1.63	1.63	1.63	1.63	1.63	1.63	1.63	1.63	2.10	
c1y	5.16	2.24	3.83	3.24	6.32	4.32	0.29	1.32	3.83	2.99	4.83	3.16	3.90	4.16	4.49	3.83	5.16	3.99	4.16	1.99	3.66	1.99	3.66	1.99	3.66	1.99	3.66	1.99	3.66	1.99	3.66	1.99	3.66	1.99	3.66	1.99	3.66	1.99	3.66	1.99	3.66	3.66	
c2x	0.63	6.51	1.97	5.51	1.44	2.44	3.67	2.11	3.63	1.44	1.63	1.63	4.51	0.97	1.53	3.97	1.97	2.11	1.30	1.78	2.54	1.30	1.78	2.54	1.30	1.78	2.54	1.30	1.78	2.54	1.30	1.78	2.54	1.30	1.78	2.54	1.30	1.78	2.54	1.30	1.78	2.54	2.54
c2y	2.65	4.06	4.65	2.40	1.95	2.95	2.00	2.95	5.99	0.28	4.99	2.65	3.73	4.65	1.32	1.32	2.32	2.95	2.65	3.95	3.02	2.65	3.95	3.02	2.65	3.95	3.02	2.65	3.95	3.02	2.65	3.95	3.02	2.65	3.95	3.02	2.65	3.95	3.02	2.65	3.95	3.02	3.02
upx	1.98	1.84	0.02	0.84	4.46	3.79	3.13	0.79	2.68	3.13	1.35	1.35	0.51	0.02	0.65	2.68	0.68	2.46	0.35	4.46	1.86	1.98	1.84	0.02	0.84	4.46	3.79	3.13	0.79	2.68	3.13	1.35	1.35	0.51	0.02	0.65	2.68	0.68	2.46	0.35	4.46	1.86	1.86
upy	1.99	0.60	1.33	0.94	0.92	1.25	2.25	1.92	1.33	1.92	2.33	1.33	0.94	1.99	1.99	1.99	1.99	1.66	1.25	1.99	1.61	1.99	0.60	1.33	0.94	0.92	1.25	2.25	1.92	1.33	1.92	2.33	1.33	0.94	1.99	1.99	1.66	1.25	1.99	2.25	1.99	2.25	1.61
downx	2.33	2.67	0.00	1.67	1.00	1.00	0.67	2.00	3.33	0.33	1.33	1.00	1.67	0.33	1.00	2.67	0.67	0.33	1.33	1.28	2.33	2.67	0.00	1.67	1.00	0.67	2.00	3.33	0.33	1.00	2.67	0.67	0.33	1.33	1.00	2.67	0.67	0.33	1.33	1.00	2.67	0.67	1.28
downy	0.33	0.00	1.00	1.67	1.00	1.00	1.00	1.00	0.33	1.00	1.67	0.67	2.00	0.33	0.33	2.00	1.33	1.00	0.33	1.33	0.95	0.33	0.00	1.00	1.67	1.00	1.00	0.33	0.33	2.00	1.33	1.00	0.33	1.33	1.00	0.33	1.33	1.00	0.33	1.33	1.00	0.95	
Average	1.68	1.95	1.43	1.86	2.33	2.00	1.96	1.42	2.25	1.60	1.67	1.43	1.62	1.77	1.37	1.92	1.61	1.66	1.34	1.97																							

Percentage (of width) Diff																																											
% Param Name	KA	DI1	KA	HA	KA	SA	KA	SU	KL	AN	KL	FE	KM	DI	KM	SA	KR	AN	MK	SA	NA	AN	NA	HA	NA	SU	NM	DI	TM	FE	TM	SA	UY	AN	UY	DI	YM	DI	YM	HA	Average		
xc	3.90	0.00	1.18	2.60	0.00	2.25	8.33	6.17	2.53	3.61	1.25	1.22	0.00	1.06	1.23	1.25	1.20	1.19	2.38	2.27	2.18	3.90	0.00	1.18	2.60	0.00	2.25	8.33	6.17	2.53	3.61	1.25	1.22	0.00	1.06	1.23	1.25	1.20	1.19	2.38	2.27	2.18	2.18
yc	0.00	1.19	0.00	6.49	9.09	1.12	1.19	2.47	0.00	2.41	1.25	3.66	0.00	4.26	2.47	1.25	8.43	5.95	1.19	0.00	2.62	0.00	1.19	0.00	6.49	9.09	1.12	1.19	2.47	0.00	2.41	1.25	3.66	0.00	4.26	2.47	1.25	8.43	5.95	1.19	0.00	2.62	
r	2.60	2.38	1.18	3.90	6.82	3.37	7.14	3.70	1.27	7.23	1.25	1.22	2.56	3.19	1.23	0.00	0.00	3.57	1.19	3.41	2.86	2.60	2.38	1.18	3.90	6.82	3.37	7.14	3.70	1.27	7.23	1.25	1.22	2.56	3.19	1.23	0.00	0.00	3.57	1.19	3.41	2.86	2.86
c1x	6.84	8.86	8.10	3.32	13.26	10.86	13.83	3.29	7.45	8.03	1.11	3.52	5.85	13.71	2.33	9.86	5.88	6.74	4.62	12.12	7.47	6.84	8.86	8.10	3.32	13.26	10.86	13.83	3.29	7.45	8.03	1.11	3.52	5.85	13.71	2.33	9.86	5.88	6.74	4.62	12.12	7.47	7.47
c1y	20.10	7.98	13.50	12.60	21.55	14.56	1.02	4.89	14.53	10.80	18.10	11.56	15.01	13.27	16.64	14.35	18.65	14.24	14.86	6.77	13.25	20.10	7.98	13.50	12.60	21.55	14.56	1.02	4.89	14.53	10.80	18.10	11.56	15.01	13.27	16.64	14.35	18.65	14.24	14.86	6.77	13.25	13.25
c2x	2.46	23.25	6.94	21.47	4.92	8.24	13.10	7.82	13.79	5.22	6.12	5.97	17.35	3.08	6.05	14.87	7.11	7.54	4.64	6.06	9.30	2.46	23.25	6.94	21.47	4.92	8.24	13.10	7.82	13.79	5.22	6.12	5.97	17.35	3.08	6.05	14.87	7.11	7.54	4.64	6.06	9.30	9.30
c2y	10.34	14.51	16.43	9.34	6.65	9.94	7.14	10.92	22.74	1.02	18.70	9.71	14.34	14.85	4.89	4.95	8.39	10.53	9.48	13.46	10.92	10.34	14.51	16.43	9.34	6.65	9.94	7.14	10.92	22.74	1.02	18.70	9.71	14.34	14.85	4.89	4.95	8.39	10.53	9.48	13.46	10.92	10.92
upx	7.72	6.58	0.06	3.29	15.20	12.78	11.16	2.93	10.20	11.30	5.07	4.94	1.96	0.06	2.40	10.07	2.48	8.78	1.26	15.20	6.67	7.72	6.58	0.06	3.29	15.20	12.78	11.16	2.93	10.20	11.30	5.07	4.94	1.96	0.06	2.40	10.07	2.48	8.78	1.26	15.20	6.67	6.67
upy	7.77	2.16	4.69	3.65	3.13	4.21	8.04	7.10	5.04	6.93	8.73	4.86	3.61	6.37	7.39	7.48	6.01	4.46	7.12	5.82	7.77	2.16	4.69	3.65	3.13	4.21	8.04	7.10	5.04	6.93	8.73	4.86	3.61	6.37	7.39	7.48	6.01	4.46	7.12	5.82	5.82		
downx	9.09	9.52	0.00	6.49	3.41	3.37	2.38	7.41	12.66	1.20	5.00	3.66	6.41	1.06	3.70	10.00	2.41	1.19	4.55	4.74	9.09	9.52	0.00	6.49	3.41	3.37	2.38	7.41	12.66	1.20	5.00	3.66	6.41	1.06	3.70	10.00	2.41	1.19	4.55	4.74	4.74		
downy	1.30	0.00	3.53	6.49	3.41	3.37	3.57	1.23	3.80	6.02	2.50	7.32	1.28	1.06	7.41	5.00	3.61	1.19	4.76	2.27	3.46	1.30	0.00	3.53	6.49	3.41	3.37	3.57	1.23	3.80	6.02	2.50	7.32	1.28	1.06	7.41	5.00	3.61	1.19	4.76	2.27	3.46	
Average	6.54	6.95	5.05	7.24	7.95	6.73	6.99	5.27	8.55	5.80	6.28	5.24	6.22	5.63	5.07	7.19	5.83	5.94	4.79	6.71																							

Figure D.1: JAFFE spline-based left eye template test results

Absolute Difference Pixel Values																					
% Param Name	KA.D11	KA.H4	KA.S4	KA.SU	KL.AN	KL.FE	KM.D1	KM.S4	KR.AN	MK.S4	NA.AN	NA.H4	NA.SU	NM.D1	TM.FE	TM.S4	UY.AN	UY.D1	YM.H4	Average	
xc	0.67	1.00	1.33	1.33	0.00	0.67	0.33	0.67	1.00	0.67	0.67	0.00	0.67	0.67	1.67	0.33	1.00	0.00	1.00	1.00	0.73
yc	1.00	0.33	0.00	0.33	2.00	1.33	0.33	1.33	2.33	0.33	2.67	0.00	0.33	1.00	0.00	1.67	1.33	2.00	0.33	0.33	0.95
r	1.00	1.00	0.33	1.00	1.00	0.00	0.00	0.67	0.33	2.00	0.67	0.67	1.33	0.33	1.00	0.67	0.67	1.00	1.00	0.67	0.77
c1x	3.19	3.19	2.37	4.52	0.55	1.29	3.11	0.45	3.04	2.54	2.22	1.63	0.19	4.85	3.11	0.04	1.45	1.11	0.71	1.55	2.06
c1y	1.90	0.10	1.16	1.57	1.65	2.49	1.32	1.32	2.49	0.38	0.99	2.49	0.43	0.76	1.32	3.49	0.99	1.99	0.49	0.32	1.38
c2x	0.16	1.51	2.70	0.18	3.44	0.63	6.11	3.78	1.03	6.33	2.78	0.63	4.84	1.16	4.11	0.37	3.11	3.11	0.70	1.78	2.42
c2y	1.73	0.40	1.32	0.06	1.38	3.35	3.62	0.38	0.35	1.67	1.05	1.65	1.27	0.60	0.95	0.35	0.62	0.62	2.65	2.95	1.35
upx	2.16	3.16	1.32	2.16	2.46	0.68	2.46	3.79	2.32	2.79	2.79	1.35	0.18	2.49	0.21	0.32	1.46	1.46	0.65	2.79	1.85
upy	1.27	0.27	0.99	1.27	1.92	1.66	3.25	1.25	1.34	1.92	1.08	1.33	0.60	1.60	1.92	0.66	1.92	1.58	2.99	2.92	1.59
downx	2.33	2.67	1.33	3.00	1.33	0.33	0.67	0.33	3.33	0.67	0.33	1.00	1.00	2.00	3.00	0.67	1.00	0.67	0.67	0.33	1.33
downy	0.67	0.67	1.33	1.00	1.33	1.33	0.67	1.67	1.00	0.33	0.67	1.67	0.00	0.33	0.33	2.00	0.00	1.33	0.33	0.67	0.87
Average	1.46	1.30	1.29	1.49	1.55	1.25	1.99	1.42	1.69	1.78	1.45	1.13	0.99	1.44	1.60	0.96	1.23	1.35	1.05	1.39	
Percentage (of width) Diff																					
% Param Name	KA.D11	KA.H4	KA.S4	KA.SU	KL.AN	KL.FE	KM.D1	KM.S4	KR.AN	MK.S4	NA.AN	NA.H4	NA.SU	NM.D1	TM.FE	TM.S4	UY.AN	UY.D1	YM.H4	Average	
xc	2.30	3.66	4.71	4.88	0.00	2.33	1.23	2.44	3.85	2.27	2.30	0.00	2.47	2.35	6.67	1.18	3.90	0.00	3.57	3.66	2.69
yc	3.45	1.22	0.00	1.22	7.14	4.65	1.23	4.88	8.97	1.14	9.20	0.00	1.23	3.53	0.00	5.88	5.19	7.69	1.19	1.22	3.45
r	3.45	3.66	1.18	3.66	3.57	0.00	0.00	2.44	1.28	6.82	2.30	2.30	4.94	1.18	4.00	2.35	2.60	3.85	3.57	2.44	2.78
c1x	10.99	11.66	8.37	16.54	1.98	4.52	11.52	1.63	11.69	8.66	7.66	5.61	0.69	17.13	12.45	0.14	5.63	4.28	2.52	5.69	7.47
c1y	6.56	0.36	4.09	5.74	5.91	8.70	4.89	4.83	9.59	1.30	3.40	8.60	1.60	2.70	5.28	12.33	3.85	7.64	1.76	1.17	5.01
c2x	0.54	5.53	9.53	0.65	12.30	2.21	22.63	13.82	3.98	21.59	9.58	2.18	17.94	4.08	16.44	1.30	12.12	11.96	2.50	6.50	8.87
c2y	5.96	1.45	4.66	0.23	4.94	11.67	13.39	1.40	1.33	5.68	3.62	5.70	4.71	2.13	3.80	1.22	2.40	2.37	9.48	10.79	4.85
upx	7.44	11.55	4.64	7.89	8.78	2.39	9.10	13.87	8.90	9.52	9.63	4.66	0.66	8.79	0.83	1.11	5.68	5.61	2.32	10.21	6.68
upy	4.38	0.99	3.51	4.65	6.85	5.80	12.04	4.57	5.15	6.53	3.74	4.58	2.24	5.66	7.67	2.33	7.47	6.09	10.70	10.67	5.78
downx	8.05	9.76	4.71	10.98	4.76	1.16	2.47	1.22	12.82	2.27	1.15	3.45	3.70	7.06	12.00	2.35	3.90	2.56	2.38	1.22	4.90
downy	2.30	2.44	4.71	3.66	4.76	4.65	2.47	6.10	3.85	1.14	2.30	5.75	0.00	1.18	1.33	7.06	0.00	5.13	1.19	2.44	3.12
Average	5.04	4.75	4.55	5.46	5.54	4.37	7.36	5.20	6.49	6.08	4.99	3.89	3.65	5.07	6.41	3.39	4.79	5.20	3.74	5.09	

Figure D.2: JAFFE spline-based right eye template test results

Absolute Difference Pixel Values																	
% Param Name	right	2.sad	brmal	brmal	sses	brmal	6.sad	right	sses	brmal	sleepy	wink	right	2.sad	subje	subje	Average
xc	1.67	11.33	1.00	1.33	1.33	0.67	1.00	1.00	2.67	0.67	1.00	118.00	2.00	1.33	2.67	1.33	1.33
yc	1.33	1.67	0.67	0.33	1.00	0.00	0.33	0.33	0.67	2.33	2.33	134.00	0.00	1.33	0.00	0.67	1.33
r	1.00	0.33	0.00	0.00	0.00	0.33	1.00	0.33	2.33	0.67	1.00	6.00	0.33	0.00	1.00	0.67	0.00
c1x	3.71	9.79	1.45	2.22	1.11	0.29	0.96	2.89	6.94	0.11	1.78	103.81	0.78	1.22	3.13	2.60	1.11
c1y	4.83	0.29	2.32	2.99	2.32	1.16	0.16	0.68	0.71	4.32	4.32	137.90	0.32	2.65	1.71	0.04	1.32
c2x	1.37	14.00	1.78	1.56	0.22	1.63	0.97	1.78	0.33	0.44	0.44	135.84	1.44	2.44	4.67	2.33	2.22
c2y	1.99	0.00	3.28	2.62	0.38	0.99	1.65	0.95	3.00	0.05	0.72	134.94	0.62	0.28	0.33	2.67	1.62
upx	2.65	7.54	2.13	4.46	3.46	0.02	0.35	2.79	4.67	3.79	3.46	117.84	2.79	2.79	1.79	0.67	2.79
upy	0.99	0.75	2.58	1.58	1.25	1.99	1.66	0.58	1.33	2.08	2.08	127.06	1.25	1.08	1.25	2.00	2.25
downx	3.00	11.00	1.33	2.33	0.00	0.00	0.00	0.00	4.67	1.00	0.33	118.00	1.00	0.00	3.33	1.33	0.00
downy	2.00	2.33	0.67	1.00	2.00	1.00	0.67	0.33	1.67	1.33	1.00	140.00	2.33	1.00	0.00	3.33	1.33
Average	2.23	5.37	1.56	1.86	1.19	0.74	0.80	1.06	2.63	1.53	1.68	NA	1.17	1.29	1.81	1.60	1.37

Percentage (of width) Diff																	
% Param Name	right	2.sad	brmal	brmal	sses	brmal	6.sad	right	sses	brmal	sleepy	wink	right	2.sad	subje	subje	Average
xc	6.49	45.95	4.11	5.41	5.88	2.50	3.57	3.49	11.76	2.74	4.41	NA	8.11	4.82	12.12	6.35	7.25
yc	5.19	6.76	2.74	1.35	4.41	0.00	1.19	1.16	2.94	9.59	10.29	NA	0.00	4.82	0.00	1.59	0.00
r	3.90	1.35	0.00	0.00	0.00	1.25	3.57	1.16	10.29	2.74	4.41	NA	1.35	0.00	4.55	4.76	2.90
c1x	14.44	39.71	5.94	9.01	4.90	1.11	3.43	10.08	30.61	0.46	7.85	NA	3.16	4.42	14.22	12.40	5.31
c1y	18.80	1.16	9.54	12.11	10.24	4.35	0.57	2.37	3.13	17.75	19.06	NA	1.30	9.59	7.79	0.20	5.74
c2x	5.33	56.76	7.30	6.31	0.98	6.12	3.45	6.20	1.47	1.82	1.96	NA	5.85	8.83	21.21	11.11	9.66
c2y	7.74	0.00	13.49	10.61	1.69	3.70	5.91	3.31	13.24	0.21	3.16	NA	2.50	1.02	1.52	12.70	7.03
upx	10.32	30.57	8.73	18.07	15.26	0.07	1.26	9.74	20.59	15.58	15.26	NA	11.32	10.09	8.14	3.17	12.14
upy	3.88	3.04	10.62	6.42	5.51	7.48	5.93	2.03	5.88	8.56	9.19	NA	5.07	3.92	5.68	9.52	9.78
downx	11.69	44.59	5.48	9.46	0.00	0.00	0.00	0.00	20.59	4.11	1.47	NA	4.05	0.00	15.15	6.35	0.00
downy	7.79	9.46	2.74	4.05	8.82	3.75	2.38	1.16	7.35	5.48	4.41	NA	9.46	3.61	0.00	15.87	5.80
Average	8.69	21.76	6.43	7.53	5.25	2.76	2.84	3.70	11.62	6.28	7.41	NA	4.74	4.65	8.22	7.64	5.96

5.10	5.54	4.38
------	------	------

Figure D.3: YALE spline-based left eye template test results

Absolute Difference Pixel Values																
% Param Name	rlight	2.sad	brmal	brmal	sses	brmal	6.sad	rlight	sses	brmal	6.sad	rlight	sses	brmal	leppy	9.wink
xc	2.00	9.00	0.33	0.00	0.00	1.00	0.33	0.67	2.33	0.33	0.33	0.00	NA	170.00	1.00	1.67
yc	1.67	2.00	1.33	0.33	0.67	0.00	1.00	0.00	1.33	2.33	3.00	NA	120.00	2.00	0.67	1.00
r	0.33	1.33	0.33	0.33	0.33	0.00	0.67	0.67	0.33	1.33	0.33	NA	5.00	0.67	1.33	0.33
c1x	4.45	6.96	1.22	3.78	0.11	0.22	0.71	0.37	5.45	1.48	1.22	NA	156.81	2.86	1.25	4.42
c1y	3.32	5.83	1.32	0.32	1.99	0.01	1.16	0.83	0.32	0.43	3.32	NA	122.83	2.17	0.13	1.20
c2x	3.11	14.97	2.89	2.78	1.56	3.44	0.03	0.97	3.11	0.52	0.78	NA	184.81	3.15	4.07	0.93
c2y	0.28	0.65	0.05	1.62	1.95	2.28	2.32	0.99	1.62	1.75	1.38	NA	120.89	1.44	0.43	1.10
upx	0.79	9.35	4.13	1.13	2.79	3.46	0.32	0.35	0.46	4.86	2.79	NA	170.23	0.43	1.95	2.95
upy	0.08	1.99	1.25	2.58	1.25	0.92	2.99	0.99	2.58	2.49	1.42	NA	113.28	4.39	1.60	3.27
downx	2.67	9.67	0.67	2.00	0.33	0.00	0.67	0.33	3.67	0.00	1.00	NA	169.84	2.16	1.33	0.33
downy	2.00	3.67	0.67	0.00	1.33	0.33	0.33	0.33	1.67	1.00	0.67	NA	124.06	2.60	0.00	0.67
Average	1.88	5.95	1.29	1.35	1.12	1.06	0.96	0.59	2.08	1.50	1.45	NA	132.52	2.08	1.31	1.50
															1.03	1.32

Percentage (of width) Diff																
% Param Name	rlight	2.sad	brmal	brmal	sses	brmal	6.sad	rlight	sses	brmal	6.sad	rlight	sses	brmal	leppy	9.wink
xc	8.82	45.00	1.49	0.00	0.00	3.61	1.22	2.50	10.77	1.28	0.00	NA	4.55	2.27	6.58	2.27
yc	7.35	10.00	5.97	1.45	2.99	0.00	3.66	0.00	6.15	8.97	11.54	NA	9.09	6.82	2.63	6.82
r	1.47	6.67	1.49	1.45	1.49	0.00	2.44	2.50	1.54	5.13	1.28	NA	3.03	2.27	5.26	2.27
c1x	19.61	34.81	5.47	16.43	0.50	0.80	2.58	1.39	25.13	5.68	4.70	NA	12.98	30.13	4.92	30.13
c1y	14.65	29.13	5.91	1.39	8.90	0.05	4.24	3.10	1.48	1.66	12.77	NA	9.87	8.19	0.52	8.19
c2x	13.72	74.83	12.94	12.07	6.97	12.45	0.12	3.62	14.36	2.01	2.99	NA	14.30	6.31	16.08	6.31
c2y	1.25	3.27	0.23	7.03	8.73	8.25	8.49	3.70	7.46	6.73	5.32	NA	6.57	7.47	1.69	7.47
upx	3.49	46.76	18.47	4.89	12.50	12.50	1.15	1.32	2.12	18.71	10.74	NA	1.96	20.10	7.69	20.10
upy	0.37	9.97	5.60	11.23	5.60	3.31	10.96	3.73	11.92	9.60	5.45	NA	19.93	22.30	6.33	22.30
downx	11.76	48.33	2.99	8.70	1.49	0.00	2.44	1.25	16.92	0.00	3.85	NA	9.80	2.27	5.26	2.27
downy	8.82	18.33	2.99	0.00	5.97	1.20	1.22	1.25	7.69	3.85	2.56	NA	11.84	4.55	0.00	4.55
Average	8.30	29.74	5.78	5.88	5.01	3.83	3.50	2.22	9.59	5.78	5.56	NA	9.45	10.24	5.18	10.24
															4.41	5.34

Figure D.4: YALE spline-based right eye template test results

Absolute Difference Pixel Values																										
% Param	s101	s105	s111	s116	s121	s1210	s155	s162	s221	s225	s231	s294	s306	s309	s39	s405	s510	s52	s71	s78	s85	s88	s94	s98	Average	
nc	0.67	0.33	1.00	1.33	0.33	0.33	0.67	1.00	1.33	1.00	2.00	1.00	0.33	8.00	0.33	1.33	0.33	1.00	0.67	0.00	1.67	1.33	2.33	2.33	1.28	
jc	0.67	0.00	0.00	0.67	0.67	0.00	0.33	1.00	0.33	0.33	0.67	0.67	1.00	2.00	0.33	0.33	0.33	1.00	0.33	0.67	0.67	0.67	1.00	0.00	0.58	
r	1.33	0.33	0.33	0.00	0.33	0.33	1.00	1.00	0.67	0.00	0.33	0.33	0.33	1.00	0.00	0.33	0.00	0.67	1.33	0.33	0.33	1.67	0.67	0.33	0.54	
c1k	4.79	3.13	4.06	4.73	0.73	3.06	2.79	5.13	0.06	2.06	4.40	3.06	2.79	9.06	2.79	1.73	3.06	3.13	3.81	3.40	2.40	1.06	3.06	3.06	3.22	
c1y	0.95	0.29	2.38	1.38	1.04	0.38	0.38	1.29	2.04	1.38	2.04	0.71	0.38	0.04	0.38	0.04	1.38	0.05	0.38	0.04	0.71	1.04	0.04	0.04	0.78	
c2x	3.00	0.33	3.67	2.67	3.67	4.67	2.00	0.33	0.33	1.67	3.67	3.33	0.67	11.67	1.00	2.00	0.67	1.00	4.67	2.00	3.67	4.67	4.67	3.33	2.89	
c2y	1.33	2.33	0.33	1.67	1.33	0.00	1.00	0.67	1.00	0.33	0.67	1.33	1.00	1.00	3.33	2.00	1.33	1.33	0.33	0.67	2.33	3.33	2.33	2.33	1.39	
upx	4.13	4.13	0.67	0.33	0.33	0.33	3.79	2.46	1.00	2.00	1.67	0.33	3.13	8.33	4.13	1.00	0.67	2.13	2.25	0.00	1.33	1.33	1.67	0.67	1.99	
upy	2.25	1.25	0.33	0.67	1.67	2.00	1.58	0.92	0.33	0.33	0.00	1.00	2.58	1.67	1.58	0.33	0.00	2.58	0.50	2.00	0.33	0.33	1.00	0.00	1.05	
downx	1.33	1.00	1.00	1.67	0.33	1.67	0.67	0.00	1.33	2.00	1.33	0.33	0.00	8.00	1.67	1.00	0.67	0.67	1.00	0.33	0.33	1.00	1.67	0.67	1.24	
downy	0.67	0.33	4.33	4.33	3.67	5.67	0.00	0.33	3.67	4.00	3.00	4.67	0.00	6.00	1.33	5.33	5.00	0.67	0.67	3.67	2.33	2.67	3.00	3.67	2.88	
Average	1.92	1.22	1.65	1.77	1.28	1.74	1.26	1.22	1.16	1.37	1.80	1.52	1.11	5.16	1.53	1.40	1.22	1.29	1.45	1.19	1.46	1.74	1.95	1.49		

Percentage (of width) Diff																										
% Param	s101	s105	s111	s116	s121	s1210	s155	s162	s221	s225	s231	s294	s306	s309	s39	s405	s510	s52	s71	s78	s85	s88	s94	s98	Average	
nc	5.26	1.96	6.38	9.52	1.75	1.89	4.26	6.67	8.16	6.38	13.04	6.12	1.96	42.86	2.00	8.16	2.44	6.12	4.55	0.00	9.62	6.78	13.21	14.29	7.64	
jc	5.26	0.00	0.00	4.76	3.51	3.77	0.00	2.22	6.12	2.13	4.35	4.08	5.88	10.71	2.00	2.04	2.44	6.12	2.27	4.55	3.85	3.39	5.66	0.00	3.55	
r	10.63	1.96	2.13	0.00	1.75	1.89	6.38	6.67	4.08	0.00	2.17	2.04	1.96	5.36	0.00	2.04	0.00	4.08	9.09	2.27	1.92	8.47	3.77	2.04	3.36	
c1k	37.85	18.40	25.93	33.78	3.84	17.33	17.84	34.18	0.38	13.16	28.67	18.75	16.44	48.55	16.77	10.59	22.41	19.15	25.99	23.15	13.82	5.40	17.33	18.75	20.35	
c1y	7.52	1.69	15.16	9.82	5.48	2.12	2.43	8.58	12.50	8.78	13.32	4.34	2.24	0.22	2.28	0.26	10.06	0.29	2.56	0.28	4.09	5.30	0.24	0.26	4.99	
c2x	23.68	1.96	23.40	19.05	19.30	26.42	12.77	2.22	2.04	10.64	23.91	20.41	3.92	62.50	6.00	12.24	4.88	6.12	31.82	13.64	21.15	23.73	26.42	20.41	17.44	
c2y	10.53	13.73	2.13	11.90	7.02	0.00	6.38	4.44	6.12	2.13	4.35	8.16	5.88	5.36	20.00	12.24	9.76	8.16	2.27	4.55	13.46	16.95	13.21	14.29	8.46	
upx	32.57	24.26	4.26	2.38	1.75	1.89	24.20	16.39	6.12	12.77	10.87	2.04	18.38	44.64	24.75	6.12	4.88	13.01	15.34	0.00	7.69	6.78	9.43	4.08	12.28	
upy	17.76	7.35	2.13	4.76	8.77	11.32	10.11	6.11	2.04	2.13	0.00	6.12	15.20	8.93	9.50	2.04	0.00	15.82	3.41	13.64	1.92	1.69	5.66	0.00	6.52	
downx	10.53	5.88	6.38	11.90	1.75	9.43	4.26	0.00	8.16	12.77	8.70	2.04	0.00	42.86	10.00	6.12	4.88	4.08	6.82	2.27	1.92	5.08	9.43	4.08	7.47	
downy	5.26	1.96	27.66	30.95	19.30	32.08	0.00	2.22	22.45	25.53	19.57	28.57	0.00	32.14	8.00	32.65	36.59	4.08	4.55	25.00	13.46	13.56	16.98	22.45	17.71	
Average	15.16	7.20	10.51	12.62	6.75	9.83	8.06	8.15	7.11	8.76	11.72	9.33	6.53	27.65	9.21	8.59	8.94	7.91	9.88	8.12	8.45	8.83	11.03	9.15		

Figure D.5: ORL spline-based left eye template test results

Absolute Difference Pixel Values																									
% Param	s101	s105	s111	s116	s121	s1210	s155	s162	s221	s225	s231	s294	s306	s309	s39	s405	s510	s52	s71	s78	s85	s88	s94	s98	Average
xc	0.67	0.00	0.33	1.00	0.67	0.33	1.00	0.67	0.67	0.67	0.67	0.67	0.00	1.33	0.67	2.00	1.00	0.33	0.33	0.33	0.33	2.33	2.00	0.33	0.76
yc	0.67	0.33	0.33	0.00	0.33	0.33	0.67	0.67	0.33	0.33	1.00	0.67	0.67	1.33	1.33	0.33	0.33	0.00	0.67	0.67	0.00	0.00	1.00	0.67	0.53
r	0.67	0.33	0.67	1.33	0.67	0.67	1.00	0.00	0.33	0.33	0.33	1.00	0.67	0.33	0.33	0.00	1.00	0.33	0.33	0.00	0.00	0.67	0.00	0.33	0.47
c1x	2.46	2.79	1.06	1.06	3.46	3.06	4.46	4.79	0.27	1.94	5.46	4.13	4.13	5.13	3.79	2.40	4.06	3.79	1.73	2.40	2.73	4.40	3.73	3.46	3.20
c1y	0.95	0.71	0.04	0.71	1.05	1.04	0.62	1.29	0.29	0.29	0.05	0.38	0.62	3.05	0.62	0.71	1.38	0.29	0.63	0.04	0.96	0.04	2.04	0.38	0.76
c2x	1.33	0.33	1.67	1.33	0.67	2.67	2.00	0.33	4.33	2.67	0.33	0.33	0.33	2.33	0.67	3.00	3.67	0.67	1.00	0.33	3.00	6.00	5.67	1.00	1.90
c2y	2.33	1.67	3.33	3.00	3.33	1.67	3.67	2.00	0.67	0.00	3.00	2.00	0.67	0.33	0.33	0.67	2.33	2.67	1.67	1.67	2.67	2.33	2.00	0.67	1.86
upx	4.13	2.79	0.67	0.33	2.79	0.67	3.13	2.46	0.67	1.33	3.13	3.46	2.13	3.13	3.46	0.33	0.67	4.13	0.00	0.00	1.33	3.33	1.33	3.13	2.02
upy	1.92	1.58	0.33	0.33	1.58	0.67	1.92	0.92	1.33	1.00	2.92	1.92	1.58	2.92	0.42	2.33	0.33	1.25	0.00	0.00	0.33	1.00	1.33	2.92	1.28
downx	0.67	0.33	1.00	1.67	0.33	0.33	0.00	0.67	0.67	0.67	0.33	0.67	1.00	3.67	0.67	1.00	1.33	1.00	0.00	0.33	0.67	3.33	2.67	0.33	0.97
downy	0.67	2.00	4.00	2.67	3.33	1.33	1.00	1.67	2.00	2.33	1.67	0.67	0.33	2.67	0.33	3.67	4.33	0.67	4.67	4.00	2.33	2.33	2.67	3.00	2.26
Average	1.50	1.17	1.22	1.22	1.66	1.16	1.77	1.41	1.05	1.05	1.72	1.44	1.10	2.38	1.15	1.49	1.86	1.37	1.00	0.89	1.30	2.34	2.22	1.47	

Percentage (of width) Diff																									
% Param	s101	s105	s111	s116	s121	s1210	s155	s162	s221	s225	s231	s294	s306	s309	s39	s405	s510	s52	s71	s78	s85	s88	s94	s98	Average
xc	4.00	0.00	2.00	6.12	3.77	2.13	5.56	4.35	3.23	3.23	4.55	4.17	0.00	7.55	3.85	12.00	6.38	1.92	2.17	2.50	2.04	13.21	11.11	1.85	4.49
yc	4.00	1.85	2.00	0.00	1.89	2.13	3.70	4.35	1.61	1.61	6.82	4.17	4.00	7.55	7.69	2.00	2.13	0.00	4.35	5.00	0.00	0.00	5.56	3.70	3.17
r	4.00	1.85	4.00	8.16	3.77	4.26	5.56	0.00	1.61	1.61	2.27	6.25	4.00	1.89	1.92	0.00	6.38	1.92	2.17	0.00	0.00	3.77	0.00	1.85	2.80
c1x	14.77	15.52	6.38	6.51	19.59	19.55	24.78	31.27	1.31	9.38	37.23	25.80	24.77	29.02	21.89	14.38	25.93	21.89	11.28	17.97	16.71	24.88	20.72	19.23	19.20
c1y	5.72	3.96	0.25	4.34	5.93	6.65	3.44	8.39	1.41	1.41	0.32	2.38	3.72	17.25	3.58	4.25	8.78	1.65	4.08	0.31	5.87	0.24	11.34	2.11	4.47
c2x	8.00	1.85	10.00	8.16	3.77	17.02	11.11	2.17	20.97	12.90	2.27	2.08	2.00	13.21	3.85	18.00	23.40	3.85	6.52	2.50	18.37	33.96	31.48	5.56	10.96
c2y	14.00	9.26	20.00	18.37	18.87	10.64	20.37	13.04	3.23	0.00	20.45	12.50	4.00	1.89	1.92	4.00	14.89	15.38	10.87	12.50	16.33	13.21	11.11	3.70	11.27
upx	24.75	15.51	4.00	2.04	15.80	4.26	17.36	16.03	3.23	6.45	21.31	21.61	12.75	17.69	19.95	2.00	4.26	23.80	0.00	0.00	8.16	18.87	7.41	17.36	11.86
upy	11.50	8.80	2.00	2.04	8.96	4.26	10.65	5.98	6.45	4.84	19.89	11.98	9.50	16.51	2.40	14.00	2.13	7.21	0.00	0.00	2.04	5.66	7.41	16.20	7.52
downx	4.00	1.85	6.00	10.20	1.89	2.13	0.00	4.35	3.23	3.23	2.27	4.17	6.00	20.75	3.85	6.00	8.51	5.77	0.00	2.50	4.08	18.87	14.81	1.85	5.68
downy	4.00	11.11	24.00	16.33	18.87	8.51	5.56	10.87	9.68	11.29	11.36	4.17	2.00	15.09	1.92	22.00	27.66	3.85	30.43	30.00	14.29	13.21	14.81	16.67	13.65
Average	8.98	6.51	7.33	7.48	9.37	7.41	9.83	9.16	5.09	5.09	11.70	9.02	6.61	13.49	6.62	8.97	11.86	7.93	6.53	6.66	7.99	13.26	12.34	8.19	

Figure D.6: ORL spline-based right eye template test results

APPENDIX E

Polygonal Eye Template Detailed Test Results

Absolute Difference Pixel Values																					
%Param Name	KADI	KA,HA	KA,SA	KA,SU	KL,AN	KL,FE	KM,DI	KM,SA	KR,AN	MK,SA	NA,AN	NA,HA	NA,SU	NM,DI	TM,FE	TM,SA	UY,AN	UY,DI	YM,DI	YMH	Average
wc	100	0.00	0.33	0.67	0.00	0.67	1.33	1.67	0.67	2.00	0.33	0.33	0.00	0.67	0.33	1.33	0.33	0.33	0.67	1.67	0.72
yc	100	0.33	0.00	1.33	2.67	0.33	0.33	1.67	2.00	0.33	0.33	1.00	2.00	1.33	0.67	1.33	2.33	1.67	1.33	1.00	1.15
r	0.67	0.33	0.33	0.00	1.00	0.00	1.00	0.00	1.33	3.00	0.33	0.33	0.67	1.00	1.33	0.00	0.00	0.00	0.33	1.00	0.63
clx	1.71	3.63	2.29	0.29	2.96	2.29	2.22	0.04	0.81	3.87	0.29	0.96	1.44	5.29	1.55	1.63	1.63	0.96	1.29	2.55	1.89
clq	6.16	3.16	3.83	7.16	7.49	5.49	1.99	3.49	4.90	0.29	4.83	3.16	7.74	4.16	3.32	4.83	5.16	5.16	5.16	2.99	4.52
c2x	0.63	3.63	1.97	2.63	1.63	0.63	1.78	0.97	6.51	3.33	1.63	1.63	4.56	1.97	1.44	2.97	1.97	0.97	1.30	2.78	2.25
c2y	1.65	4.99	4.65	0.32	1.99	2.99	1.95	1.99	3.06	1.33	4.99	2.65	2.18	4.65	1.28	0.32	2.32	2.99	1.65	2.95	2.55
upx	4.79	0.46	2.79	4.13	4.46	1.02	2.13	1.98	2.18	4.13	1.35	1.35	3.79	1.02	2.13	4.46	0.18	2.46	3.13	3.46	2.57
upy	4.63	0.63	1.25	2.75	1.92	2.33	3.25	1.99	0.06	1.92	2.33	1.33	0.75	1.99	0.92	0.92	1.27	2.25	0.92	1.25	1.73
downx	2.33	2.67	5.00	1.67	1.00	1.00	0.33	2.00	3.33	1.33	1.33	1.00	1.67	1.33	1.00	1.67	5.67	0.33	0.33	0.33	1.77
downy	1.33	1.00	1.00	0.33	2.00	0.00	2.00	2.33	2.00	0.33	0.67	2.00	2.33	0.33	1.00	2.33	1.00	1.33	2.33	1.67	1.37
Average																					
	2.46	1.98	2.24	2.09	2.51	1.68	1.63	1.58	2.49	2.15	1.78	1.38	2.48	2.34	1.40	1.94	2.09	1.71	1.61	2.00	

Percentage (of width) Diff																					
%Param Name	KADI	KA,HA	KA,SA	KA,SU	KL,AN	KL,FE	KM,DI	KM,SA	KR,AN	MK,SA	NA,AN	NA,HA	NA,SU	NM,DI	TM,FE	TM,SA	UY,AN	UY,DI	YM,DI	YMH	Average
wc	3.90	0.00	1.18	2.60	0.00	2.25	4.76	6.17	2.53	7.23	1.25	1.22	0.00	2.13	1.23	5.00	1.20	1.19	2.38	5.68	2.60
yc	3.90	1.19	0.00	5.19	9.09	1.12	1.19	6.17	7.59	1.20	1.25	3.66	7.69	4.26	2.47	5.00	8.43	5.95	4.76	3.41	4.18
r	2.60	1.19	1.18	0.00	3.41	0.00	3.57	0.00	5.06	10.84	1.25	1.22	2.56	3.19	4.94	0.00	0.00	0.00	1.19	3.41	2.28
clx	6.64	12.96	8.10	1.15	10.10	7.74	7.93	0.14	3.09	14.00	1.11	3.52	5.55	16.90	5.76	6.11	5.88	3.43	4.62	8.71	6.67
clq	24.00	11.28	13.50	27.89	25.54	18.51	7.10	12.94	18.61	1.04	18.10	11.56	29.76	13.27	12.30	18.10	18.65	18.43	18.43	10.18	16.46
c2x	2.46	12.97	6.94	10.26	5.57	2.13	6.35	3.58	24.72	12.05	6.12	5.97	17.55	6.27	5.35	11.12	7.11	3.45	4.64	9.47	8.20
c2y	6.45	17.81	16.43	1.25	6.78	10.07	6.96	7.36	11.63	4.82	18.70	9.71	8.40	14.85	4.75	1.20	8.39	10.67	5.91	10.05	9.11
upx	18.68	1.65	9.85	16.07	15.20	3.43	7.59	7.34	8.27	14.91	5.07	4.94	14.58	3.25	7.87	16.72	0.64	8.78	11.16	11.79	9.39
upy	18.04	2.25	4.41	10.71	6.53	7.85	11.61	7.39	0.24	6.93	8.73	4.86	2.88	6.37	3.40	3.44	4.59	8.04	3.27	4.26	6.29
downx	9.09	9.52	17.65	6.49	3.41	3.37	1.19	7.41	12.66	4.82	5.00	3.66	6.41	4.26	3.70	6.25	20.48	1.19	1.19	1.14	6.44
downy	5.19	3.57	3.53	1.30	6.82	0.00	7.14	8.64	7.59	1.20	2.50	7.32	8.97	1.06	3.70	8.75	3.61	4.76	8.33	5.68	4.98
Average																					
	9.18	6.76	7.52	7.54	8.40	5.13	5.94	6.10	9.27	7.19	6.28	5.24	9.49	6.89	5.04	7.43	7.18	5.99	5.99	6.71	

Figure E.1: JAFFE polygonal left eye template test results

Absolute Difference Pixel Values																					Average
%Param Name	KADiff	KAHA	KA.SA	KA.SU	KLAM	KLFE	KMDI	KMSA	KRAM	MKSA	NA.AM	NA.HA	NA.SU	NMDI	TMFE	TMSA	UY.AM	UY.DI	YMDI	YMIHA2	
xc	1.67	1.00	1.33	4.33	0.00	1.67	0.33	0.67	1.00	1.33	0.67	0.00	0.67	0.67	1.67	0.33	0.00	1.00	1.00	7.00	
yc	0.00	0.33	0.00	1.67	2.00	1.33	0.33	1.33	0.33	0.67	0.67	0.00	0.67	1.00	0.00	1.67	2.33	3.00	0.33	0.33	
r	0.00	1.00	0.33	2.00	0.00	0.00	0.00	0.67	0.33	1.00	0.33	0.67	1.33	0.33	0.00	0.67	0.33	0.00	1.00	0.67	
c1x	3.04	3.19	2.37	8.35	0.37	2.29	3.11	0.45	3.04	3.89	1.29	1.63	0.19	4.85	4.04	0.04	1.37	3.04	0.71	7.55	
c1y	1.83	0.10	1.16	6.16	2.83	2.49	1.32	1.32	0.49	2.32	0.16	2.49	0.57	0.76	2.49	3.49	3.16	4.16	0.49	0.32	
c2x	4.03	1.51	2.70	0.32	0.37	1.63	6.11	3.78	1.03	1.44	0.30	0.63	4.84	1.10	1.03	0.37	0.97	1.03	0.70	4.22	
c2y	3.65	0.40	1.32	0.93	1.35	3.35	3.62	0.38	1.65	0.62	0.99	1.65	2.27	0.15	0.99	0.35	0.35	0.35	2.65	2.95	
upx	3.16	3.16	1.46	4.69	0.32	1.68	2.46	3.79	0.46	4.79	2.79	4.13	0.18	0.79	0.21	2.46	2.46	2.82	0.65	8.79	
upy	1.27	0.27	0.92	0.04	2.99	1.66	3.25	1.25	0.58	1.92	1.92	1.25	0.40	1.92	2.92	0.58	1.92	1.27	2.99	2.92	
downx	1.67	2.67	1.33	6.00	1.33	1.33	0.67	0.33	3.33	1.33	0.33	1.00	1.00	3.00	3.00	0.67	0.00	1.67	0.67	5.67	
downy	1.33	0.67	1.33	2.00	2.33	1.33	0.67	1.67	1.00	1.67	0.33	1.67	1.00	0.33	1.33	2.00	2.00	3.33	0.33	0.67	
Average	1.97	1.30	1.30	3.32	1.26	1.71	1.99	1.42	1.21	1.91	0.89	1.37	1.19	1.36	1.61	1.15	1.35	1.97	1.05	3.74	

Percentage (of width) Diff																					Average
%Param Name	KADiff	KAHA	KA.SA	KA.SU	KLAM	KLFE	KMDI	KMSA	KRAM	MKSA	NA.AM	NA.HA	NA.SU	NMDI	TMFE	TMSA	UY.AM	UY.DI	YMDI	YMIHA2	
xc	5.75	3.66	4.71	15.85	0.00	5.81	1.23	2.44	3.85	4.55	2.30	0.00	2.47	2.35	6.67	1.18	0.00	3.85	3.57	25.61	
yc	0.00	1.22	0.00	6.10	7.14	4.65	1.23	4.88	1.28	2.27	2.30	0.00	2.47	3.53	0.00	5.88	9.09	11.54	1.19	1.22	
r	0.00	3.66	1.18	7.32	0.00	0.00	0.00	2.44	1.28	3.41	1.15	2.30	4.94	1.18	0.00	2.35	1.30	0.00	3.57	2.44	
c1x	10.48	11.66	8.37	30.54	1.33	8.00	11.52	1.63	11.69	13.26	4.46	5.61	0.69	17.13	16.15	0.14	5.35	11.69	2.52	27.64	
c1y	6.30	0.36	4.09	22.52	10.09	8.70	4.89	4.83	1.90	7.91	0.55	8.60	2.11	2.70	9.97	12.33	12.31	16.00	1.76	1.17	
c2x	13.91	5.53	9.53	1.17	1.31	5.70	22.63	13.82	3.98	4.92	1.03	2.18	17.94	3.89	4.14	1.30	3.76	3.98	2.50	15.45	
c2y	12.60	1.45	4.66	3.40	4.81	11.67	13.39	1.40	6.36	2.10	3.41	5.70	8.41	0.52	3.95	1.22	1.35	1.33	9.48	10.79	
upx	10.88	11.55	5.15	17.15	1.13	5.88	9.10	13.87	1.76	16.34	9.63	14.22	0.66	2.79	0.83	8.68	9.58	10.86	2.32	32.16	
upy	4.38	0.99	3.24	0.15	10.70	5.80	12.04	4.57	2.24	6.53	6.61	4.31	1.47	6.76	11.67	2.06	7.47	4.89	10.70	10.67	
downx	5.75	9.76	4.71	21.95	4.76	4.65	2.47	1.22	12.82	4.55	1.15	3.45	3.70	10.59	12.00	2.35	0.00	6.41	2.38	20.73	
downy	4.60	2.44	4.71	7.32	8.33	4.65	2.47	6.10	3.85	5.68	1.15	5.75	3.70	1.18	5.33	7.06	7.79	12.82	1.19	2.44	
Average	6.79	4.75	4.58	12.13	4.51	5.96	7.36	5.20	4.64	6.50	3.07	4.74	4.41	4.78	6.43	4.05	5.27	7.58	3.74	13.67	

Figure E.2: JAFFE polygonal right eye template test results

Absolute Difference Pixel Values																			
% Param	right	2.sad	brmal	brmal	sses	brmal	6.sad	right	sses	brmal	sleepy	wink	right	2.sad	subje	subje	subje	Average	
xc	1.67	6.33	1.00	1.33	0.33	0.67	1.00	2.00	2.67	0.67	1.00	NA	2.00	0.33	2.67	1.33	0.67	1.33	1.58
yc	1.33	0.67	0.33	0.33	1.00	0.00	0.67	0.33	1.67	2.33	2.33	NA	0.00	2.33	0.00	1.33	1.00	0.67	0.96
r	1.00	2.33	0.00	0.00	1.00	1.33	0.00	0.33	1.33	0.67	1.00	NA	0.33	0.00	1.00	0.00	0.67	1.33	0.70
c1x	3.71	6.37	1.45	2.22	0.54	1.22	1.89	1.89	5.54	0.11	1.78	NA	0.78	2.22	3.13	2.60	2.22	0.21	2.09
c1y	4.83	2.16	3.32	2.99	0.62	0.01	0.01	0.68	0.38	4.32	4.32	NA	0.32	3.65	1.71	1.04	0.32	0.38	2.05
c2x	1.33	3.03	1.78	1.56	1.67	1.44	2.11	2.78	3.33	0.44	0.44	NA	1.33	1.44	4.67	2.33	3.33	0.89	2.10
c2y	2.00	0.99	2.28	2.62	0.33	0.95	0.62	0.95	4.00	0.05	0.72	NA	0.67	0.72	0.33	3.67	2.67	1.67	1.33
upx	0.13	5.82	2.13	4.46	4.46	2.79	3.13	1.79	7.79	3.79	3.46	NA	0.33	3.79	1.79	0.67	3.79	2.46	3.06
upy	0.92	1.94	1.58	1.58	0.25	0.92	0.42	0.58	1.92	2.08	2.08	NA	0.00	2.08	1.25	1.00	3.25	1.92	1.25
downx	3.00	1.00	1.33	2.33	1.00	0.00	0.00	1.00	4.67	1.00	0.33	NA	1.00	1.00	3.33	1.33	1.00	0.67	1.33
downy	2.00	3.33	0.33	1.00	1.00	0.00	0.67	0.33	3.33	1.33	1.00	NA	2.33	0.00	0.00	2.33	0.33	0.67	1.25
Average	1.99	3.09	1.41	1.86	1.11	0.85	0.95	1.15	3.33	1.53	1.68	NA	0.83	1.60	1.81	1.70	1.75	1.48	1.38

Percentage (of width) Diff																			
% Param	right	2.sad	brmal	brmal	sses	brmal	6.sad	right	sses	brmal	sleepy	wink	right	2.sad	subje	subje	subje	Average	
xc	6.49	25.68	4.11	5.41	1.47	2.50	3.57	6.98	11.76	2.74	4.41	NA	8.11	1.20	12.12	6.35	2.90	6.58	6.50
yc	5.19	2.70	1.37	1.35	4.41	0.00	2.38	1.16	7.35	9.59	10.29	NA	0.00	8.43	0.00	6.35	4.35	2.63	4.01
r	3.90	9.46	0.00	0.00	4.41	5.00	0.00	1.16	5.88	2.74	4.41	NA	1.35	0.00	4.55	4.76	2.90	5.26	2.94
c1x	14.44	25.83	5.94	9.01	2.38	4.58	6.74	6.59	24.44	0.46	7.85	NA	3.16	8.03	14.22	12.40	9.66	0.81	8.65
c1y	18.80	8.75	13.64	12.11	2.73	0.05	0.05	2.37	1.68	17.75	19.06	NA	1.30	13.21	7.79	4.96	1.39	1.50	8.40
c2x	5.19	12.30	7.30	6.31	7.35	5.41	7.54	9.69	14.71	1.82	1.96	NA	5.41	5.22	21.21	11.11	14.49	18.42	8.66
c2y	7.79	4.00	9.38	10.61	1.47	3.56	2.20	3.31	17.65	0.21	3.16	NA	2.70	2.59	1.52	17.46	11.59	6.58	5.58
upx	0.49	23.61	8.73	18.07	19.67	10.47	11.16	6.25	34.38	15.58	15.26	NA	1.35	13.70	8.14	3.17	16.49	9.70	12.60
upy	3.57	7.85	6.51	6.42	1.10	3.44	1.49	2.03	8.46	8.56	9.19	NA	0.00	7.53	5.68	4.76	14.13	7.57	5.49
downx	11.69	4.05	5.48	9.46	4.41	0.00	0.00	3.49	20.59	4.11	1.47	NA	4.05	3.61	15.15	6.35	4.35	2.63	5.62
downy	7.79	13.51	1.37	4.05	4.41	0.00	2.38	1.16	14.71	5.48	4.41	NA	9.46	0.00	0.00	11.11	1.45	2.63	5.22
Average	7.76	12.52	5.80	7.53	4.89	3.18	3.41	4.02	14.69	6.28	7.41	NA	3.35	5.78	8.22	8.07	7.61	5.85	5.32

Figure E.3: YALE polygonal left eye template test results

Absolute Difference Pixel Values																					
% Param Name	right	2.sad	brmal	brmal	brmal	sses	brmal	6.sad	right	sses	brmal	leppy	β.wink	right	2.sad	subje	subje	subje	subje	Average	
xc	2.00	9.00	0.33	0.00	0.00	1.00	0.33	0.67	2.33	0.33	0.00	NA	170.00	1.00	1.67	0.33	NA	10.00	0.67	1.00	11.15
yc	1.67	2.00	1.33	0.33	0.67	0.00	1.00	0.00	1.33	2.33	3.00	NA	120.00	2.00	0.67	1.00	NA	1.00	0.67	1.00	7.78
r	0.33	1.33	0.33	0.33	0.33	0.00	0.67	0.67	0.33	1.33	0.33	NA	5.00	0.67	1.33	0.33	NA	0.33	0.33	0.00	0.78
c1x	4.45	6.96	1.22	3.78	0.11	0.22	0.71	0.37	5.45	1.48	1.22	NA	156.81	2.86	1.25	4.42	NA	10.22	0.45	2.04	11.33
c1y	3.32	5.83	1.32	0.32	1.99	0.01	1.16	0.83	0.32	0.43	3.32	NA	122.83	2.17	0.13	1.20	NA	1.99	1.99	3.83	8.50
c2x	3.11	14.97	2.89	2.78	1.56	3.44	0.03	0.97	3.11	0.52	0.78	NA	184.81	3.15	4.07	0.93	NA	8.89	0.22	1.30	13.20
c2y	0.28	0.65	0.05	1.62	1.95	2.28	2.32	0.99	1.62	1.75	1.38	NA	120.89	1.44	0.43	1.10	NA	0.28	0.28	1.01	7.80
upx	0.79	9.35	4.13	1.13	2.79	3.46	0.32	0.35	0.46	4.86	2.79	NA	170.23	0.43	1.95	2.95	NA	13.13	4.13	1.32	12.48
upy	0.08	1.99	1.25	2.58	1.25	0.92	2.99	0.99	2.58	2.49	1.42	NA	113.28	4.39	1.60	3.27	NA	1.58	0.92	0.66	8.01
downx	2.67	9.67	0.67	2.00	0.33	0.00	0.67	0.33	3.67	0.00	1.00	NA	169.84	2.16	1.33	0.33	NA	10.00	1.00	2.33	11.56
downy	2.00	3.67	0.67	0.00	1.33	0.33	0.33	0.33	1.67	1.00	0.67	NA	124.06	2.60	0.00	0.67	NA	1.67	0.67	0.00	7.87
Average	1.88	5.95	1.29	1.35	1.12	1.06	0.96	0.59	2.08	1.50	1.45	NA	132.52	2.08	1.31	1.50	NA	5.37	1.03	1.32	

Percentage (of width) Diff																					
% Param Name	right	2.sad	brmal	brmal	brmal	sses	brmal	6.sad	right	sses	brmal	leppy	β.wink	right	2.sad	subje	subje	subje	subje	Average	
xc	8.82	45.00	1.49	0.00	0.00	3.61	1.22	2.50	10.77	1.28	0.00	NA	4.55	2.27	6.58	2.27	NA	39.47	2.86	4.05	7.60
yc	7.35	10.00	5.97	1.45	2.99	0.00	3.66	0.00	6.15	8.97	11.54	NA	9.09	6.82	2.63	6.82	NA	3.95	2.86	4.05	5.24
r	1.47	6.67	1.49	1.45	1.49	0.00	2.44	2.50	1.54	5.13	1.28	NA	3.03	2.27	5.26	2.27	NA	1.32	1.43	0.00	2.28
c1x	19.61	34.81	5.47	16.43	0.50	0.80	2.58	1.39	25.13	5.68	4.70	NA	12.98	30.13	4.92	30.13	NA	40.35	1.91	8.26	13.65
c1y	14.65	29.13	5.91	1.39	8.90	0.05	4.24	3.10	1.48	1.66	12.77	NA	9.87	8.19	0.52	8.19	NA	7.84	8.52	15.51	7.88
c2x	13.72	74.83	12.94	12.07	6.97	12.45	0.12	3.62	14.36	2.01	2.99	NA	14.30	6.31	16.08	6.31	NA	35.09	0.95	5.27	13.36
c2y	1.25	3.27	0.23	7.03	8.73	8.25	8.49	3.70	7.46	6.73	5.32	NA	6.57	7.47	1.69	7.47	NA	1.12	1.21	4.10	5.00
upx	3.49	46.76	18.47	4.89	12.50	12.50	1.15	1.32	2.12	18.71	10.74	NA	1.96	20.10	7.69	20.10	NA	51.81	17.68	5.33	14.30
upy	0.37	9.97	5.60	11.23	5.60	3.31	10.96	3.73	11.92	9.60	5.45	NA	19.93	22.30	6.33	22.30	NA	6.25	3.93	2.68	8.97
downx	11.76	48.33	2.99	8.70	1.49	0.00	2.44	1.25	16.92	0.00	3.85	NA	9.80	2.27	5.26	2.27	NA	39.47	4.29	9.46	9.48
downy	8.82	18.33	2.99	0.00	5.97	1.20	1.22	1.25	7.69	3.85	2.56	NA	11.84	4.55	0.00	4.55	NA	6.58	2.86	0.00	4.68
Average	8.30	29.74	5.78	5.88	5.01	3.83	3.50	2.22	9.59	5.78	5.56	NA	9.45	10.24	5.18	10.24	NA	21.20	4.41	5.34	

Figure E.4: YALE polygonal right eye template test results

Absolute Difference Pixel Values																										
% Param	s101	s105	s111	s116	s121	s1210	s155	s162	s221	s225	s231	s294	s306	s309	s39	s405	s510	s52	s71	s78	s85	s88	s94	s98	Average	
xc	0.67	0.33	1.00	1.33	0.33	5.33	0.67	0.00	1.67	1.00	0.00	0.00	0.33	1.00	0.67	1.33	0.33	1.00	0.67	0.00	1.67	2.33	2.33	2.33	1.10	
yc	0.33	0.00	0.00	0.67	0.67	0.67	0.00	1.67	1.00	0.33	0.67	0.33	1.00	0.00	0.67	0.33	0.33	1.00	0.33	0.33	0.33	0.67	0.67	1.00	0.00	0.53
r	1.33	0.33	0.33	0.00	0.33	0.67	1.00	1.00	0.67	1.00	0.67	0.67	0.33	0.00	0.00	0.33	1.00	0.67	0.67	1.33	0.33	1.67	0.67	0.33	0.64	
c1x	4.79	3.13	4.06	4.73	0.73	9.46	2.79	4.13	3.06	5.46	3.79	3.46	2.79	3.46	3.79	1.73	4.46	3.13	4.46	4.79	2.40	2.06	3.06	3.06	3.70	
c1y	1.95	0.29	2.38	1.38	1.04	0.95	0.38	0.71	0.04	0.05	0.71	0.38	0.38	0.71	0.62	0.04	0.05	0.05	0.95	0.29	0.71	1.04	0.04	0.04	0.63	
c2x	3.00	0.33	3.67	2.67	3.67	6.67	2.00	1.33	3.33	0.67	1.33	0.67	0.67	1.67	0.00	2.00	2.33	1.00	1.33	1.00	3.67	5.67	4.67	3.33	2.36	
c2y	0.33	2.33	0.33	1.67	1.33	0.00	1.00	2.67	1.00	0.33	0.67	2.33	1.00	1.00	2.33	2.00	1.33	1.33	0.33	0.33	2.33	3.33	2.33	2.33	1.42	
upx	4.13	4.13	0.67	0.33	0.33	2.21	3.79	3.46	2.00	3.13	3.46	4.46	3.13	1.79	3.13	1.00	3.79	2.13	2.13	3.13	1.33	2.33	1.67	0.67	2.43	
upy	1.25	1.25	0.33	0.67	1.67	0.25	1.58	2.92	1.67	1.92	2.25	2.25	2.58	2.58	0.58	0.33	2.25	2.58	1.25	1.25	0.33	0.33	1.00	0.00	1.38	
downx	1.33	1.00	1.00	1.67	0.33	6.67	0.67	1.00	1.67	0.00	0.67	0.67	0.00	1.00	0.67	1.00	0.67	0.67	1.00	0.33	0.33	2.00	1.67	0.67	1.11	
downy	0.33	0.33	4.33	4.33	3.67	1.67	0.00	2.33	5.67	0.00	1.00	0.33	0.00	0.00	0.33	5.33	1.00	0.67	1.33	1.33	2.33	2.67	3.00	3.67	1.90	
Average	1.77	1.22	1.65	1.77	1.28	3.14	1.26	1.93	1.98	1.26	1.38	1.41	1.11	1.20	1.16	1.40	1.60	1.29	1.31	1.28	1.46	2.19	1.95	1.49		
Percentage (of width) Diff																										
% Param	s101	s105	s111	s116	s121	s1210	s155	s162	s221	s225	s231	s294	s306	s309	s39	s405	s510	s52	s71	s78	s85	s88	s94	s98	Average	
xc	5.26	1.96	6.38	9.52	1.75	30.19	4.26	0.00	10.20	6.38	0.00	0.00	1.96	5.36	4.00	8.16	2.44	6.12	4.55	0.00	9.62	11.86	13.21	14.29	6.56	
yc	2.63	0.00	0.00	4.76	3.51	3.77	0.00	11.11	6.12	2.13	4.35	2.04	5.88	0.00	4.00	2.04	2.44	6.12	2.27	2.27	3.85	3.39	5.66	0.00	3.26	
r	10.53	1.96	2.13	0.00	1.75	3.77	6.38	6.67	4.08	6.38	4.35	4.08	1.96	0.00	0.00	2.04	7.32	4.08	4.55	9.09	1.92	8.47	3.77	2.04	4.06	
c1x	37.85	18.40	25.93	33.78	3.84	53.55	17.84	27.52	18.75	34.86	24.75	21.19	16.44	18.54	22.77	10.59	32.64	19.15	30.42	32.69	13.82	10.49	17.33	18.75	23.41	
c1y	15.42	1.69	15.16	9.82	5.48	5.40	2.43	4.76	0.26	0.30	4.65	2.33	2.24	3.82	3.72	0.26	0.34	0.29	6.50	1.95	4.09	5.30	0.24	0.26	4.03	
c2x	23.68	1.96	23.40	19.05	19.30	37.74	12.77	8.89	20.41	4.26	8.70	4.08	3.92	8.93	0.00	12.24	17.07	6.12	9.09	6.82	21.15	28.81	26.42	20.41	14.38	
c2y	2.63	13.73	2.13	11.90	7.02	0.00	6.38	17.78	6.12	2.13	4.35	14.29	5.88	5.36	14.00	12.24	9.76	8.16	2.27	2.27	13.46	16.95	13.21	14.29	8.60	
upx	32.57	24.26	4.26	2.38	1.75	12.50	24.20	23.06	12.24	19.95	22.55	27.30	18.38	9.60	18.75	6.12	27.74	13.01	14.49	21.31	7.69	11.86	9.43	4.08	15.40	
upy	9.87	7.35	2.13	4.76	8.77	1.42	10.11	19.44	10.20	12.23	14.67	13.78	15.20	13.84	3.50	2.04	16.46	15.82	8.52	8.52	1.92	1.69	5.66	0.00	8.66	
downx	10.53	5.88	6.38	11.90	1.75	37.74	4.26	6.67	10.20	0.00	4.35	4.08	0.00	5.36	4.00	6.12	4.88	4.08	6.82	2.27	1.92	10.17	9.43	4.08	6.79	
downy	2.63	1.96	27.66	30.95	19.30	9.43	0.00	15.56	34.69	0.00	6.52	2.04	0.00	0.00	2.00	32.65	7.32	4.08	9.09	9.09	13.46	13.56	16.98	22.45	11.73	
Average	13.96	7.20	10.51	12.62	6.75	17.77	8.06	12.86	12.12	8.06	9.02	8.65	6.53	6.44	6.98	8.59	11.67	7.91	8.96	8.75	8.45	11.14	11.03	9.15		

Figure E.5: ORL polygonal left eye template test results

Absolute Difference Pixel Values																									
% Param	s101	s105	s111	s116	s121	s1210	s155	s162	s221	s225	s231	s294	s306	s309	s39	s405	s510	s52	s71	s78	s85	s88	s94	s98	Average
xc	0.33	0.00	0.33	1.00	0.67	0.33	6.00	0.33	1.67	0.33	0.67	0.67	0.00	1.33	0.67	2.00	0.00	0.33	0.67	0.33	0.67	0.67	2.00	0.33	0.89
yc	0.33	0.33	0.33	0.00	0.33	0.67	1.33	0.33	0.67	0.33	1.00	0.67	0.67	1.33	0.33	0.33	0.33	0.00	0.67	0.67	0.00	0.00	1.00	0.67	0.51
r	0.67	0.33	0.33	1.33	0.67	0.33	0.00	0.00	0.33	1.33	0.33	1.00	0.67	0.33	0.33	0.00	0.00	0.33	1.33	0.00	0.00	0.33	0.00	0.33	0.43
c1x	3.46	2.79	2.46	1.06	3.46	4.46	3.94	3.79	1.27	0.46	5.46	4.13	4.13	5.13	3.79	2.40	4.46	3.79	4.13	2.40	1.73	2.79	3.73	3.46	3.28
c1y	1.95	0.71	1.29	0.71	1.05	0.71	1.29	0.29	0.71	1.62	0.05	0.38	0.62	3.05	0.38	0.71	0.05	0.29	1.95	0.04	0.96	1.29	2.04	0.38	0.94
c2x	0.33	0.33	1.33	1.33	0.67	0.33	2.00	1.33	3.33	0.67	0.33	0.33	0.33	2.33	0.67	3.00	0.33	0.67	1.00	0.33	2.00	0.00	5.67	1.00	1.24
c2y	1.33	1.67	3.33	3.00	3.33	2.67	1.67	3.00	1.67	0.00	3.00	2.00	0.67	0.33	0.67	0.67	2.33	2.67	1.67	1.67	2.67	2.33	2.00	0.67	1.88
upx	3.13	2.79	3.79	0.33	2.79	3.79	7.00	3.46	0.33	3.46	3.13	3.46	2.13	3.13	3.46	0.33	3.46	4.13	2.13	0.00	0.33	2.79	1.33	3.13	2.66
upy	0.92	1.58	1.92	0.33	1.58	2.58	2.33	1.92	0.33	1.25	2.92	1.92	1.58	2.92	0.58	2.33	1.92	1.25	2.25	0.00	0.33	1.25	1.33	2.92	1.59
downx	0.33	0.33	1.00	1.67	0.33	0.33	7.00	0.33	0.33	0.33	0.33	0.67	1.00	3.67	0.67	1.00	0.33	1.00	1.00	0.33	0.33	0.33	2.67	0.33	1.07
downy	0.33	2.00	0.00	2.67	3.33	3.67	5.00	2.67	1.00	1.67	1.67	0.67	0.33	2.67	0.67	3.67	0.33	0.67	0.67	4.00	2.33	1.67	2.67	3.00	1.97
Average	1.19	1.17	1.47	1.22	1.66	1.81	3.41	1.59	1.06	1.04	1.72	1.44	1.10	2.38	1.11	1.49	1.23	1.37	1.59	0.89	1.03	1.22	2.22	1.47	

Percentage (of width) Diff																									
% Param	s101	s105	s111	s116	s121	s1210	s155	s162	s221	s225	s231	s294	s306	s309	s39	s405	s510	s52	s71	s78	s85	s88	s94	s98	Average
xc	2.00	0.00	2.00	6.12	3.77	2.13	33.33	2.17	8.06	1.61	4.55	4.17	0.00	7.55	3.85	12.00	0.00	1.92	4.35	2.50	4.08	3.77	11.11	1.85	5.12
yc	2.00	1.85	2.00	0.00	1.89	4.26	7.41	2.17	3.23	1.61	6.82	4.17	4.00	7.55	1.92	2.00	2.13	0.00	4.35	5.00	0.00	0.00	5.56	3.70	3.07
r	4.00	1.85	2.00	8.16	3.77	2.13	0.00	0.00	1.61	6.45	2.27	6.25	4.00	1.89	1.92	0.00	0.00	1.92	8.70	0.00	0.00	1.89	0.00	1.85	2.53
c1x	20.77	15.52	14.77	6.51	19.59	28.47	21.88	24.75	6.15	2.23	37.23	25.80	24.77	29.02	21.89	14.38	28.47	21.89	26.92	17.97	10.59	15.82	20.72	19.23	19.80
c1y	11.72	3.96	7.72	4.34	5.93	4.55	7.18	1.87	3.43	7.84	0.32	2.38	3.72	17.25	2.19	4.25	0.30	1.65	12.74	0.31	5.87	7.28	11.34	2.11	5.43
c2x	2.00	1.85	8.00	8.16	3.77	2.13	11.11	8.70	16.13	3.23	2.27	2.08	2.00	13.21	3.85	18.00	2.13	3.85	6.52	2.50	12.24	0.00	31.48	5.56	7.12
c2y	8.00	9.26	20.00	18.37	18.87	17.02	9.26	19.57	8.06	0.00	20.45	12.50	4.00	1.89	3.85	4.00	14.89	15.38	10.87	12.50	16.33	13.21	11.11	3.70	11.38
upx	18.75	15.51	22.75	2.04	15.80	24.20	38.89	22.55	1.61	16.73	21.31	21.61	12.75	17.69	19.95	2.00	22.07	23.80	13.86	0.00	2.04	15.80	7.41	17.36	15.69
upy	5.50	8.80	11.50	2.04	8.96	16.49	12.96	12.50	1.61	6.05	19.89	11.98	9.50	16.51	3.37	14.00	12.23	7.21	14.67	0.00	2.04	7.08	7.41	16.20	9.52
downx	2.00	1.85	6.00	10.20	1.89	2.13	38.89	2.17	1.61	1.61	2.27	4.17	6.00	20.75	3.85	6.00	2.13	5.77	6.52	2.50	2.04	1.89	14.81	1.85	6.20
downy	2.00	11.11	0.00	16.33	18.87	23.40	27.78	17.39	4.84	8.06	11.36	4.17	2.00	15.09	3.85	22.00	2.13	3.85	4.35	30.00	14.29	9.43	14.81	16.67	11.82
Average	7.16	6.51	8.79	7.48	9.37	11.54	18.97	10.35	5.12	5.04	11.70	9.02	6.61	13.49	6.41	8.97	7.86	7.93	10.35	6.66	6.32	6.92	12.34	8.19	

Figure E.6: ORL polygonal right eye template test results

APPENDIX F

Polygonal Mouth-Closed Template Detailed Test Results

Absolute Difference Pixel Values																					
%ParamName	KADiff	KAHA	KA.SA	KA.SU	KL.AN	KLFE	KMDI	KMSA	KR.AN	MK.SA	NA.AN	NA.HA	NA.SU	NM.DI	TM.FE	TM.SA	UY.AN	UY.DI	YMDI	YMH	Average
c1kOut	2.19	NA	2.07	2.86	3.52	2.00	NA	5.42	1.12	3.02	0.06	NA	NA	4.48	NA	1.15	0.79	7.73	3.00	NA	2.81
c1jOut	2.13	NA	0.20	2.31	0.79	2.96	NA	0.83	0.20	0.13	3.38	NA	NA	5.62	NA	2.64	2.58	4.14	1.83	NA	2.12
u1kOut	2.32	NA	2.80	0.50	2.21	5.43	NA	0.54	1.37	2.24	0.56	NA	NA	2.62	NA	0.12	1.46	1.15	5.38	NA	2.05
u1jOut	1.24	NA	0.80	1.67	1.15	0.36	NA	0.99	2.17	0.56	1.79	NA	NA	2.70	NA	2.03	0.92	3.11	1.05	NA	1.47
u2kOut	0.18	NA	0.65	4.63	0.49	3.16	NA	0.37	0.79	1.10	6.23	NA	NA	4.64	NA	4.74	2.04	3.07	7.67	NA	2.84
u2jOut	1.98	NA	0.73	3.02	0.30	0.04	NA	0.99	0.37	1.13	0.15	NA	NA	4.37	NA	1.58	2.08	0.44	1.42	NA	1.33
u3kOut	1.68	NA	1.40	0.20	0.49	1.13	NA	1.20	0.28	1.81	0.90	NA	NA	0.69	NA	0.53	4.66	1.65	1.08	NA	1.26
u3jOut	3.31	NA	2.40	4.08	2.23	1.23	NA	1.66	2.55	2.13	2.46	NA	NA	2.94	NA	2.04	2.18	1.78	2.00	NA	2.36
c2kOut	2.37	NA	3.85	6.44	1.84	2.56	NA	5.37	7.32	7.79	5.23	NA	NA	2.52	NA	0.80	6.03	5.59	7.16	NA	4.63
c2jOut	2.56	NA	5.60	1.63	0.20	4.52	NA	3.84	5.46	0.62	0.38	NA	NA	3.29	NA	2.86	1.31	0.35	1.46	NA	2.43
d3kOut	1.02	NA	0.06	0.87	2.18	4.46	NA	2.87	1.38	0.19	0.44	NA	NA	3.36	NA	0.81	1.99	0.32	2.42	NA	1.60
d3jOut	8.02	NA	7.27	5.92	3.44	3.43	NA	8.34	5.78	2.21	2.88	NA	NA	1.40	NA	3.63	2.16	2.56	0.33	NA	4.10
d2kOut	0.82	NA	0.31	4.96	0.49	3.50	NA	1.04	0.12	1.44	6.23	NA	NA	3.98	NA	4.41	3.04	0.40	7.67	NA	2.74
d2jOut	4.69	NA	3.94	5.69	2.70	2.29	NA	7.68	2.04	0.88	2.81	NA	NA	3.04	NA	0.24	3.42	1.89	3.42	NA	3.19
d1kOut	1.65	NA	3.80	0.50	1.88	5.43	NA	0.13	1.04	4.90	0.44	NA	NA	0.38	NA	1.12	3.13	0.15	8.38	NA	2.35
d1jOut	9.10	NA	7.53	6.67	4.18	2.97	NA	9.01	6.16	1.44	3.54	NA	NA	1.30	NA	1.97	2.75	2.56	0.62	NA	4.27
c1kIn	2.19	NA	2.07	2.86	3.52	2.00	NA	5.42	1.12	3.02	0.06	NA	NA	4.48	NA	1.15	0.79	7.73	3.00	NA	2.81
c1jIn	2.13	NA	0.20	2.31	0.79	2.96	NA	0.83	0.20	0.13	3.38	NA	NA	5.62	NA	2.64	2.58	4.14	1.83	NA	2.12
u1kIn	3.65	NA	4.47	1.50	1.54	5.10	NA	0.87	4.37	2.30	1.56	NA	NA	3.95	NA	0.55	2.79	2.48	6.05	NA	2.98
u1jIn	5.60	NA	5.53	3.50	3.68	3.64	NA	6.51	3.33	1.77	2.04	NA	NA	3.96	NA	2.64	3.32	2.39	4.12	NA	3.76
u2kIn	0.82	NA	0.02	4.29	0.17	2.16	NA	1.04	0.12	1.77	6.90	NA	NA	2.31	NA	5.41	2.04	1.73	8.67	NA	2.68
u2jIn	3.52	NA	3.94	8.52	3.20	2.96	NA	4.51	3.20	1.21	2.65	NA	NA	5.37	NA	2.24	3.92	2.72	6.25	NA	3.87
u3kIn	2.98	NA	3.94	3.47	0.85	7.79	NA	3.20	4.05	4.19	1.10	NA	NA	4.03	NA	2.47	2.32	0.68	0.75	NA	2.99
u3jIn	4.19	NA	4.27	3.42	3.61	3.10	NA	6.18	3.95	1.88	2.04	NA	NA	3.73	NA	2.29	2.99	3.06	2.17	NA	3.35
c2kIn	2.37	NA	3.85	6.44	1.84	2.56	NA	5.37	7.32	7.79	5.23	NA	NA	2.52	NA	0.80	6.03	5.59	7.16	NA	4.63
c2jIn	2.56	NA	5.60	1.63	0.20	4.52	NA	3.84	5.46	0.62	0.38	NA	NA	3.29	NA	2.86	1.31	0.35	1.46	NA	2.43
d3kIn	2.98	NA	3.94	3.47	0.85	7.79	NA	3.20	4.05	4.19	1.10	NA	NA	4.03	NA	2.47	2.32	0.68	0.75	NA	2.99
d3jIn	4.19	NA	4.27	3.42	3.61	3.10	NA	6.18	3.95	1.88	2.04	NA	NA	3.73	NA	2.29	2.99	3.06	2.17	NA	3.35
d2kIn	0.82	NA	0.02	4.29	0.17	2.16	NA	1.04	0.12	1.77	6.90	NA	NA	2.31	NA	5.41	2.04	1.73	8.67	NA	2.68
d2jIn	3.52	NA	3.94	8.52	3.20	2.96	NA	4.51	3.20	1.21	2.65	NA	NA	5.37	NA	2.24	3.92	2.72	6.25	NA	3.87
d1kIn	9.10	NA	7.53	6.67	4.18	2.97	NA	9.01	6.16	1.44	3.54	NA	NA	1.30	NA	1.97	2.75	2.56	0.62	NA	4.27
d1jIn	2.19	NA	2.07	2.86	3.52	2.00	NA	5.42	1.12	3.02	0.06	NA	NA	4.48	NA	1.15	0.79	7.73	3.00	NA	2.81
c1jIn	2.13	NA	0.20	2.31	0.79	2.96	NA	0.83	0.20	0.13	3.38	NA	NA	5.62	NA	2.64	2.58	4.14	1.83	NA	2.12
u1jIn	3.65	NA	4.47	1.50	1.54	5.10	NA	0.87	4.37	2.30	1.56	NA	NA	3.95	NA	0.55	2.79	2.48	6.05	NA	2.98
u1jIn	5.60	NA	5.53	3.50	3.68	3.64	NA	6.51	3.33	1.77	2.04	NA	NA	3.96	NA	2.64	3.32	2.39	4.12	NA	3.76
u2kIn	0.82	NA	0.02	4.29	0.17	2.16	NA	1.04	0.12	1.77	6.90	NA	NA	2.31	NA	5.41	2.04	1.73	8.67	NA	2.68
u2jIn	3.52	NA	3.94	8.52	3.20	2.96	NA	4.51	3.20	1.21	2.65	NA	NA	5.37	NA	2.24	3.92	2.72	6.25	NA	3.87
u3kIn	2.98	NA	3.94	3.47	0.85	7.79	NA	3.20	4.05	4.19	1.10	NA	NA	4.03	NA	2.47	2.32	0.68	0.75	NA	2.99
u3jIn	4.19	NA	4.27	3.42	3.61	3.10	NA	6.18	3.95	1.88	2.04	NA	NA	3.73	NA	2.29	2.99	3.06	2.17	NA	3.35
c2kIn	2.37	NA	3.85	6.44	1.84	2.56	NA	5.37	7.32	7.79	5.23	NA	NA	2.52	NA	0.80	6.03	5.59	7.16	NA	4.63
c2jIn	2.56	NA	5.60	1.63	0.20	4.52	NA	3.84	5.46	0.62	0.38	NA	NA	3.29	NA	2.86	1.31	0.35	1.46	NA	2.43
d3kIn	2.98	NA	3.94	3.47	0.85	7.79	NA	3.20	4.05	4.19	1.10	NA	NA	4.03	NA	2.47	2.32	0.68	0.75	NA	2.99
d3jIn	4.19	NA	4.27	3.42	3.61	3.10	NA	6.18	3.95	1.88	2.04	NA	NA	3.73	NA	2.29	2.99	3.06	2.17	NA	3.35
d2kIn	0.82	NA	0.02	4.29	0.17	2.16	NA	1.04	0.12	1.77	6.90	NA	NA	2.31	NA	5.41	2.04	1.73	8.67	NA	2.68
d2jIn	3.52	NA	3.94	8.52	3.20	2.96	NA	4.51	3.20	1.21	2.65	NA	NA	5.37	NA	2.24	3.92	2.72	6.25	NA	3.87
d1kIn	9.10	NA	7.53	6.67	4.18	2.97	NA	9.01	6.16	1.44	3.54	NA	NA	1.30	NA	1.97	2.75	2.56	0.62	NA	4.27
d1jIn	2.19	NA	2.07	2.86	3.52	2.00	NA	5.42	1.12	3.02	0.06	NA	NA	4.48	NA	1.15	0.79	7.73	3.00	NA	2.81
c1jIn	2.13	NA	0.20	2.31	0.79	2.96	NA	0.83	0.20	0.13	3.38	NA	NA	5.62	NA	2.64	2.58	4.14	1.83	NA	2.12
u1jIn	3.65	NA	4.47	1.50	1.54	5.10	NA	0.87	4.37	2.30	1.56	NA	NA	3.95	NA	0.55	2.79	2.48	6.05	NA	2.98
u1jIn	5.60	NA	5.53	3.50	3.68	3.64	NA	6.51	3.33	1.77	2.04	NA	NA	3.96	NA	2.64	3.32	2.39	4.12	NA	3.76
u2kIn	0.82	NA	0.02	4.29	0.17	2.16	NA	1.04	0.12	1.77	6.90	NA	NA	2.31	NA	5.41	2.04	1.73	8.67	NA	2.68
u2jIn	3.52	NA	3.94	8.52	3.20	2.96	NA	4.51	3.20	1.21	2.65	NA	NA	5.37	NA	2.24	3.92	2.72	6.25	NA	3.87
u3kIn	2.98	NA	3.94	3.47	0.85	7.79	NA	3.20	4.05	4.19	1.10	NA	NA	4.03	NA	2.47	2.32	0.68	0.75	NA	2.99
u3jIn	4.19	NA	4.27	3.42	3.61	3.10	NA	6.18	3.95	1.88	2.04	NA	NA	3.73	NA	2.29	2.99	3.06	2.17	NA	3.35
c2kIn	2.37	NA	3.85	6.44	1.84	2.56	NA	5.37	7.32	7.79	5.23	NA	NA	2.52	NA	0.80	6.03	5.59	7.16	NA	4.63
c2jIn	2.56	NA	5.60	1.63	0.20	4.52	NA	3.84	5.46	0.62	0.38	NA	NA	3.29	NA	2.86	1.31	0.35	1.46	NA	2.43
d3kIn	2.98	NA	3.94	3.47	0.85	7.79	NA	3.20	4.05	4.19	1.10	NA	NA	4.03	NA	2.47	2.32	0.68	0.75	NA	2.99
d3jIn	4.19	NA	4.27	3.42	3.61	3.10	NA	6.18	3.95	1.88	2.04	NA	NA	3.73	NA	2.29	2.99	3.06	2.17	NA	3.35
d2kIn	0.82	NA	0.02	4.29	0.17	2.16	NA	1.04	0.12	1.77	6.90	NA	NA	2.31	NA	5.41	2.04	1.73	8.67	NA	2.68
d2jIn	3.52	NA	3.94	8.52	3.20	2.96	NA	4.51	3.20	1.21	2.65	NA	NA	5.37	NA	2.24	3.92	2.72	6.25	NA	3.87
d1kIn	9.10	NA	7.53	6.67	4.18	2.97	NA	9.01	6.16	1.44	3.54	NA	NA	1.30	NA	1.97	2.75	2.56	0.62	NA	4.27
d1jIn	2.19	NA	2.07	2.86	3.52	2.00	NA	5.42	1.12	3.02	0.06	NA	NA	4.48	NA	1.15	0.79	7.73	3.00	NA	2.81
c1jIn	2.13	NA	0.20	2.31	0.79	2.96	NA	0.83	0.20	0.13	3.38	NA	NA	5.62	NA	2.64	2.58	4.14	1.83	NA	2.12
u1jIn	3.65	NA	4.47	1.50	1.54	5.10	NA	0.87	4.37	2.30	1.56	NA	NA	3.95	NA	0.55	2.79	2.48	6.05	NA	2.98
u1jIn	5.60	NA	5.53	3.50	3.68	3.64	NA	6.51	3.33	1.77	2.04	NA	NA	3.96	NA	2.64	3.32	2.39	4.12	NA	3.76
u2kIn	0.82	NA	0.02	4.29																	

Percentage (of width) Diff		K.A.DI	K.A.HA	K.A.SA	K.A.SU	KL.AN	KL.FE	KM.DI	KM.SA	KR.AN	MK.SA	NA.AN	NA.HA	NA.SU	NM.DI	TM.FE	TM.SA	UY.AN	UY.DI	YM.DI	YM.HA	Average
% Param Name																						
c1kOut		4.84	NA	4.73	6.70	8.51	4.68	NA	13.66	2.44	6.25	0.13	NA	NA	9.33	NA	2.47	1.86	18.27	6.25	NA	6.44
c1jOut		4.70	NA	0.45	5.42	1.91	6.93	NA	2.10	0.44	0.26	7.28	NA	NA	11.71	NA	5.69	6.05	9.78	3.82	NA	4.75
u1kOut		5.11	NA	6.42	1.17	5.35	12.74	NA	1.35	2.98	4.83	1.21	NA	NA	5.45	NA	0.25	3.42	2.72	11.21	NA	4.57
u1jOut		2.72	NA	1.84	3.91	2.79	0.85	NA	2.49	4.72	1.16	3.87	NA	NA	5.63	NA	4.37	2.15	7.35	2.18	NA	3.29
u2kOut		0.40	NA	1.48	10.84	1.20	7.41	NA	0.93	1.72	2.28	13.44	NA	NA	9.67	NA	10.23	4.79	7.25	15.97	NA	6.26
u2jOut		4.36	NA	1.68	7.08	0.74	0.10	NA	2.49	0.80	2.33	0.31	NA	NA	9.10	NA	3.41	4.88	1.05	2.95	NA	2.95
u3kOut		3.71	NA	3.20	0.47	1.18	2.64	NA	3.03	0.61	3.75	1.93	NA	NA	1.45	NA	1.14	10.32	3.90	2.26	NA	2.87
u3jOut		7.31	NA	5.49	9.56	5.39	2.89	NA	4.18	5.55	4.40	5.31	NA	NA	6.12	NA	4.40	5.10	4.20	4.17	NA	5.29
c2kOut		5.23	NA	8.82	15.09	4.45	6.01	NA	13.54	15.92	16.12	11.29	NA	NA	5.26	NA	1.73	14.14	13.20	14.91	NA	10.41
c2jOut		5.64	NA	12.83	3.81	0.47	10.59	NA	9.69	11.87	1.27	0.81	NA	NA	6.84	NA	6.17	3.08	0.84	3.05	NA	5.50
d3kOut		2.24	NA	0.15	2.03	5.28	10.45	NA	7.23	3.01	0.39	0.94	NA	NA	7.00	NA	1.74	4.67	0.75	5.03	NA	3.64
d3jOut		17.69	NA	16.65	13.88	8.32	8.04	NA	21.03	12.57	4.57	6.21	NA	NA	2.91	NA	7.83	5.06	6.04	0.69	NA	9.39
d2kOut		1.80	NA	0.72	11.62	1.20	8.19	NA	2.61	0.27	2.37	13.44	NA	NA	8.29	NA	9.52	7.13	0.95	15.97	NA	6.05
d2jOut		10.34	NA	9.01	13.33	6.52	5.36	NA	19.35	4.43	1.81	6.07	NA	NA	6.32	NA	0.53	8.01	4.46	7.12	NA	7.33
d1kOut		3.64	NA	8.71	1.17	4.54	12.74	NA	0.33	2.25	10.15	0.94	NA	NA	0.80	NA	2.41	7.32	0.36	17.46	NA	5.20
d1jOut		20.07	NA	17.24	15.63	10.11	6.96	NA	22.72	13.39	2.38	7.64	NA	NA	2.70	NA	4.26	6.45	6.04	1.29	NA	9.82
c1kIn		4.84	NA	4.73	6.70	8.51	4.68	NA	13.66	2.44	6.25	0.13	NA	NA	9.33	NA	2.47	1.86	18.27	6.25	NA	6.44
c1jIn		4.70	NA	0.45	5.42	1.91	6.93	NA	2.10	0.44	0.26	7.28	NA	NA	11.71	NA	5.69	6.05	9.78	3.82	NA	4.75
u1kIn		8.05	NA	10.23	3.52	3.73	11.95	NA	2.19	9.50	6.01	3.37	NA	NA	8.23	NA	1.19	6.54	5.87	12.59	NA	6.64
u1jIn		12.35	NA	12.66	8.20	8.90	8.52	NA	16.41	7.23	3.67	4.41	NA	NA	8.26	NA	5.70	9.18	5.65	8.58	NA	8.55
u2kIn		1.80	NA	0.04	10.06	0.42	5.07	NA	2.61	0.27	3.66	14.88	NA	NA	4.81	NA	11.67	4.79	4.10	18.06	NA	5.87
u2jIn		7.77	NA	9.01	19.97	7.73	6.93	NA	11.37	6.96	2.50	5.71	NA	NA	11.18	NA	4.84	9.18	6.43	13.02	NA	8.76
u3kIn		6.58	NA	9.01	8.12	2.05	18.26	NA	8.08	8.81	8.66	2.38	NA	NA	8.39	NA	5.33	5.45	1.61	1.56	NA	6.74
u3jIn		9.24	NA	9.78	8.02	8.73	7.26	NA	15.57	8.58	3.88	4.41	NA	NA	7.77	NA	4.95	7.01	7.22	4.51	NA	7.64
c2kIn		5.23	NA	8.82	15.09	4.45	6.01	NA	13.54	15.92	16.12	11.29	NA	NA	5.26	NA	1.73	14.14	13.20	14.91	NA	10.41
c2jIn		5.64	NA	12.83	3.81	0.47	10.59	NA	9.69	11.87	1.27	0.81	NA	NA	6.84	NA	6.17	3.08	0.84	3.05	NA	5.50
d3kIn		6.58	NA	9.01	8.12	2.05	18.26	NA	8.08	8.81	8.66	2.38	NA	NA	8.39	NA	5.33	5.45	1.61	1.56	NA	6.74
d3jIn		9.24	NA	9.78	8.02	8.73	7.26	NA	15.57	8.58	3.88	4.41	NA	NA	7.77	NA	4.95	7.01	7.22	4.51	NA	7.64
d2kIn		1.80	NA	0.04	10.06	0.42	5.07	NA	2.61	0.27	3.66	14.88	NA	NA	4.81	NA	11.67	4.79	4.10	18.06	NA	5.87
d2jIn		7.77	NA	9.01	19.97	7.73	6.93	NA	11.37	6.96	2.50	5.71	NA	NA	11.18	NA	4.84	9.18	6.43	13.02	NA	8.76
d1kIn		8.05	NA	10.23	3.52	3.73	11.95	NA	2.19	9.50	6.01	3.37	NA	NA	8.23	NA	1.19	6.54	5.87	12.59	NA	6.64
d1jIn		12.35	NA	12.66	8.20	8.90	0.00	NA	16.41	7.23	3.67	4.41	NA	NA	8.26	NA	5.70	9.18	5.65	8.58	NA	7.94
Average		4.21	NA	4.28	6.01	3.39	5.94	NA	5.52	4.55	3.89	4.23	NA	NA	7.05	NA	3.78	5.55	6.30	6.53	NA	

Figure F.2: JAFFE polygonal mouth-closed template test results (%)

Absolute Difference Pixel Values																			
% Param	flight	2.sad	brmal	brmal	brmal	brmal	brmal	brmal	brmal	brmal	brmal	brmal	brmal	brmal	brmal	brmal	brmal	brmal	brmal
c1kOut	8.76	0.68	10.50	11.11	7.83	6.69	0.76	5.67	2.68	2.184	22.81	15.60	21.50	10.33	14.67	8.94	2.15	NA	6.74
c1yOut	2.93	1.94	4.50	4.64	1.17	0.76	3.41	1.50	3.98	11.79	10.45	0.30	12.67	2.50	4.67	10.89	2.71	NA	0.39
u1kOut	2.29	1.59	1.80	2.82	10.15	2.33	1.59	5.50	2.59	15.42	16.47	14.52	15.33	9.92	1.42	8.02	2.23	NA	3.34
u1yOut	0.57	0.06	1.74	0.28	0.67	1.33	0.93	1.00	1.15	0.54	1.14	0.80	1.33	0.33	15.33	5.28	0.54	NA	1.40
u2kOut	1.58	1.84	2.83	0.39	9.69	2.33	2.24	7.00	1.84	16.18	17.31	17.65	13.00	9.17	3.52	6.27	1.31	NA	0.03
u2yOut	6.26	15.94	2.00	1.03	3.74	0.67	0.07	0.67	1.48	1.70	1.20	7.91	2.67	0.67	12.38	6.36	1.54	NA	5.22
u3kOut	6.79	3.43	3.17	2.02	2.58	6.00	5.08	9.75	2.76	16.59	18.47	16.69	9.00	6.75	3.07	16.85	1.06	NA	2.18
u3yOut	0.57	1.06	0.00	1.36	0.33	0.33	0.07	0.07	0.81	0.63	0.47	0.14	0.67	0.33	18.92	4.61	0.13	NA	0.38
c2kOut	5.37	1.34	4.17	12.23	8.50	11.54	3.91	0.83	7.16	21.01	22.97	19.27	9.33	7.67	5.17	13.60	0.15	NA	9.51
c2yOut	1.07	2.60	2.00	3.31	0.17	3.94	5.41	0.42	1.10	16.87	15.86	14.36	2.33	0.50	0.75	2.78	2.71	NA	1.85
d3kOut	4.12	2.43	5.50	0.98	3.58	8.33	6.74	8.09	1.81	17.93	20.14	17.35	13.00	7.75	0.74	11.19	0.94	NA	2.84
d3yOut	1.90	1.60	0.33	0.64	3.00	1.33	0.07	0.60	3.48	1.63	2.14	1.14	3.00	2.00	15.25	4.61	5.54	NA	0.38
d2kOut	0.75	0.51	4.93	0.73	10.69	3.33	1.91	4.67	1.18	17.94	19.64	19.31	13.00	8.17	1.85	4.27	0.35	NA	0.03
d2yOut	6.59	16.60	0.33	0.69	5.74	3.00	1.59	2.33	2.81	2.63	3.80	12.24	5.67	3.33	6.38	8.36	2.21	NA	3.56
d1kOut	3.96	2.93	0.53	0.49	8.48	1.33	0.41	5.17	0.93	19.09	19.47	15.85	14.00	9.25	2.75	9.35	0.90	NA	4.01
d1yOut	2.57	2.94	0.74	4.05	3.66	0.67	1.41	0.33	3.48	0.21	2.14	1.80	4.67	1.00	10.67	4.61	4.21	NA	0.40
c1kIn	8.76	0.68	10.50	11.11	7.83	6.69	0.76	5.67	2.68	2.184	22.81	15.60	21.50	10.33	14.67	8.94	2.15	NA	6.74
c1yIn	2.93	1.94	4.50	4.64	1.17	0.76	3.41	1.50	3.98	11.79	10.45	0.30	12.67	2.50	4.67	10.89	2.71	NA	0.39
u1kIn	3.96	2.59	0.47	2.82	6.15	0.67	1.41	6.83	1.93	14.42	16.14	13.52	14.00	8.25	1.08	10.02	2.23	NA	4.34
u1yIn	1.40	2.60	3.41	6.05	0.83	1.17	1.41	1.50	2.31	1.63	0.53	1.36	1.00	0.17	15.00	2.45	3.04	NA	2.73
u2kIn	0.42	2.18	5.83	0.39	12.35	5.00	2.91	4.67	0.16	17.84	18.64	18.65	13.67	7.83	1.19	2.60	0.98	NA	0.70
u2yIn	5.42	17.60	2.33	1.31	3.91	1.17	1.07	1.83	2.31	1.87	1.53	7.41	1.00	0.83	11.71	6.20	3.38	NA	6.89
u3kIn	3.79	2.43	6.17	0.64	9.25	9.67	5.41	6.42	1.24	19.26	20.81	19.02	13.67	9.75	0.26	10.19	1.60	NA	4.51
u3yIn	1.07	2.27	1.33	3.31	2.83	2.17	2.74	1.57	2.31	2.20	1.53	2.70	2.00	1.50	19.25	1.78	3.38	NA	2.05
c2kIn	5.37	1.34	4.17	12.23	8.50	11.54	3.91	0.83	7.16	21.01	22.97	19.27	9.33	7.67	5.17	13.60	0.15	NA	9.51
c2yIn	1.07	2.60	2.00	3.31	0.17	3.94	5.41	0.42	1.10	16.87	15.86	14.36	2.33	0.50	0.75	2.78	2.71	NA	1.85
d3kIn	3.79	2.43	6.17	0.64	9.25	9.67	5.41	6.42	1.24	19.26	20.81	19.02	13.67	9.75	0.26	10.19	1.60	NA	4.51
d3yIn	1.07	2.27	1.33	3.31	2.83	2.17	2.74	1.57	2.31	2.20	1.53	2.70	2.00	1.50	19.25	1.78	3.38	NA	2.05
d2kIn	0.42	2.18	5.83	0.39	12.35	5.00	2.91	4.67	0.16	17.84	18.64	18.65	13.67	7.83	1.19	2.60	0.98	NA	0.70
d2yIn	5.42	17.60	2.33	1.31	3.91	1.17	1.07	1.83	2.31	1.87	1.53	7.41	1.00	0.83	11.71	6.20	3.38	NA	6.89
d1kIn	3.96	2.59	0.47	2.82	6.15	0.67	1.41	6.83	1.93	14.42	16.14	13.52	14.00	8.25	1.08	10.02	2.23	NA	4.34
d1yIn	1.40	2.60	3.41	6.05	0.83	1.17	1.41	1.50	2.31	1.63	0.53	1.36	1.00	0.17	15.00	2.45	3.04	NA	2.73
Average	3.32	3.86	3.29	3.35	5.26	3.64	2.47	3.36	2.34	11.50	12.03	10.93	8.68	4.92	7.49	7.15	2.05	NA	3.22

Figure F.3: YALE polygonal mouth-closed template test results

Percentage (of width) Diff																			
% Param	light	2.sad	bm	l	bm	l	bm	l	bm	l	bm	l	bm	l	bm	l	bm	l	Average
c1wOut	17.88	1.86	23.68	25.44	16.21	15.08	1.67	11.64	7.30	67.56	66.43	41.80	52.87	21.68	24.31	23.73	4.99	N/A	15.32
c1yOut	5.98	5.33	10.15	10.63	2.41	1.72	7.51	3.08	10.85	36.45	30.43	0.81	31.15	5.24	7.73	28.90	6.30	N/A	0.88
u1wOut	4.67	4.39	4.06	6.46	20.99	5.26	3.50	11.30	7.07	47.70	47.98	38.90	37.70	20.80	2.35	21.29	5.18	N/A	7.80
u1yOut	1.16	0.17	3.93	0.65	1.39	3.01	2.05	2.05	3.12	1.67	3.31	2.15	3.28	0.70	25.41	14.02	1.26	N/A	3.17
u2wOut	3.23	5.07	6.39	0.90	20.04	5.26	4.95	14.38	5.03	50.03	50.41	47.27	31.97	19.23	5.84	16.65	3.05	N/A	0.08
u2yOut	12.77	43.86	4.51	2.35	7.74	1.50	0.16	1.37	4.03	5.27	3.49	21.18	6.56	1.40	20.51	16.90	3.59	N/A	11.87
u3wOut	13.86	9.43	7.14	4.63	5.34	13.53	11.20	20.04	7.53	51.32	53.81	44.70	22.13	14.16	5.09	44.75	2.47	N/A	4.95
u3yOut	1.16	2.92	0.00	3.11	0.69	0.75	0.16	0.14	2.22	1.95	1.37	0.36	1.64	0.70	31.36	12.25	0.29	N/A	0.87
e2wOut	10.96	3.70	9.40	28.00	17.59	26.03	8.63	1.71	19.52	64.98	66.91	51.62	22.95	16.08	8.56	36.12	0.34	N/A	21.61
e2yOut	2.18	7.17	4.51	7.57	0.34	8.88	11.93	0.86	3.01	52.17	46.21	38.48	5.74	1.05	1.24	7.38	6.30	N/A	4.21
d3wOut	8.41	6.68	12.41	2.24	7.41	18.80	14.88	16.61	5.20	55.44	58.66	46.48	31.97	16.26	1.22	29.70	2.18	N/A	6.46
d3yOut	3.88	4.42	0.75	1.47	6.21	3.01	0.16	1.23	9.49	5.04	6.22	3.04	7.38	4.20	25.28	12.25	12.89	N/A	0.87
d2wOut	1.54	1.40	10.90	1.66	22.11	7.52	4.22	9.59	3.21	55.19	57.21	51.73	31.97	17.13	3.07	11.34	0.82	N/A	0.08
d2yOut	13.45	45.70	0.75	1.59	11.87	6.77	3.52	4.79	7.67	8.13	11.07	32.78	13.93	6.99	10.57	22.21	5.14	N/A	8.08
d1wOut	8.07	8.06	1.20	1.12	17.54	3.01	0.91	10.62	2.53	59.04	56.72	42.47	34.43	19.41	4.56	24.83	2.08	N/A	9.11
d1yOut	5.24	8.08	1.68	9.28	7.58	1.50	3.10	0.68	9.49	0.84	6.22	4.83	11.48	2.10	17.68	12.25	9.79	N/A	0.90
e1wIn	17.88	1.86	23.68	25.44	16.21	15.08	1.67	11.64	7.30	67.56	66.43	41.80	52.87	21.68	24.31	23.73	4.99	N/A	15.32
e1yIn	5.98	5.33	10.15	10.63	2.41	1.72	7.51	3.08	10.85	36.45	30.43	0.81	31.15	5.24	7.73	28.90	6.30	N/A	0.88
u1wIn	8.07	7.14	1.05	6.46	12.71	1.50	3.11	14.04	5.26	44.60	47.01	36.22	34.43	17.31	1.80	26.60	5.18	N/A	9.87
u1yIn	2.86	7.17	7.69	13.86	1.71	2.63	3.10	3.08	6.31	5.03	1.55	3.66	2.46	0.35	24.86	6.50	7.07	N/A	6.20
u2wIn	0.86	5.99	13.16	0.90	25.56	11.28	6.42	9.59	0.43	55.19	54.29	49.94	33.61	16.43	1.97	6.91	2.28	N/A	1.59
u2yIn	11.07	48.45	5.26	2.99	8.08	2.63	2.37	3.77	6.31	5.78	4.46	19.84	2.46	1.75	19.41	16.45	7.85	N/A	15.66
u3wIn	7.73	6.68	13.91	1.47	19.14	21.80	11.94	13.19	3.38	59.57	60.60	50.95	33.61	20.45	0.43	27.05	3.73	N/A	10.25
u3yIn	2.18	6.25	3.01	7.57	5.86	4.89	6.04	3.22	6.31	6.81	4.46	7.23	4.92	3.15	31.91	4.73	7.85	N/A	4.65
e2wIn	10.96	3.70	9.40	28.00	17.59	26.03	8.63	1.71	19.52	64.98	66.91	51.62	22.95	16.08	8.56	36.12	0.34	N/A	21.61
e2yIn	2.18	7.17	4.51	7.57	0.34	8.88	11.93	0.86	3.01	52.17	46.21	38.48	5.74	1.05	1.24	7.38	6.30	N/A	4.21
d3wIn	7.73	6.68	13.91	1.47	19.14	21.80	11.94	13.19	3.38	59.57	60.60	50.95	33.61	20.45	0.43	27.05	3.73	N/A	10.25
d3yIn	2.18	6.25	3.01	7.57	5.86	4.89	6.04	3.22	6.31	6.81	4.46	7.23	4.92	3.15	31.91	4.73	7.85	N/A	4.65
d2wIn	0.86	5.99	13.16	0.90	25.56	11.28	6.42	9.59	0.43	55.19	54.29	49.94	33.61	16.43	1.97	6.91	2.28	N/A	1.59
d2yIn	11.07	48.45	5.26	2.99	8.08	2.63	2.37	3.77	6.31	5.78	4.46	19.84	2.46	1.75	19.41	16.45	7.85	N/A	15.66
d1wIn	8.07	8.06	1.20	1.12	17.54	3.01	0.91	10.62	2.53	59.04	56.72	42.47	34.43	19.41	4.56	24.83	2.08	N/A	9.11
d1yIn	5.24	8.08	1.68	9.28	7.58	1.50	3.10	0.68	9.49	0.84	6.22	4.83	11.48	2.10	17.68	12.25	9.79	N/A	0.90
Average	6.78	10.61	7.42	7.66	10.88	8.21	5.45	6.91	6.37	35.55	35.04	29.28	21.26	10.31	12.42	18.97	4.77	N/A	7.33

Figure F.4: YALE polygonal mouth-closed template test results (%)

Absolute Difference Pixel Values																										
% Param	s101	s105	s111	s116	s121	s1210	s155	s162	s221	s225	s231	s294	s306	s309	s39	s405	s510	s52	s71	s78	s85	s88	s94	s98	Average	
c1kOut	NA	0.17	NA	4.67	1.45	NA	0.90	2.68	NA	NA	2.90	1.47	3.01	1.06	1.43	NA	NA	NA	NA	10.70	4.63	NA	2.41	0.87	0.94	2.62
c1yOut	NA	0.53	NA	13.02	2.06	NA	3.57	1.87	NA	NA	3.61	1.77	2.34	0.60	2.05	NA	NA	NA	NA	0.46	0.42	NA	0.12	19.11	1.33	3.52
u1kOut	NA	1.77	NA	0.95	1.20	NA	0.48	1.04	NA	NA	5.97	0.47	1.65	0.72	2.26	NA	NA	NA	NA	8.20	4.29	NA	1.64	2.76	1.62	2.34
u1yOut	NA	0.26	NA	14.96	1.44	NA	1.30	1.48	NA	NA	0.41	0.40	0.21	0.07	0.45	NA	NA	NA	NA	0.71	0.65	NA	0.36	10.39	0.30	2.22
u2xOut	NA	0.68	NA	1.95	1.80	NA	1.04	2.28	NA	NA	2.44	2.15	1.81	3.87	0.89	NA	NA	NA	NA	7.41	4.38	NA	0.77	0.19	1.78	2.23
u2yOut	NA	0.59	NA	13.62	0.77	NA	0.64	1.71	NA	NA	0.13	0.16	0.54	1.07	1.72	NA	NA	NA	NA	0.29	0.65	NA	2.24	7.89	0.63	2.18
u3xOut	NA	0.07	NA	2.62	2.03	NA	0.56	0.73	NA	NA	1.52	1.20	1.31	1.72	0.93	NA	NA	NA	NA	9.20	4.13	NA	0.98	2.93	0.05	2.00
u3yOut	NA	0.93	NA	14.96	1.77	NA	2.24	0.75	NA	NA	0.13	0.73	0.21	0.93	0.11	NA	NA	NA	NA	1.04	0.65	NA	1.69	9.72	0.30	2.41
e2xOut	NA	0.48	NA	5.10	0.35	NA	0.77	0.83	NA	NA	0.40	2.14	6.44	1.06	2.24	NA	NA	NA	NA	8.37	4.21	NA	0.52	7.10	2.70	2.85
e2yOut	NA	2.24	NA	15.57	0.23	NA	2.24	0.14	NA	NA	1.88	1.10	0.98	3.93	1.89	NA	NA	NA	NA	1.46	1.85	NA	0.53	12.43	2.62	3.27
d3xOut	NA	1.73	NA	0.95	3.03	NA	2.22	1.73	NA	NA	0.81	0.47	0.98	2.06	0.60	NA	NA	NA	NA	9.87	4.46	NA	0.36	4.26	1.05	2.31
d3yOut	NA	2.07	NA	16.29	0.11	NA	1.10	1.09	NA	NA	2.54	0.40	1.21	0.07	0.45	NA	NA	NA	NA	0.71	2.35	NA	1.31	8.72	1.30	2.65
d2xOut	NA	1.35	NA	2.29	1.14	NA	1.29	2.62	NA	NA	0.44	3.15	1.81	5.54	0.23	NA	NA	NA	NA	8.75	4.04	NA	3.43	0.15	1.45	2.51
d2yOut	NA	2.07	NA	16.96	1.23	NA	2.64	0.04	NA	NA	2.21	0.49	0.21	2.60	1.39	NA	NA	NA	NA	0.71	2.01	NA	4.24	8.55	1.63	3.13
d1xOut	NA	3.77	NA	1.62	2.53	NA	1.48	3.71	NA	NA	4.30	1.14	1.98	0.72	2.60	NA	NA	NA	NA	8.54	3.29	NA	1.36	2.43	1.28	2.72
d1yOut	NA	2.74	NA	16.62	0.11	NA	2.70	2.15	NA	NA	2.92	0.27	1.21	1.73	1.11	NA	NA	NA	NA	0.71	2.01	NA	2.97	9.72	1.96	3.26
e1kIn	NA	0.17	NA	4.67	1.45	NA	0.90	2.68	NA	NA	2.90	1.47	3.01	1.06	1.43	NA	NA	NA	NA	10.70	4.63	NA	2.41	0.87	0.94	2.62
e1yIn	NA	0.53	NA	13.02	2.06	NA	3.57	1.87	NA	NA	3.61	1.77	2.34	0.60	2.05	NA	NA	NA	NA	0.46	0.42	NA	0.12	19.11	1.33	3.52
u1kIn	NA	2.10	NA	1.95	0.53	NA	0.48	2.04	NA	NA	4.97	0.14	1.31	0.06	2.26	NA	NA	NA	NA	9.20	5.29	NA	1.31	2.76	2.38	2.45
u1yIn	NA	1.91	NA	13.96	1.73	NA	1.86	3.81	NA	NA	1.59	1.44	3.71	0.40	0.39	NA	NA	NA	NA	0.13	1.18	NA	2.81	8.05	1.54	2.97
u2xIn	NA	1.35	NA	1.29	1.80	NA	1.62	2.95	NA	NA	1.44	2.81	1.48	3.54	1.23	NA	NA	NA	NA	6.75	3.71	NA	3.10	0.52	0.12	2.25
u2yIn	NA	0.43	NA	13.62	1.27	NA	2.81	2.38	NA	NA	1.88	1.34	2.04	0.40	1.55	NA	NA	NA	NA	0.79	1.18	NA	4.40	5.89	0.87	2.72
u3xIn	NA	0.07	NA	1.29	4.36	NA	4.22	1.73	NA	NA	0.48	3.47	0.31	0.39	0.74	NA	NA	NA	NA	9.54	3.79	NA	1.02	2.60	0.38	2.29
u3yIn	NA	1.24	NA	11.96	1.06	NA	1.60	2.75	NA	NA	1.88	1.10	3.38	1.27	0.39	NA	NA	NA	NA	0.46	1.18	NA	1.47	7.05	1.87	2.58
e2xIn	NA	0.48	NA	5.10	0.35	NA	0.77	0.83	NA	NA	0.40	2.14	6.44	1.06	2.24	NA	NA	NA	NA	8.37	4.21	NA	0.52	7.10	2.70	2.85
e2yIn	NA	2.24	NA	15.57	0.23	NA	2.24	0.14	NA	NA	1.88	1.10	0.98	3.93	1.89	NA	NA	NA	NA	1.46	1.85	NA	0.53	12.43	2.62	3.27
d3xIn	NA	0.07	NA	1.29	4.36	NA	4.22	1.73	NA	NA	0.48	3.47	0.31	0.39	0.74	NA	NA	NA	NA	9.54	3.79	NA	1.02	2.60	0.38	2.29
d3yIn	NA	1.24	NA	11.96	1.06	NA	1.60	2.75	NA	NA	1.88	1.10	3.38	1.27	0.39	NA	NA	NA	NA	0.46	1.18	NA	1.47	7.05	1.87	2.58
d2xIn	NA	1.35	NA	1.29	1.80	NA	1.62	2.95	NA	NA	1.44	2.81	1.48	3.54	1.23	NA	NA	NA	NA	6.75	3.71	NA	3.10	0.52	0.12	2.25
d2yIn	NA	0.43	NA	13.62	1.27	NA	2.81	2.38	NA	NA	1.88	1.34	2.04	0.40	1.55	NA	NA	NA	NA	0.79	1.18	NA	4.40	5.89	0.87	2.72
d1xIn	NA	2.10	NA	1.95	0.53	NA	0.48	2.04	NA	NA	4.97	0.14	1.31	0.06	2.26	NA	NA	NA	NA	9.20	5.29	NA	1.31	2.76	2.38	2.45
d1yIn	NA	1.91	NA	13.96	1.73	NA	1.86	3.81	NA	NA	1.59	1.44	3.71	0.40	0.39	NA	NA	NA	NA	0.13	1.18	NA	2.81	8.05	1.54	2.97
Average	NA	1.22	NA	8.39	1.46	NA	1.81	1.93	NA	NA	2.06	1.39	1.97	1.45	1.28	NA	NA	NA	NA	4.75	2.74	NA	1.77	6.26	1.34	

Figure F.5: ORL polygonal mouth-closed template test results

Percentage (of width) Diff																									
% Param	s101	s105	s111	s116	s121	s1210	s155	s162	s221	s225	s231	s294	s306	s309	s39	s405	s510	s52	s71	s78	s85	s88	s94	s98	Average
c1xOut	NA	0.61	NA	18.45	5.17	NA	3.30	9.91	NA	NA	10.00	6.29	10.50	3.78	5.96	NA	NA	NA	37.78	19.31	NA	8.02	3.02	3.13	9.68
c1yOut	NA	1.88	NA	51.39	7.36	NA	13.07	6.94	NA	NA	12.46	7.59	8.16	2.15	8.55	NA	NA	NA	162	176	NA	0.39	66.65	4.45	12.96
u1xOut	NA	6.31	NA	3.76	4.27	NA	1.77	3.85	NA	NA	20.59	2.01	5.74	2.59	9.43	NA	NA	NA	28.95	17.89	NA	5.48	9.64	5.39	8.51
u1yOut	NA	0.93	NA	59.04	5.14	NA	4.77	5.48	NA	NA	1.42	1.70	0.73	0.23	1.86	NA	NA	NA	2.50	2.72	NA	1.20	36.23	0.99	8.33
u2xOut	NA	2.44	NA	7.70	6.44	NA	3.81	8.46	NA	NA	8.41	9.20	6.32	13.82	3.73	NA	NA	NA	26.17	18.24	NA	2.56	0.65	5.95	8.26
u2yOut	NA	2.12	NA	53.78	2.75	NA	2.36	6.33	NA	NA	0.43	0.69	1.89	3.82	7.17	NA	NA	NA	1.02	2.72	NA	7.46	27.51	2.10	8.14
u3xOut	NA	0.24	NA	10.34	7.25	NA	2.03	2.71	NA	NA	5.24	5.13	4.58	6.16	3.88	NA	NA	NA	32.48	17.20	NA	3.26	10.22	0.16	7.39
u3yOut	NA	3.31	NA	59.04	6.33	NA	8.19	2.79	NA	NA	0.43	3.12	0.73	3.34	0.47	NA	NA	NA	3.67	2.72	NA	5.64	33.91	0.99	8.98
c2xOut	NA	1.73	NA	20.12	1.23	NA	2.80	3.08	NA	NA	1.36	9.15	22.46	3.78	9.35	NA	NA	NA	29.54	17.54	NA	1.74	24.75	8.98	10.51
c2yOut	NA	8.00	NA	61.46	0.81	NA	8.19	0.51	NA	NA	6.47	4.73	3.42	14.05	7.90	NA	NA	NA	5.15	7.70	NA	1.75	43.36	8.73	12.15
d3xOut	NA	6.19	NA	3.76	10.82	NA	8.13	6.41	NA	NA	2.80	2.01	3.42	7.35	2.49	NA	NA	NA	34.84	18.58	NA	1.19	14.87	3.50	8.42
d3yOut	NA	7.40	NA	64.30	0.38	NA	4.01	4.02	NA	NA	8.76	1.70	4.22	0.23	1.86	NA	NA	NA	2.50	9.78	NA	4.36	30.42	4.32	9.88
d2xOut	NA	4.82	NA	9.02	4.06	NA	4.72	9.69	NA	NA	1.51	13.48	6.32	19.78	0.95	NA	NA	NA	30.88	16.85	NA	11.45	0.51	4.84	9.26
d2yOut	NA	7.40	NA	86.93	4.40	NA	9.67	0.16	NA	NA	7.61	2.12	0.73	9.28	5.78	NA	NA	NA	2.51	8.39	NA	14.12	29.83	5.43	11.62
d1xOut	NA	13.45	NA	6.39	9.04	NA	5.43	13.73	NA	NA	14.84	4.87	6.90	2.59	10.82	NA	NA	NA	30.13	13.72	NA	4.52	8.47	4.28	9.95
d1yOut	NA	9.78	NA	65.62	0.38	NA	9.86	7.95	NA	NA	10.08	1.16	4.22	6.19	4.64	NA	NA	NA	2.50	8.39	NA	9.91	33.91	6.95	12.07
c1xIn	NA	0.61	NA	18.45	5.17	NA	3.30	9.91	NA	NA	10.00	6.29	10.50	3.78	5.96	NA	NA	NA	37.78	19.31	NA	8.02	3.02	3.13	9.68
c1yIn	NA	1.88	NA	51.39	7.36	NA	13.07	6.94	NA	NA	12.46	7.59	8.16	2.15	8.55	NA	NA	NA	162	176	NA	0.39	66.65	4.45	12.96
u1xIn	NA	7.50	NA	7.70	1.89	NA	1.77	7.56	NA	NA	17.14	0.58	4.58	0.21	9.43	NA	NA	NA	32.48	22.06	NA	4.37	9.64	7.94	8.99
u1yIn	NA	6.81	NA	55.09	6.17	NA	6.81	14.12	NA	NA	5.48	6.16	12.94	1.43	1.61	NA	NA	NA	0.45	4.92	NA	9.36	28.09	5.12	10.97
u2xIn	NA	4.82	NA	5.07	6.44	NA	5.94	10.93	NA	NA	4.96	12.05	5.16	12.63	5.12	NA	NA	NA	23.82	15.46	NA	10.34	1.81	0.39	8.33
u2yIn	NA	1.53	NA	53.78	4.53	NA	10.28	8.80	NA	NA	6.47	5.74	7.12	1.44	6.48	NA	NA	NA	2.78	4.92	NA	14.68	20.53	2.90	10.13
u3xIn	NA	0.24	NA	5.07	15.58	NA	15.45	6.41	NA	NA	1.65	14.87	1.09	1.40	3.07	NA	NA	NA	33.66	15.81	NA	3.41	9.05	1.28	8.54
u3yIn	NA	4.43	NA	47.20	3.79	NA	5.84	10.19	NA	NA	6.47	4.73	11.77	4.53	1.61	NA	NA	NA	162	4.92	NA	4.91	24.61	6.23	9.52
c2xIn	NA	1.73	NA	20.12	1.23	NA	2.80	3.08	NA	NA	1.36	9.15	22.46	3.78	9.35	NA	NA	NA	29.54	17.54	NA	1.74	24.75	8.98	10.51
c2yIn	NA	8.00	NA	61.46	0.81	NA	8.19	0.51	NA	NA	6.47	4.73	3.42	14.05	7.90	NA	NA	NA	5.15	7.70	NA	1.75	43.36	8.73	12.15
d3xIn	NA	0.24	NA	5.07	15.58	NA	15.45	6.41	NA	NA	1.65	14.87	1.09	1.40	3.07	NA	NA	NA	33.66	15.81	NA	3.41	9.05	1.28	8.54
d3yIn	NA	4.43	NA	47.20	3.79	NA	5.84	10.19	NA	NA	6.47	4.73	11.77	4.53	1.61	NA	NA	NA	162	4.92	NA	4.91	24.61	6.23	9.52
d2xIn	NA	4.82	NA	5.07	6.44	NA	5.94	10.93	NA	NA	4.96	12.05	5.16	12.63	5.12	NA	NA	NA	23.82	15.46	NA	10.34	1.81	0.39	8.33
d2yIn	NA	1.53	NA	53.78	4.53	NA	10.28	8.80	NA	NA	6.47	5.74	7.12	1.44	6.48	NA	NA	NA	2.78	4.92	NA	14.68	20.53	2.90	10.13
d1xIn	NA	7.50	NA	7.70	1.89	NA	1.77	7.56	NA	NA	17.14	0.58	4.58	0.21	9.43	NA	NA	NA	32.48	22.06	NA	4.37	9.64	7.94	8.99
d1yIn	NA	6.81	NA	55.09	6.17	NA	6.81	14.12	NA	NA	5.48	6.16	12.94	1.43	1.61	NA	NA	NA	0.45	4.92	NA	9.36	28.09	5.12	10.97
Average	NA	4.36	NA	33.14	5.22	NA	6.61	7.14	NA	NA	7.09	5.97	6.88	5.19	5.35	NA	NA	NA	16.75	11.44	NA	5.91	21.85	4.46	

Figure F.6: ORL polygonal mouth-closed template test results (%)

APPENDIX G

Spline-based Mouth-Closed Template Detailed Test Results

Absolute Difference Pixel Values																					
%ParamName	K.A.DI	K.A.HI	K.A.SA	K.A.SU	KL.AN	KL.FE	KM.DI	KM.SA	KR.AN	MK.SA	NA.AN	NA.HI	NA.SU	NM.DI	TM.FE	TM.SA	UY.AN	UY.DI	YM.DI	YM.HI	Average
c1kOut	0.41	NA	2.54	0.16	1.44	1.62	NA	0.18	1.83	2.33	3.56	NA	NA	1.50	NA	0.47	2.63	4.09	0.03	NA	1.63
c1jOut	3.43	NA	1.38	2.56	2.03	0.92	NA	1.47	0.03	2.50	0.35	NA	NA	1.72	NA	2.01	1.07	1.38	1.44	NA	1.59
u1kOut	8.37	NA	0.99	0.00	1.60	5.39	NA	0.18	0.34	0.67	2.19	NA	NA	0.57	NA	1.32	0.05	3.50	6.89	NA	2.29
u1jOut	0.17	NA	1.75	1.67	2.14	0.68	NA	0.31	1.30	1.33	0.24	NA	NA	1.85	NA	0.35	0.04	0.12	2.14	NA	1.01
u2kOut	4.28	NA	0.42	2.05	3.10	0.78	NA	1.85	4.66	1.07	0.17	NA	NA	2.70	NA	4.15	5.77	3.92	3.36	NA	2.73
u2jOut	1.28	NA	1.10	1.20	0.47	1.06	NA	0.31	0.99	0.97	4.11	NA	NA	3.32	NA	3.71	1.02	2.54	0.51	NA	1.61
u3kOut	1.38	NA	2.08	4.33	1.68	6.31	NA	2.51	1.33	3.00	1.97	NA	NA	0.90	NA	0.87	1.55	1.00	2.93	NA	2.28
u3jOut	1.51	NA	2.77	3.67	2.21	1.18	NA	0.36	1.64	3.00	0.43	NA	NA	1.85	NA	0.33	0.04	1.21	1.43	NA	1.54
c2kOut	2.90	NA	3.04	3.00	0.77	0.18	NA	0.15	2.17	1.33	3.90	NA	NA	3.27	NA	2.05	0.97	2.58	0.25	NA	1.90
c2jOut	0.40	NA	2.39	3.00	0.03	0.21	NA	2.14	0.36	0.50	0.58	NA	NA	2.32	NA	0.15	1.05	2.04	1.40	NA	1.18
d3kOut	0.72	NA	0.75	5.00	0.98	2.97	NA	0.85	0.34	1.00	3.31	NA	NA	1.77	NA	0.47	4.21	0.33	4.26	NA	1.92
d3jOut	3.83	NA	5.90	5.33	3.46	1.49	NA	3.64	3.70	0.33	0.90	NA	NA	0.52	NA	4.00	0.29	1.54	2.90	NA	2.70
d2kOut	3.28	NA	0.75	1.72	3.10	0.45	NA	1.18	5.33	1.40	0.17	NA	NA	3.37	NA	4.49	4.77	1.25	3.36	NA	2.47
d2jOut	0.61	NA	2.57	2.87	2.53	1.39	NA	2.97	0.34	0.03	2.78	NA	NA	1.02	NA	0.38	1.64	0.88	3.49	NA	1.68
d1kOut	7.71	NA	1.99	1.00	1.27	5.39	NA	0.85	0.67	2.00	1.19	NA	NA	3.57	NA	0.32	1.62	2.50	9.89	NA	2.86
d1jOut	4.51	NA	5.58	5.67	3.19	2.01	NA	4.31	4.03	0.33	1.57	NA	NA	0.85	NA	2.35	0.38	1.54	2.19	NA	2.75
c1kIn	0.41	NA	2.54	0.16	1.44	1.62	NA	0.18	1.83	2.33	3.56	NA	NA	1.50	NA	0.47	2.63	4.09	0.03	NA	1.63
c1jIn	3.43	NA	1.38	2.56	2.03	0.92	NA	1.47	0.03	2.50	0.35	NA	NA	1.72	NA	2.01	1.07	1.38	1.44	NA	1.59
u1kIn	9.71	NA	2.66	1.00	0.94	5.06	NA	0.15	2.66	0.00	3.19	NA	NA	0.77	NA	1.99	1.29	4.84	7.55	NA	2.99
u1jIn	4.01	NA	4.08	3.00	2.69	3.68	NA	4.81	2.70	0.50	2.07	NA	NA	3.32	NA	4.02	2.79	3.38	4.31	NA	3.24
u2kIn	3.28	NA	1.08	2.39	2.44	1.78	NA	1.18	5.33	1.74	0.84	NA	NA	5.03	NA	3.49	5.77	2.59	4.36	NA	2.95
u2jIn	1.22	NA	3.07	6.20	3.03	3.06	NA	2.81	2.33	0.86	4.61	NA	NA	2.82	NA	3.38	0.86	3.71	2.34	NA	2.88
u3kIn	3.28	NA	3.25	0.67	0.35	0.36	NA	0.51	3.01	3.00	3.97	NA	NA	2.43	NA	2.13	3.88	1.33	2.59	NA	2.20
u3jIn	2.99	NA	3.40	3.33	3.63	2.15	NA	4.47	3.36	0.50	2.07	NA	NA	3.32	NA	3.66	3.12	4.04	2.60	NA	3.05
c2kIn	2.90	NA	3.04	3.00	0.77	0.18	NA	0.15	2.17	1.33	3.90	NA	NA	3.27	NA	2.05	0.97	2.58	0.25	NA	1.90
c2jIn	0.40	NA	2.39	3.00	0.03	0.21	NA	2.14	0.36	0.50	0.58	NA	NA	2.32	NA	0.15	1.05	2.04	1.40	NA	1.18
d3kIn	3.28	NA	3.25	0.67	0.35	0.36	NA	0.51	3.01	3.00	3.97	NA	NA	2.43	NA	2.13	3.88	1.33	2.59	NA	2.20
d3jIn	2.99	NA	3.40	3.33	3.63	2.15	NA	4.47	3.36	0.50	2.07	NA	NA	3.32	NA	3.66	3.12	4.04	2.60	NA	3.05
d2kIn	3.28	NA	1.08	2.39	2.44	1.78	NA	1.18	5.33	1.74	0.84	NA	NA	5.03	NA	3.49	5.77	2.59	4.36	NA	2.95
d2jIn	1.22	NA	3.07	6.20	3.03	3.06	NA	2.81	2.33	0.86	4.61	NA	NA	2.82	NA	3.38	0.86	3.71	2.34	NA	2.88
d1kIn	9.71	NA	2.66	1.00	0.94	5.06	NA	0.15	2.66	0.00	3.19	NA	NA	0.77	NA	1.99	1.29	4.84	7.55	NA	2.99
d1jIn	4.01	NA	4.08	3.00	2.69	3.68	NA	4.81	2.70	0.50	2.07	NA	NA	3.32	NA	4.02	2.79	3.38	4.31	NA	3.24
Average	2.26	NA	1.75	2.42	1.50	1.94	NA	0.94	1.36	1.61	1.89	NA	NA	1.98	NA	1.44	1.67	2.07	2.24	NA	NA

Figure G.1: JAFFE spline-based mouth-closed template test results

Percentage (of width) Diff																					
%ParamName	KADiff	KAHA	KASA	KASU	KLAN	KLFE	KMDI	KMSA	KRAN	MKSA	NAAR	NAHA	NASU	NMDI	TMFE	TMSA	UYAN	UYDI	YMDI	YMH4	Average
c1kOut	0.90	NA	5.82	0.39	3.47	3.79	NA	0.45	3.97	4.83	7.68	NA	NA	3.13	NA	1.02	6.16	9.66	0.05	NA	3.67
c1jOut	7.58	NA	3.16	6.00	4.90	2.16	NA	3.71	0.06	5.17	0.75	NA	NA	3.58	NA	4.34	2.50	3.25	3.00	NA	3.58
u1kOut	18.47	NA	2.27	0.00	3.88	12.64	NA	0.45	0.74	1.38	4.73	NA	NA	1.18	NA	2.86	0.11	8.28	14.35	NA	5.09
u1jOut	0.38	NA	4.02	3.91	5.18	1.58	NA	0.77	2.84	2.76	0.51	NA	NA	3.86	NA	0.76	0.10	0.30	4.46	NA	2.24
u2kOut	9.45	NA	0.96	4.82	7.51	1.84	NA	4.66	10.13	2.21	0.37	NA	NA	5.63	NA	8.96	13.52	9.26	7.00	NA	6.16
u2jOut	2.82	NA	2.52	2.82	1.14	2.49	NA	0.77	2.16	2.02	8.87	NA	NA	6.91	NA	8.00	2.40	6.00	1.06	NA	3.57
u3kOut	3.05	NA	4.77	10.16	4.07	14.78	NA	6.34	2.89	6.21	4.26	NA	NA	1.88	NA	1.87	3.82	2.37	6.10	NA	5.17
u3jOut	3.33	NA	6.33	8.59	5.34	2.77	NA	0.91	3.56	6.21	0.93	NA	NA	3.86	NA	0.72	0.10	2.85	2.98	NA	3.46
c2kOut	6.40	NA	6.95	7.03	1.86	0.42	NA	0.39	4.72	2.76	8.43	NA	NA	6.80	NA	4.42	2.28	6.09	0.52	NA	4.22
c2jOut	0.89	NA	5.48	7.03	0.07	0.49	NA	5.40	0.79	1.03	1.25	NA	NA	4.82	NA	0.32	2.45	4.82	2.91	NA	2.70
d3kOut	1.58	NA	1.72	11.72	2.38	6.97	NA	2.13	0.74	2.07	7.14	NA	NA	3.68	NA	1.00	9.87	0.78	8.87	NA	4.33
d3jOut	8.44	NA	13.51	12.50	8.37	3.48	NA	9.18	8.03	0.69	1.95	NA	NA	1.08	NA	8.63	0.68	3.64	6.05	NA	6.16
d2kOut	7.24	NA	1.72	4.03	7.51	1.06	NA	2.98	11.58	2.90	0.37	NA	NA	7.02	NA	9.68	11.17	2.96	7.00	NA	5.52
d2jOut	1.35	NA	5.88	6.73	6.11	3.27	NA	7.50	0.74	0.05	5.99	NA	NA	2.12	NA	0.81	3.85	2.07	7.27	NA	3.84
d1kOut	17.00	NA	4.56	2.34	3.07	12.64	NA	2.13	1.46	4.14	2.57	NA	NA	7.43	NA	0.70	3.80	5.32	20.60	NA	6.31
d1jOut	9.94	NA	12.78	13.28	7.73	4.71	NA	10.86	8.76	0.69	3.39	NA	NA	1.77	NA	5.08	0.89	3.64	4.56	NA	6.29
c1kIn	0.90	NA	5.82	0.39	3.47	3.79	NA	0.45	3.97	4.83	7.68	NA	NA	3.13	NA	1.02	6.16	9.66	0.05	NA	3.67
c1jIn	7.58	NA	3.16	6.00	4.90	2.16	NA	3.71	0.06	5.17	0.75	NA	NA	3.58	NA	4.34	2.50	3.25	3.00	NA	3.58
u1kIn	21.41	NA	6.08	2.34	2.26	11.86	NA	0.39	5.79	0.00	6.89	NA	NA	1.60	NA	4.29	3.02	11.43	15.74	NA	6.65
u1jIn	8.84	NA	9.34	7.03	6.52	8.61	NA	12.12	5.86	1.03	4.47	NA	NA	6.91	NA	8.68	6.54	7.97	8.98	NA	7.35
u2kIn	7.24	NA	2.48	5.60	5.89	4.18	NA	2.98	11.58	3.59	1.80	NA	NA	10.49	NA	7.52	13.52	6.11	9.08	NA	6.58
u2jIn	2.69	NA	7.03	14.54	7.32	7.17	NA	7.08	5.06	1.78	9.95	NA	NA	5.87	NA	7.28	2.00	8.76	4.88	NA	6.53
u3kIn	7.24	NA	7.44	1.56	0.85	0.85	NA	1.29	6.53	6.21	8.58	NA	NA	5.07	NA	4.60	9.09	3.14	5.40	NA	4.85
u3jIn	6.60	NA	7.79	7.81	8.78	5.04	NA	11.28	7.31	1.03	4.47	NA	NA	6.91	NA	7.91	7.32	9.55	5.41	NA	6.94
c2kIn	6.40	NA	6.95	7.03	1.86	0.42	NA	0.39	4.72	2.76	8.43	NA	NA	6.80	NA	4.42	2.28	6.09	0.52	NA	4.22
c2jIn	0.89	NA	5.48	7.03	0.07	0.49	NA	5.40	0.79	1.03	1.25	NA	NA	4.82	NA	0.32	2.45	4.82	2.91	NA	2.70
d3kIn	7.24	NA	7.44	1.56	0.85	0.85	NA	1.29	6.53	6.21	8.58	NA	NA	5.07	NA	4.60	9.09	3.14	5.40	NA	4.85
d3jIn	6.60	NA	7.79	7.81	8.78	5.04	NA	11.28	7.31	1.03	4.47	NA	NA	6.91	NA	7.91	7.32	9.55	5.41	NA	6.94
d2kIn	7.24	NA	2.48	5.60	5.89	4.18	NA	2.98	11.58	3.59	1.80	NA	NA	10.49	NA	7.52	13.52	6.11	9.08	NA	6.58
d2jIn	2.69	NA	7.03	14.54	7.32	7.17	NA	7.08	5.06	1.78	9.95	NA	NA	5.87	NA	7.28	2.00	8.76	4.88	NA	6.53
d1kIn	21.41	NA	6.08	2.34	2.26	11.86	NA	0.39	5.79	0.00	6.89	NA	NA	1.60	NA	4.29	3.02	11.43	15.74	NA	6.65
d1jIn	8.84	NA	9.34	7.03	6.52	8.61	NA	12.12	5.86	1.03	4.47	NA	NA	6.91	NA	8.68	6.54	7.97	8.98	NA	6.73
Average	4.99	NA	4.00	5.68	3.62	4.54	NA	2.36	2.96	3.33	4.08	NA	NA	4.12	NA	3.12	3.92	4.88	4.66	NA	

Figure G.2: JAFFE spline-based mouth-closed template test results(%)

Percentage (of width) Diff																				
	% Param	lflight	l2.sad	brml	brml	brml	brml	brml	brml	brml	brml	brml	brml	brml	brml	brml	brml	brml	brml	brml
c1kOut	157	27.15	0.23	0.81	5.86	2.67	8.65	2.10	5.72	50.19	38.65	33.93	24.59	1.75	25.76	12.28	8.16	N/A	7.50	N/A
c1yOut	102	4.43	4.76	3.72	6.55	5.61	11.70	4.88	6.68	22.15	23.42	0.45	28.69	5.24	20.58	18.81	4.12	N/A	2.90	N/A
u1kOut	0.74	30.36	11.43	6.77	9.66	7.93	2.95	2.44	4.82	43.48	38.17	27.68	18.85	4.02	11.89	5.86	5.64	N/A	13.73	N/A
u1yOut	2.70	0.30	5.51	0.95	4.14	3.41	1.17	4.37	1.05	1.56	0.61	0.89	5.74	0.70	21.01	20.58	1.41	N/A	7.27	N/A
u2kOut	7.77	31.74	14.81	8.11	10.3	18.84	7.55	0.64	8.14	28.66	16.81	27.68	22.13	5.22	6.46	17.15	5.45	N/A	9.07	N/A
u2yOut	4.74	3.05	7.01	0.19	0.69	6.55	1.04	0.94	15.20	20.15	3.52	37.50	4.10	2.87	23.77	13.50	3.73	N/A	5.58	N/A
u3kOut	5.39	36.78	27.26	4.87	10.84	1.84	9.94	0.39	6.00	45.55	38.17	17.05	29.51	3.67	4.90	21.35	3.71	N/A	11.91	N/A
u3yOut	2.70	2.45	4.04	0.57	4.12	1.16	1.04	0.94	3.08	1.56	2.55	1.99	0.82	0.70	26.66	18.81	0.15	N/A	5.68	N/A
c2kOut	0.96	73.02	23.08	14.03	9.31	14.06	3.50	0.47	3.37	32.66	27.97	30.36	26.23	8.74	5.04	11.17	5.28	N/A	3.95	N/A
c2yOut	4.74	47.55	2.50	3.63	3.79	6.04	16.11	6.98	3.04	3.08	6.43	0.45	3.28	1.05	20.30	25.22	2.70	N/A	6.55	N/A
d3kOut	0.06	34.03	22.00	11.74	8.77	7.10	13.61	3.81	18.73	41.42	33.31	18.84	19.67	5.77	1.04	6.31	8.36	N/A	10.39	N/A
d3yOut	7.46	2.14	4.23	10.88	1.40	1.16	7.66	5.91	4.19	10.84	2.31	0.69	9.84	4.20	28.87	21.46	8.38	N/A	3.30	N/A
d2kOut	3.00	28.07	10.30	8.87	3.10	16.58	6.81	4.15	9.96	23.51	10.01	32.14	22.13	7.32	3.69	11.84	9.33	N/A	9.07	N/A
d2yOut	7.46	2.14	7.27	7.82	4.83	3.54	3.98	1.11	18.84	0.56	18.08	49.11	16.39	5.52	22.12	21.46	0.63	N/A	0.49	N/A
d1kOut	2.66	34.03	6.16	12.12	6.21	5.68	7.36	3.13	0.27	32.14	29.43	31.25	22.13	2.62	14.10	9.40	8.75	N/A	15.24	N/A
d1yOut	8.82	5.81	5.77	17.75	4.83	0.35	10.60	5.22	5.31	6.72	2.31	3.57	13.93	2.10	21.56	21.46	5.28	N/A	2.72	N/A
c1kIn	157	27.15	0.23	0.81	5.86	2.67	8.65	2.10	5.72	50.19	38.65	33.93	24.59	1.75	25.76	12.28	8.16	N/A	7.50	N/A
c1yIn	102	4.43	4.76	3.72	6.55	5.61	11.70	4.88	6.68	22.15	23.42	0.45	28.69	5.24	20.58	18.81	4.12	N/A	2.90	N/A
u1kIn	2.66	33.11	8.42	6.77	1.38	1.17	9.57	0.30	3.00	46.58	39.14	25.00	22.13	0.52	11.34	11.17	5.64	N/A	16.00	N/A
u1yIn	5.42	6.26	4.76	18.89	1.03	3.35	7.29	4.88	2.13	2.05	5.46	4.91	0.00	0.35	24.60	14.38	4.89	N/A	9.16	N/A
u2kIn	3.68	32.65	8.04	8.11	6.55	12.82	9.02	4.15	13.59	23.51	12.92	30.36	20.49	8.02	2.59	7.41	6.23	N/A	7.55	N/A
u2yIn	4.06	6.26	3.25	8.97	1.03	11.81	6.55	5.57	17.47	17.57	2.55	36.16	0.00	0.27	26.81	14.38	5.67	N/A	8.23	N/A
u3kIn	0.74	34.03	20.50	10.97	2.95	10.11	10.67	7.23	16.91	37.30	31.37	23.30	18.03	9.97	0.62	3.65	9.91	N/A	6.61	N/A
u3yIn	4.74	5.35	2.54	13.55	1.06	5.61	10.23	6.25	1.01	4.11	8.37	9.58	2.46	3.15	31.35	12.61	5.67	N/A	8.23	N/A
c2kIn	0.96	73.02	23.08	14.03	9.31	14.06	3.50	0.47	3.37	32.66	27.97	30.36	26.23	8.74	5.04	11.17	5.28	N/A	3.95	N/A
c2yIn	4.74	47.55	2.50	3.63	3.79	6.04	16.11	6.98	3.04	3.08	6.43	0.45	3.28	1.05	20.30	25.22	2.70	N/A	6.55	N/A
d3kIn	0.74	34.03	20.50	10.97	2.95	10.11	10.67	7.23	16.91	37.30	31.37	23.30	18.03	9.97	0.62	3.65	9.91	N/A	6.61	N/A
d3yIn	4.74	5.35	2.54	13.55	1.06	5.61	10.23	6.25	1.01	4.11	8.37	9.58	2.46	3.15	31.35	12.61	5.67	N/A	8.23	N/A
d2kIn	3.68	32.65	8.04	8.11	6.55	12.82	9.02	4.15	13.59	23.51	12.92	30.36	20.49	8.02	2.59	7.41	6.23	N/A	7.55	N/A
d2yIn	4.06	6.26	3.25	8.97	1.03	11.81	6.55	5.57	17.47	17.57	2.55	36.16	0.00	0.27	26.81	14.38	5.67	N/A	8.23	N/A
d1kIn	2.66	33.11	8.42	6.77	1.38	1.17	9.57	0.30	3.00	46.58	39.14	25.00	22.13	0.52	11.34	11.17	5.64	N/A	16.00	N/A
d1yIn	5.42	6.26	4.76	18.89	1.03	3.35	7.29	4.88	2.13	2.05	5.46	4.91	0.00	0.35	24.60	14.38	4.89	N/A	9.16	N/A
Average	3.52	23.45	8.81	8.42	4.33	6.90	8.13	3.71	7.54	22.95	18.37	19.92	14.91	3.84	16.38	14.10	5.54	N/A	7.74	N/A

Percentage (of width) Diff																			
% Param	flight	b2.sad	brml	brml	brml	asses	brml	6.sad	rflight	asses	brml	leepg	wink	rflight	2.sad	subje	subje	subje	Average
c1kOut	157	27.15	0.23	0.81	5.86	2.67	8.65	2.10	5.72	50.19	38.65	33.93	24.59	1.75	25.76	12.28	8.16	NA	14.31
c1yOut	102	4.43	4.76	3.72	6.55	5.61	11.70	4.88	6.68	22.15	23.42	0.45	28.69	5.24	20.58	18.81	4.12	NA	9.76
u1kOut	0.74	30.36	11.43	6.77	9.66	7.93	2.95	2.44	4.82	43.48	38.17	27.68	18.85	4.02	11.89	5.86	5.64	NA	13.69
u1yOut	2.70	0.30	5.51	0.95	4.14	3.41	1.17	4.37	1.05	1.56	0.61	0.89	5.74	0.70	21.01	20.58	1.41	NA	4.63
u2kOut	7.77	31.74	14.81	8.11	10.3	18.84	7.55	0.64	8.14	28.66	16.81	27.68	22.13	5.22	6.46	17.15	5.45	NA	13.18
u2yOut	4.74	3.05	7.01	0.19	0.69	6.55	1.04	0.94	15.20	20.15	3.52	37.50	4.10	2.87	23.77	13.50	3.73	NA	8.56
u3kOut	5.39	36.78	27.26	4.87	10.84	1.84	9.94	0.39	6.00	45.55	38.17	17.05	29.51	3.67	4.90	21.35	3.71	NA	15.51
u3yOut	2.70	2.45	4.04	0.57	4.12	1.16	1.04	0.94	3.08	1.56	2.55	1.99	0.82	0.70	26.66	18.81	0.15	NA	4.38
c2kOut	0.96	73.02	23.08	14.03	9.31	14.06	3.50	0.47	3.37	32.66	27.97	30.36	26.23	8.74	5.04	21.22	5.28	NA	16.29
c2yOut	4.74	47.55	2.50	3.63	3.79	6.04	16.11	6.98	3.04	3.08	6.43	0.45	3.28	1.05	20.30	25.22	2.70	NA	9.08
d3kOut	0.06	34.03	22.00	11.74	8.77	7.10	13.61	3.81	18.73	41.42	33.31	18.84	19.67	5.77	1.04	6.31	8.36	NA	14.72
d3yOut	7.46	2.14	4.23	10.88	1.40	1.16	7.66	5.91	4.19	10.84	2.31	0.69	9.84	4.20	28.87	21.46	8.38	NA	7.49
d2kOut	3.00	28.07	10.30	8.87	3.10	16.58	6.81	4.15	9.96	23.51	10.01	32.14	22.13	7.32	3.69	11.84	9.33	NA	12.22
d2yOut	7.46	2.14	7.27	7.82	4.83	3.54	3.98	1.11	18.84	0.56	18.08	49.11	16.39	5.52	22.12	21.46	0.63	NA	10.63
d1kOut	2.66	34.03	6.16	12.12	6.21	5.68	7.36	3.13	0.27	32.14	29.43	31.25	22.13	2.62	14.10	9.40	8.75	NA	13.48
d1yOut	8.82	5.81	5.77	17.75	4.83	0.35	10.60	5.22	5.31	6.72	2.31	3.57	13.93	2.10	21.56	12.46	5.28	NA	8.01
c1kIn	157	27.15	0.23	0.81	5.86	2.67	8.65	2.10	5.72	50.19	38.65	33.93	24.59	1.75	25.76	12.28	8.16	NA	14.31
c1yIn	102	4.43	4.76	3.72	6.55	5.61	11.70	4.88	6.68	22.15	23.42	0.45	28.69	5.24	20.58	18.81	4.12	NA	9.76
u1kIn	2.68	33.11	8.42	6.77	1.38	1.17	9.57	0.30	3.00	46.58	39.14	25.00	22.13	0.52	11.34	11.17	5.64	NA	13.55
u1yIn	5.42	6.26	4.76	18.89	103	3.35	7.29	4.88	2.13	2.05	5.46	4.91	0.00	0.35	24.60	14.38	4.89	NA	6.66
u2kIn	3.68	32.65	8.04	8.11	6.55	12.82	9.02	4.15	13.59	23.51	12.92	30.36	20.49	8.02	2.59	7.41	6.23	NA	12.09
u2yIn	4.06	6.26	3.25	8.97	1.03	11.81	6.55	5.57	17.47	17.57	2.55	36.16	0.00	0.27	26.81	14.38	5.67	NA	9.81
u3kIn	0.74	34.03	20.50	10.97	2.95	10.11	10.67	7.23	16.91	37.30	31.37	23.30	18.03	9.97	0.62	3.65	9.91	NA	14.16
u3yIn	4.74	5.35	2.54	13.55	106	5.61	10.23	6.25	1.01	4.11	8.37	9.58	2.46	3.15	31.35	12.61	5.67	NA	7.55
c2kIn	0.96	73.02	23.08	14.03	9.31	14.06	3.50	0.47	3.37	32.66	27.97	30.36	26.23	8.74	5.04	11.17	5.28	NA	16.29
c2yIn	4.74	47.55	2.50	3.63	3.79	6.04	16.11	6.98	3.04	3.08	6.43	0.45	3.28	1.05	20.30	25.22	2.70	NA	9.08
d3kIn	0.74	34.03	20.50	10.97	2.95	10.11	10.67	7.23	16.91	37.30	31.37	23.30	18.03	9.97	0.62	3.65	9.91	NA	14.16
d3yIn	4.74	5.35	2.54	13.55	106	5.61	10.23	6.25	1.01	4.11	8.37	9.58	2.46	3.15	31.35	12.61	5.67	NA	7.55
d2kIn	3.68	32.65	8.04	8.11	6.55	12.82	9.02	4.15	13.59	23.51	12.92	30.36	20.49	8.02	2.59	7.41	6.23	NA	12.09
d2yIn	4.06	6.26	3.25	8.97	1.03	11.81	6.55	5.57	17.47	17.57	2.55	36.16	0.00	0.27	26.81	14.38	5.67	NA	9.81
d1kIn	2.66	34.03	6.16	12.12	6.21	5.68	7.36	3.13	0.27	32.14	29.43	31.25	22.13	2.62	14.10	9.40	8.75	NA	13.48
d1yIn	8.82	5.81	5.77	17.75	4.83	0.35	10.60	5.22	5.31	6.72	2.31	3.57	13.93	2.10	21.56	12.46	5.28	NA	8.01
c1kIn	157	27.15	0.23	0.81	5.86	2.67	8.65	2.10	5.72	50.19	38.65	33.93	24.59	1.75	25.76	12.28	8.16	NA	14.31
c1yIn	102	4.43	4.76	3.72	6.55	5.61	11.70	4.88	6.68	22.15	23.42	0.45	28.69	5.24	20.58	18.81	4.12	NA	9.76
u1kIn	2.68	33.11	8.42	6.77	1.38	1.17	9.57	0.30	3.00	46.58	39.14	25.00	22.13	0.52	11.34	11.17	5.64	NA	13.55
u1yIn	5.42	6.26	4.76	18.89	103	3.35	7.29	4.88	2.13	2.05	5.46	4.91	0.00	0.35	24.60	14.38	4.89	NA	6.66
u2kIn	3.68	32.65	8.04	8.11	6.55	12.82	9.02	4.15	13.59	23.51	12.92	30.36	20.49	8.02	2.59	7.41	6.23	NA	12.09
u2yIn	4.06	6.26	3.25	8.97	1.03	11.81	6.55	5.57	17.47	17.57	2.55	36.16	0.00	0.27	26.81	14.38	5.67	NA	9.81
u3kIn	0.74	34.03	20.50	10.97	2.95	10.11	10.67	7.23	16.91	37.30	31.37	23.30	18.03	9.97	0.62	3.65	9.91	NA	14.16
u3yIn	4.74	5.35	2.54	13.55	106	5.61	10.23	6.25	1.01	4.11	8.37	9.58	2.46	3.15	31.35	12.61	5.67	NA	7.55
c2kIn	0.96	73.02	23.08	14.03	9.31	14.06	3.50	0.47	3.37	32.66	27.97	30.36	26.23	8.74	5.04	11.17	5.28	NA	16.29
c2yIn	4.74	47.55	2.50	3.63	3.79	6.04	16.11	6.98	3.04	3.08	6.43	0.45	3.28	1.05	20.30	25.22	2.70	NA	9.08
d3kIn	0.74	34.03	20.50	10.97	2.95	10.11	10.67	7.23	16.91	37.30	31.37	23.30	18.03	9.97	0.62	3.65	9.91	NA	14.16
d3yIn	4.74	5.35	2.54	13.55	106	5.61	10.23	6.25	1.01	4.11	8.37	9.58	2.46	3.15	31.35	12.61	5.67	NA	7.55
d2kIn	3.68	32.65	8.04	8.11	6.55	12.82	9.02	4.15	13.59	23.51	12.92	30.36	20.49	8.02	2.59	7.41	6.23	NA	12.09
d2yIn	4.06	6.26	3.25	8.97	1.03	11.81	6.55	5.57	17.47	17.57	2.55	36.16	0.00	0.27	26.81	14.38	5.67	NA	9.81
d1kIn	2.66	34.03	6.16	12.12	6.21	5.68	7.36	3.13	0.27	32.14	29.43	31.25	22.13	2.62	14.10	9.40	8.75	NA	13.48
d1yIn	8.82	5.81	5.77	17.75	4.83	0.35	10.60	5.22	5.31	6.72	2.31	3.57	13.93	2.10	21.56	12.46	5.28	NA	8.01
Average	3.52	23.45	8.81	8.42	4.33	6.90	8.13	3.71	7.54	22.95	18.37	19.92	14.91	3.84	16.38	14.10	5.54	NA	7.74

Figure G.4: YALE spline-based mouth-closed template test results(%)

Absolute Difference Pixel Values																										
% Param	s101	s105	s111	s116	s121	s1210	s155	s162	s221	s225	s231	s294	s306	s309	s39	s405	s510	s52	s71	s78	s85	s88	s94	s98	Average	
c1kOut	N/A	1.84	N/A	2.67	0.71	N/A	0.84	2.61	N/A	N/A	1.15	4.12	0.35	0.70	2.81	N/A	N/A	N/A	N/A	0.50	0.43	N/A	0.86	0.15	2.27	1.47
c1yOut	N/A	1.69	N/A	14.83	0.25	N/A	0.86	2.70	N/A	N/A	2.04	0.11	2.04	0.37	2.14	N/A	N/A	N/A	N/A	0.71	2.54	N/A	1.17	13.76	0.57	3.05
c1yOut	N/A	3.35	N/A	1.19	1.99	N/A	1.63	0.98	N/A	N/A	2.35	2.56	0.60	1.13	4.03	N/A	N/A	N/A	N/A	0.24	1.73	N/A	1.26	0.55	0.52	1.61
u1yOut	N/A	0.76	N/A	14.94	0.29	N/A	0.34	1.75	N/A	N/A	0.06	0.25	0.21	1.80	1.06	N/A	N/A	N/A	N/A	1.24	0.23	N/A	0.68	9.46	1.77	2.32
u2xOut	N/A	1.77	N/A	3.67	1.99	N/A	3.38	0.33	N/A	N/A	1.69	3.97	2.63	2.30	2.63	N/A	N/A	N/A	N/A	2.34	0.90	N/A	3.43	0.26	3.64	2.33
u2yOut	N/A	1.10	N/A	14.00	0.04	N/A	1.01	2.69	N/A	N/A	0.13	0.25	1.01	1.13	1.40	N/A	N/A	N/A	N/A	0.21	0.23	N/A	1.15	7.99	11.47	2.92
u3xOut	N/A	0.52	N/A	1.22	1.24	N/A	3.46	0.83	N/A	N/A	1.58	5.72	0.44	3.13	2.70	N/A	N/A	N/A	N/A	1.74	0.40	N/A	5.60	5.34	1.56	2.37
u3yOut	N/A	1.43	N/A	15.10	0.70	N/A	0.32	1.03	N/A	N/A	0.11	0.08	0.21	0.80	0.73	N/A	N/A	N/A	N/A	1.57	0.23	N/A	0.61	7.98	2.37	2.22
e2xOut	N/A	5.23	N/A	6.23	0.99	N/A	1.14	0.33	N/A	N/A	2.85	0.61	2.13	0.68	1.20	N/A	N/A	N/A	N/A	1.16	1.03	N/A	1.87	9.08	1.51	2.40
e2yOut	N/A	0.30	N/A	14.40	2.54	N/A	1.90	2.69	N/A	N/A	2.38	1.13	0.57	4.35	1.27	N/A	N/A	N/A	N/A	1.93	0.73	N/A	2.29	14.58	1.36	3.49
d3xOut	N/A	1.15	N/A	0.45	0.24	N/A	1.80	0.17	N/A	N/A	0.75	4.06	0.77	2.80	2.36	N/A	N/A	N/A	N/A	2.41	0.07	N/A	6.93	6.67	0.56	2.08
d3yOut	N/A	0.57	N/A	17.43	1.03	N/A	1.99	0.64	N/A	N/A	3.56	1.75	0.79	1.20	0.30	N/A	N/A	N/A	N/A	0.76	2.23	N/A	3.39	7.98	2.37	3.05
d2xOut	N/A	2.43	N/A	4.00	1.32	N/A	1.05	0.01	N/A	N/A	0.31	2.97	2.63	0.63	3.30	N/A	N/A	N/A	N/A	3.67	1.23	N/A	6.10	0.07	3.31	2.20
d2yOut	N/A	0.57	N/A	18.33	3.96	N/A	1.99	0.97	N/A	N/A	3.21	2.08	1.32	1.80	2.07	N/A	N/A	N/A	N/A	0.79	1.90	N/A	4.15	9.65	11.47	4.28
d1xOut	N/A	5.35	N/A	1.86	0.65	N/A	0.63	3.65	N/A	N/A	0.68	1.89	0.27	1.13	4.36	N/A	N/A	N/A	N/A	0.58	2.73	N/A	1.74	0.22	0.86	1.77
d1yOut	N/A	1.24	N/A	17.61	0.96	N/A	0.66	0.42	N/A	N/A	4.28	1.08	0.79	0.46	0.73	N/A	N/A	N/A	N/A	0.76	1.90	N/A	3.65	9.79	2.43	3.12
c1kIn	N/A	1.84	N/A	2.67	0.71	N/A	0.84	2.61	N/A	N/A	1.15	4.12	0.35	0.70	2.81	N/A	N/A	N/A	N/A	0.50	0.43	N/A	0.86	0.15	2.27	1.47
c1yIn	N/A	1.69	N/A	14.83	0.25	N/A	0.86	2.70	N/A	N/A	2.04	0.11	2.04	0.37	2.14	N/A	N/A	N/A	N/A	0.71	2.54	N/A	1.17	13.76	0.57	3.05
u1kIn	N/A	3.68	N/A	2.19	2.65	N/A	1.63	1.98	N/A	N/A	1.35	2.89	0.94	1.80	4.03	N/A	N/A	N/A	N/A	1.24	0.73	N/A	0.92	0.55	4.52	2.07
u1yIn	N/A	0.90	N/A	14.44	1.87	N/A	1.01	3.09	N/A	N/A	2.44	1.08	2.71	0.63	0.27	N/A	N/A	N/A	N/A	0.60	1.56	N/A	2.99	7.62	0.57	2.79
u2xIn	N/A	2.43	N/A	3.00	1.99	N/A	0.71	0.34	N/A	N/A	0.69	3.31	2.29	2.63	2.30	N/A	N/A	N/A	N/A	1.67	1.57	N/A	5.76	0.60	1.98	2.08
u2yIn	N/A	1.43	N/A	14.50	0.46	N/A	0.68	2.36	N/A	N/A	2.38	0.75	1.51	0.30	1.73	N/A	N/A	N/A	N/A	1.29	1.56	N/A	3.82	6.49	9.47	3.25
u3xIn	N/A	0.52	N/A	0.11	1.09	N/A	0.20	0.17	N/A	N/A	0.42	1.06	1.44	4.47	1.03	N/A	N/A	N/A	N/A	2.08	0.73	N/A	7.60	5.01	1.23	1.81
u3yIn	N/A	0.24	N/A	12.60	1.14	N/A	1.01	2.03	N/A	N/A	2.39	0.75	2.38	1.04	0.27	N/A	N/A	N/A	N/A	0.93	1.56	N/A	3.06	5.81	0.30	2.37
e2xIn	N/A	5.23	N/A	6.23	0.99	N/A	1.14	0.33	N/A	N/A	2.85	0.61	2.13	0.68	1.20	N/A	N/A	N/A	N/A	1.16	1.03	N/A	1.87	9.08	1.51	2.40
e2yIn	N/A	0.30	N/A	14.40	2.54	N/A	1.90	2.69	N/A	N/A	2.38	1.13	0.57	4.35	1.27	N/A	N/A	N/A	N/A	1.93	0.73	N/A	2.29	14.58	1.36	3.49
d3xIn	N/A	0.52	N/A	0.11	1.09	N/A	0.20	0.17	N/A	N/A	0.42	1.06	1.44	4.47	1.03	N/A	N/A	N/A	N/A	2.08	0.73	N/A	7.60	5.01	1.23	1.81
d3yIn	N/A	0.24	N/A	12.60	1.14	N/A	1.01	2.03	N/A	N/A	2.39	0.75	2.38	1.04	0.27	N/A	N/A	N/A	N/A	0.93	1.56	N/A	3.06	5.81	0.30	2.37
d2xIn	N/A	2.43	N/A	3.00	1.99	N/A	0.71	0.34	N/A	N/A	0.69	3.31	2.29	2.63	2.30	N/A	N/A	N/A	N/A	1.67	1.57	N/A	5.76	0.60	1.98	2.08
d2yIn	N/A	1.43	N/A	14.50	0.46	N/A	0.68	2.36	N/A	N/A	2.38	0.75	1.51	0.30	1.73	N/A	N/A	N/A	N/A	1.29	1.56	N/A	3.82	6.49	9.47	3.25
d1xIn	N/A	3.68	N/A	2.19	2.65	N/A	1.63	1.98	N/A	N/A	1.35	2.89	0.94	1.80	4.03	N/A	N/A	N/A	N/A	1.24	0.73	N/A	0.92	0.55	4.52	2.07
d1yIn	N/A	0.90	N/A	14.44	1.87	N/A	1.01	3.09	N/A	N/A	2.44	1.08	2.71	0.63	0.27	N/A	N/A	N/A	N/A	0.60	1.56	N/A	2.99	7.62	0.57	2.79
Average	N/A	1.77	N/A	8.74	1.31	N/A	1.19	1.56	N/A	N/A	1.71	1.82	1.39	1.63	1.86	N/A	N/A	N/A	N/A	1.27	1.21	N/A	3.11	6.04	2.81	

Figure G.5: ORL spline-based mouth-closed template test results

Percentage (of width) Diff		s116	s121	s1210	s155	s162	s221	s225	s231	s294	s306	s309	s39	s405	s510	s52	s71	s78	s85	s88	s94	s98	Average
% Param	s101 s105 s111																						
c1wOut	NA 6.59 NA	10.53 2.54 NA	58.55 0.91 NA	3.15 3.08 NA	9.65 NA NA	3.95 17.64 NA	7.12 1.32 8.92 NA	NA NA	NA NA	NA NA	NA NA	NA NA	NA NA	NA NA	NA NA	NA NA	1.77 1.78 NA	2.88 0.51 7.58	NA NA	2.88 0.51 7.58	NA NA	NA NA	5.59
c1yOut	NA 6.04 NA	58.55 0.91 NA	3.15 3.08 NA	9.65 NA NA	3.95 17.64 NA	7.12 1.32 8.92 NA	NA NA	NA NA	NA NA	NA NA	NA NA	NA NA	NA NA	NA NA	NA NA	NA NA	2.51 10.57 NA	3.90 48.00 1.89	NA NA	3.90 48.00 1.89	NA NA	NA NA	11.36
u1wOut	NA 11.97 NA	4.70 7.10 NA	5.96 3.64 NA	8.11 10.96 NA	8.11 10.96 NA	8.11 10.96 NA	2.11 4.05 16.80 NA	NA NA	NA NA	NA NA	NA NA	NA NA	NA NA	NA NA	NA NA	NA NA	0.86 7.22 NA	4.19 1.92 1.74	NA NA	4.19 1.92 1.74	NA NA	NA NA	6.09
u1yOut	NA 2.72 NA	58.97 1.05 NA	1.26 6.49 NA	0.19 1.07 NA	0.73 6.42 4.43 NA	NA NA	NA NA	NA NA	NA NA	NA NA	NA NA	NA NA	NA NA	NA NA	NA NA	NA NA	4.37 0.96 NA	2.27 32.99 5.89	NA NA	2.27 32.99 5.89	NA NA	NA NA	8.65
u2xOut	NA 6.31 NA	14.47 7.10 NA	12.37 1.21 NA	5.82 17.03 NA	8.21 10.96 NA	NA NA	NA NA	NA NA	NA NA	NA NA	NA NA	NA NA	NA NA	NA NA	NA NA	NA NA	8.26 3.74 NA	11.43 0.92 12.14	NA NA	11.43 0.92 12.14	NA NA	NA NA	8.61
u2yOut	NA 3.91 NA	55.26 0.14 NA	3.70 9.97 NA	0.43 1.07 NA	3.52 4.04 5.83 NA	NA NA	NA NA	NA NA	NA NA	NA NA	NA NA	NA NA	NA NA	NA NA	NA NA	NA NA	0.75 0.96 NA	3.84 27.86 38.25	NA NA	3.84 27.86 38.25	NA NA	NA NA	10.64
u3xOut	NA 1.85 NA	4.81 4.43 NA	12.67 3.06 NA	5.46 24.53 NA	1.19 11.24 NA	NA NA	NA NA	NA NA	NA NA	NA NA	NA NA	NA NA	NA NA	NA NA	NA NA	NA NA	6.15 1.66 NA	18.66 18.62 5.21	NA NA	18.66 18.62 5.21	NA NA	NA NA	8.74
u3yOut	NA 5.10 NA	59.60 2.49 NA	1.18 3.80 NA	0.36 0.36 NA	0.73 2.85 3.04 NA	NA NA	NA NA	NA NA	NA NA	NA NA	NA NA	NA NA	NA NA	NA NA	NA NA	NA NA	5.55 0.96 NA	2.03 27.83 7.89	NA NA	2.03 27.83 7.89	NA NA	NA NA	8.25
e2xOut	NA 18.68 NA	24.58 3.53 NA	4.17 1.21 NA	9.84 2.61 NA	2.42 4.99 NA	NA NA	NA NA	NA NA	NA NA	NA NA	NA NA	NA NA	NA NA	NA NA	NA NA	NA NA	4.09 4.29 NA	6.24 31.69 5.03	NA NA	6.24 31.69 5.03	NA NA	NA NA	8.72
e2yOut	NA 1.07 NA	56.83 9.07 NA	6.96 9.97 NA	8.19 4.83 NA	2.00 15.52 5.30 NA	NA NA	NA NA	NA NA	NA NA	NA NA	NA NA	NA NA	NA NA	NA NA	NA NA	NA NA	6.81 3.04 NA	7.63 50.87 4.54	NA NA	7.63 50.87 4.54	NA NA	NA NA	12.84
d3xOut	NA 4.11 NA	1.77 0.86 NA	6.57 0.64 NA	2.59 17.39 NA	2.69 10.00 9.85 NA	NA NA	NA NA	NA NA	NA NA	NA NA	NA NA	NA NA	NA NA	NA NA	NA NA	NA NA	8.50 0.27 NA	23.10 23.27 1.87	NA NA	23.10 23.27 1.87	NA NA	NA NA	7.57
d3yOut	NA 2.04 NA	68.81 3.68 NA	7.28 2.38 NA	12.28 7.51 NA	2.76 4.29 0.26 NA	NA NA	NA NA	NA NA	NA NA	NA NA	NA NA	NA NA	NA NA	NA NA	NA NA	NA NA	2.69 0.29 NA	11.30 27.83 7.89	NA NA	11.30 27.83 7.89	NA NA	NA NA	11.35
d2xOut	NA 8.69 NA	15.79 4.72 NA	3.83 0.02 NA	1.08 12.74 NA	9.16 2.26 13.74 NA	NA NA	NA NA	NA NA	NA NA	NA NA	NA NA	NA NA	NA NA	NA NA	NA NA	NA NA	12.97 5.13 NA	20.32 0.24 11.03	NA NA	20.32 0.24 11.03	NA NA	NA NA	8.11
d2yOut	NA 2.04 NA	72.37 14.14 NA	7.28 3.61 NA	11.06 8.93 NA	6.42 8.60 NA	NA NA	NA NA	NA NA	NA NA	NA NA	NA NA	NA NA	NA NA	NA NA	NA NA	NA NA	2.78 7.90 NA	13.84 33.68 38.25	NA NA	13.84 33.68 38.25	NA NA	NA NA	15.70
d1xOut	NA 19.11 NA	7.33 2.34 NA	2.31 13.51 NA	2.36 8.10 NA	4.05 18.19 NA	NA NA	NA NA	NA NA	NA NA	NA NA	NA NA	NA NA	NA NA	NA NA	NA NA	NA NA	2.03 11.38 NA	5.81 0.76 2.86	NA NA	5.81 0.76 2.86	NA NA	NA NA	6.74
d1yOut	NA 4.42 NA	69.50 3.43 NA	2.40 1.55 NA	14.75 4.65 NA	2.76 1.66 3.04 NA	NA NA	NA NA	NA NA	NA NA	NA NA	NA NA	NA NA	NA NA	NA NA	NA NA	NA NA	2.69 7.90 NA	12.17 34.15 8.11	NA NA	12.17 34.15 8.11	NA NA	NA NA	11.55
c1xIn	NA 6.59 NA	10.53 2.54 NA	3.08 9.65 NA	3.95 17.64 NA	7.12 1.32 8.92 NA	NA NA	NA NA	NA NA	NA NA	NA NA	NA NA	NA NA	NA NA	NA NA	NA NA	NA NA	1.77 1.78 NA	2.88 0.51 7.58	NA NA	2.88 0.51 7.58	NA NA	NA NA	5.59
c1yIn	NA 6.04 NA	58.55 0.91 NA	3.15 3.08 NA	9.65 NA NA	3.95 17.64 NA	7.12 1.32 8.92 NA	NA NA	NA NA	NA NA	NA NA	NA NA	NA NA	NA NA	NA NA	NA NA	NA NA	2.51 10.57 NA	3.90 48.00 1.89	NA NA	3.90 48.00 1.89	NA NA	NA NA	11.36
u1xIn	NA 13.16 NA	8.65 9.48 NA	5.96 7.34 NA	4.66 12.39 NA	3.27 6.43 16.80 NA	NA NA	NA NA	NA NA	NA NA	NA NA	NA NA	NA NA	NA NA	NA NA	NA NA	NA NA	4.39 3.05 NA	3.08 1.92 15.08	NA NA	3.08 1.92 15.08	NA NA	NA NA	7.71
u1yIn	NA 3.23 NA	57.00 6.69 NA	3.70 11.43 NA	8.43 4.64 NA	2.26 1.13 NA	NA NA	NA NA	NA NA	NA NA	NA NA	NA NA	NA NA	NA NA	NA NA	NA NA	NA NA	2.10 6.52 NA	9.95 26.59 1.89	NA NA	9.95 26.59 1.89	NA NA	NA NA	10.33
u2xIn	NA 8.69 NA	11.84 7.10 NA	2.61 1.26 NA	2.37 14.17 NA	7.99 9.41 9.57 NA	NA NA	NA NA	NA NA	NA NA	NA NA	NA NA	NA NA	NA NA	NA NA	NA NA	NA NA	5.91 6.52 NA	19.21 2.08 6.59	NA NA	19.21 2.08 6.59	NA NA	NA NA	7.69
u2yIn	NA 5.10 NA	57.24 1.64 NA	2.48 8.74 NA	8.19 3.21 NA	5.27 1.06 7.22 NA	NA NA	NA NA	NA NA	NA NA	NA NA	NA NA	NA NA	NA NA	NA NA	NA NA	NA NA	4.54 6.52 NA	12.73 22.63 31.58	NA NA	12.73 22.63 31.58	NA NA	NA NA	11.88
u3xIn	NA 1.85 NA	4.81 4.43 NA	12.67 3.06 NA	5.46 24.53 NA	1.19 11.24 NA	NA NA	NA NA	NA NA	NA NA	NA NA	NA NA	NA NA	NA NA	NA NA	NA NA	NA NA	7.33 3.05 NA	25.33 17.46 4.10	NA NA	25.33 17.46 4.10	NA NA	NA NA	6.41
u3yIn	NA 5.10 NA	59.60 2.49 NA	1.18 3.80 NA	0.36 0.36 NA	0.73 2.85 3.04 NA	NA NA	NA NA	NA NA	NA NA	NA NA	NA NA	NA NA	NA NA	NA NA	NA NA	NA NA	3.28 6.52 NA	10.19 20.27 1.00	NA NA	10.19 20.27 1.00	NA NA	NA NA	8.78
e2xIn	NA 0.85 NA	49.73 4.06 NA	3.70 7.50 NA	8.26 3.21 NA	8.28 3.70 1.13 NA	NA NA	NA NA	NA NA	NA NA	NA NA	NA NA	NA NA	NA NA	NA NA	NA NA	NA NA	3.28 6.52 NA	10.19 20.27 1.00	NA NA	10.19 20.27 1.00	NA NA	NA NA	8.78
e2yIn	NA 18.68 NA	24.58 3.53 NA	4.17 1.21 NA	9.84 2.61 NA	2.42 4.99 NA	NA NA	NA NA	NA NA	NA NA	NA NA	NA NA	NA NA	NA NA	NA NA	NA NA	NA NA	4.09 4.29 NA	6.24 31.69 5.03	NA NA	6.24 31.69 5.03	NA NA	NA NA	8.72
d3xIn	NA 1.07 NA	56.83 9.07 NA	6.96 9.97 NA	8.19 4.83 NA	2.00 15.52 5.30 NA	NA NA	NA NA	NA NA	NA NA	NA NA	NA NA	NA NA	NA NA	NA NA	NA NA	NA NA	6.81 3.04 NA	7.63 50.87 4.54	NA NA	7.63 50.87 4.54	NA NA	NA NA	12.84
d3yIn	NA 1.85 NA	4.81 4.43 NA	12.67 3.06 NA	5.46 24.53 NA	1.19 11.24 NA	NA NA	NA NA	NA NA	NA NA	NA NA	NA NA	NA NA	NA NA	NA NA	NA NA	NA NA	7.33 3.05 NA	25.33 17.46 4.10	NA NA	25.33 17.46 4.10	NA NA	NA NA	6.41
d2xIn	NA 0.85 NA	49.73 4.06 NA	3.70 7.50 NA	8.26 3.21 NA	8.28 3.70 1.13 NA	NA NA	NA NA	NA NA	NA NA	NA NA	NA NA	NA NA	NA NA	NA NA	NA NA	NA NA	3.28 6.52 NA	10.19 20.27 1.00	NA NA	10.19 20.27 1.00	NA NA	NA NA	8.78
d2yIn	NA 5.10 NA	57.24 1.64 NA	2.48 8.74 NA	8.19 3.21 NA	5.27 1.06 7.22 NA	NA NA	NA NA	NA NA	NA NA	NA NA	NA NA	NA NA	NA NA	NA NA	NA NA	NA NA	4.54 6.52 NA	12.73 22.63 31.58	NA NA	12.73 22.63 31.58	NA NA	NA NA	11.88
d1xIn	NA 13.16 NA	8.65 9.48 NA	5.96 7.34 NA	4.66 12.39 NA	3.27 6.43 16.80 NA	NA NA	NA NA	NA NA	NA NA	NA NA	NA NA	NA NA	NA NA	NA NA	NA NA	NA NA	4.39 3.05 NA	3.08 1.92 15.08	NA NA	3.08 1.92 15.08	NA NA	NA NA	7.71
d1yIn	NA 3.23 NA	57.00 6.69 NA	3.70 11.43 NA	8.43 4.64 NA	2.26 1.13 NA	NA NA	NA NA	NA NA	NA NA	NA NA	NA NA	NA NA	NA NA	NA NA	NA NA	NA NA	2.10 6.52 NA	9.95 26.59 1.89	NA NA	9.95 26.59 1.89	NA NA	NA NA	10.33
Average		NA 6.34 NA	34.51 4.67 NA	4.37 5.79 NA	5.91 7.80 NA	4.84 5.83 7.75 NA	4.84 5.83 7.75 NA	NA NA	NA NA	NA NA	4.84 5.83 7.75 NA	4.84 5.83 7.75 NA	NA NA	NA NA	NA NA	NA NA	4.47 5.03 NA	10.35 21.07 9.36	NA NA	10.35 21.07 9.36	NA NA	NA NA	9.36

Figure G.6: ORL spline-based mouth-closed template test results (%)

APPENDIX H

Polygonal Mouth-Open Template Detailed Test Results

Absolute Difference Pixel Values																				
% Param Name	KA,DI1	KA,H2	KA,S4	KA,SU	KL,AN	KL,FE2	KM,DI	KM,S4	KR,AN	MK,S4	NA,AN	NA,H2	NA,SU	NM,DI	TM,FE	TM,S4	UY,AN	UY,DI2	YM,H2	Average
c1xOut	NA	4.92	NA	NA	NA	NA	4.87	NA	NA	NA	NA	0.29	0.34	NA	0.08	NA	NA	NA	NA	1.88
c1yOut	NA	8.76	NA	NA	NA	NA	2.63	NA	NA	NA	NA	8.32	4.71	NA	1.08	NA	NA	NA	NA	5.81
u1xOut	NA	3.59	NA	NA	NA	NA	0.04	NA	NA	NA	NA	2.96	0.32	NA	0.59	NA	NA	NA	NA	1.46
u1yOut	NA	2.07	NA	NA	NA	NA	3.46	NA	NA	NA	NA	3.15	1.21	NA	1.75	NA	NA	NA	NA	2.08
u2xOut	NA	3.26	NA	NA	NA	NA	1.04	NA	NA	NA	NA	3.70	0.53	NA	0.41	NA	NA	NA	NA	1.77
u2yOut	NA	2.07	NA	NA	NA	NA	7.79	NA	NA	NA	NA	4.79	10.98	NA	0.09	NA	NA	NA	NA	4.33
u3xOut	NA	3.59	NA	NA	NA	NA	1.79	NA	NA	NA	NA	1.04	3.68	NA	0.08	NA	NA	NA	NA	2.10
u3yOut	NA	2.41	NA	NA	NA	NA	2.13	NA	NA	NA	NA	1.82	0.54	NA	0.91	NA	NA	NA	NA	1.33
c2xOut	NA	5.26	NA	NA	NA	NA	5.46	NA	NA	NA	NA	2.04	3.01	NA	0.59	NA	NA	NA	NA	3.21
c2yOut	NA	6.09	NA	NA	NA	NA	0.63	NA	NA	NA	NA	5.99	3.71	NA	1.75	NA	NA	NA	NA	4.53
d3xOut	NA	4.77	NA	NA	NA	NA	0.84	NA	NA	NA	NA	0.26	2.40	NA	1.84	NA	NA	NA	NA	2.07
d3yOut	NA	4.49	NA	NA	NA	NA	0.75	NA	NA	NA	NA	3.17	1.14	NA	3.97	NA	NA	NA	NA	2.52
d2xOut	NA	4.98	NA	NA	NA	NA	0.94	NA	NA	NA	NA	1.98	0.53	NA	1.43	NA	NA	NA	NA	1.93
d2yOut	NA	11.79	NA	NA	NA	NA	5.81	NA	NA	NA	NA	8.65	3.52	NA	6.92	NA	NA	NA	NA	7.13
d1xOut	NA	2.97	NA	NA	NA	NA	1.31	NA	NA	NA	NA	1.66	3.82	NA	2.19	NA	NA	NA	NA	2.15
d1yOut	NA	5.10	NA	NA	NA	NA	4.03	NA	NA	NA	NA	4.56	0.71	NA	1.05	NA	NA	NA	NA	2.99
c1xIn	NA	4.26	NA	NA	NA	NA	5.87	NA	NA	NA	NA	0.71	1.66	NA	0.75	NA	NA	NA	NA	2.39
c1yIn	NA	7.43	NA	NA	NA	NA	0.96	NA	NA	NA	NA	6.32	3.37	NA	0.25	NA	NA	NA	NA	4.45
u1xIn	NA	4.59	NA	NA	NA	NA	2.62	NA	NA	NA	NA	0.96	0.34	NA	0.08	NA	NA	NA	NA	2.09
u1yIn	NA	1.32	NA	NA	NA	NA	4.79	NA	NA	NA	NA	6.69	1.21	NA	1.25	NA	NA	NA	NA	2.92
u2xIn	NA	5.59	NA	NA	NA	NA	0.29	NA	NA	NA	NA	3.36	1.47	NA	0.75	NA	NA	NA	NA	2.14
u2yIn	NA	0.99	NA	NA	NA	NA	5.79	NA	NA	NA	NA	7.67	9.64	NA	0.09	NA	NA	NA	NA	4.67
u3xIn	NA	7.92	NA	NA	NA	NA	2.88	NA	NA	NA	NA	2.96	7.68	NA	0.59	NA	NA	NA	NA	4.24
u3yIn	NA	1.66	NA	NA	NA	NA	5.46	NA	NA	NA	NA	5.36	1.54	NA	2.58	NA	NA	NA	NA	3.48
c2xIn	NA	7.92	NA	NA	NA	NA	11.13	NA	NA	NA	NA	1.62	6.68	NA	2.92	NA	NA	NA	NA	5.81
c2yIn	NA	5.43	NA	NA	NA	NA	1.96	NA	NA	NA	NA	5.99	3.04	NA	0.08	NA	NA	NA	NA	4.03
d3xIn	NA	7.40	NA	NA	NA	NA	5.21	NA	NA	NA	NA	2.48	5.66	NA	0.43	NA	NA	NA	NA	4.41
d3yIn	NA	1.71	NA	NA	NA	NA	3.71	NA	NA	NA	NA	0.27	1.19	NA	1.13	NA	NA	NA	NA	1.61
d2xIn	NA	3.66	NA	NA	NA	NA	1.08	NA	NA	NA	NA	0.28	0.59	NA	2.36	NA	NA	NA	NA	1.63
d2yIn	NA	3.99	NA	NA	NA	NA	3.62	NA	NA	NA	NA	2.32	5.70	NA	6.81	NA	NA	NA	NA	3.77
d1xIn	NA	0.45	NA	NA	NA	NA	5.61	NA	NA	NA	NA	0.62	5.24	NA	2.04	NA	NA	NA	NA	2.76
d1yIn	NA	2.03	NA	NA	NA	NA	3.37	NA	NA	NA	NA	2.99	0.66	NA	2.76	NA	NA	NA	NA	2.55
Average	NA	4.45	NA	NA	NA	NA	3.37	NA	NA	NA	NA	3.28	3.03	NA	1.55	NA	NA	NA	NA	3.11

Figure H.1: JAFFE polygonal mouth-open template test results

Percentage (of width) Diff		KA,DI1	KA,HA	KA,SA	KA,SU	KL,AN	KL,FE2	KM,DI1	KM,SA	KR,AN	MK,SA	NA,AN	NA,HA	NA,SU	NM,DI	TM,FE	TM,SA	UY,AM	UY,DI2	YM,HA	Average
c1xOut		NA	9.53	NA	NA	NA	NA	12.60	NA	NA	NA	NA	0.47	0.70	NA	0.19	NA	NA	NA	NA	4.13
c1yOut		NA	16.96	NA	NA	NA	NA	6.79	NA	NA	NA	NA	13.35	9.54	NA	2.49	NA	NA	NA	NA	10.86
u1xOut		NA	6.95	NA	NA	NA	NA	0.12	NA	NA	NA	NA	4.74	0.65	NA	1.35	NA	NA	NA	NA	2.67
u1yOut		NA	4.01	NA	NA	NA	NA	8.94	NA	NA	NA	NA	5.06	2.44	NA	0.04	NA	NA	NA	NA	4.32
u2xOut		NA	6.30	NA	NA	NA	NA	2.69	NA	NA	NA	NA	5.93	1.07	NA	0.96	NA	NA	NA	NA	3.31
u2yOut		NA	4.01	NA	NA	NA	NA	20.15	NA	NA	NA	NA	7.69	22.25	NA	0.20	NA	NA	NA	NA	9.12
u3xOut		NA	6.95	NA	NA	NA	NA	4.63	NA	NA	NA	NA	1.67	7.46	NA	0.19	NA	NA	NA	NA	4.16
u3yOut		NA	4.66	NA	NA	NA	NA	5.50	NA	NA	NA	NA	2.92	1.09	NA	2.11	NA	NA	NA	NA	2.76
c2xOut		NA	10.17	NA	NA	NA	NA	14.12	NA	NA	NA	NA	3.28	6.10	NA	1.35	NA	NA	NA	NA	6.66
c2yOut		NA	11.79	NA	NA	NA	NA	1.62	NA	NA	NA	NA	9.60	7.51	NA	4.03	NA	NA	NA	NA	8.33
d3xOut		NA	9.23	NA	NA	NA	NA	2.17	NA	NA	NA	NA	0.41	4.87	NA	4.23	NA	NA	NA	NA	4.15
d3yOut		NA	8.69	NA	NA	NA	NA	1.94	NA	NA	NA	NA	5.09	2.30	NA	9.16	NA	NA	NA	NA	4.99
d2xOut		NA	9.65	NA	NA	NA	NA	2.42	NA	NA	NA	NA	3.17	1.07	NA	3.29	NA	NA	NA	NA	3.76
d2yOut		NA	22.82	NA	NA	NA	NA	15.03	NA	NA	NA	NA	13.88	7.14	NA	15.96	NA	NA	NA	NA	14.22
d1xOut		NA	5.74	NA	NA	NA	NA	3.40	NA	NA	NA	NA	2.66	7.74	NA	5.05	NA	NA	NA	NA	4.36
d1yOut		NA	9.87	NA	NA	NA	NA	10.43	NA	NA	NA	NA	7.32	1.44	NA	2.42	NA	NA	NA	NA	5.96
c1xIn		NA	8.24	NA	NA	NA	NA	15.19	NA	NA	NA	NA	1.14	3.36	NA	1.72	NA	NA	NA	NA	5.26
c1yIn		NA	14.37	NA	NA	NA	NA	2.48	NA	NA	NA	NA	10.14	6.84	NA	0.58	NA	NA	NA	NA	8.12
u1xIn		NA	8.88	NA	NA	NA	NA	6.78	NA	NA	NA	NA	1.54	0.70	NA	0.19	NA	NA	NA	NA	4.14
u1yIn		NA	2.56	NA	NA	NA	NA	12.39	NA	NA	NA	NA	10.74	2.44	NA	2.88	NA	NA	NA	NA	5.82
u2xIn		NA	10.82	NA	NA	NA	NA	0.76	NA	NA	NA	NA	5.40	2.98	NA	1.72	NA	NA	NA	NA	4.01
u2yIn		NA	1.92	NA	NA	NA	NA	14.98	NA	NA	NA	NA	12.30	19.55	NA	0.20	NA	NA	NA	NA	9.26
u3xIn		NA	15.33	NA	NA	NA	NA	7.44	NA	NA	NA	NA	4.74	15.56	NA	1.35	NA	NA	NA	NA	8.38
u3yIn		NA	3.21	NA	NA	NA	NA	14.12	NA	NA	NA	NA	8.60	3.12	NA	5.96	NA	NA	NA	NA	7.06
c2xIn		NA	15.33	NA	NA	NA	NA	28.78	NA	NA	NA	NA	2.61	13.54	NA	6.74	NA	NA	NA	NA	12.47
c2yIn		NA	10.50	NA	NA	NA	NA	5.07	NA	NA	NA	NA	9.60	6.16	NA	0.19	NA	NA	NA	NA	7.45
d3xIn		NA	14.32	NA	NA	NA	NA	13.49	NA	NA	NA	NA	3.98	11.47	NA	0.99	NA	NA	NA	NA	8.89
d3yIn		NA	3.31	NA	NA	NA	NA	9.60	NA	NA	NA	NA	0.44	2.41	NA	2.62	NA	NA	NA	NA	3.54
d2xIn		NA	7.08	NA	NA	NA	NA	2.80	NA	NA	NA	NA	0.45	1.20	NA	5.44	NA	NA	NA	NA	3.34
d2yIn		NA	7.73	NA	NA	NA	NA	9.36	NA	NA	NA	NA	3.72	11.55	NA	15.72	NA	NA	NA	NA	8.06
d1xIn		NA	0.88	NA	NA	NA	NA	14.51	NA	NA	NA	NA	1.00	10.62	NA	4.71	NA	NA	NA	NA	6.02
d1yIn		NA	3.93	NA	NA	NA	NA	8.72	NA	NA	NA	NA	4.80	1.34	NA	6.37	NA	NA	NA	NA	5.18
Average		NA	8.62	NA	NA	NA	NA	8.72	NA	NA	NA	NA	5.26	6.13	NA	3.58	NA	NA	NA	NA	5.33

Figure H.2: JAFFE polygonal mouth-open template test results (%)

Absolute Difference Pixel Values																			
% Param	01	02	03	04	05	06	07	08	09	10	11	12	13	14	15	16	17	Average	
c1xOut	NA	NA	NA	NA	NA	NA	NA	NA	NA	NA	NA	NA	NA	NA	NA	NA	NA	7.03	
c1yOut	NA	NA	NA	NA	NA	NA	NA	NA	NA	NA	NA	NA	NA	NA	NA	NA	NA	6.14	
u1xOut	NA	NA	NA	NA	NA	NA	NA	NA	NA	NA	NA	NA	NA	NA	NA	NA	NA	5.93	
u1yOut	NA	NA	NA	NA	NA	NA	NA	NA	NA	NA	NA	NA	NA	NA	NA	NA	NA	0.96	
u2xOut	NA	NA	NA	NA	NA	NA	NA	NA	NA	NA	NA	NA	NA	NA	NA	NA	NA	4.78	
u2yOut	NA	NA	NA	NA	NA	NA	NA	NA	NA	NA	NA	NA	NA	NA	NA	NA	NA	9.80	
u3xOut	NA	NA	NA	NA	NA	NA	NA	NA	NA	NA	NA	NA	NA	NA	NA	NA	NA	3.43	
u3yOut	NA	NA	NA	NA	NA	NA	NA	NA	NA	NA	NA	NA	NA	NA	NA	NA	NA	0.29	
c2xOut	NA	NA	NA	NA	NA	NA	NA	NA	NA	NA	NA	NA	NA	NA	NA	NA	NA	7.02	
c2yOut	NA	NA	NA	NA	NA	NA	NA	NA	NA	NA	NA	NA	NA	NA	NA	NA	NA	7.40	
d3xOut	NA	NA	NA	NA	NA	NA	NA	NA	NA	NA	NA	NA	NA	NA	NA	NA	NA	2.47	
d3yOut	NA	NA	NA	NA	NA	NA	NA	NA	NA	NA	NA	NA	NA	NA	NA	NA	NA	1.44	
d2xOut	NA	NA	NA	NA	NA	NA	NA	NA	NA	NA	NA	NA	NA	NA	NA	NA	NA	1.70	
d2yOut	NA	NA	NA	NA	NA	NA	NA	NA	NA	NA	NA	NA	NA	NA	NA	NA	NA	3.83	
d1xOut	NA	NA	NA	NA	NA	NA	NA	NA	NA	NA	NA	NA	NA	NA	NA	NA	NA	3.19	
d1yOut	NA	NA	NA	NA	NA	NA	NA	NA	NA	NA	NA	NA	NA	NA	NA	NA	NA	1.12	
c1xIn	NA	NA	NA	NA	NA	NA	NA	NA	NA	NA	NA	NA	NA	NA	NA	NA	NA	2.68	
c1yIn	NA	NA	NA	NA	NA	NA	NA	NA	NA	NA	NA	NA	NA	NA	NA	NA	NA	6.62	
u1xIn	NA	NA	NA	NA	NA	NA	NA	NA	NA	NA	NA	NA	NA	NA	NA	NA	NA	3.93	
u1yIn	NA	NA	NA	NA	NA	NA	NA	NA	NA	NA	NA	NA	NA	NA	NA	NA	NA	5.01	
u2xIn	NA	NA	NA	NA	NA	NA	NA	NA	NA	NA	NA	NA	NA	NA	NA	NA	NA	6.12	
u2yIn	NA	NA	NA	NA	NA	NA	NA	NA	NA	NA	NA	NA	NA	NA	NA	NA	NA	12.85	
u3xIn	NA	NA	NA	NA	NA	NA	NA	NA	NA	NA	NA	NA	NA	NA	NA	NA	NA	6.43	
c2xIn	NA	NA	NA	NA	NA	NA	NA	NA	NA	NA	NA	NA	NA	NA	NA	NA	NA	4.01	
c2yIn	NA	NA	NA	NA	NA	NA	NA	NA	NA	NA	NA	NA	NA	NA	NA	NA	NA	8.34	
c3xIn	NA	NA	NA	NA	NA	NA	NA	NA	NA	NA	NA	NA	NA	NA	NA	NA	NA	8.18	
d3xIn	NA	NA	NA	NA	NA	NA	NA	NA	NA	NA	NA	NA	NA	NA	NA	NA	NA	5.90	
d3yIn	NA	NA	NA	NA	NA	NA	NA	NA	NA	NA	NA	NA	NA	NA	NA	NA	NA	8.74	
d2xIn	NA	NA	NA	NA	NA	NA	NA	NA	NA	NA	NA	NA	NA	NA	NA	NA	NA	2.71	
d2yIn	NA	NA	NA	NA	NA	NA	NA	NA	NA	NA	NA	NA	NA	NA	NA	NA	NA	0.28	
d1xIn	NA	NA	NA	NA	NA	NA	NA	NA	NA	NA	NA	NA	NA	NA	NA	NA	NA	1.17	
d1yIn	NA	NA	NA	NA	NA	NA	NA	NA	NA	NA	NA	NA	NA	NA	NA	NA	NA	6.02	
Average	NA	NA	NA	NA	NA	NA	NA	NA	NA	NA	NA	NA	NA	NA	NA	NA	NA	7.35	4.77

Figure H.3: YALE polygonal mouth-open template test results

Percentage (of width) Diff																				
% Param	01	02	03	04	05	06	07	08	09	10	11	12	13	14	15	16	17	18	19	Average
c1wOut	N/A	N/A	N/A	N/A	N/A	N/A	N/A	N/A	N/A	N/A	N/A	N/A	N/A	N/A	N/A	N/A	N/A	N/A	N/A	13.45
c1yOut	N/A	N/A	N/A	N/A	N/A	N/A	N/A	N/A	N/A	N/A	N/A	N/A	N/A	N/A	N/A	N/A	N/A	N/A	N/A	12.13
u1wOut	N/A	N/A	N/A	N/A	N/A	N/A	N/A	N/A	N/A	N/A	N/A	N/A	N/A	N/A	N/A	N/A	N/A	N/A	N/A	13.95
u1yOut	N/A	N/A	N/A	N/A	N/A	N/A	N/A	N/A	N/A	N/A	N/A	N/A	N/A	N/A	N/A	N/A	N/A	N/A	N/A	1.46
u2wOut	N/A	N/A	N/A	N/A	N/A	N/A	N/A	N/A	N/A	N/A	N/A	N/A	N/A	N/A	N/A	N/A	N/A	N/A	N/A	14.01
u2yOut	N/A	N/A	N/A	N/A	N/A	N/A	N/A	N/A	N/A	N/A	N/A	N/A	N/A	N/A	N/A	N/A	N/A	N/A	N/A	11.23
u3wOut	N/A	N/A	N/A	N/A	N/A	N/A	N/A	N/A	N/A	N/A	N/A	N/A	N/A	N/A	N/A	N/A	N/A	N/A	N/A	14.78
u3yOut	N/A	N/A	N/A	N/A	N/A	N/A	N/A	N/A	N/A	N/A	N/A	N/A	N/A	N/A	N/A	N/A	N/A	N/A	N/A	0.46
c2wOut	N/A	N/A	N/A	N/A	N/A	N/A	N/A	N/A	N/A	N/A	N/A	N/A	N/A	N/A	N/A	N/A	N/A	N/A	N/A	19.43
c2yOut	N/A	N/A	N/A	N/A	N/A	N/A	N/A	N/A	N/A	N/A	N/A	N/A	N/A	N/A	N/A	N/A	N/A	N/A	N/A	14.58
d3wOut	N/A	N/A	N/A	N/A	N/A	N/A	N/A	N/A	N/A	N/A	N/A	N/A	N/A	N/A	N/A	N/A	N/A	N/A	N/A	14.18
d3yOut	N/A	N/A	N/A	N/A	N/A	N/A	N/A	N/A	N/A	N/A	N/A	N/A	N/A	N/A	N/A	N/A	N/A	N/A	N/A	5.73
d2wOut	N/A	N/A	N/A	N/A	N/A	N/A	N/A	N/A	N/A	N/A	N/A	N/A	N/A	N/A	N/A	N/A	N/A	N/A	N/A	10.80
d2yOut	N/A	N/A	N/A	N/A	N/A	N/A	N/A	N/A	N/A	N/A	N/A	N/A	N/A	N/A	N/A	N/A	N/A	N/A	N/A	15.01
d1wOut	N/A	N/A	N/A	N/A	N/A	N/A	N/A	N/A	N/A	N/A	N/A	N/A	N/A	N/A	N/A	N/A	N/A	N/A	N/A	9.21
d1yOut	N/A	N/A	N/A	N/A	N/A	N/A	N/A	N/A	N/A	N/A	N/A	N/A	N/A	N/A	N/A	N/A	N/A	N/A	N/A	6.56
c1wIn	N/A	N/A	N/A	N/A	N/A	N/A	N/A	N/A	N/A	N/A	N/A	N/A	N/A	N/A	N/A	N/A	N/A	N/A	N/A	12.76
c1yIn	N/A	N/A	N/A	N/A	N/A	N/A	N/A	N/A	N/A	N/A	N/A	N/A	N/A	N/A	N/A	N/A	N/A	N/A	N/A	11.82
u1wIn	N/A	N/A	N/A	N/A	N/A	N/A	N/A	N/A	N/A	N/A	N/A	N/A	N/A	N/A	N/A	N/A	N/A	N/A	N/A	11.88
u1yIn	N/A	N/A	N/A	N/A	N/A	N/A	N/A	N/A	N/A	N/A	N/A	N/A	N/A	N/A	N/A	N/A	N/A	N/A	N/A	9.57
u2wIn	N/A	N/A	N/A	N/A	N/A	N/A	N/A	N/A	N/A	N/A	N/A	N/A	N/A	N/A	N/A	N/A	N/A	N/A	N/A	16.01
u2yIn	N/A	N/A	N/A	N/A	N/A	N/A	N/A	N/A	N/A	N/A	N/A	N/A	N/A	N/A	N/A	N/A	N/A	N/A	N/A	16.75
u3wIn	N/A	N/A	N/A	N/A	N/A	N/A	N/A	N/A	N/A	N/A	N/A	N/A	N/A	N/A	N/A	N/A	N/A	N/A	N/A	18.19
u3yIn	N/A	N/A	N/A	N/A	N/A	N/A	N/A	N/A	N/A	N/A	N/A	N/A	N/A	N/A	N/A	N/A	N/A	N/A	N/A	8.84
c2wIn	N/A	N/A	N/A	N/A	N/A	N/A	N/A	N/A	N/A	N/A	N/A	N/A	N/A	N/A	N/A	N/A	N/A	N/A	N/A	22.97
c2yIn	N/A	N/A	N/A	N/A	N/A	N/A	N/A	N/A	N/A	N/A	N/A	N/A	N/A	N/A	N/A	N/A	N/A	N/A	N/A	14.05
d3wIn	N/A	N/A	N/A	N/A	N/A	N/A	N/A	N/A	N/A	N/A	N/A	N/A	N/A	N/A	N/A	N/A	N/A	N/A	N/A	20.25
d3yIn	N/A	N/A	N/A	N/A	N/A	N/A	N/A	N/A	N/A	N/A	N/A	N/A	N/A	N/A	N/A	N/A	N/A	N/A	N/A	10.12
d2wIn	N/A	N/A	N/A	N/A	N/A	N/A	N/A	N/A	N/A	N/A	N/A	N/A	N/A	N/A	N/A	N/A	N/A	N/A	N/A	12.16
d2yIn	N/A	N/A	N/A	N/A	N/A	N/A	N/A	N/A	N/A	N/A	N/A	N/A	N/A	N/A	N/A	N/A	N/A	N/A	N/A	0.92
d1wIn	N/A	N/A	N/A	N/A	N/A	N/A	N/A	N/A	N/A	N/A	N/A	N/A	N/A	N/A	N/A	N/A	N/A	N/A	N/A	7.21
d1yIn	N/A	N/A	N/A	N/A	N/A	N/A	N/A	N/A	N/A	N/A	N/A	N/A	N/A	N/A	N/A	N/A	N/A	N/A	N/A	6.81
Average	N/A	N/A	N/A	N/A	N/A	N/A	N/A	N/A	N/A	N/A	N/A	N/A	N/A	N/A	N/A	N/A	N/A	N/A	N/A	9.87

Figure H.4: YALE polygonal mouth-open template test results (%)

Absolute Difference Pixel Values																									
% Param	s101	s105	s111	s116	s121	s1210	s155	s162	s221	s225	s231	s294	s306	s309	s39	s405	s510	s52	s71	s78	s85	s88	s94	s98	Average
c1kOut	2.29	NA	0.52	NA	NA	1.30	NA	NA	4.35	3.26	NA	NA	NA	NA	NA	0.20	0.51	1.40	NA	NA	1.66	NA	NA	NA	1.79
c1yOut	4.61	NA	0.80	NA	NA	0.82	NA	NA	3.20	1.82	NA	NA	NA	NA	NA	5.58	0.87	2.77	NA	NA	5.00	NA	NA	NA	2.80
u1kOut	0.46	NA	0.69	NA	NA	0.99	NA	NA	4.52	4.10	NA	NA	NA	NA	NA	2.58	1.15	0.73	NA	NA	0.33	NA	NA	NA	1.73
u1yOut	1.11	NA	0.14	NA	NA	5.85	NA	NA	0.80	1.35	NA	NA	NA	NA	NA	1.10	0.04	0.56	NA	NA	0.33	NA	NA	NA	1.25
u2kOut	0.96	NA	1.85	NA	NA	1.07	NA	NA	3.35	6.26	NA	NA	NA	NA	NA	1.20	3.85	0.60	NA	NA	0.33	NA	NA	NA	2.16
u2yOut	0.22	NA	0.80	NA	NA	5.85	NA	NA	0.20	1.02	NA	NA	NA	NA	NA	2.24	0.16	0.89	NA	NA	0.66	NA	NA	NA	1.34
u3kOut	1.46	NA	2.35	NA	NA	1.18	NA	NA	2.18	6.10	NA	NA	NA	NA	NA	0.20	0.51	1.60	NA	NA	0.01	NA	NA	NA	1.73
u3yOut	0.11	NA	0.14	NA	NA	5.85	NA	NA	0.13	0.02	NA	NA	NA	NA	NA	0.91	0.37	0.89	NA	NA	1.67	NA	NA	NA	1.12
c2kOut	1.29	NA	1.85	NA	NA	0.57	NA	NA	2.35	9.60	NA	NA	NA	NA	NA	1.47	1.15	0.94	NA	NA	1.99	NA	NA	NA	2.36
c2yOut	2.28	NA	0.14	NA	NA	0.18	NA	NA	6.20	7.15	NA	NA	NA	NA	NA	1.58	2.54	1.77	NA	NA	0.67	NA	NA	NA	2.50
d3kOut	2.37	NA	2.62	NA	NA	1.73	NA	NA	1.52	6.08	NA	NA	NA	NA	NA	0.82	0.49	1.41	NA	NA	1.66	NA	NA	NA	2.08
d3yOut	0.72	NA	1.04	NA	NA	4.40	NA	NA	3.37	4.11	NA	NA	NA	NA	NA	0.20	1.04	1.14	NA	NA	0.16	NA	NA	NA	1.80
d2kOut	1.44	NA	0.04	NA	NA	2.06	NA	NA	5.54	5.94	NA	NA	NA	NA	NA	1.63	0.75	1.02	NA	NA	2.22	NA	NA	NA	2.29
d2yOut	1.78	NA	2.27	NA	NA	4.77	NA	NA	4.77	3.45	NA	NA	NA	NA	NA	1.85	4.62	2.05	NA	NA	2.80	NA	NA	NA	3.15
d1kOut	0.24	NA	0.28	NA	NA	0.47	NA	NA	5.44	4.77	NA	NA	NA	NA	NA	0.92	1.52	0.61	NA	NA	1.69	NA	NA	NA	1.77
d1yOut	2.86	NA	1.30	NA	NA	2.21	NA	NA	1.87	3.30	NA	NA	NA	NA	NA	1.44	1.05	0.85	NA	NA	3.70	NA	NA	NA	2.06
c1kIn	1.29	NA	0.52	NA	NA	2.57	NA	NA	5.02	3.26	NA	NA	NA	NA	NA	0.53	1.18	0.06	NA	NA	2.33	NA	NA	NA	1.86
c1yIn	3.94	NA	1.14	NA	NA	1.18	NA	NA	2.20	0.48	NA	NA	NA	NA	NA	5.24	0.13	1.11	NA	NA	5.00	NA	NA	NA	2.27
u1kIn	2.13	NA	0.69	NA	NA	1.32	NA	NA	4.18	4.76	NA	NA	NA	NA	NA	2.58	0.51	0.40	NA	NA	1.33	NA	NA	NA	1.99
u1yIn	2.85	NA	3.07	NA	NA	2.58	NA	NA	1.07	1.45	NA	NA	NA	NA	NA	2.10	3.24	2.18	NA	NA	2.60	NA	NA	NA	2.35
u2kIn	2.63	NA	1.52	NA	NA	0.40	NA	NA	4.35	6.60	NA	NA	NA	NA	NA	0.47	4.18	0.60	NA	NA	1.33	NA	NA	NA	2.45
u2yIn	2.18	NA	2.41	NA	NA	3.58	NA	NA	1.40	1.78	NA	NA	NA	NA	NA	3.58	2.37	1.85	NA	NA	1.93	NA	NA	NA	2.34
u3kIn	3.13	NA	1.69	NA	NA	1.15	NA	NA	3.52	9.10	NA	NA	NA	NA	NA	1.47	1.82	0.94	NA	NA	1.33	NA	NA	NA	2.68
u3yIn	2.18	NA	2.41	NA	NA	2.24	NA	NA	1.40	3.78	NA	NA	NA	NA	NA	2.91	3.24	2.18	NA	NA	1.27	NA	NA	NA	2.40
c2kIn	1.96	NA	2.85	NA	NA	1.57	NA	NA	2.68	13.60	NA	NA	NA	NA	NA	2.14	3.82	1.40	NA	NA	4.33	NA	NA	NA	3.82
c2yIn	1.94	NA	1.47	NA	NA	0.52	NA	NA	5.20	5.48	NA	NA	NA	NA	NA	2.58	1.54	1.77	NA	NA	0.00	NA	NA	NA	2.28
d3kIn	3.44	NA	2.39	NA	NA	3.11	NA	NA	4.42	8.44	NA	NA	NA	NA	NA	1.53	3.73	1.84	NA	NA	4.09	NA	NA	NA	3.67
d3yIn	0.77	NA	1.08	NA	NA	5.18	NA	NA	3.79	3.93	NA	NA	NA	NA	NA	0.30	2.74	0.32	NA	NA	0.93	NA	NA	NA	2.12
d2kIn	2.09	NA	1.06	NA	NA	0.50	NA	NA	3.70	5.36	NA	NA	NA	NA	NA	0.59	1.84	0.60	NA	NA	1.91	NA	NA	NA	1.96
d2yIn	1.56	NA	0.44	NA	NA	6.57	NA	NA	3.51	2.39	NA	NA	NA	NA	NA	2.84	1.65	0.38	NA	NA	0.72	NA	NA	NA	2.23
d1kIn	1.24	NA	0.89	NA	NA	1.06	NA	NA	2.99	2.56	NA	NA	NA	NA	NA	1.92	0.96	2.32	NA	NA	0.41	NA	NA	NA	1.61
d1yIn	1.85	NA	0.66	NA	NA	6.19	NA	NA	1.24	1.30	NA	NA	NA	NA	NA	2.10	2.86	1.48	NA	NA	2.27	NA	NA	NA	2.22
Average	1.86	NA	1.29	NA	NA	2.48	NA	NA	3.14	4.46	NA	NA	NA	NA	NA	1.77	1.76	1.21	NA	NA	1.77	NA	NA	NA	NA

Figure H.5: ORL polygonal mouth-open template test results

Percentage (of width) Diff		s101	s105	s111	s116	s121	s1210	s155	s162	s221	s225	s231	s294	s306	s309	s39	s405	s510	s52	s71	s78	s85	s88	s94	s98	Average
% Param																										
ckOut	8.49	NA	2.10	NA	NA	5.89	NA	NA	NA	10.88	7.47	NA	NA	NA	NA	NA	0.75	1.69	4.07	NA	NA	5.24	NA	NA	NA	5.18
cljOut	17.08	NA	3.25	NA	NA	1.59	NA	NA	NA	8.01	4.16	NA	NA	NA	NA	NA	21.18	2.87	8.07	NA	NA	15.77	NA	NA	NA	9.11
ukOut	1.70	NA	2.78	NA	NA	3.05	NA	NA	NA	11.29	9.38	NA	NA	NA	NA	NA	9.81	3.80	2.12	NA	NA	1.03	NA	NA	NA	5.00
uljOut	4.12	NA	0.55	NA	NA	18.09	NA	NA	NA	1.99	3.10	NA	NA	NA	NA	NA	4.19	0.12	1.63	NA	NA	1.04	NA	NA	NA	3.87
u2xOut	3.55	NA	7.51	NA	NA	3.31	NA	NA	NA	8.38	14.34	NA	NA	NA	NA	NA	4.55	12.69	1.76	NA	NA	1.03	NA	NA	NA	6.35
u2jOut	0.82	NA	3.25	NA	NA	18.09	NA	NA	NA	0.51	2.33	NA	NA	NA	NA	NA	8.52	0.52	2.61	NA	NA	2.09	NA	NA	NA	4.31
u3xOut	5.41	NA	9.54	NA	NA	3.65	NA	NA	NA	5.46	13.96	NA	NA	NA	NA	NA	0.75	1.69	4.67	NA	NA	0.02	NA	NA	NA	5.02
u3jOut	0.41	NA	0.55	NA	NA	18.09	NA	NA	NA	0.32	0.04	NA	NA	NA	NA	NA	3.46	1.22	2.61	NA	NA	5.28	NA	NA	NA	3.55
e2xOut	4.79	NA	7.51	NA	NA	1.76	NA	NA	NA	5.88	21.97	NA	NA	NA	NA	NA	5.58	3.80	2.73	NA	NA	6.29	NA	NA	NA	6.70
e2jOut	8.44	NA	0.55	NA	NA	0.56	NA	NA	NA	15.51	16.37	NA	NA	NA	NA	NA	5.59	8.36	5.16	NA	NA	2.12	NA	NA	NA	7.01
d3xOut	8.78	NA	10.63	NA	NA	5.36	NA	NA	NA	3.80	13.92	NA	NA	NA	NA	NA	3.13	1.61	4.11	NA	NA	5.25	NA	NA	NA	6.29
d3jOut	2.66	NA	4.20	NA	NA	13.60	NA	NA	NA	8.42	9.40	NA	NA	NA	NA	NA	0.75	3.42	3.32	NA	NA	0.50	NA	NA	NA	5.14
d2xOut	5.33	NA	0.16	NA	NA	6.37	NA	NA	NA	13.85	13.61	NA	NA	NA	NA	NA	6.18	2.46	2.98	NA	NA	7.02	NA	NA	NA	6.44
d2jOut	6.61	NA	9.19	NA	NA	14.76	NA	NA	NA	11.93	7.89	NA	NA	NA	NA	NA	7.04	15.22	5.98	NA	NA	8.84	NA	NA	NA	9.72
dlxOut	0.89	NA	1.15	NA	NA	1.46	NA	NA	NA	13.59	10.93	NA	NA	NA	NA	NA	3.48	5.02	1.77	NA	NA	5.35	NA	NA	NA	4.85
dljOut	10.58	NA	5.28	NA	NA	6.94	NA	NA	NA	4.67	7.55	NA	NA	NA	NA	NA	5.45	3.48	2.46	NA	NA	11.69	NA	NA	NA	6.44
ckIn	4.79	NA	2.10	NA	NA	7.95	NA	NA	NA	12.54	7.47	NA	NA	NA	NA	NA	2.02	3.89	0.18	NA	NA	7.34	NA	NA	NA	5.37
cljIn	14.61	NA	4.61	NA	NA	3.66	NA	NA	NA	5.51	1.10	NA	NA	NA	NA	NA	19.92	0.43	3.22	NA	NA	15.77	NA	NA	NA	7.65
ukIn	7.88	NA	2.78	NA	NA	4.08	NA	NA	NA	10.46	10.90	NA	NA	NA	NA	NA	9.81	1.69	1.15	NA	NA	4.19	NA	NA	NA	5.88
uljIn	10.56	NA	12.46	NA	NA	7.97	NA	NA	NA	2.67	3.32	NA	NA	NA	NA	NA	7.98	10.70	6.34	NA	NA	8.21	NA	NA	NA	7.80
u2xIn	9.73	NA	6.16	NA	NA	1.25	NA	NA	NA	10.88	15.10	NA	NA	NA	NA	NA	1.78	13.79	1.76	NA	NA	4.19	NA	NA	NA	7.18
u2jIn	8.09	NA	9.76	NA	NA	11.07	NA	NA	NA	3.51	4.09	NA	NA	NA	NA	NA	13.59	7.80	5.37	NA	NA	6.10	NA	NA	NA	7.71
u3xIn	11.58	NA	6.83	NA	NA	3.57	NA	NA	NA	8.79	20.83	NA	NA	NA	NA	NA	5.58	6.00	2.73	NA	NA	4.19	NA	NA	NA	7.79
u3jIn	8.09	NA	9.76	NA	NA	6.94	NA	NA	NA	3.51	8.67	NA	NA	NA	NA	NA	11.06	10.70	6.34	NA	NA	4.00	NA	NA	NA	7.67
e2xIn	7.26	NA	11.56	NA	NA	4.86	NA	NA	NA	6.71	31.13	NA	NA	NA	NA	NA	8.11	12.59	4.07	NA	NA	13.66	NA	NA	NA	11.11
e2jIn	7.20	NA	5.96	NA	NA	1.59	NA	NA	NA	13.01	12.55	NA	NA	NA	NA	NA	9.79	5.07	5.16	NA	NA	0.01	NA	NA	NA	6.71
d3xIn	12.75	NA	9.70	NA	NA	9.61	NA	NA	NA	11.06	19.32	NA	NA	NA	NA	NA	5.80	12.31	5.36	NA	NA	12.92	NA	NA	NA	10.98
d3jIn	2.87	NA	4.39	NA	NA	16.01	NA	NA	NA	9.48	9.00	NA	NA	NA	NA	NA	1.15	9.03	0.94	NA	NA	2.94	NA	NA	NA	6.20
d2xIn	7.74	NA	4.29	NA	NA	1.56	NA	NA	NA	9.26	12.28	NA	NA	NA	NA	NA	2.25	6.06	1.76	NA	NA	6.04	NA	NA	NA	5.69
d2jIn	5.77	NA	1.80	NA	NA	20.32	NA	NA	NA	8.78	5.47	NA	NA	NA	NA	NA	10.77	5.45	1.12	NA	NA	2.28	NA	NA	NA	6.86
dlxIn	4.60	NA	4.03	NA	NA	3.28	NA	NA	NA	7.47	5.86	NA	NA	NA	NA	NA	7.27	3.15	6.77	NA	NA	1.30	NA	NA	NA	4.86
dljIn	6.86	NA	2.67	NA	NA	19.14	NA	NA	NA	3.10	2.98	NA	NA	NA	NA	NA	7.98	9.42	4.31	NA	NA	7.18	NA	NA	NA	7.07
Average	6.88	NA	5.22	NA	NA	7.67	NA	NA	NA	7.85	###	NA	NA	NA	NA	NA	6.74	5.81	3.52	NA	NA	5.59	NA	NA	NA	NA

Figure H.6: ORL polygonal mouth-open template test results (%)

APPENDIX I

Spline-based Mouth-Open Template Detailed Test Results

Absolute Difference Pixel Values																				
% Param Name	K.A.Diff	K.A.HA	K.A.SA	K.A.SU	KL.AN	KL.FE	KM.DH	KM.SA	KR.AN	MK.SA	NA.AN	NA.HA	NA.SU	NM.DH	TM.FE	TM.SA	UY.AN	UY.DH	YM.HA	Average
c1kOut	NA	5.11	NA	NA	NA	NA	2.24	NA	NA	NA	NA	4.06	3.46	NA	1.70	NA	NA	NA	2.58	3.19
c1yOut	NA	7.98	NA	NA	NA	NA	6.71	NA	NA	NA	NA	7.87	6.38	NA	2.87	NA	NA	NA	10.05	6.98
u1kOut	NA	2.27	NA	NA	NA	NA	0.43	NA	NA	NA	NA	6.23	2.29	NA	0.53	NA	NA	NA	2.17	2.32
u1yOut	NA	1.86	NA	NA	NA	NA	1.55	NA	NA	NA	NA	2.21	1.88	NA	1.96	NA	NA	NA	0.12	1.60
u2xOut	NA	0.44	NA	NA	NA	NA	2.91	NA	NA	NA	NA	5.06	3.46	NA	1.03	NA	NA	NA	4.26	2.86
u2yOut	NA	1.86	NA	NA	NA	NA	5.88	NA	NA	NA	NA	2.21	3.22	NA	0.29	NA	NA	NA	1.12	2.43
u3xOut	NA	0.73	NA	NA	NA	NA	5.91	NA	NA	NA	NA	1.23	5.07	NA	0.20	NA	NA	NA	7.01	3.36
u3yOut	NA	2.19	NA	NA	NA	NA	0.21	NA	NA	NA	NA	0.87	0.21	NA	0.71	NA	NA	NA	0.55	0.79
e2xOut	NA	0.56	NA	NA	NA	NA	0.91	NA	NA	NA	NA	0.27	4.12	NA	0.97	NA	NA	NA	10.76	2.93
e2yOut	NA	5.31	NA	NA	NA	NA	4.71	NA	NA	NA	NA	5.54	5.38	NA	3.54	NA	NA	NA	9.72	5.70
d3xOut	NA	0.24	NA	NA	NA	NA	3.17	NA	NA	NA	NA	1.65	4.23	NA	2.09	NA	NA	NA	7.36	3.12
d3yOut	NA	2.43	NA	NA	NA	NA	7.37	NA	NA	NA	NA	2.80	0.91	NA	2.42	NA	NA	NA	5.01	3.49
d2xOut	NA	1.77	NA	NA	NA	NA	0.69	NA	NA	NA	NA	3.83	3.11	NA	2.32	NA	NA	NA	3.91	2.60
d2yOut	NA	2.18	NA	NA	NA	NA	2.17	NA	NA	NA	NA	1.72	3.79	NA	0.44	NA	NA	NA	3.68	2.33
d1xOut	NA	1.06	NA	NA	NA	NA	0.39	NA	NA	NA	NA	3.04	0.17	NA	3.65	NA	NA	NA	2.88	1.86
d1yOut	NA	3.66	NA	NA	NA	NA	8.75	NA	NA	NA	NA	3.49	3.55	NA	0.04	NA	NA	NA	5.80	4.21
e1kIn	NA	4.44	NA	NA	NA	NA	3.24	NA	NA	NA	NA	3.06	1.46	NA	2.37	NA	NA	NA	2.24	2.80
e1yIn	NA	6.64	NA	NA	NA	NA	5.05	NA	NA	NA	NA	5.87	5.05	NA	1.54	NA	NA	NA	9.05	5.53
u1kIn	NA	3.27	NA	NA	NA	NA	2.24	NA	NA	NA	NA	4.23	2.96	NA	1.20	NA	NA	NA	4.84	3.12
u1yIn	NA	0.87	NA	NA	NA	NA	1.72	NA	NA	NA	NA	5.61	1.61	NA	1.44	NA	NA	NA	0.88	2.02
u2xIn	NA	2.77	NA	NA	NA	NA	1.57	NA	NA	NA	NA	4.73	5.46	NA	1.37	NA	NA	NA	4.59	3.41
u2yIn	NA	0.54	NA	NA	NA	NA	2.72	NA	NA	NA	NA	4.95	1.61	NA	0.10	NA	NA	NA	0.88	1.80
u3xIn	NA	3.61	NA	NA	NA	NA	1.24	NA	NA	NA	NA	5.23	9.07	NA	0.47	NA	NA	NA	6.01	4.27
u3yIn	NA	1.20	NA	NA	NA	NA	2.39	NA	NA	NA	NA	4.28	0.94	NA	2.77	NA	NA	NA	2.88	2.41
e2xIn	NA	2.11	NA	NA	NA	NA	4.76	NA	NA	NA	NA	3.39	7.79	NA	3.30	NA	NA	NA	9.09	5.07
e2yIn	NA	4.64	NA	NA	NA	NA	6.05	NA	NA	NA	NA	5.54	4.72	NA	1.87	NA	NA	NA	8.38	5.20
d3xIn	NA	2.95	NA	NA	NA	NA	1.27	NA	NA	NA	NA	4.32	7.49	NA	0.11	NA	NA	NA	4.43	3.43
d3yIn	NA	0.98	NA	NA	NA	NA	0.17	NA	NA	NA	NA	0.01	1.98	NA	0.91	NA	NA	NA	2.61	1.11
d2xIn	NA	0.52	NA	NA	NA	NA	2.61	NA	NA	NA	NA	2.20	2.01	NA	3.27	NA	NA	NA	3.94	2.43
d2yIn	NA	2.08	NA	NA	NA	NA	4.07	NA	NA	NA	NA	0.16	2.45	NA	6.40	NA	NA	NA	1.75	2.82
d1xIn	NA	2.30	NA	NA	NA	NA	4.72	NA	NA	NA	NA	0.79	1.26	NA	3.75	NA	NA	NA	4.50	2.89
d1yIn	NA	3.39	NA	NA	NA	NA	4.09	NA	NA	NA	NA	0.33	0.96	NA	2.55	NA	NA	NA	0.46	1.96
Average																				
NA	2.56	NA	NA	NA	NA	NA	3.18	NA	NA	NA	NA	3.34	3.38	NA	1.82	NA	NA	NA	4.48	

Figure I.1: JAFFE spline-based mouth-open template test results

Percentage (of width) Diff																					
% Param Name	KADiff	KA.HA	KA.SA	KA.SU	KL.AN	KL.FE2	KM.DH	KM.SA	KR.AN	MK.SA	NA.AN	NA.HA	NA.SU	NM.DI	TM.FE	TM.SA	UY.AN	UY.DI2	YM.DH	YMH2	Average
c1xOut	NA	9.89	NA	NA	NA	NA	5.79	NA	NA	NA	NA	6.51	7.00	NA	3.93	NA	NA	NA	NA	4.42	6.26
c1yOut	NA	15.44	NA	NA	NA	NA	17.36	NA	NA	NA	NA	12.63	12.94	NA	6.63	NA	NA	NA	NA	17.23	13.70
u1xOut	NA	4.40	NA	NA	NA	NA	1.11	NA	NA	NA	NA	9.99	4.64	NA	1.23	NA	NA	NA	NA	3.72	4.18
u1yOut	NA	3.60	NA	NA	NA	NA	4.00	NA	NA	NA	NA	3.54	3.81	NA	4.52	NA	NA	NA	NA	0.20	3.28
u2xOut	NA	0.85	NA	NA	NA	NA	7.51	NA	NA	NA	NA	8.12	7.00	NA	2.39	NA	NA	NA	NA	7.30	5.53
u2yOut	NA	3.60	NA	NA	NA	NA	15.21	NA	NA	NA	NA	3.54	6.52	NA	0.68	NA	NA	NA	NA	1.92	5.24
u3xOut	NA	140	NA	NA	NA	NA	15.27	NA	NA	NA	NA	1.97	10.28	NA	0.46	NA	NA	NA	NA	12.01	6.90
u3yOut	NA	4.24	NA	NA	NA	NA	0.55	NA	NA	NA	NA	1.40	0.43	NA	1.63	NA	NA	NA	NA	0.94	1.53
c2xOut	NA	108	NA	NA	NA	NA	2.34	NA	NA	NA	NA	0.44	8.36	NA	2.23	NA	NA	NA	NA	18.44	5.48
c2yOut	NA	10.27	NA	NA	NA	NA	12.19	NA	NA	NA	NA	8.89	10.91	NA	8.17	NA	NA	NA	NA	16.66	11.18
d3xOut	NA	0.46	NA	NA	NA	NA	8.20	NA	NA	NA	NA	2.64	8.57	NA	4.82	NA	NA	NA	NA	12.61	6.22
d3yOut	NA	4.71	NA	NA	NA	NA	19.05	NA	NA	NA	NA	4.50	1.84	NA	5.58	NA	NA	NA	NA	8.58	7.38
d2xOut	NA	3.43	NA	NA	NA	NA	1.78	NA	NA	NA	NA	6.14	6.30	NA	5.35	NA	NA	NA	NA	6.70	4.95
d2yOut	NA	4.21	NA	NA	NA	NA	5.60	NA	NA	NA	NA	2.77	7.69	NA	1.01	NA	NA	NA	NA	6.31	4.60
d1xOut	NA	2.04	NA	NA	NA	NA	1.00	NA	NA	NA	NA	4.88	0.35	NA	8.42	NA	NA	NA	NA	4.93	3.60
d1yOut	NA	7.08	NA	NA	NA	NA	22.63	NA	NA	NA	NA	5.59	7.19	NA	0.09	NA	NA	NA	NA	9.94	8.75
c1xIn	NA	8.60	NA	NA	NA	NA	8.38	NA	NA	NA	NA	4.91	2.95	NA	5.46	NA	NA	NA	NA	3.85	5.69
c1yIn	NA	12.86	NA	NA	NA	NA	13.05	NA	NA	NA	NA	9.42	10.23	NA	3.55	NA	NA	NA	NA	15.51	10.77
u1xIn	NA	6.34	NA	NA	NA	NA	5.79	NA	NA	NA	NA	6.78	5.99	NA	2.77	NA	NA	NA	NA	8.30	5.99
u1yIn	NA	1.69	NA	NA	NA	NA	4.46	NA	NA	NA	NA	9.01	3.27	NA	3.31	NA	NA	NA	NA	1.51	3.87
u2xIn	NA	5.37	NA	NA	NA	NA	4.07	NA	NA	NA	NA	7.58	11.06	NA	3.16	NA	NA	NA	NA	7.87	6.52
u2yIn	NA	1.04	NA	NA	NA	NA	7.05	NA	NA	NA	NA	7.94	3.27	NA	0.24	NA	NA	NA	NA	1.51	3.51
u3xIn	NA	6.98	NA	NA	NA	NA	3.20	NA	NA	NA	NA	8.39	18.38	NA	1.07	NA	NA	NA	NA	10.30	8.05
u3yIn	NA	2.33	NA	NA	NA	NA	6.18	NA	NA	NA	NA	6.87	1.91	NA	6.39	NA	NA	NA	NA	4.94	4.77
c2xIn	NA	4.08	NA	NA	NA	NA	12.31	NA	NA	NA	NA	5.44	15.79	NA	7.61	NA	NA	NA	NA	15.58	10.14
c2yIn	NA	8.98	NA	NA	NA	NA	15.64	NA	NA	NA	NA	8.89	9.56	NA	4.32	NA	NA	NA	NA	14.37	10.29
d3xIn	NA	5.71	NA	NA	NA	NA	3.28	NA	NA	NA	NA	6.93	15.18	NA	0.26	NA	NA	NA	NA	7.60	6.49
d3yIn	NA	1.90	NA	NA	NA	NA	0.43	NA	NA	NA	NA	0.02	4.01	NA	2.10	NA	NA	NA	NA	4.47	2.15
d2xIn	NA	1.00	NA	NA	NA	NA	6.76	NA	NA	NA	NA	3.54	4.07	NA	7.54	NA	NA	NA	NA	6.76	4.95
d2yIn	NA	4.03	NA	NA	NA	NA	10.53	NA	NA	NA	NA	0.26	4.96	NA	14.78	NA	NA	NA	NA	3.00	6.26
d1xIn	NA	4.45	NA	NA	NA	NA	12.22	NA	NA	NA	NA	1.27	2.56	NA	8.66	NA	NA	NA	NA	7.71	6.15
d1yIn	NA	6.55	NA	NA	NA	NA	10.57	NA	NA	NA	NA	0.53	1.94	NA	5.89	NA	NA	NA	NA	0.79	4.38
Average		NA	4.96	NA	NA	NA	8.24	NA	NA	NA	NA	5.35	6.84	NA	4.20	NA	NA	NA	NA	7.69	

Figure I.2: JAFFE spline-based mouth-open template test results (%)

Absolute Difference Pixel Values																						
% Param	01.cen	02.ct	03.npt	04.npt	05.npt	06.glt	06.npt	08.cen	09.npt	09.npt	09.npt	09.npt	12.cen	12.ct	13.cen	14.ct	15.npt	15.npt	15.npt	15.npt	15.npt	Average
c1xOut	NA	NA	NA	NA	NA	NA	NA	NA	NA	NA	NA	NA	NA	NA	NA	NA	7.23	NA	3.09	NA	5.16	
c1yOut	NA	NA	NA	NA	NA	NA	NA	NA	NA	NA	NA	NA	NA	NA	NA	NA	8.31	NA	13.15	NA	10.73	
u1xOut	NA	NA	NA	NA	NA	NA	NA	NA	NA	NA	NA	NA	NA	NA	NA	NA	3.14	NA	4.43	NA	3.79	
u1yOut	NA	NA	NA	NA	NA	NA	NA	NA	NA	NA	NA	NA	NA	NA	NA	NA	0.36	NA	4.98	NA	2.67	
u2xOut	NA	NA	NA	NA	NA	NA	NA	NA	NA	NA	NA	NA	NA	NA	NA	NA	2.73	NA	2.03	NA	2.38	
u2yOut	NA	NA	NA	NA	NA	NA	NA	NA	NA	NA	NA	NA	NA	NA	NA	NA	1.02	NA	13.82	NA	7.42	
u3xOut	NA	NA	NA	NA	NA	NA	NA	NA	NA	NA	NA	NA	NA	NA	NA	NA	3.31	NA	0.57	NA	1.94	
u3yOut	NA	NA	NA	NA	NA	NA	NA	NA	NA	NA	NA	NA	NA	NA	NA	NA	0.02	NA	4.31	NA	2.17	
c2xOut	NA	NA	NA	NA	NA	NA	NA	NA	NA	NA	NA	NA	NA	NA	NA	NA	2.56	NA	1.24	NA	1.90	
c2yOut	NA	NA	NA	NA	NA	NA	NA	NA	NA	NA	NA	NA	NA	NA	NA	NA	9.64	NA	13.15	NA	11.39	
d3xOut	NA	NA	NA	NA	NA	NA	NA	NA	NA	NA	NA	NA	NA	NA	NA	NA	3.63	NA	2.78	NA	3.20	
d3yOut	NA	NA	NA	NA	NA	NA	NA	NA	NA	NA	NA	NA	NA	NA	NA	NA	8.43	NA	7.80	NA	8.12	
d2xOut	NA	NA	NA	NA	NA	NA	NA	NA	NA	NA	NA	NA	NA	NA	NA	NA	2.41	NA	0.84	NA	1.62	
d2yOut	NA	NA	NA	NA	NA	NA	NA	NA	NA	NA	NA	NA	NA	NA	NA	NA	6.11	NA	12.49	NA	9.30	
d1xOut	NA	NA	NA	NA	NA	NA	NA	NA	NA	NA	NA	NA	NA	NA	NA	NA	0.44	NA	2.42	NA	1.43	
d1yOut	NA	NA	NA	NA	NA	NA	NA	NA	NA	NA	NA	NA	NA	NA	NA	NA	8.09	NA	7.80	NA	7.94	
c1xIn	NA	NA	NA	NA	NA	NA	NA	NA	NA	NA	NA	NA	NA	NA	NA	NA	7.23	NA	2.43	NA	4.83	
c1yIn	NA	NA	NA	NA	NA	NA	NA	NA	NA	NA	NA	NA	NA	NA	NA	NA	7.98	NA	13.15	NA	10.56	
u1xIn	NA	NA	NA	NA	NA	NA	NA	NA	NA	NA	NA	NA	NA	NA	NA	NA	3.14	NA	2.43	NA	2.79	
u1yIn	NA	NA	NA	NA	NA	NA	NA	NA	NA	NA	NA	NA	NA	NA	NA	NA	4.17	NA	7.42	NA	5.79	
u2xIn	NA	NA	NA	NA	NA	NA	NA	NA	NA	NA	NA	NA	NA	NA	NA	NA	3.39	NA	3.36	NA	3.38	
u2yIn	NA	NA	NA	NA	NA	NA	NA	NA	NA	NA	NA	NA	NA	NA	NA	NA	3.17	NA	15.26	NA	9.22	
u3xIn	NA	NA	NA	NA	NA	NA	NA	NA	NA	NA	NA	NA	NA	NA	NA	NA	3.64	NA	2.43	NA	3.04	
u3yIn	NA	NA	NA	NA	NA	NA	NA	NA	NA	NA	NA	NA	NA	NA	NA	NA	4.51	NA	6.42	NA	5.46	
c2xIn	NA	NA	NA	NA	NA	NA	NA	NA	NA	NA	NA	NA	NA	NA	NA	NA	4.89	NA	2.09	NA	3.49	
c2yIn	NA	NA	NA	NA	NA	NA	NA	NA	NA	NA	NA	NA	NA	NA	NA	NA	8.64	NA	12.48	NA	10.56	
d3xIn	NA	NA	NA	NA	NA	NA	NA	NA	NA	NA	NA	NA	NA	NA	NA	NA	6.22	NA	159	NA	3.90	
d3yIn	NA	NA	NA	NA	NA	NA	NA	NA	NA	NA	NA	NA	NA	NA	NA	NA	5.66	NA	1.81	NA	3.69	
d2xIn	NA	NA	NA	NA	NA	NA	NA	NA	NA	NA	NA	NA	NA	NA	NA	NA	2.71	NA	0.32	NA	1.51	
d2yIn	NA	NA	NA	NA	NA	NA	NA	NA	NA	NA	NA	NA	NA	NA	NA	NA	1.87	NA	11.39	NA	6.63	
d1xIn	NA	NA	NA	NA	NA	NA	NA	NA	NA	NA	NA	NA	NA	NA	NA	NA	0.49	NA	1.91	NA	1.20	
d1yIn	NA	NA	NA	NA	NA	NA	NA	NA	NA	NA	NA	NA	NA	NA	NA	NA	2.09	NA	2.46	NA	2.28	
Average	NA	NA	NA	NA	NA	NA	NA	NA	NA	NA	NA	NA	NA	NA	NA	NA	4.29	NA	NA	NA	5.68	

Figure I.3: YALE spline-based mouth-open template test results

Percentage (of width) Diff																															
01.correct		02.t03		04.npt		05.npt		06.gst		06.nlect		08.cer		09.nopt		09.nlect		09.sect		12.correct		13.correct		14.ctt		15.net		15.su		Average	
clt	Out	NA	NA	NA	NA	NA	NA	NA	NA	NA	NA	NA	NA	NA	NA	NA	NA	NA	NA	NA	NA	NA	NA	NA	NA	NA	NA	NA	NA	NA	NA
clt	Out	NA	NA	NA	NA	NA	NA	NA	NA	NA	NA	NA	NA	NA	NA	NA	NA	NA	NA	NA	NA	NA	NA	NA	NA	NA	NA	NA	NA	NA	NA
ult	Out	NA	NA	NA	NA	NA	NA	NA	NA	NA	NA	NA	NA	NA	NA	NA	NA	NA	NA	NA	NA	NA	NA	NA	NA	NA	NA	NA	NA	NA	NA
ult	Out	NA	NA	NA	NA	NA	NA	NA	NA	NA	NA	NA	NA	NA	NA	NA	NA	NA	NA	NA	NA	NA	NA	NA	NA	NA	NA	NA	NA	NA	NA
u2	Out	NA	NA	NA	NA	NA	NA	NA	NA	NA	NA	NA	NA	NA	NA	NA	NA	NA	NA	NA	NA	NA	NA	NA	NA	NA	NA	NA	NA	NA	NA
u2	Out	NA	NA	NA	NA	NA	NA	NA	NA	NA	NA	NA	NA	NA	NA	NA	NA	NA	NA	NA	NA	NA	NA	NA	NA	NA	NA	NA	NA	NA	NA
u2	Out	NA	NA	NA	NA	NA	NA	NA	NA	NA	NA	NA	NA	NA	NA	NA	NA	NA	NA	NA	NA	NA	NA	NA	NA	NA	NA	NA	NA	NA	NA
u3	Out	NA	NA	NA	NA	NA	NA	NA	NA	NA	NA	NA	NA	NA	NA	NA	NA	NA	NA	NA	NA	NA	NA	NA	NA	NA	NA	NA	NA	NA	NA
u3	Out	NA	NA	NA	NA	NA	NA	NA	NA	NA	NA	NA	NA	NA	NA	NA	NA	NA	NA	NA	NA	NA	NA	NA	NA	NA	NA	NA	NA	NA	NA
c2	Out	NA	NA	NA	NA	NA	NA	NA	NA	NA	NA	NA	NA	NA	NA	NA	NA	NA	NA	NA	NA	NA	NA	NA	NA	NA	NA	NA	NA	NA	NA
c2	Out	NA	NA	NA	NA	NA	NA	NA	NA	NA	NA	NA	NA	NA	NA	NA	NA	NA	NA	NA	NA	NA	NA	NA	NA	NA	NA	NA	NA	NA	NA
d3	Out	NA	NA	NA	NA	NA	NA	NA	NA	NA	NA	NA	NA	NA	NA	NA	NA	NA	NA	NA	NA	NA	NA	NA	NA	NA	NA	NA	NA	NA	NA
d3	Out	NA	NA	NA	NA	NA	NA	NA	NA	NA	NA	NA	NA	NA	NA	NA	NA	NA	NA	NA	NA	NA	NA	NA	NA	NA	NA	NA	NA	NA	NA
d2	Out	NA	NA	NA	NA	NA	NA	NA	NA	NA	NA	NA	NA	NA	NA	NA	NA	NA	NA	NA	NA	NA	NA	NA	NA	NA	NA	NA	NA	NA	NA
d2	Out	NA	NA	NA	NA	NA	NA	NA	NA	NA	NA	NA	NA	NA	NA	NA	NA	NA	NA	NA	NA	NA	NA	NA	NA	NA	NA	NA	NA	NA	NA
d1	Out	NA	NA	NA	NA	NA	NA	NA	NA	NA	NA	NA	NA	NA	NA	NA	NA	NA	NA	NA	NA	NA	NA	NA	NA	NA	NA	NA	NA	NA	NA
d1	Out	NA	NA	NA	NA	NA	NA	NA	NA	NA	NA	NA	NA	NA	NA	NA	NA	NA	NA	NA	NA	NA	NA	NA	NA	NA	NA	NA	NA	NA	NA
c1	in	NA	NA	NA	NA	NA	NA	NA	NA	NA	NA	NA	NA	NA	NA	NA	NA	NA	NA	NA	NA	NA	NA	NA	NA	NA	NA	NA	NA	NA	NA
c1	in	NA	NA	NA	NA	NA	NA	NA	NA	NA	NA	NA	NA	NA	NA	NA	NA	NA	NA	NA	NA	NA	NA	NA	NA	NA	NA	NA	NA	NA	NA
u1	in	NA	NA	NA	NA	NA	NA	NA	NA	NA	NA	NA	NA	NA	NA	NA	NA	NA	NA	NA	NA	NA	NA	NA	NA	NA	NA	NA	NA	NA	NA
u2	in	NA	NA	NA	NA	NA	NA	NA	NA	NA	NA	NA	NA	NA	NA	NA	NA	NA	NA	NA	NA	NA	NA	NA	NA	NA	NA	NA	NA	NA	NA
u2	in	NA	NA	NA	NA	NA	NA	NA	NA	NA	NA	NA	NA	NA	NA	NA	NA	NA	NA	NA	NA	NA	NA	NA	NA	NA	NA	NA	NA	NA	NA
u3	in	NA	NA	NA	NA	NA	NA	NA	NA	NA	NA	NA	NA	NA	NA	NA	NA	NA	NA	NA	NA	NA	NA	NA	NA	NA	NA	NA	NA	NA	NA
u3	in	NA	NA	NA	NA	NA	NA	NA	NA	NA	NA	NA	NA	NA	NA	NA	NA	NA	NA	NA	NA	NA	NA	NA	NA	NA	NA	NA	NA	NA	NA
u3	in	NA	NA	NA	NA	NA	NA	NA	NA	NA	NA	NA	NA	NA	NA	NA	NA	NA	NA	NA	NA	NA	NA	NA	NA	NA	NA	NA	NA	NA	NA
u3	in	NA	NA	NA	NA	NA	NA	NA	NA	NA	NA	NA	NA	NA	NA	NA	NA	NA	NA	NA	NA	NA	NA	NA	NA	NA	NA	NA	NA	NA	NA
u3	in	NA	NA	NA	NA	NA	NA	NA	NA	NA	NA	NA	NA	NA	NA	NA	NA	NA	NA	NA	NA	NA	NA	NA	NA	NA	NA	NA	NA	NA	NA
u3	in	NA	NA	NA	NA	NA	NA	NA	NA	NA	NA	NA	NA	NA	NA	NA	NA	NA	NA	NA	NA	NA	NA	NA	NA	NA	NA	NA	NA	NA	NA
u3	in	NA	NA	NA	NA	NA	NA	NA	NA	NA	NA	NA	NA	NA	NA	NA	NA	NA	NA	NA	NA	NA	NA	NA	NA	NA	NA	NA	NA	NA	NA
u3	in	NA	NA	NA	NA	NA	NA	NA	NA	NA	NA	NA	NA	NA	NA	NA	NA	NA	NA	NA	NA	NA	NA	NA	NA	NA	NA	NA	NA	NA	NA
u3	in	NA	NA	NA	NA	NA	NA	NA	NA	NA	NA	NA	NA	NA	NA	NA	NA	NA	NA	NA	NA	NA	NA	NA	NA	NA	NA	NA	NA	NA	NA
u3	in	NA	NA	NA	NA	NA	NA	NA	NA	NA	NA	NA	NA	NA	NA	NA	NA	NA	NA	NA	NA	NA	NA	NA	NA	NA	NA	NA	NA	NA	NA
u3	in	NA	NA	NA	NA	NA	NA	NA	NA	NA	NA	NA	NA	NA	NA	NA	NA	NA	NA	NA	NA	NA	NA	NA	NA	NA	NA	NA	NA	NA	NA
u3	in	NA	NA	NA	NA	NA	NA	NA	NA	NA	NA	NA	NA	NA	NA	NA	NA	NA	NA	NA	NA	NA	NA	NA	NA	NA	NA	NA	NA	NA	NA
u3	in	NA	NA	NA	NA	NA	NA	NA	NA	NA	NA	NA	NA	NA	NA	NA	NA	NA	NA	NA	NA	NA	NA	NA	NA	NA	NA	NA	NA	NA	NA
u3	in	NA	NA	NA	NA	NA	NA	NA	NA	NA	NA	NA	NA	NA	NA	NA	NA	NA	NA	NA	NA	NA	NA	NA	NA	NA	NA	NA	NA	NA	NA
u3	in	NA	NA	NA	NA	NA	NA	NA	NA	NA	NA	NA	NA	NA	NA	NA	NA	NA	NA	NA	NA	NA	NA	NA	NA	NA	NA	NA	NA	NA	NA
u3	in	NA	NA	NA	NA	NA	NA	NA	NA	NA	NA	NA	NA	NA	NA	NA	NA	NA	NA	NA	NA	NA	NA	NA	NA	NA	NA	NA	NA	NA	NA
u3	in	NA	NA	NA	NA	NA	NA	NA	NA	NA	NA	NA	NA	NA	NA	NA	NA	NA	NA	NA	NA	NA	NA	NA	NA	NA	NA	NA	NA	NA	NA
u3	in	NA	NA	NA	NA	NA	NA	NA	NA	NA	NA	NA	NA	NA	NA	NA	NA	NA	NA	NA	NA	NA	NA	NA	NA	NA	NA	NA	NA	NA	NA
u3	in	NA	NA	NA	NA	NA	NA	NA	NA	NA	NA	NA	NA	NA	NA	NA	NA	NA	NA	NA	NA	NA	NA	NA	NA	NA	NA	NA	NA	NA	NA
u3	in	NA	NA	NA	NA	NA	NA	NA	NA	NA	NA	NA	NA	NA	NA	NA	NA	NA	NA	NA	NA	NA	NA	NA	NA	NA	NA	NA	NA	NA	NA
u3	in	NA	NA	NA	NA	NA	NA	NA	NA	NA	NA	NA	NA	NA	NA	NA	NA	NA	NA	NA	NA	NA	NA	NA	NA	NA	NA	NA	NA	NA	NA
u3	in	NA	NA	NA	NA	NA	NA	NA	NA	NA	NA	NA	NA	NA	NA	NA	NA	NA	NA	NA	NA	NA	NA	NA	NA	NA	NA	NA	NA	NA	NA
u3	in	NA	NA	NA	NA	NA	NA	NA	NA	NA	NA	NA	NA	NA	NA	NA	NA	NA	NA	NA	NA	NA	NA	NA	NA	NA	NA	NA	NA	NA	NA
u3	in	NA	NA	NA	NA	NA	NA	NA	NA	NA	NA	NA	NA	NA	NA	NA	NA	NA	NA	NA	NA	NA	NA	NA	NA	NA	NA	NA	NA	NA	NA
u3	in	NA	NA	NA	NA	NA	NA	NA	NA	NA	NA	NA	NA	NA	NA	NA	NA	NA	NA	NA	NA	NA	NA	NA	NA	NA	NA	NA	NA	NA	NA
u3	in	NA	NA	NA	NA	NA	NA	NA	NA	NA	NA	NA	NA	NA	NA	NA	NA	NA	NA	NA	NA	NA	NA	NA	NA	NA	NA	NA	NA	NA	NA
u3	in	NA	NA	NA	NA	NA	NA	NA	NA	NA	NA	NA	NA	NA	NA	NA	NA	NA	NA	NA	NA	NA	NA	NA	NA	NA	NA	NA	NA	NA	NA
u3	in	NA	NA	NA	NA	NA	NA	NA	NA	NA	NA	NA	NA	NA	NA	NA	NA	NA	NA	NA	NA	NA	NA	NA	NA	NA	NA	NA	NA	NA	NA
u3	in	NA	NA	NA	NA	NA	NA	NA	NA	NA	NA	NA	NA	NA	NA	NA	NA	NA	NA	NA	NA	NA	NA	NA	NA	NA	NA	NA	NA	NA	NA
u3	in	NA	NA	NA	NA	NA	NA	NA	NA	NA	NA	NA	NA	NA	NA	NA	NA	NA	NA	NA	NA	NA	NA	NA	NA	NA	NA	NA	NA	NA	NA
u3	in	NA	NA	NA	NA	NA	NA	NA	NA	NA	NA	NA	NA	NA	NA	NA	NA	NA	NA	NA	NA	NA	NA	NA	NA	NA	NA	NA	NA	NA	NA
u3	in	NA	NA	NA	NA	NA	NA	NA	NA	NA	NA	NA	NA	NA	NA	NA	NA	NA	NA	NA	NA	NA	NA	NA	NA	NA	NA	NA	NA	NA	NA
u3	in	NA	NA	NA	NA	NA	NA	NA	NA	NA	NA	NA	NA	NA	NA	NA	NA	NA	NA	NA	NA	NA	NA	NA	NA	NA	NA	NA	NA	NA	NA
u3	in	NA	NA	NA	NA	NA	NA	NA	NA	NA	NA	NA	NA	NA	NA	NA	NA	NA	NA												

Absolute Difference Pixel Values		s101	s105	s111	s116	s121	s1210	s155	s162	s221	s225	s231	s294	s306	s309	s39	s405	s510	s52	s71	s78	s85	s88	s94	s98	Average
% Param		2.80	N/A	0.63	N/A	1.36	N/A	1.15	N/A	0.56	2.30	N/A	N/A	N/A	N/A	N/A	1.00	0.37	2.44	N/A	N/A	3.07	N/A	N/A	N/A	1.59
c1kOut		3.49	N/A	0.90	N/A	1.15	N/A	1.15	N/A	0.38	1.73	N/A	N/A	N/A	N/A	N/A	1.07	1.37	2.71	N/A	N/A	5.62	N/A	N/A	N/A	2.50
c1yOut		1.03	N/A	1.05	N/A	0.19	N/A	1.85	N/A	1.85	1.89	N/A	N/A	N/A	N/A	N/A	1.50	0.30	1.02	N/A	N/A	3.65	N/A	N/A	N/A	1.39
u1kOut		0.80	N/A	0.24	N/A	4.18	N/A	4.18	N/A	0.88	1.43	N/A	N/A	N/A	N/A	N/A	2.33	0.96	0.62	N/A	N/A	0.45	N/A	N/A	N/A	1.32
u1yOut		1.27	N/A	2.46	N/A	7.52	N/A	7.52	N/A	2.94	2.80	N/A	N/A	N/A	N/A	N/A	2.67	0.70	1.06	N/A	N/A	2.90	N/A	N/A	N/A	2.70
u2xOut		2.85	N/A	0.90	N/A	7.93	N/A	7.93	N/A	1.88	1.10	N/A	N/A	N/A	N/A	N/A	2.33	0.04	0.96	N/A	N/A	0.78	N/A	N/A	N/A	2.09
u3xOut		1.77	N/A	3.21	N/A	2.48	N/A	2.48	N/A	4.02	1.39	N/A	N/A	N/A	N/A	N/A	2.17	1.32	2.81	N/A	N/A	2.49	N/A	N/A	N/A	2.41
u3yOut		2.51	N/A	0.24	N/A	4.18	N/A	4.18	N/A	1.54	0.10	N/A	N/A	N/A	N/A	N/A	3.67	0.52	0.96	N/A	N/A	1.55	N/A	N/A	N/A	1.70
e2xOut		1.60	N/A	2.96	N/A	0.98	N/A	0.98	N/A	6.44	3.64	N/A	N/A	N/A	N/A	N/A	0.33	2.70	2.89	N/A	N/A	0.26	N/A	N/A	N/A	2.42
e2yOut		1.15	N/A	0.24	N/A	1.49	N/A	1.49	N/A	6.38	7.07	N/A	N/A	N/A	N/A	N/A	0.50	3.04	1.71	N/A	N/A	0.05	N/A	N/A	N/A	2.40
d3xOut		2.12	N/A	3.70	N/A	0.86	N/A	0.86	N/A	3.34	1.34	N/A	N/A	N/A	N/A	N/A	0.50	2.25	2.96	N/A	N/A	0.57	N/A	N/A	N/A	1.96
d3yOut		0.02	N/A	1.74	N/A	3.51	N/A	3.51	N/A	3.90	4.86	N/A	N/A	N/A	N/A	N/A	0.33	1.84	4.26	N/A	N/A	0.57	N/A	N/A	N/A	2.34
d2xOut		1.52	N/A	0.97	N/A	5.77	N/A	5.77	N/A	5.08	2.32	N/A	N/A	N/A	N/A	N/A	1.33	1.37	1.80	N/A	N/A	1.08	N/A	N/A	N/A	2.36
d2yOut		0.31	N/A	3.50	N/A	3.30	N/A	3.30	N/A	4.40	2.03	N/A	N/A	N/A	N/A	N/A	1.00	3.04	3.08	N/A	N/A	1.06	N/A	N/A	N/A	2.41
d1xOut		0.40	N/A	0.30	N/A	6.88	N/A	6.88	N/A	2.84	2.40	N/A	N/A	N/A	N/A	N/A	0.17	2.09	1.17	N/A	N/A	2.55	N/A	N/A	N/A	2.09
d1yOut		0.32	N/A	1.85	N/A	2.18	N/A	2.18	N/A	4.19	6.42	N/A	N/A	N/A	N/A	N/A	1.00	3.09	1.30	N/A	N/A	4.24	N/A	N/A	N/A	2.73
c1kIn		1.60	N/A	0.63	N/A	2.02	N/A	2.02	N/A	0.10	2.30	N/A	N/A	N/A	N/A	N/A	1.00	1.04	1.11	N/A	N/A	2.40	N/A	N/A	N/A	1.36
c1yIn		2.82	N/A	1.24	N/A	0.49	N/A	0.49	N/A	2.38	0.40	N/A	N/A	N/A	N/A	N/A	2.17	0.37	1.04	N/A	N/A	5.62	N/A	N/A	N/A	1.84
u1kIn		0.63	N/A	1.05	N/A	0.52	N/A	0.52	N/A	1.52	2.55	N/A	N/A	N/A	N/A	N/A	0.83	1.37	0.69	N/A	N/A	2.85	N/A	N/A	N/A	1.31
u1yIn		1.00	N/A	3.17	N/A	1.38	N/A	1.38	N/A	4.08	0.90	N/A	N/A	N/A	N/A	N/A	0.67	1.37	1.65	N/A	N/A	2.59	N/A	N/A	N/A	1.87
u2xIn		2.93	N/A	2.13	N/A	6.86	N/A	6.86	N/A	3.94	3.14	N/A	N/A	N/A	N/A	N/A	1.00	0.37	1.06	N/A	N/A	1.90	N/A	N/A	N/A	2.59
u2yIn		0.38	N/A	2.51	N/A	6.13	N/A	6.13	N/A	4.42	1.23	N/A	N/A	N/A	N/A	N/A	0.67	1.37	1.32	N/A	N/A	1.92	N/A	N/A	N/A	2.22
u3xIn		3.43	N/A	2.55	N/A	0.14	N/A	0.14	N/A	5.35	4.39	N/A	N/A	N/A	N/A	N/A	0.17	1.01	2.14	N/A	N/A	1.15	N/A	N/A	N/A	2.26
u3yIn		0.38	N/A	2.51	N/A	1.04	N/A	1.04	N/A	4.42	3.23	N/A	N/A	N/A	N/A	N/A	1.00	2.52	1.65	N/A	N/A	1.25	N/A	N/A	N/A	2.00
e2xIn		2.27	N/A	1.68	N/A	0.02	N/A	0.02	N/A	6.77	7.64	N/A	N/A	N/A	N/A	N/A	0.33	0.04	0.56	N/A	N/A	2.60	N/A	N/A	N/A	2.43
e2yIn		0.82	N/A	1.45	N/A	1.15	N/A	1.15	N/A	5.38	5.40	N/A	N/A	N/A	N/A	N/A	0.50	2.04	1.71	N/A	N/A	0.62	N/A	N/A	N/A	2.12
d3xIn		3.70	N/A	2.61	N/A	2.52	N/A	2.52	N/A	6.45	3.70	N/A	N/A	N/A	N/A	N/A	0.17	0.59	0.46	N/A	N/A	1.73	N/A	N/A	N/A	2.44
d3yIn		2.30	N/A	0.35	N/A	3.38	N/A	3.38	N/A	4.54	1.89	N/A	N/A	N/A	N/A	N/A	1.00	1.21	0.27	N/A	N/A	0.56	N/A	N/A	N/A	1.72
d2xIn		2.45	N/A	1.90	N/A	8.19	N/A	8.19	N/A	3.56	1.99	N/A	N/A	N/A	N/A	N/A	1.00	0.37	1.39	N/A	N/A	1.29	N/A	N/A	N/A	2.45
d2yIn		3.07	N/A	1.30	N/A	8.13	N/A	8.13	N/A	4.70	0.83	N/A	N/A	N/A	N/A	N/A	0.67	1.71	0.47	N/A	N/A	3.63	N/A	N/A	N/A	2.72
d1xIn		1.71	N/A	0.23	N/A	5.49	N/A	5.49	N/A	0.59	0.23	N/A	N/A	N/A	N/A	N/A	0.83	2.78	2.76	N/A	N/A	4.52	N/A	N/A	N/A	2.13
d1yIn		0.99	N/A	0.15	N/A	3.71	N/A	3.71	N/A	5.23	0.19	N/A	N/A	N/A	N/A	N/A	0.67	0.05	0.20	N/A	N/A	5.32	N/A	N/A	N/A	1.83
Average		1.70	N/A	1.57	N/A	3.29	N/A	3.29	N/A	3.66	2.58	N/A	N/A	N/A	N/A	N/A	1.11	1.35	1.57	N/A	N/A	2.21	N/A	N/A	N/A	N/A

Figure I.5: ORL spline-based mouth-open template test results

Percentage (of width) Diff		s101	s105	s111	s116	s121	s1210	s155	s162	s221	s225	s231	s294	s306	s309	s39	s405	s510	s52	s71	s78	s85	s88	s94	s98	Average
% Param																										
c1%Out		9.63	NA	2.56	NA	4.20	NA	NA	NA	1.41	5.27	NA	NA	NA	NA	NA	3.95	1.22	7.11	NA	NA	9.69	NA	NA	NA	5.00
c1%In		12.91	NA	3.66	NA	3.57	NA	NA	NA	8.44	3.97	NA	NA	NA	NA	NA	8.55	4.53	7.90	NA	NA	17.74	NA	NA	NA	7.92
u1%Out		3.83	NA	4.25	NA	0.59	NA	NA	NA	4.64	4.32	NA	NA	NA	NA	NA	5.92	0.98	2.98	NA	NA	11.54	NA	NA	NA	4.34
u1%In		2.97	NA	0.96	NA	12.92	NA	NA	NA	2.19	3.28	NA	NA	NA	NA	NA	9.21	3.16	1.81	NA	NA	1.42	NA	NA	NA	4.22
u2%Out		4.69	NA	9.99	NA	23.27	NA	NA	NA	7.34	6.42	NA	NA	NA	NA	NA	10.53	2.32	3.09	NA	NA	9.17	NA	NA	NA	8.54
u2%In		10.54	NA	3.66	NA	24.52	NA	NA	NA	4.69	2.52	NA	NA	NA	NA	NA	9.21	0.13	2.78	NA	NA	2.47	NA	NA	NA	6.73
u3%Out		6.54	NA	13.03	NA	7.66	NA	NA	NA	10.05	3.17	NA	NA	NA	NA	NA	8.55	4.35	8.19	NA	NA	7.85	NA	NA	NA	7.71
u3%In		9.31	NA	0.96	NA	12.92	NA	NA	NA	3.85	0.23	NA	NA	NA	NA	NA	14.47	1.70	2.78	NA	NA	4.89	NA	NA	NA	5.68
c2%Out		5.93	NA	12.02	NA	3.02	NA	NA	NA	16.09	8.33	NA	NA	NA	NA	NA	1.32	8.91	8.43	NA	NA	0.83	NA	NA	NA	7.21
c2%In		4.27	NA	0.96	NA	4.60	NA	NA	NA	15.94	16.18	NA	NA	NA	NA	NA	1.97	10.02	4.98	NA	NA	0.16	NA	NA	NA	6.57
d3%Out		7.85	NA	14.99	NA	2.65	NA	NA	NA	8.35	3.08	NA	NA	NA	NA	NA	1.97	7.41	8.62	NA	NA	1.81	NA	NA	NA	6.30
d3%In		0.07	NA	7.07	NA	10.86	NA	NA	NA	9.74	11.13	NA	NA	NA	NA	NA	1.32	6.07	12.41	NA	NA	1.79	NA	NA	NA	6.72
d2%Out		5.64	NA	3.93	NA	17.86	NA	NA	NA	12.69	5.32	NA	NA	NA	NA	NA	5.26	4.52	5.26	NA	NA	3.41	NA	NA	NA	7.10
d2%In		1.16	NA	14.20	NA	10.22	NA	NA	NA	11.00	4.65	NA	NA	NA	NA	NA	3.95	10.02	8.96	NA	NA	3.34	NA	NA	NA	7.50
d1%Out		1.49	NA	1.21	NA	21.28	NA	NA	NA	7.11	5.49	NA	NA	NA	NA	NA	0.66	6.89	3.42	NA	NA	8.05	NA	NA	NA	6.18
d1%In		1.17	NA	7.50	NA	6.74	NA	NA	NA	10.48	14.70	NA	NA	NA	NA	NA	3.95	10.19	3.78	NA	NA	13.39	NA	NA	NA	7.99
c1%In		5.93	NA	2.56	NA	6.26	NA	NA	NA	0.26	5.27	NA	NA	NA	NA	NA	3.95	3.42	3.22	NA	NA	7.59	NA	NA	NA	4.27
c1%In		10.45	NA	5.01	NA	1.51	NA	NA	NA	5.94	0.91	NA	NA	NA	NA	NA	8.55	1.23	3.04	NA	NA	17.74	NA	NA	NA	6.04
u1%In		2.34	NA	4.25	NA	1.62	NA	NA	NA	3.80	5.84	NA	NA	NA	NA	NA	3.29	4.52	2.01	NA	NA	8.38	NA	NA	NA	4.01
u1%In		3.70	NA	12.87	NA	4.26	NA	NA	NA	10.21	2.06	NA	NA	NA	NA	NA	2.63	4.53	4.80	NA	NA	8.17	NA	NA	NA	5.91
u2%In		10.87	NA	8.64	NA	21.21	NA	NA	NA	9.84	7.18	NA	NA	NA	NA	NA	3.95	1.22	3.09	NA	NA	6.01	NA	NA	NA	8.00
u3%In		12.72	NA	10.33	NA	18.95	NA	NA	NA	11.04	2.82	NA	NA	NA	NA	NA	2.63	4.53	3.83	NA	NA	6.06	NA	NA	NA	6.83
u3%In		1.40	NA	10.17	NA	3.23	NA	NA	NA	11.04	7.40	NA	NA	NA	NA	NA	3.95	8.30	4.80	NA	NA	3.96	NA	NA	NA	6.03
c2%In		8.40	NA	6.81	NA	0.08	NA	NA	NA	16.93	17.49	NA	NA	NA	NA	NA	1.32	0.12	1.63	NA	NA	8.20	NA	NA	NA	6.77
c2%In		3.04	NA	5.89	NA	3.57	NA	NA	NA	13.44	12.36	NA	NA	NA	NA	NA	1.97	6.73	4.98	NA	NA	1.95	NA	NA	NA	5.99
d3%In		13.72	NA	10.60	NA	7.81	NA	NA	NA	16.13	8.47	NA	NA	NA	NA	NA	0.66	1.96	1.34	NA	NA	5.45	NA	NA	NA	7.35
d3%In		8.51	NA	1.40	NA	10.44	NA	NA	NA	11.35	4.32	NA	NA	NA	NA	NA	3.95	3.99	0.79	NA	NA	1.76	NA	NA	NA	5.17
d2%In		9.07	NA	7.72	NA	25.33	NA	NA	NA	8.89	4.33	NA	NA	NA	NA	NA	3.95	1.22	4.06	NA	NA	4.08	NA	NA	NA	7.63
d2%In		11.39	NA	5.25	NA	25.13	NA	NA	NA	11.74	1.90	NA	NA	NA	NA	NA	2.63	5.63	1.36	NA	NA	11.45	NA	NA	NA	8.50
d1%In		6.33	NA	0.94	NA	16.98	NA	NA	NA	1.46	0.52	NA	NA	NA	NA	NA	3.29	9.15	8.04	NA	NA	14.27	NA	NA	NA	6.78
d1%In		3.68	NA	0.60	NA	11.48	NA	NA	NA	13.07	0.43	NA	NA	NA	NA	NA	2.63	0.16	0.58	NA	NA	16.79	NA	NA	NA	5.49
Average		6.28	NA	6.38	NA	10.16	NA	NA	NA	9.14	5.92	NA	NA	NA	NA	NA	4.40	4.45	4.57	NA	NA	6.97	NA	NA	NA	NA

Figure I.6: ORL spline-based mouth-open template test results (%)

APPENDIX J

Face Detection Training Set



Figure J.1: Face detection training set (part 1)



Figure J.2: Face detection training set (part 2)



Figure J.3: Face detection training set (part 3)

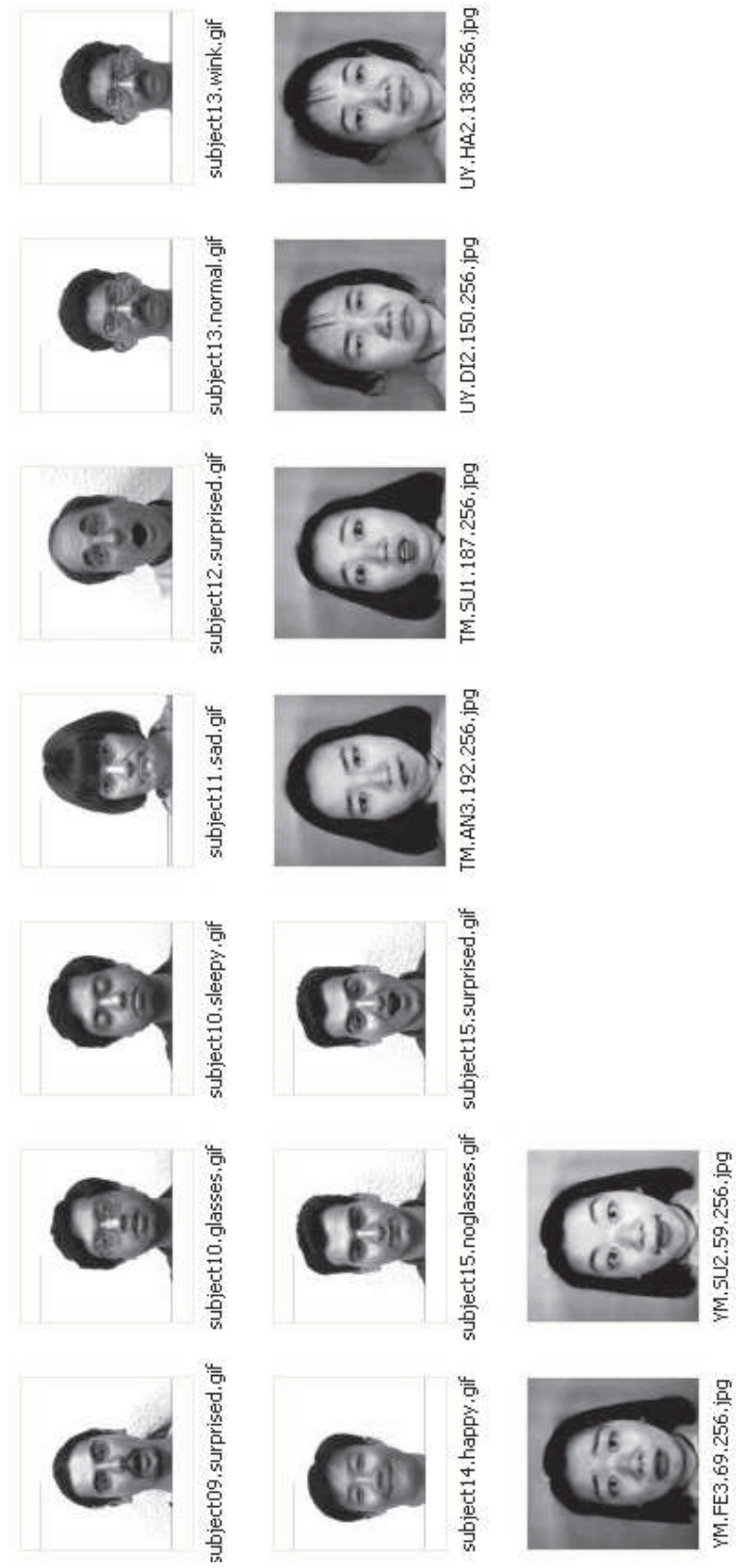


Figure J.4: Face detection training set (part 4)